PERVAPORATION DEHYDRATION OF ISOPROPANOL-WATER SYSTEMS USING CHITOSAN MEMBRANES

by

Mohd. Ghazali Mohd. Nawawi

A thesis
presented to the University of Waterloo
in fulfilment of the
thesis requirement for the degree of
Doctor of Philosophy
in Chemical Engineering

Waterloo, Ontario, 1997

©Mohd. Ghazali Mohd. Nawawi

National Library of Canada
Acquisitions and Bibliographic Services
395 Wellington Street
Ottawa ON K1A 0N4
Canada

Bibliothèque nationale du Canada
Acquisitions et services bibliographiques
395, rue Wellington
Ottawa ON K1A 0N4
Canada

Your file Votre référence

Our file Notre référence

The author has granted a non-exclusive licence allowing the National Library of Canada to reproduce, loan, distribute or sell copies of his/her thesis by any means and in any form or format, making this thesis available to interested persons.

The author retains ownership of the copyright in his/her thesis. Neither the thesis nor substantial extracts from it may be printed or otherwise reproduced with the author's permission.

L'auteur a accordé une licence non exclusive permettant à la Bibliothèque nationale du Canada de reproduire, prêter, distribuer ou vendre des copies de sa thèse de quelque manière et sous quelque forme que ce soit pour mettre des exemplaires de cette thèse à la disposition des personnes intéressées.

L'auteur conserve la propriété du droit d'auteur qui protège sa thèse. Ni la thèse ni des extraits substantiels de celle-ci ne doivent être imprimés ou autrement reproduits sans son autorisation.

0-612-21370-6

Canada

The University of Waterloo requires the signature of all persons using or photocopying the thesis. Please sign below, and give address and date.

Abstract

Sorption and pervaporation for the dehydration of isopropanol/water mixtures using chitosan membranes were investigated. The chitosan membranes showed preferential water sorption and permeation. It was clarified that both sorption selectivity and diffusion selectivity are important to the overall permeation selectivity. Preferential sorption affects and leads to preferential permeation.

Composite chitosan membranes consisting of a dense skin layer and a porous substrate were developed for dehydration of isopropanol. At 30 °C, a permeation flux of 375 g/m^2.hr and a separation factor of 348 were achieved for the dehydration of 90 wt. % isopropanol aqueous solution; a significantly larger separation factor (807) with a lower permeation flux (265 g/m^2.hr) were obtained for the dehydration of 95 wt. % isopropanol solution. It was shown that the composite membranes' performance was affected not only by the dense skin layer but also the porous substrate.

Modifications of chitosan membranes via crosslinking and polymer blending for the dehydration of isopropanol were studied. It was shown that

the chitosan membranes crosslinked with diisocyanate and the chitosan/poly(vinyl alcohol) blended membranes were preferentially permeable to water. The crosslinked chitosan membranes increased the separation factors up to 1238 while the blended chitosan membranes increased the separation factors up to 1806, for the dehydration of 90 wt. % isopropanol aqueous solution. Optimal conditions and overall performances for the crosslinking and the polymer blending were determined based on the use of the pervaporation separation index (PSI).

A comparison between pervaporation (PVAP) and vapor phase pervaporation (VPVAP) for the separation of isopropanol/water mixtures using chitosan membranes was also investigated. Preliminary results showed that significantly higher separation factor could be obtained via VPVAP, but due to the common permeability-selectivity trade-off, PVAP was more effective.

A relatively new technique to determine diffusion coefficients using thin-channel inverse gas chromatography was developed. This new technique was shown to be potentially useful for determining diffusion coefficients and especially applicable to pervaporation membranes. The technique provides a simple, fast and efficient alternative to the more conventional sorption and desorption methods for measuring diffusion coefficients of permeants through thin membrane films.

A polar pathway model to describe the mass transport in hydrophilic

chitosan pervaporation membranes was developed. This model was based on the solution-diffusion model and incorporated hydrophilic polar pathways to describe single component permeation of water and isopropanol in the chitosan membrane. Reasonable agreements between the calculated and the experimental values of single permeabilities were obtained. The free volume model approach based on the free volume theory and thermodynamics was employed to conduct the modelling of the binary component permeation of isopropanol-water mixtures through the chitosan membranes. Reasonable estimates of the pervaporation parameters were achieved.

Acknowledgements

I wish to express my sincere appreciation and gratitude to my supervisor Professor Emeritus Robert Y.M. Huang for his invaluable guidance, direction, encouragement and aspiration throughout the course of this study and in the preparation of this thesis. I also wish to express my gratitude to Professor C. Burns for co-supervising my thesis preparation and my oral defense.

My appreciation is due to Professor A. Plumtree, Professor R. Pal, Professor W. A. Anderson, and Professor M. Pritzker for their interest and helpful comments. My appreciation is also due to Dr. J. Hoff for his assistance and guidance throughout the inverse gas chromatography experiments.

The financial support in the form of graduate scholarship provided to this study by Universiti Teknologi Malaysia and the Malaysian government is gratefully acknowledged.

My special appreciation goes to my wife for her patience, understanding and caring, and all the difficulties she had in raising our children during the last few years . Finally, my deepest appreciation goes to my parents for their proper upbringing, education, unceasing support and encouragement.

to

my wife, Zuhana

and my children, Amira, Afiqa, Anisa,and Fareez.

Table of Contents

Table of Contents			ix
List of Tables			xvi
List of Figures			xvii
1	**Introduction**		1
	1.1	Background	1
	1.2	Scope of the Thesis	8
2	**Literature Review**		11
	2.1	Brief History of Pervaporation	11
	2.2	Characteristics of Pervaporation	15
	2.3	Pervaporation Membranes	18
		2.3.1 Membrane Performance	19
		2.3.2 Selection of Polymer Membrane Materials	20
		2.3.3 Modifications of Membranes	26
		2.3.4 Fabrications of Membranes	32
	2.4	Polymers for Pervaporation Applications	34
		2.4.1 Dehydration of Organic Solvents	36
		2.4.2 Removal of Organic Compounds from Aqueous Solutions	38
		2.4.3 Separation of Organic Mixtures	40
	2.5	Pervaporation Transport Mechanism	43

2.5.1 The Solution-Diffusion Model 43
2.5.2 The Pore Flow Model 48
2.6 Effects of Process Conditions 51
2.6.1 Feed Concentration 51
2.6.2 Feed and Permeate Pressures 52
2.6.3 Temperature 53

3 Pervaporation Properties of Chitosan Membranes 55
3.1 Introduction 55
3.1.1 Chitosan (CS) Membranes 56
3.2 Theoretical 58
3.3 Experimental 62
3.3.1 Materials 62
3.3.2 Preparation of Homogeneous Chitosan Membranes 62
3.3.3 Pervaporation Experiments 64
3.3.4 Liquid Sorption Experiments 67
3.4 Results and Discussion 68
3.4.1 Fabrication of Chitosan Membranes 68
3.4.2 Liquid Sorption 70
3.4.3 Pervaporation 74
3.4.4 Sorption versus Diffusion 78
3.4.5 Temperature Effect 84
3.5 Conclusions 88

4 Composite Chitosan Membranes for Dehydration of Isopropanol 89

4.1 Introduction 89
4.2 Theoretical 92
4.3 Experimental 94
4.3.1 Materials 94
4.3.2 Membrane Preparation 95
4.3.3 Scanning Electron Microscopy (SEM) 96
4.3.4 Pervaporation 96
4.4 Results and Discussion 97
4.4.1 Membranes Morphology 97
4.4.2 Pervaporation Performance of Composite Membranes 101
4.4.3 Composite Membranes vs. Homogeneous Membranes 106
4.5 Conclusions 114

5 Modified Chitosan Membranes for the Pervaporation of Isopropanol/Water Mixtures 116
5.1 Introduction 116
5.2 Experimental 119
5.2.1 Materials 119
5.2.2 Membrane Preparation 119
5.2.3 Fourier Transform Infrared Spectroscopy (FT-IR) Measurement 121
5.2.4 SEM Experiment 121
5.2.5 Differential Scanning Calorimeter (DSC) 122
5.2.6 Swelling Measurement 122
5.2.7 Pervaporation Experiment 123

5.3 Results and Discussion 123
5.3.1 Crosslinking of Chitosan Membranes 123
5.3.2 Polymer Blending of Chitosan-Poly(vinyl alcohol) (CS-PVA) 131
5.3.3 Relative Degree of Swelling 133
5.3.4 Pervaporation with Chemically Crosslinked Chitosan Membranes 137
5.3.5 Pervaporation with CS-PVA Blends Membranes 145
5.4 Conclusions 156

6 Vapor Phase Pervaporation Dehydration of Isopropanol with Chitosan Membranes 158
6.1 Introduction 158
6.2 Experimental 163
6.2.1 Materials 163
6.2.2 VPVAP Permeation Cell Design 163
6.2.3 Membrane Preparation 165
6.2.4 Vapor Phase Pervaporation 165
6.3 Results and Discussion 167
6.4 Conclusions 179

7 Diffusion Coefficients Estimations by Thin-Channel Column Inverse Gas Chromatography 181
7.1 Background 181
7.2 Theoretical 185
7.3 Experimental 189
7.3.1 Materials and Equipment 189

7.3.2 Column Design 191
7.3.3 Stationary Phase Preparation 193
7.3.4 Experimental Procedure 194
7.3.5 Measurement of Retention Time, Peak Variance, Partition Coefficient and Diffusion Coefficient 196
7.4 Results and Discussion 200
7.4.1 Effect of Temperature 210
7.4.2 Effect of Penetrant Size 216
7.5 Accuracy of Measurements 220
7.5 Conclusions 222

8 **Pervaporation Transport Mechanism in Hydrophilic Chitosan Membranes** 225
8.1 Introduction 225
8.2 Theoretical 228
8.2.1 Single Component Permeation 228
8.2.2 Binary Component Permeation 230
8.3 Transport Through Chitosan Membranes 233
8.3.1 Single Component Permeation 238
8.3.2 Estimation of Parameters 247
8.4 Binary Component Permeation 249
8.4.1 Free Volume Model Approach 249
8.5 Results and Discussion 256
8.5.1 Single Component Permeation 256
8.5.2 Equilibrium Sorption of Individual Component 261
8.5.3 Free Volume Parameters 263
8.5.4 Concentration Profile of Individual Component 265

8.5.5 Estimation of the Individual Permeability 265
8.5.6 Plasticization by Permeant during Pervaporation 269
8.6 Conclusions 272

9 Conclusions and Contributions to Original Research 274
10 Recommendations for Future Work 277
Nomenclature 280
Bibliography 287
Appendix
A Sorption Data of Isopropanol/Water Mixtures in Homogeneous Chitosan Membranes 306
B Degree of Swelling Data of Chitosan Membranes in Water/Isopropanol Mixtures 309
C Pervaporation Data of Water/Isopropanol Mixtures with Chitosan Membranes 311
D Results of IGC Experiments 319
E Diffusion Coefficients Data in Chitosan Membranes 323
F Binary Component Permeation in Chitosan Membrane : Derivation of Model Equations 326
G Calculation of Concentration Profile 330

List of Tables

1.1	Technically relevant membrane processes.	5
5.1	Relative infrared (IR) peaks intensity for crosslinked chitosan membranes.	130
5.2	Glass transition temperature of CS-PVA blends membranes.	133
7.1	A comparison between the experimental and theoretical values of retention time of methane, t_m.	201
7.2	Experimental data of the peak-spreading processes of methane, water and isopropanol.	208
7.3	Diffusion coefficients in chitosan membrane determined by the thin-channel column GC technique.	211
7.4	Diffusion coefficients from gas chromatographic measurements on dry chitosan membrane.	212
7.5	Diffusion activation energy for water and isopropanol determined by IGC technique.	216
7.6	Diffusion activation energy of alcohols determined by IGC technique.	220
7.7	Literature data of experimental diffusion coefficients	

measured by gas chromatography technique. 222

8.1 Estimated surface area fraction of polar pathway k, diffusion coefficient D, and solubility c, in chitosan membrane 257

8.2 Estimated model parameters of components in chitosan membrane. 258

8.3 Comparison between experimental permeation and theoretical permeation of pure components in chitosan membrane. 260

8.4 Equilibrium sorption of chitosan membrane with isopropanol/ water mixture at 30 °C. 262

8.5 Free volume parameters of water and chitosan at 30 °C. 264

8.6 Experimental and calculated permeability of individual component through the chitosan membrane at 30 °C. 267

8.7 Plasticizing coefficient of individual component at 30 °C. 270

8.8 The amount of plasticization action of individual component on the upstream side of chitosan membrane at 30 °C. 271

List of Figures

1.1	Separation processes play a critical role in the chemical process industries (CPI)	2
2.1	Standard pervaporation process	13
2.2	The solution-diffusion mechanism	45
2.3	The pore flow model	49
3.1	The deacetylation of chitin to chitosan	57
3.2	Sequence of preparation of homogeneous chitosan membrane	63
3.3	A schematic diagram of the pervaporation separation apparatus	65
3.4	A schematic diagram of the pervaporation cell structure	66
3.5	Fabricating chitosan membrane	69
3.6	Sorption data for isopropanol/water mixtures in chitosan membrane	71
3.7	Sorption ratio versus liquid composition	72
3.8	Weight fraction of isopropanol in membrane sorbed phase vs. weight fraction of isopropanol in bulk liquid phase	73
3.9	The total and partial permeation fluxes versus feed concentration	75
3.10	Permeation ratio versus feed concentration	77
3.11	Weight fraction of isopropanol in the permeate versus weight fraction of isopropanol in liquid feed	79

3.12	Partial permeation and sorption of isopropanol versus weight fraction of isopropanol in feed	80
3.13	Separation factor and sorption selectivity versus weight fraction of isopropanol in feed	83
3.14	Effect of temperature on permeation flux. Isopropanol weight fraction in feed: 0.90	85
3.15	Effect of temperature on separation factor	86
4.1	Scanning electron microscopy (SEM) photographs of homogeneous chitosan membranes: (a) cross-section; (b) surface layer	98
4.2	SEM photographs of composite chitosan membranes showing both (a) the chitosan top layer and (b) the polysulfone porous substrate	99
4.3	SEM photographs of composite chitosan membranes taken from the opposite angle and without the nonwoven fabric: (a) polysulfone support; (b) chitosan dense layer	100
4.4	The total and partial permeation fluxes versus feed concentration for composite chitosan membrane	102
4.5	Separation performance for the composite chitosan membrane as a function of feed concentration	104
4.6	The effect of temperature on the permeation flux and the separation factor for the composite membrane	105
4.7	The isopropanol partial permeation for the homogeneous membrane and the composite membrane as a function of feed concentration	107
4.8	The separation factor for the homogeneous membrane and composite membrane as a function of feed concentration	109

4.9	The permeation rate ratio and the separation factor ratio of homogeneous and composite membrane	111
4.10	The pervaporation separation index for the homogeneous and composite membrane vs. feed concentration	113
5.1	A model of the structural change between the chitosan membrane and the crosslinked chitosan membrane	125
5.2	Fourier Transform Infrared Spectroscopy (FT-IR) spectra of the chitosan and crosslinked chitosan membranes: (a) unmodified, (b) 24-hr-crosslinked, (c) 30-hr-crosslinked, (d)48-hr-crosslinked chitosan membranes	126
5.3	The resulted FT-IR subtraction spectra for the crosslinked chitosan membranes after: (a) 24 hr crosslinking, (b) 30 hr crosslinking and (c) 48 hr crosslinking	128
5.4	SEM photographs of CS-PVA blended membranes. (a) 5:5 CS to PVA weight ratio; (b) 8:2 CS to PVA weight ratio	132
5.5	The Differential Scanning Calorimetry (DSC) thermogram of some of the blended CS-PVA films. Weight fraction of chitosan (a) 70 %, (b) 30 %, (c) 10 %.	134
5.6	The swelling degree of chitosan membranes as a function of membrane treatment time	136
5.7	The total permeation fluxes for crosslinked and uncrosslinked chitosan membranes versus feed composition	138
5.8	The separation factor for the crosslinked and uncrosslinked chitosan membranes versus feed composition	139
5.9	The pervaporation separation index for the crosslinked and uncrosslinked chitosan membranes versus feed composition	140
5.10	The pervaporation data of the crosslinked membranes as a	

function of the membrane treatment time. Feed isopropanol concentration: 90 wt. %. 143

5.11 The individual fluxes for the crosslinked chitosan membranes as a function of the membrane treatment time. Feed isopropanol concentration: 90 wt. %. 144

5.12 The pervaporation data for the CS-PVA blended membranes as a function of blend compositions. Feed isopropanol concentration: 90 wt. %. 146

5.13 The pervaporation separation index for the CS-PVA membranes as a function of blend composition, Feed isopropanol concentration: 90 wt. % 148

5.14 The individual sorptions for the CS-PVA blended membrane versus feed composition. Blend composition: 40/60 149

5.15 The individual permeation for the CS-PVA blended membrane versus feed composition. Blend composition 40/60. 150

5.16 The separation factor and sorption selectivity of the CS-PVA blended membrane versus feed composition. Blend composition 40/60. 152

5.17 The pervaporation separation index of chitosan membranes as a function of feed composition. 153

5.18 The pervaporation data of the CS-PVA blended membrane versus operating temperature. Feed isopropanol concentration: 0.90; blend composition: 40/60. 155

6.1 Comparison between the (a) PVAP and (b) VPVAP 161

6.2 A schematic diagram of the VPVAP permeation cell 164

6.3 A schematic diagram of the VPVAP separation apparatus 166

6.4 The total and partial permeation fluxes as a function of

feed composition. Temperature 30 °C. 168
6.5 The total permeation flux in PVAP and in VPVAP as a function of feed composition. Temperature 30 °C. 169
6.6 The isopropanol fluxes in VPVAP and in PVAP versus feed composition. Temperature 30 °C. 171
6.7 The separation factors for PVAP and VPVAP versus feed composition. 173
6.8 The pervaporation separation index in PVAP and in VPVAP as a function of feed composition. 175
6.9 The permeability of composite chitosan membranes in VPVAP as a function of feed composition. 176
6.10 The separation factors of homogeneous and composite chitosan membranes versus feed composition. 178
7.1 Schematic diagram of apparatus used for the IGC 191
7.2 Schematic diagram of the thin-channel GC column. 192
7.3 Schematic of the injection unit of the TC column. 195
7.4 Times on peak concentration profile, measured from mass center of injection profile. 199
7.5 Partition coefficient of water and isopropanol as a function of carrier gas velocity. Operating temperature 30 °C. 202
7.6 Van Deemter curves for thin-channel column with chitosan stationary phase. 204
7.7 Arrhenius plots of diffusion coefficients for water and isopropanol in chitosan. 214
7.8 Arrhenius plots of diffusion coefficients of methanol, ethanol and isopropanol. 218
8.1 Transport mechanism of water by direct hydrogen bonding

between water molecules and carboxylic acid. 234

8.2 The schematic of transport mechanism through chitosan membrane. 235

8.3 The schematic of permeation through a membrane. 240

8.4 Calculated concentration profile inside the chitosan membrane. Feed isopropanol concentration : 50 wt. %; feed temperature 30 °C. 266

CHAPTER 1

Introduction

1.1 Background

Separation processes are the main cog in the manufacturing wheel of the chemical process industries. They are used for such essential chores such as removal of contaminants from raw materials, recovery and purification of primary products, and elimination of contaminants from effluent water and air streams as illustrated in Figure 1.1. The heart of the separating process is the mass-separating agent. In distillation, it is heat; in extraction, the solvent; in adsorption, the adsorbent; and in the membrane separation processes, the membrane material. Membrane processes separate the components of a gas or liquid mixture on the basis of their relative permeation rates through the membrane material. Although it is still considered as a relatively new

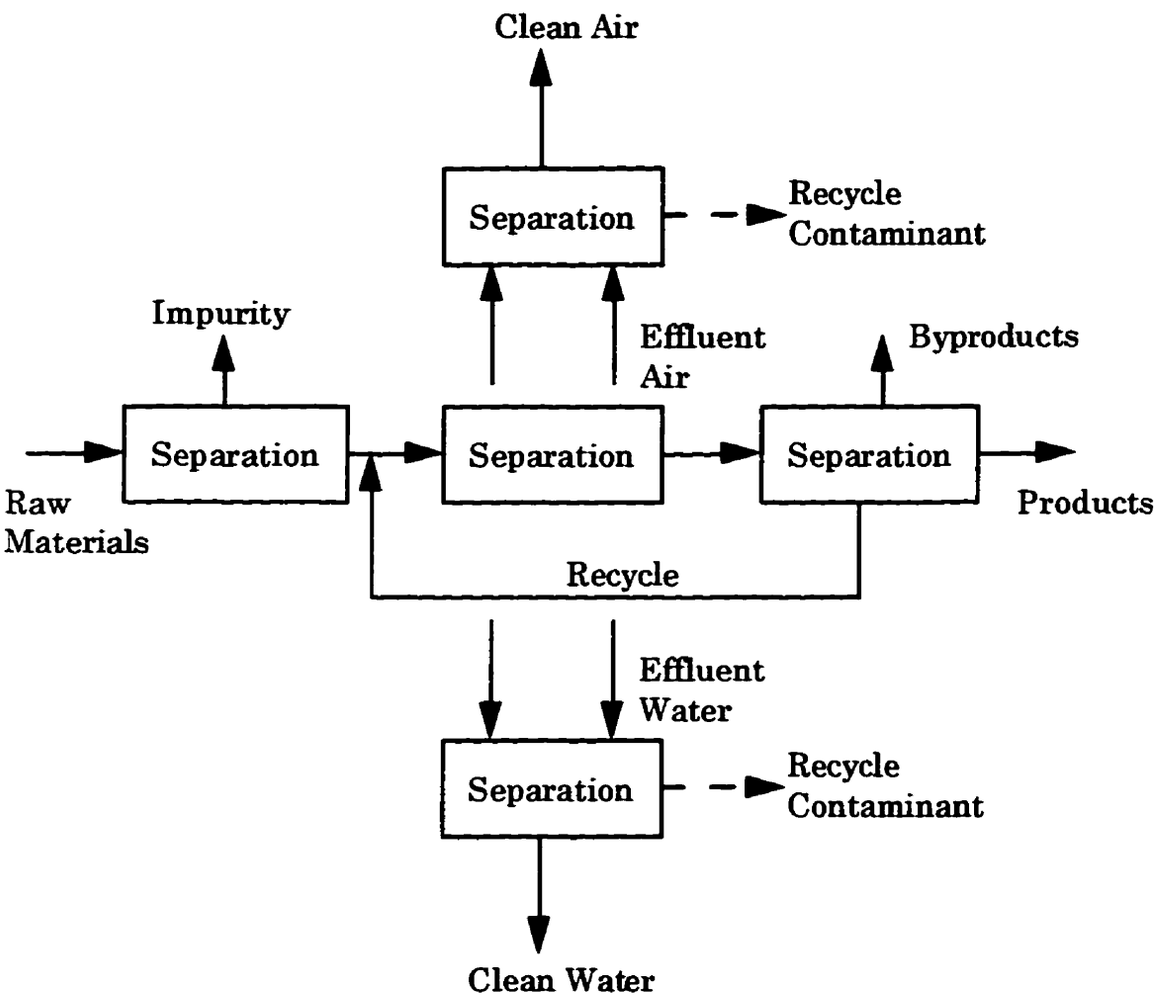


Figure 1.1 Separation processes play a critical role in the chemical process industries (CPI) [King, 1980].

commercial process, membrane separation raises significant expectations in the process plant of the future.

In recent years membranes and membrane processes have become industrial products of substantial technical and commercial importance. Membranes and membrane processes have found a very broad range applications. They are used today to produce potable water from seawater, to treat industrial effluents, to recover hydrogen from off-gases or to fractionate, concentrate, and purify molecular solutions in the chemical and pharmaceutical industry. Membranes are also key elements in artificial kidneys and controlled drug delivery systems.

The growing significance of membranes and membrane processes as efficient tools for laboratory and industrial scale mass separations is based on the several properties, characteristic of all membrane separation processes, which make them superior to many conventional mass separation methods. The mass separation by means of a membrane is a physical procedure carried out at ambient temperature, thus the constituents to be separated are not exposed to thermal stress or chemical alteration. This is of particular importance for biochemical or microbiological applications where often mixtures of sensitive biological materials have to be separated. Furthermore, membrane processes are energy efficient and rather simple to operate in a continuous mode. Up- or downscaling is easy and process costs depend only

marginally on the plant size.

Membrane processes are just as heterogeneous as the membranes. Significant differences occur in the membranes used, the driving forces for the mass transport, the applications and also in their technical and economical significance. Technically relevant membrane processes and their most important characteristics are given in Table 1.1. In some of the processes the membranes as well as the processes have reached such a level that completely new developments can not be expected. Some examples of this are in microfiltration, ultrafiltration, reverse osmosis, dialysis or electrodialysis. In these processes only improvements and optimization of existing systems and their adaptation to special applications are to be expected. Other processes, such as pervaporation and vapor permeation, are in the very beginning of their industrial application and offer the possibility of totally new developments of membranes and modules.

Pervaporation, which name originates from a combination of the terms permeation and vaporization, is a hybrid between a liquid and a gas separation process.Pervaporation which was first developed by Kober [1917] is a relatively new membrane separation process and potentially applicable to numerous cases [Baker *et. al,* 1991; Wijmans and Baker, 1993; Fleming, 1993].There are three current applications of pervaporation; dehydration of organic solvents (water removal from organics), removal of organic compounds

Table 1.1 Technically Relevant Membrane Processes [Strathmann, 1991]

Membrane Separation Process	Driving force for mass transport	Type of membranes employed	Separation mechanism of the membrane	Application
Microfiltration	Hydrostatic pressure dif. 50-100 kPa	Symmetrical porous membrane with a pore radius of 0.1 to 20 µm	Sieving effect	Separation of suspended materials
Ultrafiltration	Hydrostatic pressure dif. 100-1000 kPa	Symmetrical porous membrane with a radius of 1-20 µm	Sieving effect	Concentration fractionation and cleaning of macromolecular solutions
Reverse Osmosis	Hydrostatic pressure dif. 1000-10000 kPa	Asymmetric membrane from different homogeneous polymers	Solubility and diffusion in the homogeneous polymer matrix	Concentration of components with low molecular weight
Dialysis	Concentration difference	Symmetrical porous membrane	Diffusion in a convection-free layer	Separation of components with low molecular from macromolecular solutions
Electrodialysis	Difference in electrical potential	Ion exchange membrane	Different charges of the components in solutions	Desalting and deacidifying of solutions containing neutral components
Pervaporation, Vapor permeation	Partial pressure dif. 0-100 kPa	Asymmetrical solubility membrane from a homogeneous polymer	Solution and diffusion in the homogeneous polymer matrix	Separation of solvents and azeotropic mixtures

from aqueous solution (organic removal from water), and the separation of organic mixtures.The most important category of separation problems for which pervaporation is promising are mixtures with azeotrope and/or small differences in boiling characteristics.Removal of water from liquid organic mixtures now accounts for the largest segment of industrial pervaporation plants.Currently, dehydration of solvents, in particular ethanol and isopropanol, is the only process installed on a large scale. A specific example of alcohol dehydration includes pervaporation dehydration of isopropanol to allow in-plant recycle as a cleaning agent in compact disk manufacturing. Dehydration of fermentation product directly, or following primary distillation, has become the classic example of membrane pervaporation. In mid-1970s, Gesellschaft fur Trenntechnik (GFT), Co., Germany, commercialized an economical pervaporation process for dehydrating ethanol and producing high purities that rivalled azeotropic distillation.

The permselectivity of pervaporation process is determined by the membrane materials itself.The selection of these polymers is, therefore, a key task in the development of pervaporation membranes.Membranes used for pervaporation separation process are generally dense (non-porous), homogeneous thin polymer films, or membranes that have a dense polymer top-layer (skinned or composite). In fact the key to commercialization of pervaporation has been the development of asymmetric composite

membranes.The predominant commercial membranes are generally those from the poly (vinyl alcohol) (PVA) family in asymmetric composites;comprise of a supporting layer of nonwoven porous polyester, on which is cast either polyacrylonitrile (PAN) or polysulfone (PS) ultrafiltration membrane, and finally a thin layer of crosslinked poly(vinyl alcohol). A number of hydrophilic polymeric materials have been found that exhibit favorable selectivities and fluxes for water.

Smooth, mechanically resistant films are preferable for the manufacturing of pervaporation membranes. In most cases, the films should also maintain a proper hydrophilic-hydrophobic balance because the introduction of hydrophilic groups swells the membranes significantly under aqueous mixture due to its plasticization action which results in poor selectivity. Usually, a membrane with high flux gives a low selectivity, and *vice versa*, so that an optimal combination of flux and selectivity should be determined by adjusting and controlling hydrophilic-hydrophobic balance properties of a membrane [Huang and Xu, 1989; Uragami *et al.*, 1990]. In order to control the hydrophilic-hydrophobic balance properties of a membrane, several techniques have been tried. These include blending a hydrophilic polymer with a hydrophobic polymer, crosslinking a polymer, grafting a selective species onto an inert film , and copolymerization [Mochizuki *et al.*, 1990].Since the early history of pervaporation, the most

common method used in the preparation of the membranes is the solvent casting technique.

Research in pervaporation can be categorized into three main aspects : i) engineering aspects of pervaporation such as module development and process design, ii) modelling to describe pervaporation transport mechanism, and iii) development of pervaporation membranes.The development and optimization of high performance membrane have been the focus and motive of research in pervaporation. On the other hand, mathematical model equations to describe the pervaporation transport mechanism are also necessary.

1.2 Scope of the Thesis

The motives of the research project have been derived in light of the aforementioned background discussions. The development of effective pervaporation membranes along with the mathematical modelling have been emphasized throughout this thesis.The structure of the thesis is as follow :

Chapter 2 provides a brief history of pervaporation and an overview of pervaporation characteristics as well as a review of the current pervaporation literature concerning its industrial applications, mass transport model, membrane materials selection and membrane fabrication.

The sorption and pervaporation properties of the produced chitosan membranes are investigated with isopropanol-water mixtures. It has been shown by experimental results, which are presented in Chapter 3, that the chitosan membranes show preferential sorption and permeation to water, making chitosan membranes effective for the dehydration of isopropanol.

In Chapter 4, composite chitosan/polysulfone membranes for dehydration of isopropanol are developed and tested. Their pervaporation performance was compared to the homogeneous chitosan membranes in terms of the pervaporation separation index (PSI).

Modifications of chitosan membranes via chemical crosslinking and polymer blending with poly(vinyl alcohol) (PVA) are tested for pervaporation dehydration of isopropanol-water systems, and the results are presented in Chapter 5. The modified chitosan membrane performance is investigated in terms of feed concentrations, degree of crosslinking and blend compositions of the blended membranes.

Vapor phase pervaporation for dehydration of isopropanol using chitosan membranes is also investigated, the results are presented in Chapter 6. In comparison with the *traditional* pervaporation, vapor phase pervaporation tends to produce higher separation factors but lower permeation rates.

A novel technique for measuring diffusion coefficients by inverse gas

chromatography applicable to pervaporation membranes is illustrated in Chapter 7. A thin-channel column with a thin layer of dense membrane film as a stationary phase is designed and used to measure diffusion coefficients of alcohols and water as a function temperature and molecular size.

Chapter 8 is concerned with the modelling of pervaporation using chitosan membrane based on the solution-diffusion model. The modified model is used to interpret the transport mechanism in the highly hydropilic chitosan membrane.

Finally, the conclusions and contributions of this study to original research are summarized in Chapter 9. The recommendations for future study in which the present study may be extended are given in Chapter 10.

CHAPTER 2

Literature Review

2.1 Brief History of Pervaporation

Pervaporation is a novel liquid separation process used to separate mixtures of dissolved solvents. In fact, pervaporation is a very effective and economical technique for the separation of water from organic solvents and solvent mixtures. This membrane process has emerged in recent years as a novel liquid separation process which may eventually compete with conventional distillation for the final dehydration stages of ethanol production, separation of organic-organic liquid mixtures, removal of dissolved organic contaminants from aqueous streams and continuous removal of biosolvents with inhibitory effects on the production rate from fermentation broths [Strathmann and Gudernatsch, 1991].

In essence, as shown in Figure 2.1, the liquid to be separated (feed) contacts the upstream membrane face, a vapor permeate leaves the downstream face. The chemical potential gradient across the membrane is the driving force for the mass transport. The driving force can be created by applying either vacuum pump or an inert purge (air or steam) on the permeate side so that the permeate vapor pressure is always lower than the partial pressure of the liquid feed.

In principle, vapor permeation or vapor phase pervaporation is similar to membrane pervaporation. The feed stream is a mixture of vapors, rather than a liquid. As in the pervaporation, the permeate partial pressure is maintained by the use of inert sweep gas or a vacuum. Because requirements for the membranes are similar to those in pervaporation, membranes currently being employed in vapor permeation are generally the same as those used in pervaporation.

Although the origins of pervaporation can be traced to 1917 [Kober, 1917], but most of the work in this field was done only in the past several years [Slater and Hickey, 1989]. The first major research effort in pervaporation was undertaken by Binning and co-workers [1958, 1961]. It was their work that established the principles and highlighted the potential applications of pervaporation separation. Although this work was pursued for a number of years and several patents were obtained, the process was not

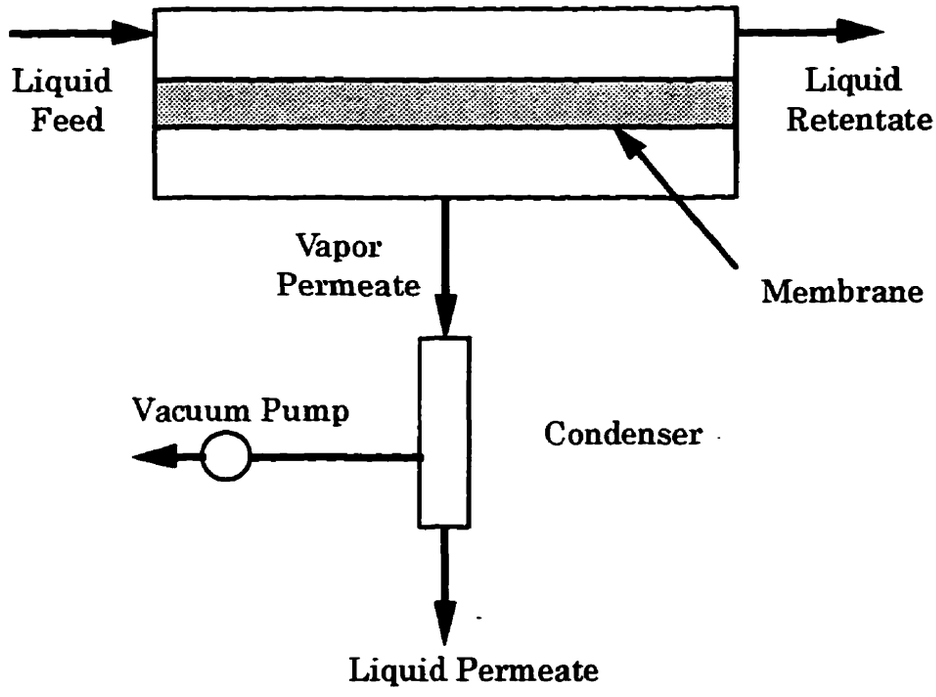


Figure 2.1 Standard pervaporation process

commercialized. The major problem was that the membrane fabrication technology available then did not allow the high-performance modules and modules required for a commercially competitive process to be made. Traditional separation technologies including distillation, extraction, and adsorption were deemed sufficient. Further,the membranes then being utilized lacked the high selectivity and permeability necessary to make pervaporation economically attractive.

The energy crisis in the 1970s refocused interest in separation technologies that possessed a high potential for energy savings. Pervaporation was aggressively pursued, primarily in Europe, because of its demonstrated ability to dewater aqueous mixtures for fuel utilization. By the 1980s,better membrane materials were being developed in the analogous technologies of reverse osmosis and gas permeation, so that the potential for economically attractive separations by pervaporation was greatly enhanced.In the mid-1980s multiple membrane options were developed, all based on novel proprietary asymmetric composite polymer technology for producing economical, chemically and thermally stable membranes in a flat plate geometry. A number of composite membranes were developed including poly(vinyl alcohol), silicone, and modified cellulose esters composites, each exhibiting high selectivities (10 to 1000) for specific separations [Brueschke, 1988]. Advancements in membrane technology made it possible to prepare

economically viable pervaporation systems.A breakthrough was achieved in West Germany which led to the successful commercialization of the poly(vinyl alcohol) composite membrane (GFT membrane) for the separation of ethanol-water mixtures [Hauser *et al.*, 1987, 1988; Rautenbach *et al.*, 1988; Bruschke, 1987; Tusel, 1987].

In the last decade, pervaporation has become one of the most popular membrane separation processes after numerous technical breakthroughs had been achieved [Asada, 1988; Sander and Soukup, 1988; Rapin, 1988]. Many reports and articles provide substantial amount of information on pervaporation membrane separation process. Already 7 international conferences on the subject have been held.The first comprehensive pervaporation book edited by Huang [1991] covers exclusively the various aspects of pervaporation process, such as transport principles, process thermodynamics, evaluation of pervaporation membrane materials, and plant design as well as industrial applications.

2.2 Characteristics of Pervaporation

The pervaporation technique is a fractionation process which uses a dense membrane as a separation barrier between the vapor permeant and the liquid feed. Pervaporation is a membrane process which differs from all other

membrane processes (except may be membrane distillation) because of the permeate phase change from liquid to vapor. This means that at least the heat of evaporation of the permeant has to be supplied to the process. As a consequence pervaporation requires higher energy input compared to other membrane processes. Therefore pervaporation will especially be attractive when the amount of the component that has to be removed is relatively small.

The pervaporation separation of various components from a liquid mixture is not only determined by differences in their vapor pressure but also by their permeation rate through the membrane.The separation is governed by the chemical nature of the macromolecules that comprise the membrane, the physical structure of the membrane, the physiochemical properties of the mixtures to be separated, and the permeant-permeant and permeant-membrane interactions. The actual driving force for the permeation of the different components through the membrane is their chemical potential gradient across the membrane. This chemical potential gradient may be established by a temperature difference between the two phases separated by the membrane or by lowering the partial pressure of the different components in the permeate. The driving force is generally controlled by applying a vacuum.

A gradient of the chemical potential, best expressed as the gradient of partial vapor pressures, acts as the driving force for the transport of matter

across the membrane. The separation characteristic of the membrane is thus solely determined by the ratio of the permeation rates and not by thermodynamic equilibria. By the pervaporation process the feed is separated into two streams :

i) a permeate, in which the preferentially permeating substance is enriched to a concentration higher than the initial feed concentration,

ii) a retentate, which is depleted of the preferentially permeating substance.

As in reverse osmosis, the liquid in contact with the membrane tends to dissolve into the membrane and cause membrane swelling. Swelling tends to alter the membrane properties and generally leads to higher permeability and lower selectivity. However, in pervaporation, because a vacuum exists at the downstream face of the membrane, less average swelling and associated loss in mobility selectivity of the membrane occurs than under equivalent feed conditions for reverse osmosis.

Unlike reverse osmosis, pervaporation transport is not limited by osmotic pressure because the driving force for mass transfer is provided by the large drop in activity between the liquid and vapor phase of the permeant, and consequently a large transmembrane pressure difference is unnecessary. For a given membrane and a given liquid mixture, both the permeation flux and

separation factor in pervaporation are higher than in reverse osmosis [Tanimura *et al.*, 1990].On the downstream side of the membrane, the partial vapor pressure of a component affects its permeation rate significantly.Hence the downstream vapor pressure must be maintained as low as economically feasible to maximize the driving force for the permeation.

Unlike reverse osmosis and membrane gas separation, pervaporation involves a phase change of permeating species from the liquid to the vapor state. Consequently, energy is needed for the vaporization of the permeate. Thus, from an energy consumption point of view, pervaporation is especially promising when the concentration of the preferentially permeating species in the liquid feed is low.

2.3 Pervaporation Membranes

For the practical application of pervaporation, the membrane must have a high permeation rate and a large separation factor. Although a so-called trade-off relationship exists between permeability and selectivity, acceptable membrane materials with both high permeability and high selectivity may be synthesized by polymer design. Very selective and solvent stable membranes are commercially available, using materials such as poly(vinyl alcohol), poly(dimethylsiloxane), poly(acrylate), *etc*. At the same

time, new membrane materials exhibiting good permseletivity are being developed for given separation problems.

2.3.1 Membrane Performance

As for most membrane processes, pervaporation and vapor permeation membranes are characterized by the transport rate through the membrane and the separation performance. Usually, the transport rate is represented by the flux or permeation rate, J : the amount of liquid transported through the membrane per unit area per unit time. Note that permeation rate depends on both the intrinsic permeability and the effective thickness of a membrane. In some cases, permeabilities, the product of flux and membrane thickness, may be used as a normalized permeation to characterize the transport rate.

The selectivity of a membrane for the separation of a mixture composed of components i and j is represented by the separation factor, α, which is defined as

$$\alpha=\left(\frac{Y}{1-Y}\right)\left(\frac{1-X}{X}\right) \qquad (2.1)$$

where X and Y are the weight fractions of the more permeable component i in the feed and permeate, respectively. When the separation factor is unity, no

separation occurs; when it approaches infinity, the membrane become perfectly "semi-permeable".It is the membrane selectivity that forms the basis for separating a mixture.

Another alternative parameter used to express the separation characteristic of membrane is the enrichment factor, β, which is defined as

$$\beta_{i,j} = \frac{Y_i}{X_i} \qquad (2.2)$$

In both cases, component i is the preferentially permeating component from the i/j mixture.From the physiochemical point of view, α is more significant term than β, although the β term is more convenient to use when dealing with very dilute feed solutions.

Membrane stability is the ability of a membrane to maintain both the permeability and selectivity under specific system conditions for an extended period of time.Membrane stability is affected by the chemical, mechanical and thermal properties of the membrane. Thus, when considering polymeric membranes for the separation of organic mixtures, the membrane stability is of prime importance.

2.3.2 Selection of Polymer Membrane Materials

In pervaporation, the membrane performance is governed by the

chemical nature as well as the physical structure of the membrane, the physiochemical properties of the liquid mixtures to be separated, and the interactions between the permeant and membrane material. Many commercially available polymers have been investigated as the membrane materials for miscellaneous pervaporation applications.PVA- and PAA-based polymers are the most widely used membrane materials for the dehydration of organic mixtures, silicone-based polymers are useful for the removal of organic compounds from aqueous solutions, and polyacetylene derivatives are being developed as a potential material.However, due to the complicated nature of pervaporation process, a well-established criterion for the selection of membrane materials is not yet available, and the materials for pervaporation membranes are usually selected empirically.Polymers with high selectivity are often preferred for further study because the disadvantage associated with low permeability can be partly compensated by introducing asymmetricity to the membrane structure, thereby reducing the effective thickness of the membrane.On the other hand, recognition of the fact that membrane permeation is governed by both the chemical nature of the membrane material and the physical structure of the membrane facilitates the selection of an appropriate membrane material; theoretical approaches have been developed to predict membrane performance and used as guides for membrane material selection.

Solubility Parameter Approach.According to the solution-diffusion mechanism, the permeation rate and separation factor are dependent on the solubility and diffusivity of components in the membranes.In general, diffusion of small molecules through a dense membrane is favored, and the solubility of a component in a polymeric membrane is governed by the chemical affinity between the permeant and the membrane.When the difference in molecular size of two components to be separated in a mixture is large, permeation through the membrane may be preferential for the smaller molecular size component, although the solubility of the larger molecular size component in the membrane is large.For this reason, many polymers are preferentially permeable to water rather than organic components because water molecules are much smaller than the organic molecules.

Based on the perception that preferential sorption is the prerequisite to the preferential permeation [Mulder *et al.*, 1985], the solubility aspect of pervaporation has been emphasized in the selection of membrane materials.Considering a permeant A and a membrane M, the greater their mutual solubility, the smaller the difference in their solubility parameters Δ_{AM}. Lloyd and Meluch [1985] used the ratio Δ_{AM}/Δ_{BM} as a measure of preferential sorption for the component A and B in the membrane M. Although the ratio Δ_{AM}/Δ_{BM} cannot quantitatively describe the separation property of

pervaporation membrane, it is still convenient to use it as a first estimate in the selection of membrane material.It is suggested that if it is desired to permeate component *B* and reject component *A*, the membrane material should be selected to maximize the ratio Δ_{AM}/Δ_{BM}.

However, there are some restrictions in using the solubility parameter approach to select membrane material for pervaporation.First, this approach is based on the perception that preferential sorption is the prerequisite to selective permeation, but there is no guarantee at all that this is always the case. In fact in some cases the diffusivity contribution is also significant [Deng *et al.*, 1990; Bell *et al.* 1988; Neel *et al.*, 1985].Therefore, this approach may be misleading for the situations where selective diffusion dominates the separation.The other restriction in the solubility parameter approach is the limitations in using solubility parameter itself.Generally, solubility parameter predicts the mixing of solvent and polymer from the properties of pure substances, which means the interactions involved in the ternary system (membrane *M* and permeant *A* and *B*) are not fully considered.Further, the numerical value of solubility parameter is usually obtained by applying group contributions using the numerical values assigned to the various structural groups in the polymer repeat unit; the numerical value of solubility parameter for a given polymer is subject to some indefinite variations depending on the

source of the data involved.

Polarity Parameter Approach. The concept of membrane polarity has also been adopted as a guideline for the development of novel membrane materials. Based on the comparison of membrane polarity in terms of Dimroth's solvent polarity parameter value (E_t at 25°C), Shimizu and Yoshikawa [1991] observed that if the membrane polarity is close to water polarity (63.1 kcal/mol), the membrane tends to be water selective, and the separation factor tends to decrease as the polarity parameter of the membrane deviates from that of water.As no knowledge of precise polymer structure is required, E_t value seems to be useful in the development of novel polymer membranes for the separation of organic-water mixtures. This approach has been shown to be applicable for the so-called "fixed carrier membranes" used for water-ethanol separations, but its validity for other membrane systems has yet to be testified.

Surface Thermodynamics Approach. This particular approach was originally proposed by van Oss *et al.* [1983] and was considered as an alternative method for screening membrane materials by Lee *et al.* [1989].In this approach, two interfacial free energy parameters, ΔF_{123} and ΔF_{132}, are required to interpret the interactions between water (1), organic component (2) and membrane (3).These parameters are calculated using the interfacial

tension values that are available in literature [Nuemann *et al.*, 1974; van Krevelen, 1976]. According to the surface thermodynamics, a negative value of ΔF_{123} implies preferential sorption of organic component into the polymer and a large value of ΔF_{132} suggests good separation of organic component from water in the polymer.When the value of $\Delta F_{132} > 2$, water transport is favored; when the value of $\Delta F_{132} < 2$, organic transport is favored.Also, a large value of ΔF_{123} suggests a strong water-polymer interaction and indicates preferential organic transport, while a small or more negative value indicates preferential water transport.However, this approach is also limited to the same restrictions as discussed in the solubility parameter approach.

Contact Angle Approach. A simplified surface thermodynamics approach was used by Farnand and Noh [1989] to preliminarily evaluate membrane materials for the separation of methanol from C_4 hydrocarbons.This particular method was intended to measure the contact angle , which is a variable in interfacial tension calculation, of methanol with the membrane surface in order to give an approximation determination if the membrane could be used to reject or attract methanol in the separation process. However, it seems that experimental results do not show an obvious relation between the contact angle and the pervaporation performance.

2.3.3 Modifications of Membranes

The feasibility of a membrane process depends largely on the characteristics of the membrane material. In the pervaporation process, it is desirable to have a polymeric membrane with the combined characteristics of high permeation and good selectivity. Since usually a single polymer does not posses the optimum properties for a given separation, new membrane materials are essential and have to be developed to achieve the desired balance of pervaporation properties.Over the years, numerous membrane materials have been developed in order to create a polymer material whose properties correspond to the separation purposes. Most of the work have been focused at balancing the hydrophilicity-hydrophobicity of the polymer materials by incorporating some special groups into the polymer structure.In order to adjust and control the hydrophobic and hydrophilic balance of a polymer membrane, various modification techniques including co-polymerization, polymer blending and crosslinking have been investigated.

Copolymerization. Two or more different monomers can be polymerized to produce polymers that are covalent bonded.In general, the purpose is to blend the properties of each polymer that would occur if each monomer was individually polymerized. One of the monomer units may impart the structural integrity and mechanical property to the polymer chain.The

second monomer unit may interact with the desired component of the feed. (e.g. The monomer and feed component may have similar solubility parameters. The monomer unit may be soluble in one feed component but not in the other component.) Therefore, copolymerization can tailor the polymer to dilute too strong an interaction between feed and membrane that would be detrimental to membrane structural integrity. There are three structural types of copolymers:

i) Random copolymer : the structural units are completely irregularly distributed and its properties are strongly dependent on the ratio of the structural unit;

ii) Block copolymer : each monomer unit is distributed in blocks throughout the polymer chain and because of the miscibility of different oligomer blocks, phase separation might occur;

iii) Graft copolymer : it consists of a regular main chain with irregular distribution of side chains of different monomer blocks. These monomer blocks can be covalently bonded to the main chain by chemical reaction or by irradiation.

Much attention has been directed toward graft polymerization processes as a means of the preparation of pervaporation membranes. By graft copolymerization, much higher permselective layers can be introduced into the separation membrane without dissolution to the solvents [Chapiro, 1988].

In addition to such characteristics, this procedure has the following advantages:

i) the permselective layer composed of graft polymers is chemically bonded to the substrate film, and therefore mechanically stable;

ii) graft polymers can be further modified to improve the permselectivity, e.g., by metal-ionization, coupling, and other chemical reactions without causing faults on the substrates.

Among the methods for the initiation of graft polymerization, irradiation-induced grafting is the most popular and has been applied to improve significantly the membrane performance [Aptel *et al.*, 1972, 1974, 1976; Shantora, 1981; Huang, 1989;]. Plasma graft copolymerization, which is initiated by the surface-specific activation by glow discharge plasmas, is another hopeful means for the preparation of pervaporation membranes [Hirotsu, 1987, 1991; Lee *et al.*, 1992]. As the effects of plasmas are formed generally in a surface-specific manner, and the bulk chemical structure and therefore its properties can be preserved.

Copolymer membranes have been used extensively in pervaporation process for the separation of various liquid mixtures. Among others, acrylonitrile-based [Yoshikawa *et al.*, 1984, 1986a; Shimizu and Okushita, 1988] and PDMS [Okamoto *et al.*, 1987] block copolymer membranes have been investigated for the separation of water-alcohol and cyclohexanone-

cyclohexanol mixtures by pervaporation.Nitrile Butadiene Rubber and Styrene Butadiene Rubber were studied by Brun *et al.* [1985] and Larchet *et al.* [1983] for the removal of benzene and chloroform from water.

Polymer Blending.Polymer properties can also be blended at a molecular level by blending one polymer with another.A mixture of two or more polymers which are not covalently bonded is called a polymer blend.Polymer blending is a convenient technique for studying the influence of the modifications of the membrane nature on its pervaporation characteristics.

In general, two kinds of blends can be distinguished :

i) homogeneous blends, in which the two polymers are miscible on a molecular scale for all compositions;

ii) heterogeneous blends, in which the two polymer are not totally miscible.

The properties of a homogeneous blend differ substantially from those of a heterogeneous blend. The properties of the individual polymers disappear in a homogeneous blend and often the properties of the blend lie between those of the two polymers.Since the homogeneous polymer blends are compatible at the molecular level, the new distinctive polymeric material thus combines the properties of the polymeric components.The properties of both materials are still present in a heterogeneous blend. In this case, heterogeneous blends are

comparable to random copolymers where domains of one polymer within the matrix of the other polymer can be observed. As potential membrane materials, only homogeneous blends are considered because heterogeneous blends will not give enough mechanical strength to the thin membrane.

Two polymers mix homogeneously when the free energy of mixing, ΔG_M is negative.

$$\Delta G_M = \Delta H_M - T\Delta S_M \qquad (2.3)$$

The entropy of mixing, ΔS_M , is very small for polymers, which makes the influence of $T\Delta S_M$ very small too. This means that the enthalpy of mixing, ΔH_M , must be smaller than $T\Delta S_M$ or even negative to produce a homogeneous polymer blend.Specific intermolecular interactions such as hydrogen bonding, are often necessary to ensure compatibility.

Polymer blends represent an attractive low-cost alternative to the synthesis of entirely new macromolecules and in the past decade polymer blend technology has gained increasing interest from both the scientific and industrial communities.Cabasso *et al.* [1974] successfully used cellulose-polyphosphonate alloys for the separation of benzene-cyclohexane mixtures by pervaporation.The similar blend, cellulose acetate-poly(bromophenylene oxide, dimethylphosphonate), was found to be highly selective in the pervaporation of a methanol-hexane mixture [Cabasso and Tran, 1979].

Nguyen *et al.* [1985] reported the first membranes made of non cellulosic polymer blends, (blend of poly(acrylonitrile) and poly(vinylpyrrolidone)), whose properties in pervaporation were similar to that of the equivalent membranes obtained by radiative grafting. Several other polymer blend systems including poly (vinyl alcohol)-poly(ethylene glycol) [Elyassini *et al.*,1987], polyamide-poly(acrylic acid) [Huang, 1987; Zhao, 1990] and poly(vinyl alcohol)-poly(acrylic acid) [Park, 1994] have also been investigated for the pervaporation separation process.

Crosslinking.In general, crosslinking is used to enhance resistance of a polymer material to its environment. In membrane technology, there are two reasons why a polymer is crosslinked. The first reason is to make the polymer insoluble for the feed mixture and the second reason is to decrease the degree of swelling of a polymer to maintain selectivity, especially for hydrophilic polymers such PVA and PAA. A good example is the chemically crosslinked PVA top layer of the GFT composite membranes which show excellent resistant to many solvents.Crosslinking can be achieved by chemical reaction [Huang, 1991a, 1991b, 1993, 1993a] of a compound connecting two polymer chains, by irradiation [Katz, 1982] or by ionization [Huang, 1987; Takegami, 1992a]. The degree of crosslinking is important; too low a level of crosslinking will allow excessive swelling and loss of selectivity, while too high a level of crosslinking reduces flux and may cause brittleness and mechanical failure.

2.3.4 Fabrications of Membranes

The ability of a membrane to regulate permeation lies not only in the selection of an appropriate membrane material, but also in the physical structure of the membrane. The physical structure and the physical properties of a membrane can be directly related to membrane preparation procedures.

Dense Membranes. Dense homogeneous membranes are often used in research work to characterize membrane properties. These membranes can be prepared by melt extrusion, compression moulding or solution casting.Since permeation is inversely related to membrane thickness, the concept of reducing the effective thickness of dense membranes has led to the development of thin asymmetric and composite membranes.In fact, dense homogeneous membranes are rarely used commercially in large scale industrial separation processes because the transmembrane flux is too low for practical applications.

Asymmetric Membranes. Asymmetric membranes consist of a thin, relatively dense layer supported by a porous layer.The advantage of the asymmetric membranes over the homogeneous membrane lies in the extreme thinness of the top skin layer, and thus the ability to achieve high fluxes without any loss in selectivity. Whether the skin layer of a membrane is dense or finely porous often depends on the method of membrane preparation. The

asymmetric membrane prepared from phase inversion process was first introduced by Loeb [1960].Since then, various techniques have been developed to prepare this kind of membranes [Wijmans, 1986]. Kesting [1985] discussed in detail the process variables involved in the procedure for membrane preparation and their effects on the structure of the resulting membranes.Skin layers deposited from solution or plasma onto a porous support are probably homogeneous, while skin layers resulting from phase inversion processes may be finely porous or dense, depending upon casting solution composition, casting conditions and post-formation thermal or chemical treatment. Regardless of the origin or structure, it is the top skin layer which predominantly determine the permeation properties of the membrane.

The top skin layer and the porous support layer may be comprised of the same material. In this case, the asymmetric membrane may be referred to as an integrally skinned asymmetric membrane. Alternatively, the top skin and the support layer may be comprised of different materials. These non-integrally skinned structures are referred to as composite membranes.

Composite Membranes. Two major steps are involved in the preparation of composite membranes: first, casting of the microporous support, followed by deposition of the selective dense layer on the surface of the porous support. One of the advantages of using the composite approach is that different polymers may be used as the barrier layer and the porous

support, which allows a combination of properties that may not be available in a single material.

The key to commercialization of pervaporation has been the development of asymmetric composite membranes.The predominant commercial membranes are generally those from the poly (vinyl alcohol) (PVA) family in asymmetric composites; comprised of a supporting layer of nonwoven porous polyester, on which is cast either a polyacrylonitrile (PAN) or a polysulfone (PS) ultrafiltration membrane, and finally a thin layer of crosslinked poly(vinyl alcohol).Several methods have been developed to prepare composite membranes and were described by Heinzelmann [1991]. However, currently direct casting of polymer solution onto a porous support is the most widely used method for preparing composite membranes. A classic example of composite membranes for pervaporation is the GFT membranes and it is believed that these membranes which are comprised of crosslinked PVA top skin layer and poly(acrylonitrile) (PAN) support, are manufactured by the direct casting technique. In this way, the PVA polymer solution was cast directly onto the PAN microporous support film.

2.4 Polymers for Pervaporation Applications

Pervaporation is potentially applicable to mixtures that are difficult to

separate by more conventional techniques, such as azeotropic mixtures, or mixtures of close-boiling point components.The typical possible applications of pervaporation can be classified into three categories :

i) dehydration of organic solvents,

ii) removal of organic compounds from aqueous solutions,

iii) separation of organic mixtures.

Currently dehydration of solvents, in particular ethanol and isopropanol, is the only process installed on a large scale. However, as technology develops, the other applications are expected to grow.Separation of organic mixtures, in particular, could become a major application.

The key to successful pervaporation lies in the membrane. Selectivity and, to a large extent, flux are essentially controlled by this permselectivity barrier between the feed liquid and the gaseous permeate.In distillation, relative volatilities are indicators of the ease of separation. In pervaporation, by contrast, the flux and selectivity of the permeating species depend on the membrane-sorption and membrane-diffusion properties of the species.Sorption properties can be controlled by choosing the membrane material. The selectivity of pervaporation membranes can vary substantially and has a critical effect on the overall separation obtained. The acetone-selective, silicone rubber membrane is best used to treat dilute acetone feed streams, concentrating most of the acetone in a small volume of permeate.

The water-selective, poly(vinyl alcohol) membrane is best used to treat concentrated acetone feed streams containing only a few percent water. Most of the water is then removed and concentrated in the permeate. Since diffusion through the membrane often is rate-limiting, the transport rate can be controlled by properly choosing the membrane thickness.

2.4.1 Dehydration of Organic Solvents

Today, the most successful application of pervaporation process is the dehydration of aqueous alcoholic solutions. It has been shown that pervaporation is effective for the recovery of alcohols from fermentation broths [Hickey and Slater, 1990; Strathmann and Gudernatsch, 1991] and the removal of hazardous organic compounds from waste water [Boddeker *et al.*, 1990, 1993; Lipski and Cote, 1990; Jian and Pintauro, 1993].

Generally, the membranes used for dehydration are prepared from hydrophilic polymers such as poly(vinyl alcohol) (PVA) and polyacrylic acid (PAA).A number of hydrophilic polymeric materials have been found that exhibit favorable selectivities and fluxes for water. Selection of the proper hydrophillic material such as poly(vinyl alcohol) [Shantora and Huang, 1981; Huang and Jarvis, 1970; Huang and Yeom, 1990], cellulose [Nagy *et al*, 1980], polysaccharide [Mochizuki *et al.*, 1989a; Mochizuki *et al.*, 1989b; Mochizuki *et*

al.,1989c], sulfonated polyethylene [Cabasso *et al.*, 1985], poly-(hydroxymethylene) [Terada *et al.*, 1988], poly(maleimide-co-acrylonitrile) [Yoshikawa *et al.*, 1986a,1986b] and polyion complex consisting of poly(acrylic) and polycation [Karakane *et al.*, 1991; Huang *et al.*, 1988] have been investigated for the dehydration of ethanol mixtures because they provide both mobility and solubility selectivity of water over the larger organic molecule.Many plants have been installed for the dehydration of ethanol by pervaporation. This is a particularly favorable application because ethanol forms an azeotrope with water at 95% and there is a need for a 99.5% pure product. Although most of the installed solvent dehydration systems have been for ethanol dehydration, dehydration of other solvents including isopropanol, glycols, acetone and methylene chloride, has been considered.

Generally, the hydrophilic group containing polymers have high solubility parameters and show relatively large water solubility. However, the introduction of hydrophilic groups sometimes swells the membranes significantly under aqueous mixture due to its plasticization action which results in poor selectivity. Usually, a membrane with high flux gives a low selectivity, and *vice versa*, so that an optimal combination of flux and selectivity should be determined by adjusting and controlling hydrophilic-hydrophobic balance properties of a membrane [Huang and Xu, 1989; Uragami *et al.*, 1990]. In order to control the hydrophilic-hydrophobic balance

properties of a membrane, several techniques have been tried. These include blending a hydrophilic polymer with a hydrophobic polymer, crosslinking a polymer, grafting a selective species onto an inert film , and copolymerization [Mochizuki *et al.*, 1990].

2.4.2 Removal of Organic Compounds from Aqueous Solutions

A number of applications exist for pervaporation in the removal or recovery of organic solvents from water.If the aqueous stream is very dilute, pollution control is the principal economic driving force. However, if the stream contains more than 1-2% solvent, recovery for eventual reuse can significantly enhance the process economics.For the enrichment or removal of organic compounds from their dilute aqueous solutions, the most effective separation is extracting the organic compounds from the bulk solutions; therefore, organophilic or hydrophobic membranes are used.Since the smaller water molecule will diffuse faster through the membrane than the larger organic molecules, the membrane must posses very high affinity to organic compounds to achieve a reasonable permeability.

A number of membranes have been used for the separation of solvents from water and are discussed in the literature [Lee *et al.*, 1987; Nijhuis *et al.*,

1988; Bell, 1988]. Usually the membranes are made from rubbery polymers such as polydimethyl siloxane (PDMS) or silicone rubber, polybutadiene, natural rubber, polyether copolymers and the like [Baker *et al.*, 1991].Silicon-containing polymers generally exhibit good organophilicity and silicon rubber-based membranes mainly PDMS, have been the most investigated materials for the separation of many organic-water mixture systems.Sorption and permeation properties of organic compounds through silicone rubber membranes have been reported by Watson [1990] and Blume [1989].In general selectivities of rubbery membranes can be improved by incorporation of special sorptive materials such as molecular sieve particles into the membrane matrices. Both hydrophobic and hydrophilic zeolites have been investigated and found to increase the selectivity of the membrane in the direction of the sorption selection of the zeolite. Incorporating zeolites into PDMS membrane increased the separation factor without affecting permeation rate [Jia *et al.*, 1992].A number of silicon-containing polymer membranes have been used for the extraction of alcohols from aqueous solutions and are discussed in literature [Nyugen *et al.* 1987; Jopski *et al.*, 1989; Slater *et al.*, 1990; Volkov *et al.*, 1989, 1991].The most promising results so far have been obtained with silicone rubber containing zeolite dispersed particles. It appears that ethanol preferentially permeates through the pores of the zeolite particles [te Hennepe *et al.*, 1987].Non-silicon synthetic

membranes for the separation of dilute organic aqueous solutions have also been reported in recent years [Masuoka *et al*, 1992; Boddeker, 1990, 1990a, 1993; Takegami, 1992, Yoshikawa, 1993; Matsumoto, 1992]. The most investigated materials is the polyetheramide block copolymer (PEBA), used for the extraction of alcohols and aromatic hydrocarbons; the membrane exhibits good selectivity for high boiling bioproducts.

Pervaporation would be more widely applied in solvent recovery operations if membranes more selective for hydrophilic polar solvents were available.Existing materials, such as silicone rubber, have relatively low pervaporation selectivities for this type of solvents. If materials having reasonably high selectivities (in the range 40-50) could be made for solvents such as acetic acid, formic acid, ethanol or methanol, pervaporation could easily compete with distillation or extraction.

2.4.3 Separation of Organic Mixtures

The final application of pervaporation membranes is the separation of organic solvent mixtures. Although widely investigated in the beginning of extensive pervaporation research almost 40 years ago,the separations of organic/organic mixtures represent the least developed and largest potential commercial impact of pervaporation.Historically, the earliest interest in

pervaporation was focused on this type of application [Binning and James, 1958] for benzene/cyclohexane separation.The lack of membranes and modules able to withstand aggressive solvent mixtures under the operating conditions of pervaporation is the key problem hindering the application of pervaporation to organic mixtures.

In this area, only laboratory scale work has been published and as of 1991, no known commercial plant was reported for organic-organic separations.The first pilot plant for organic-organic separation by pervaporation was reported by Air Products [Chen *et al.* 1989] for the removal of methanol from methyl-tert-butyl ether (MTBE) in the production of octane enhancer for fuel blends. The success of this application lies in the high selectivity for the spiral wound cellulose acetate membrane for methanol over MTBE. When aqueous-organic mixtures have to be separated, hydrophilicity or hydrophobicity of a polymer can be used as a guideline in membrane development.In organic-organic separation such a fairly easy concept does not exist. Therefore, screening of polymers can only make use of the concept of solubility parameters, as far as these are known for polymer-organic pairs. The presence of a second organic component, however, may change the solubility parameter of the first component, and *vice versa*,and thus reducing the applicability of the concept. Polyethylene [Wessling *et al*, 1991] and polypropylene [Wytcherley and McCandles, 1992] have been used to separate

aromatic C_8-isomers mixtures such as ethylenebenzene/xylene, *p*-xylene/*o*-xylene and *m*-xylene/*p*-xylene. Sheng [1991] reported the separation of dichloroethane/trichloroethylene using a block copolymer membrane of polyamide and polyether and showed high permeability but low selectivity for dichloroethane. Poly(methyl acrylate) membranes prepared by plasma-graft polymerization were used for the pervaporation of organic liquid mixtures. The membrane possess high permselectivity for benzene/cyclohexane, chloroform/*n*-hexane, methyl acetate/cyclohexane, chloroform/CCl_4, and acetone/CCl_4 mixture.

Current membranes exhibit only marginal performance for most organic/organic separations of industrial interest. Membranes must be custom-designed for specific process objectives. This factor, combined with the large inertia in the chemical industry toward conventional processing with distillation, has retarded the development of applications for organic/organic separations. However, if problems associated with membrane and module stability under the relatively harsh conditions required for these separations can be solved, this could prove to be major membrane application in the future. Ho *et al.* [1996] synthesized hard/soft segment polyimide based copolymer membranes for the separation of aromatic/saturates through high temperature pervaporation separation. They reported that the hard segments

of the membranes provide temperature stability and solvent resistance in aggressive solvents such as *N*-methyl-2-pyrrolidone (NMP) and *N,N*-Dimethyl formamide (DMF).

2.5 Pervaporation Transport Mechanism

In pervaporation, the driving force for transport is generally recognized as a gradient in chemical potential between the liquid and the vapor. The selectivity of the membrane is then the determining factor in the relative flow of the different components. On one hand, because of the complicated penetrants-membrane interactions, it is difficult to formulate a single explanation to the complex transport process. On the other hand, a proper understanding of the membrane separation mechanism may provide direct information for research and development of an appropriate membrane. In order to describe the transport phenomena in pervaporation process, two distinctive approaches have been developed: the solution-diffusion mechanism and the pore flow mechanism.

2.5.1 The Solution-Diffusion Model

Pervaporation through a nonporous membrane can be described by the widely accepted solution - diffusion model [Binning and James, 1958a, 1958b;

Binning *et al.*, 1961; Lee, 1975] . According to this mechanism, pervaporation consists of three successive steps (see Fig. 2-2):

i) sorption of permeant from the feed liquid to the membrane;

ii) diffusion of the permeant in the membrane; and

iii) desorption of the permeant to the vapor phase on the downstream of the membrane.

The solution-diffusion model suggests that, the selectivity and permeation rate are governed by sorption and diffusion of each component of the feed mixture to be separated. In contrast, the desorption is considered to have no major influence on the pervaporation process as long as the permeate pressure is kept low enough, that is below the saturation vapor pressure, and the desorption rate is so fast that the mass transport resistance resulting from it is negligible [Rautenbach and Albrecht, 1985].

Sorption is a thermodynamic property and diffusion is a kinetic property. The sorption process is determined primarily by the chemical nature of the membrane polymer and permeating molecules, and the diffusion is determined by the physical structure of the polymer and the size of the permeating molecules. In the solution-diffusion model, it is assumed that the sorption process is much faster than the diffusion process, thus the former which occurs at the membrane interface can be considered as a thermodynamic equilibrium. For ideal systems, where interactions between

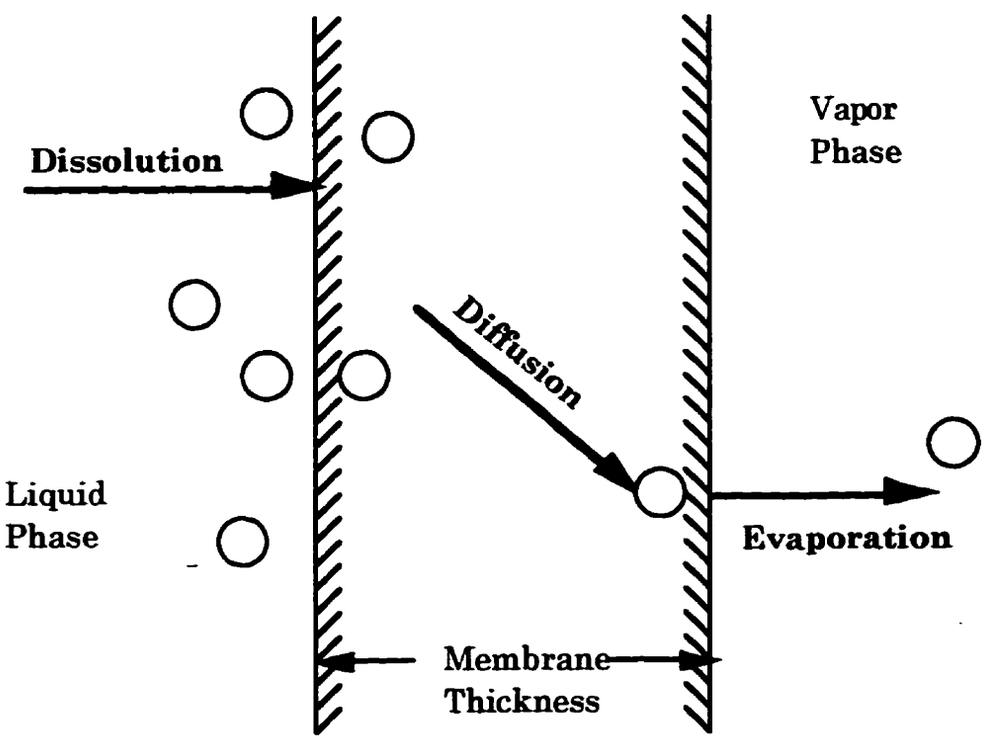


Figure 2.2 The solution-diffusion mechanism.

the solution and polymer are weak, the sorption isotherm is linear and Henry's law is applicable. For non-ideal system such as in pervaporation, where interactions between solution and polymer are strong, the sorption behavior can be described by Flory-Huggins thermodynamics [1953]. However, to simplify pervaporation modelling, most workers [Brun *et al.*, 1985; Greenlaw *et al.*, 1977; Lee, 1975] assumed ideal sorption.

Many attempts have been made to derive relationships for calculating the concentration dependence of diffusivities from molecular models. The most important one is the Fujita's free volume theory [Rautenbach and Albrecht, 1980] which is widely accepted for determining diffusion coefficients, and was adapted for binary mixtures permeation by Fels and Huang [1970, 1971]. More recently, the Fels and Huang model was modified by introducing the permeant-polymer interaction parameters based on the Flory-Huggins thermodynamics [Fels and Huang, 1970a; Mulder *et al.*, 1985; Rhim and Huang, 1989; Huang and Rhim, 1990; Yeom and Huang, 1992] and was able to predict and interpret pervaporation performance for a given system.

Single component permeation through a homogeneous polymeric membrane can be described by Fick's first law (Eq. 2.3) and this equation has been used as the starting point for modelling pervaporation processes by several workers [Merten, 1966; Aptel *et al.*, 1974, 1974a; Greenlaw *et al.*, 1977,

Blume *et al.*, 1990]

$$J_i = -D_i \frac{dC_i}{dx} \tag{2.4}$$

where J_i is the flux of single component i, D_i is the concentration dependent diffusion coefficient of component i in the polymer fixed frame of reference, and dC_i/dx is the concentration gradient across the membrane.

In pervaporation the actual driving force for the permeation of the different components through the membrane is their chemical potential gradient across the membrane. Merten [1966] proposed an equation to relate the diffusive flux to the chemical potential and the equation has been used by several workers [Lee, 1975; Psaume *et al.*, 1988]. In this approach the diffusive flux of a component i through the membrane can be described by the product of concentration, mobility and driving force

$$J_i = -C_i m_i \frac{d\mu_i}{dx} \tag{2.5}$$

where J_i is the flux of component i, C_i is the concentration of component i in the membrane system, m_i is the mobility of component i and $d\mu/dx$ is the chemical potential gradient of component i across the membrane. This equation presents a relationship between non-equilibrium thermodynamics and solution-diffusion model by replacing the phenomenological coefficient

with the terms having a more concrete physical significance.

2.5.2 The Pore Flow Model

The pore flow model to describe transport mechanism in pervaporation was originally proposed by Sourirajan *et al.* [1987] and supported by experimental work conducted by Matsuura and co-workers [Okada and Matsuura, 1991; Okada *et al.*, 1991; Matsuura, 1994]. According to this model, the pervaporation process is regarded as a combination of liquid permeation and vapor permeation in series. It is assumed that there are a bundle of straight cylindrical pores of length δ penetrating across the active surface layer of the membrane perpendicular to the membrane surface. The mass transport by this mechanism consists of three steps: (1) liquid transport from the pore inlet to a liquid-vapor phase boundary, (2) evaporation at the phase boundary, and (3) vapor transport from the boundary to the pore outlet, as shown in Figure 2.3. The distinctive characteristic of the pore flow model is that a liquid-vapor phase boundary exists inside the membrane at a certain distance from the membrane surface. Accordingly, there is a change in the transport mechanism from liquid permeation to vapor permeation at the liquid-vapor phase boundary. Therefore, in order to design an appropriate pervaporation membrane, it is important to locate the position of the phase

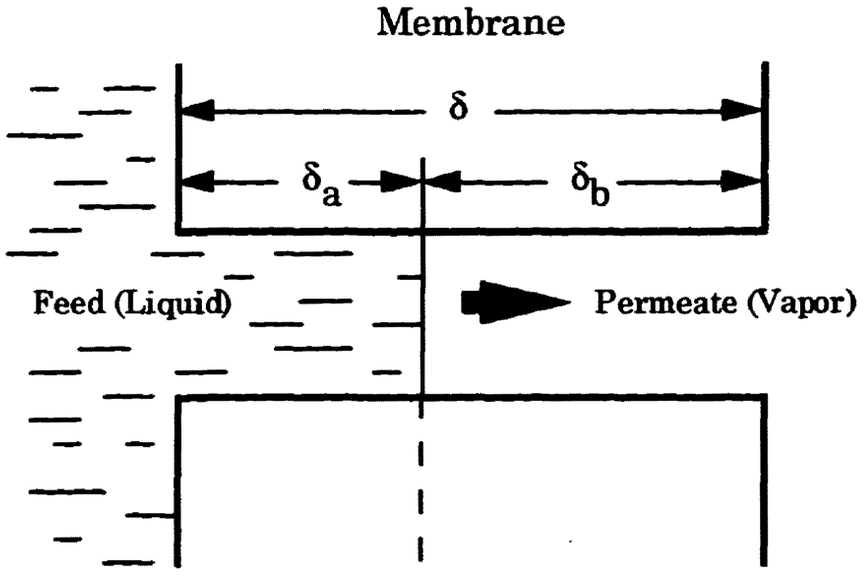


Figure 2.2 The Pore Flow Model

boundary since the selective barrier component of the membrane should be in contact with the vapor phase to take full advantage of its high selectivity. However, it seems rather misleading to say that the pore is filled with "liquid" and with "vapor" and there is a clear boundary separating liquid and vapor phases in the membrane [Matsuura, 1994].

There has been some controversy regarding the existence of pores in pervaporation membranes. The term pore and the nature of the pore as defined in the solution-diffusion model are not exactly the same as they are described in the pore flow model. The pores in the pore flow model are defined as the space between non-bound material entities in the polymer matrix through which mass transfer takes place. Therefore, the equivalent size of such as pore is expressed by any distance (however small) greater than zero [Sourirajan and Matsuura, 1985]. In this case, the pore size of effective pervaporation membranes can be viewed to be as small as those of gas separation membranes. On the other hand, the pores in the solution-diffusion model are defined in terms of dynamic free volume and energy requirements for polymer segmental motion; it depends on the thermally agitated motion of chain segments comprising the polymer matrix to generate penetrant-scale transient gaps in the matrix [Koros and Hellums, 1989].

Clearly, the concept of pore in the solution-diffusion model is different from that perceived in the pore flow model and the two models represent

different approaches to describe the pervaporation process. The solution-diffusion model has been widely accepted to describe the transport mechanism in pervaporation, at the same time, several features of pervaporation observed experimentally could be explained semi-quantitatively by the pore flow model.

2.6 Effects of Process Conditions

The pervaporation process is continually driven by condensation of the permeate, therefore, creating a significant vacuum on the permeate side of the membrane. The transport mechanism is considered to be one of dissolution in the "liquid" or swollen membrane phase and diffusion down the chemical potential gradient, from the upstream to the downstream surface of the membrane. Permeation rate and sometimes selectivity are affected by the feed liquid concentration, feed and/or permeate pressure, and temperature.

2.6.1 Feed Concentration

Changes in feed composition directly affects the sorption phenomena of the liquid-membrane interface. Because the diffusion of the components in the membrane is dependent on the concentration of the components, the permeation characteristics are obviously dependent on the feed concentration.

In addition, the effects of coupling, membrane swelling or shrinking, and the concentration polarization, which result from the change of feed concentration, all play important role in pervaporation process [Psaume *et al.*, 1988]. Pervaporation process is more highly concentration - dependent than other membrane separation processes.

2.5.2 Feed and Permeate Pressures

For pervaporation, the driving force for mass transport is the difference in chemical potential across the membrane. Since the chemical potential is not significantly influenced by liquid pressure, the feed pressure shows relatively small effects on the pervaporation performance. The main contribution to the driving force is the activity gradient of the components in the membrane. Because the permeate pressure is directly related to the activity of the components at the permeate side of the membrane, the permeate pressure has a strong influence on the pervaporation performance. Since the maximum driving force is obtained at zero permeate pressure, an increase in the permeate pressure results in a decrease in driving force, and thus decreases permeation rate. When the permeate pressure reaches the saturation pressure of the permeate, the activity gradient reduces to its minimum, leading to a steep decrease in permeation rate. This was described

mathematically and confirmed experimentally [Greenlaw *et al.*, 1977; Shelden and Thompson, 1978, 1984; Neel *et al.*, 1980; Knight *et al.*, 1986; Duggal and Thompson, 1986]. The selectivity can increase or decrease with increasing permeate pressure, depending on the relative volatility of the permeating component.

2.5.3 Temperature

Since the solubility and diffusivity of permeant in the membrane are generally dependent on the operating temperature, pervaporation performance characteristics in terms of permeation rate are also dependent on the temperature. When the feed temperature increases, the permeation rate generally follows an Arrhenius-type equation [Huang and Jarvis, 1970; Cabasso *et al.*, 1974], as

$$J = J_0 exp(E_p / RT) \qquad (2.6)$$

The value of the apparent "activation energy", E_p, of permeation varies usually in the range of 15 - 65 *KJ/mol*. The permeation rates may increase many times for each 10 °C temperature increment. Also since diffusion rates in membrane increase with increasing temperature, permeation rates also increase with increasing temperature. The selectivity is not so strongly dependent on the temperature, in most cases a small decrease of selectivity is

found at increasing temperature [Aptel *et al.*, 1974; Cabasso *et al.*, 1974; Carter, 1964]; in fact, a higher selectivity has been reported [Fels and Huang, 1971; Carter, 1964].

CHAPTER 3

Pervaporation Properties of Chitosan Membranes[1]

3.1 Introduction

In general, membranes used for research and development (R & D) in pervaporation separation processes are dense homogeneous thin films and mostly are prepared by means of the solvent casting technique. Pervaporation polymer membranes used for dehydration of aqueous alcohol solutions should be highly water permselective. Since the size of water molecules is smaller than that of organic molecules, the diffusion of water molecules through a dense membrane is faster than that of organic molecules although the

---

[1]Portions of this chapter have been published in *J. Memb. Sci.*, 124,53 (1997)

solubility is higher for the organic molecules. For this reason, many polymers are preferentially permeable to water rather than to organic components. However, it is better to use hydrophilic polymers as membrane materials in order to get a high water/organic separation factor for a pervaporation dehydration process.

3.1.1 Chitosan (CS) Membranes

Chitosan, a natural, non-toxic, biodegradable, high molecular weight polymer, is the name used for low acetyl forms of chitin and is composed primarily of glucosamine, 2-amino-2-deoxy-D-glucose (see Figure 3.1) [Charles, 1984]. Chitin is the second most abundant natural biopolymer, cellulose being the most abundant. The most easily exploited sources of chitin are the protective shells of crustaceans such as crabs and shrimp.

Chitosan, because of the amino group in its repeating units, undergoes reactions typical of amines. When in the free amine form, chitosan is not soluble in water at neutral pH's, but at acidic pH's, the free amino groups ($-NH_2$) become protonated to form cationic amine groups ($-NH_3$). Thus, in general chitosan is not soluble in water and in organic solvents; however, in the presence of a limited amount of acid, it is soluble in water-methanol, water-ethanol, water-acetone and other mixtures [Muzzarelli, 1977]. Owing to

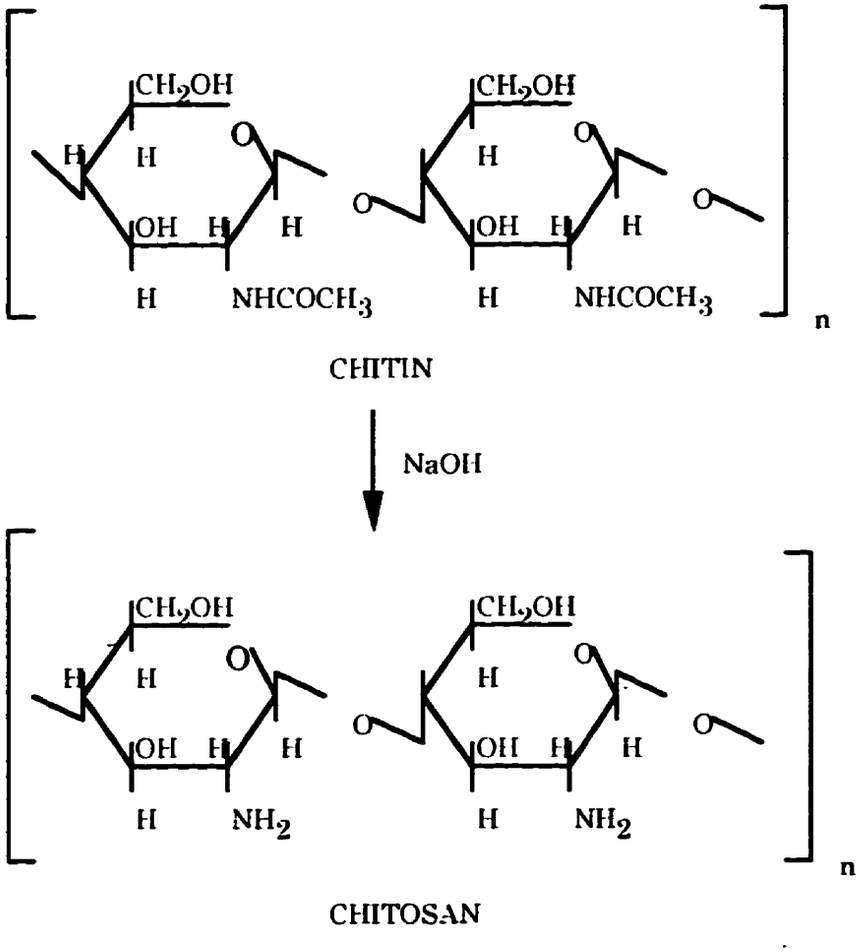


Figure 3.1 The deacetylation of chitin to chitosan .

its high solubility to formic or acetic acid, chitosan is apt for the preparation of a membrane; therefore a chelating membrane becomes feasible on the basis of the film-forming ability and of the chelating properties of chitosan. Chitosan has been studied as membranes [Yang and Zall, 1984; Mochizuki *et al.*, 1989 a,b,c, 1990 a,b] because of its good film forming properties, highly hydrophilic, and good chemical resistant properties.

3.2 Theoretical

Mass transfer through dense solvent cast membranes is usually described by the solution-diffusion model although alternative approaches have been developed [Neel, 1991; Huang and Rhim; 1991; Okada and Matsuura, 1991; Matsuura, 1994]. It is widely accepted that sorption and diffusion govern the permeability and selectivity. The applicability of the solution-diffusion model has been reported by several researchers, assuming an ideal sorption and a concentration dependent diffusion. However, the assumption of ideal sorption has been experimentally proven not to be the case normally, i.e, the concentration of a component in the membrane is not proportional to its concentration in the bulk solution [Deng *et al.*, 1990; Masuda *et al.*, 1990; Mulder and Smolders, 1986]. This means that one of the components is preferentially sorbed by the membrane. In general, hydrophilic

membranes tend to sorb hydrophilic components, however, in some hydrophobic polymers, pure water is hardly sorbed, whereas in the presence of ethanol, water is sorbed preferentially [Mulder *et al.*, 1985].

For the pervaporation of a binary mixture, there is usually no linear relationship between the permeation flux and its concentration in the feed mixture. The presence of one component may have significant influence on the permeation of the other. This effect is often addressed as the coupling effect, which can be further broken down into two factors: the plasticizing effect (the free volume factor) and the interaction factor [Huang and Lin, 1968; Brun *et al.*, 1985]. The presence of one component in the membrane, more or less, plasticizes the polymer, which is equivalent to increasing the free volume. This plasticization may or may not enhance the sorption and diffusion of the other component, depending on the interaction between the feed components and the membrane. The interaction between the two components, especially when polar groups are present in the molecules, usually results in the formation of larger molecular clusters, so as to cause deviation from the ideal permeation. If either of these effects exists, the actual permeation of one component during pervaporation may not be proportional to its concentration in the feed mixture.

Defining an ideal permeation as that permeation in which permeation flux of a component is proportional to its feed concentration, Huang and Lin

[1968] introduced the permeation ratio, to measure deviation of the actual permeation flux from the ideal one,

$$\theta_i = \frac{J_i}{X_i J_i^o} \tag{3.1}$$

where θ is the permeation ratio, J and J^o are the partial flux in mixture permeation and the permeation flux of pure component, respectively; X is the weight fraction in the feed mixture; and subscripts i represents component i.When $\theta_i > 1$, the permeation of component i is enhanced by the presence of the other component; when $\theta_i < 1$, the permeation of component i is retarded by the other component.

Analogous to the permeation ratio defined by eqn. (3.1), a sorption ratio is used to characterize the non-ideal sorption of a binary liquid mixture in the polymer membranes,

$$\phi_i = \frac{Q_i}{X_i Q_i^o} \tag{3.2}$$

where ϕ_i is the sorption ratio of component i and Q^o and Q are the amount of component i sorbed from the pure and mixed solutions, respectively, per unit weight of polymer membrane. When $\phi_i > 1$, the sorption of component i is increased by the presence of the other component, when $\phi_i < 1$, the sorption of

component i is reduced by the other component. When $\phi_i = 1$, the two components sorb onto the polymer membrane independently, i.e., an ideal sorption occurs.

According to the solution-diffusion model, when the permeate pressure is very small, then the permeation selectivity α, is the product of sorption and diffusion selectivities,

$$\alpha = \alpha_S \times \alpha_D \tag{3.3}$$

where α_D is the diffusion selectivity and α_S is the sorption selectivity. As a first approximation the sorption selectivity may be defined as,

$$\alpha_s = \left(\frac{X_p}{1-X_p}\right)\left(\frac{1-X}{X}\right) \tag{3.4}$$

where X_p represents the weight fraction of component i in the polymer sorbed phase. It is obvious that if component i is preferentially sorbed, then $\alpha_S > 1$.

From eqn. (3.3), the selective diffusion can be interpreted as the ratio of permeation selectivity and sorption selectivity. Combining this definition with the definitions of the selectivities in eqns. (2.1) and (3.4) results in,

$$\alpha_D = \frac{\alpha}{\alpha_S} = \left(\frac{Y}{1-Y}\right)\left(\frac{1-X_p}{X_p}\right) \tag{3.5}$$

If Fick's first law is applicable to the diffusion, and equilibrium and isotherm conditions are assumed, the following expression has been obtained by Spitzen [1988],

$$\alpha_D = \frac{D_i}{D_j} \tag{3.6}$$

which indicates that the diffusion selectivity measures the difference in the diffusion coefficients D, of the permeates i and j.

3.3 Experimental

3.3.1 Materials

Chitosan polymer (MW : 50,000 - 100,000) was generously donated by Kyowa Tecnos Co. Ltd., Japan. Reagent grade acetic acid was purchased from Canlab. The isopropanol-water mixtures used for the pervaporation tests were prepared by mixing known quantities of isopropanol purchased from Commercial Alcohols Inc. in Toronto and deionized water.

3.3.2 Preparation of Homogeneous Chitosan Membranes

The preparation of the homogeneous chitosan membrane involved a sequence of procedures as shown in Figure 3.2. A preweighed chitosan was

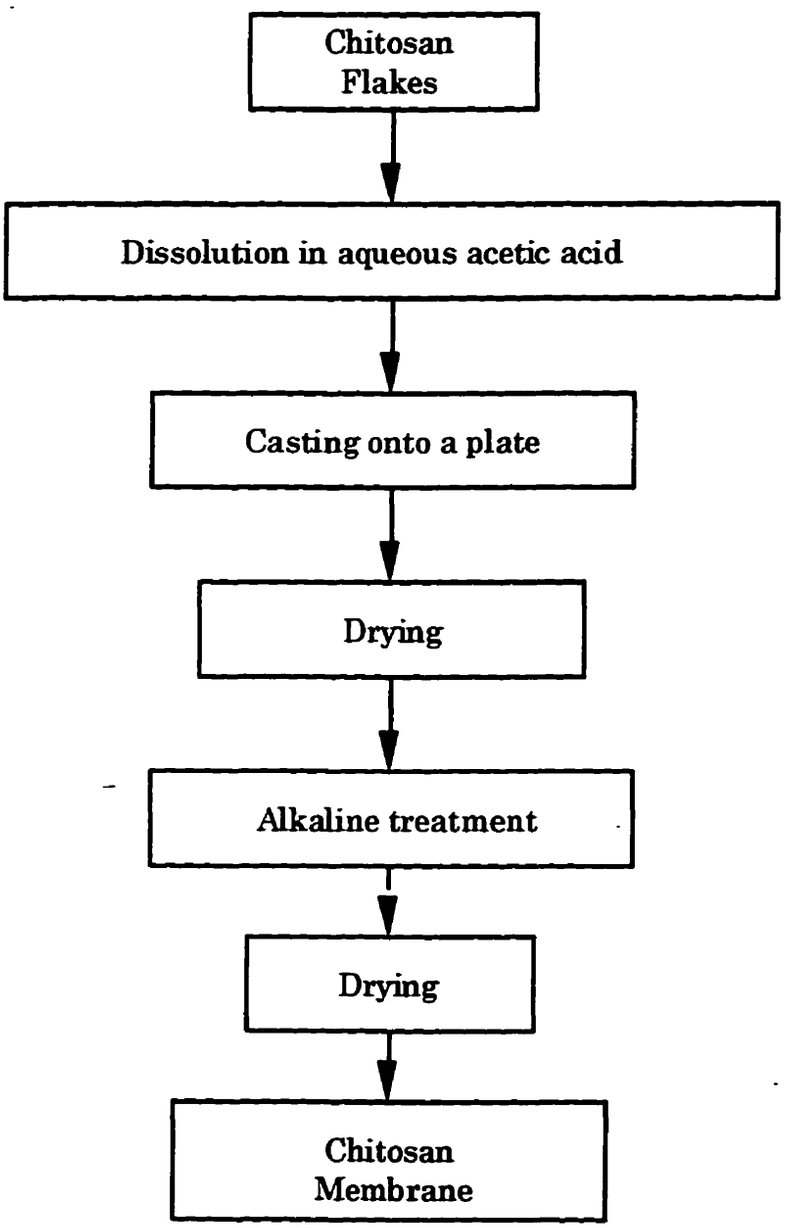


Figure 3.2 Sequence of preparation of homogeneous chitosan membrane

first dissolved in 10 wt. % aqueous acetic acid solution at room temperature for 24 hours to produce a casting solution consisting of 1 wt. % of chitosan. The polymer solution was filtered to remove impurities and undissolved chitosan to produce a clear homogeneous casting solution. The resulting casting solution was cast onto a PVC plate with the aid of a Gardner casting knife, allowing the casting solvent to evaporate at room temperature for 24 hours. The formed membranes were peeled off from the plate, treated in 3 wt. % NaOH solution containing 50 wt. % isopropanol for 24 hours at room temperature, washed thoroughly with deionized water to completely remove NaOH and dried at room temperature under vacuum. The thickness of the dried chitosan membrane was 20 - 30 μm.

3.3.3 Pervaporation Experiments

The experiments were carried out using the pervaporation unit as shown in Figure 3.3, which is a continuously feeding type. The pervaporation experiments were performed by employing two stainless steel pervaporation cells (Fig. 3.4).The feed mixture enters the cell through the inlet opening , flows through the thin channel and leaves the cell through the outlet opening on the opposite side,which allows relatively higher fluid velocity parallel to the membrane surface. The effective membrane area in each cell is 14.2 cm^2.

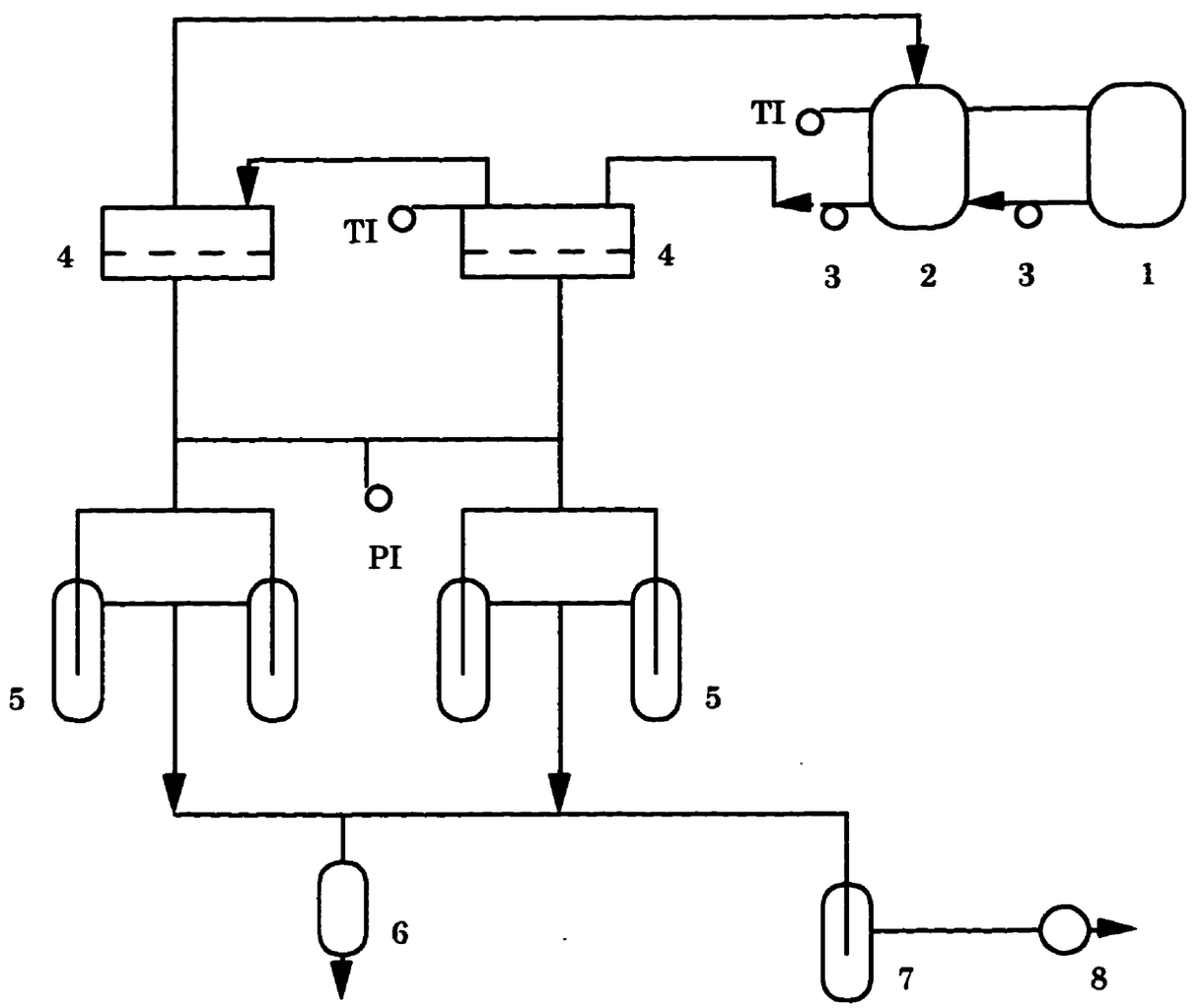


Figure 3.3 A schematic diagram of the pervaporation separation apparatus. (1) water bath; (2) feed tank; (3) circulation pump; (4) membrane cells; (5) permeant collection traps; (6) vent to atmosphere; (7) cold trap; (8) vacuum pump, and TI: Temperature indicator, PI: Pressure indicator.

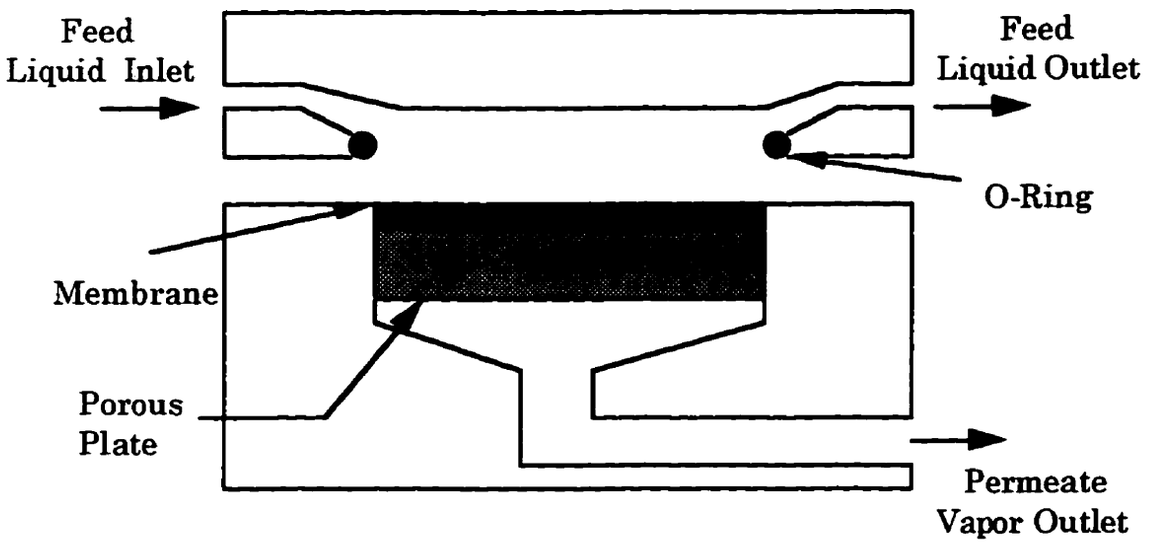


Figure 3.4 A schematic diagram of the pervaporation cell structure.

The glass feed tank has a feed solution capacity of approximately 1000 ml. From the feed tank, which was kept constant at a desired temperature, the feed mixture was circulated through the cells by a circulation pump. The pressure at the downstream side was maintained at approximately 3 mm Hg by using a Welch duo-seal vacuum pump. Each pervaporation process was run for at least two hours to reach the steady state before the collection of permeant. The permeant was collected in one of the glass traps which were immersed in liquid nitrogen. The permeant was warmed up to ambient temperature, removed, weighed and analyzed for permeate composition.

The analysis of the permeate compositions was conducted by using a Hewlett Packard 5890 Series II gas chromatography equipped with a 6' x 0.125"-column packed with Porapak T 80/100 mesh. Flame Ionization Detector (FID) was used and the oven and injection temperatures were kept constant at 150 °C and 200 °C, respectively. Helium was used as the carrier gas with a flow rate of 20 ml/min. An adjustable 10 μl-syringe was used to inject a fixed volume of liquid permeates.

3.3.4 Liquid Sorption Experiment

The predried membranes were immersed in a liquid sorbate of known composition of water/isopropanol mixtures in closed bottles at room

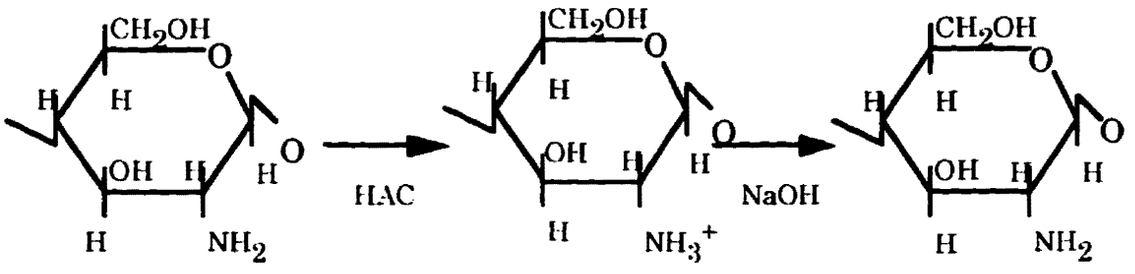
temperature for 48 hours. The swollen membranes were removed, pressed between Kimwipes tissue papers, and weighed immediately.

The membrane was then placed in a dry container that was connected to a cold trap followed by a vacuum pump. The liquid sorbed by the membrane was thus desorbed under vacuum for up to 4 hours and collected in the trap. The collected liquid was then weighed and analyzed for composition by using the gas chromatography unit used in the pervaporation experiments. The same vacuum and trapping system as used in the pervaporation (see Figure 3.3) was used for the sorption measurements. The total of amount of liquid sorbed by the membrane was determined from the sorption uptake, and the sorption data so obtained was ensured by weighing the liquid collected in the cold trap during desorption.

3.4 Results and Discussion

3.4.1 Fabrication of Chitosan Membranes

Chitosan, being a high molecular weight polymer, is a linear polyamine whose amino groups are readily available for chemical reactions and salt formation with acids. Figure 3.5 shows the chemical reactions involved in the production of chitosan membrane by dissolving chitosan flakes in acetic acid aqueous solution and followed by neutralizing the chitosan salt with sodium



Chitosan **Chitosan salt** **Chitosan**

Figure 3.5 Fabricating chitosan membrane.

hydroxide solution.

3.4.2 Liquid Sorption

Figure 3.6 shows the results of the liquid sorption experiments. At low concentration of isopropanol in the bulk liquid, the sorption of isopropanol in the chitosan membrane increases with an increase in isopropanol concentration. At isopropanol weight fractions in the liquid higher than 0.30, the isopropanol sorption decreases slightly to a minimum at an isopropanol weight fraction about 0.70, then increases again. While the water sorption decreases gradually with an increase in isopropanol concentration in the liquid feed. It is observed that the water uptake is higher than the isopropanol uptake especially at low isopropanol concentration in the bulk liquid, suggesting different degrees of polymer-permeant interaction for the two components. Being relatively hydrophilic, chitosan is significantly swollen in water and the presence of isopropanol reduces the relative degree of swelling of the membrane.As a result, the total sorption of the isopropanol/water mixtures reaches a maximum at an isopropanol weight fraction of about 0.10.

The sorption ratio is shown in Figure 3.7. At low isopropanol content in the bulk liquid, a sorption greater than unity is observed for both components in the binary mixture, indicating positive deviation from ideal sorption. The

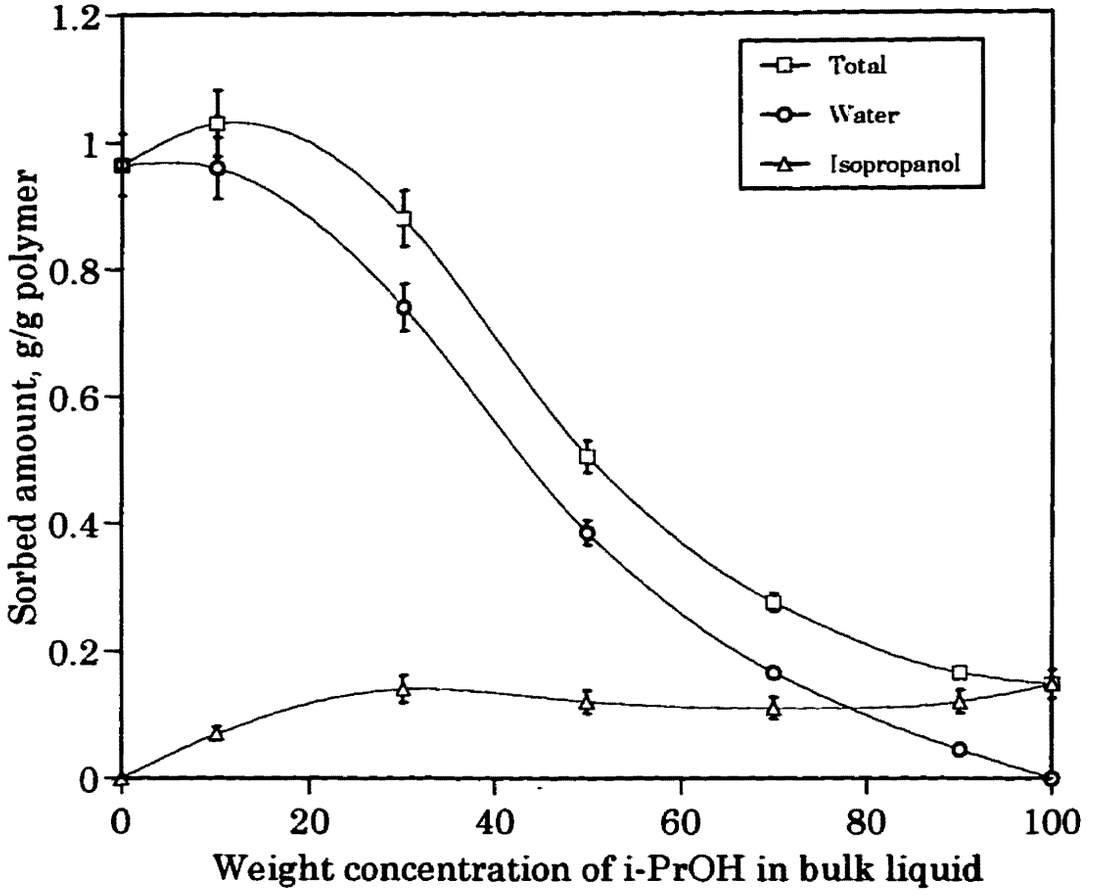


Figure 3.6 **Sorption data for isopropanol/water mixtures in chitosan membrane. Temperature 30 °C.**

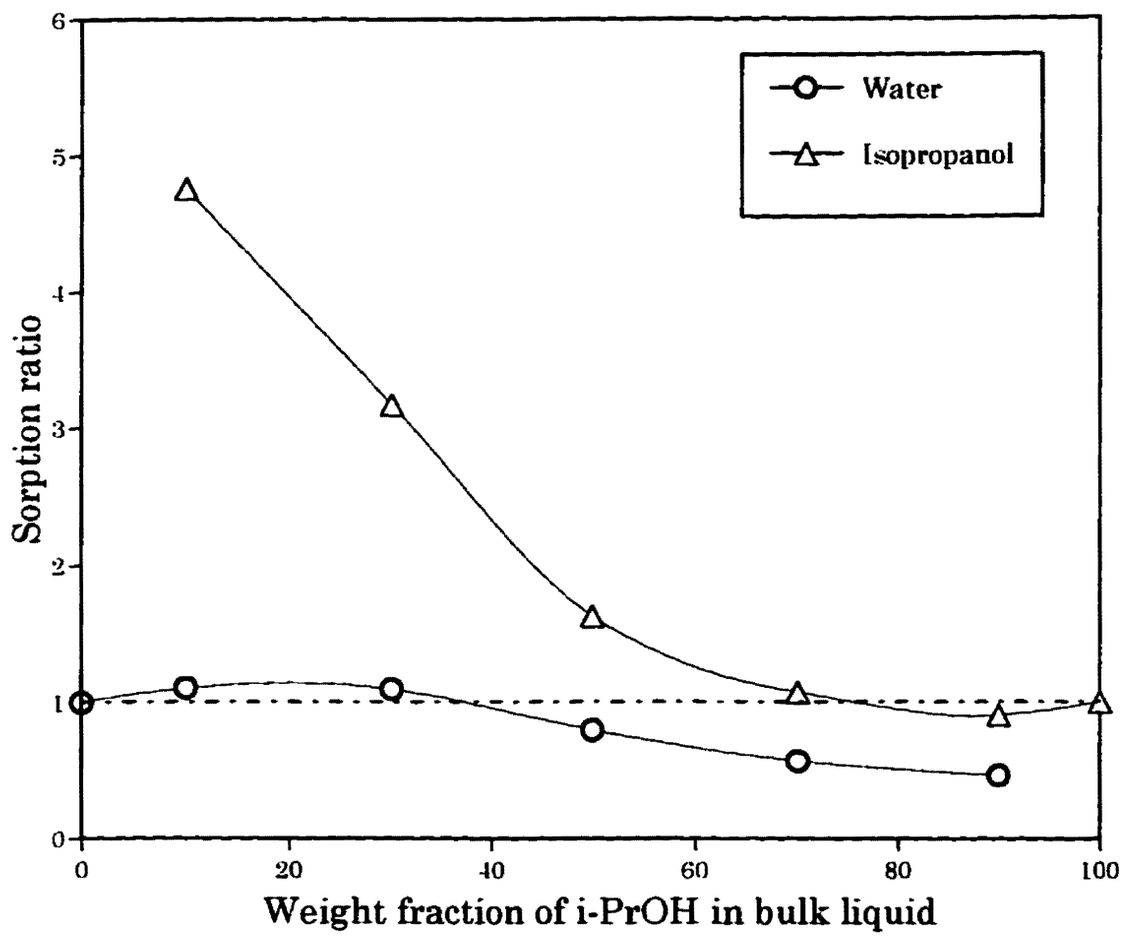


Figure 3.7 Sorption ratio versus liquid composition. Temperature 30 °C.

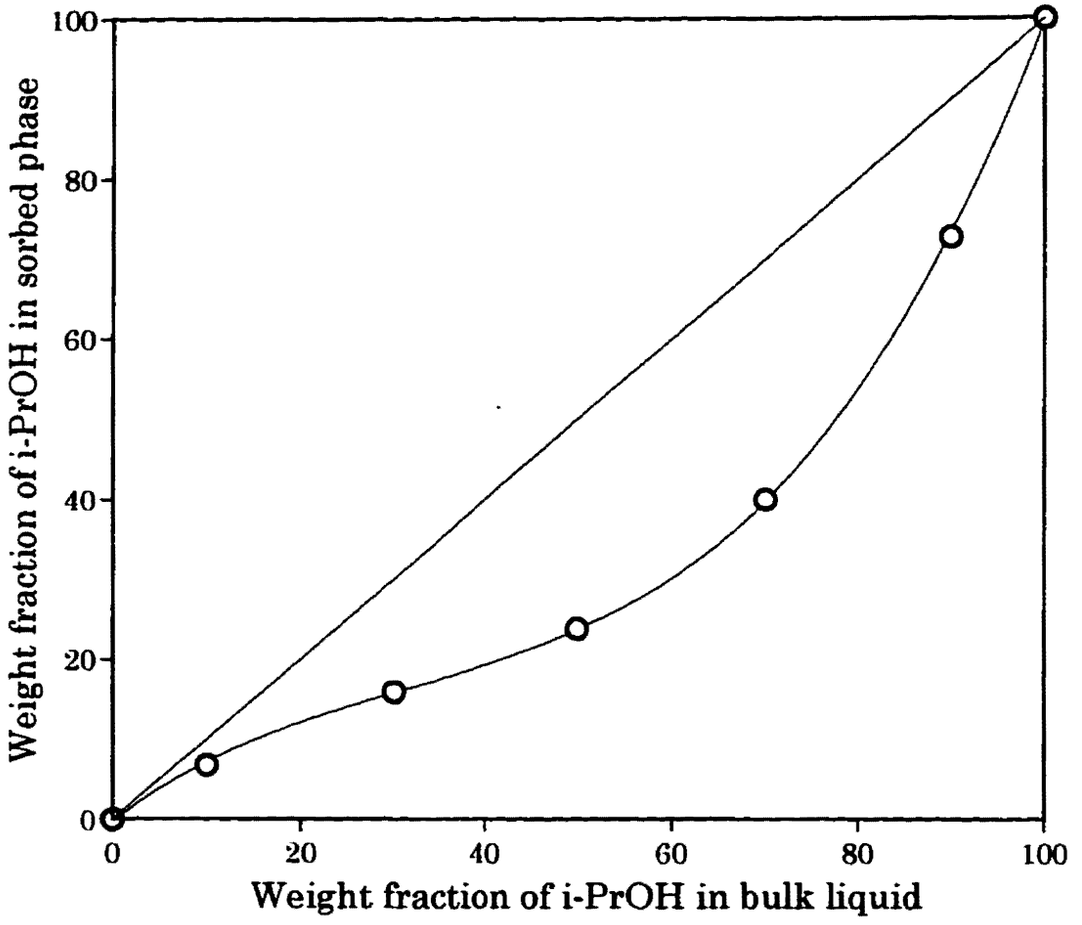


Figure 3.8 **Weight fraction of isopropanol in membrane sorbed phase vs weight fraction of isopropanol in bulk liquid phase. Temperature 30 °C.**

sorption of one component increases with the addition of the other component; the two components enhance each other with respect to their sorption due to polymer-permeant and permeant-permeant interactions. The isopropanol sorption ratio is well above unity especially at very low weight fraction of isopropanol in the bulk solution, suggesting that the sorption of isopropanol to the chitosan membrane is greatly enhanced by the presence of water. However, when isopropanol weight fraction is higher than 0.70, both the components show negative deviation from ideal sorption; the presence of one component decreases the sorption of the other component.

The weight fraction of isopropanol in the membrane sorbed phase versus the weight fraction of isopropanol in the bulk liquid is plotted in Figure 3.8. For the entire range of compositions of isopropanol/water in the bulk solution, water is sorbed preferentially; the water component is enriched in the membrane sorbed phase.

3.4.3 Pervaporation

The total and partial permeation fluxes for the binary isopropanol/water mixtures at 30 °C and at a permeate pressure of 3 mm Hg are plotted in Figure 3.9. As the concentration of isopropanol in the feed increases, isopropanol flux increases to a maximum, then decreases, while

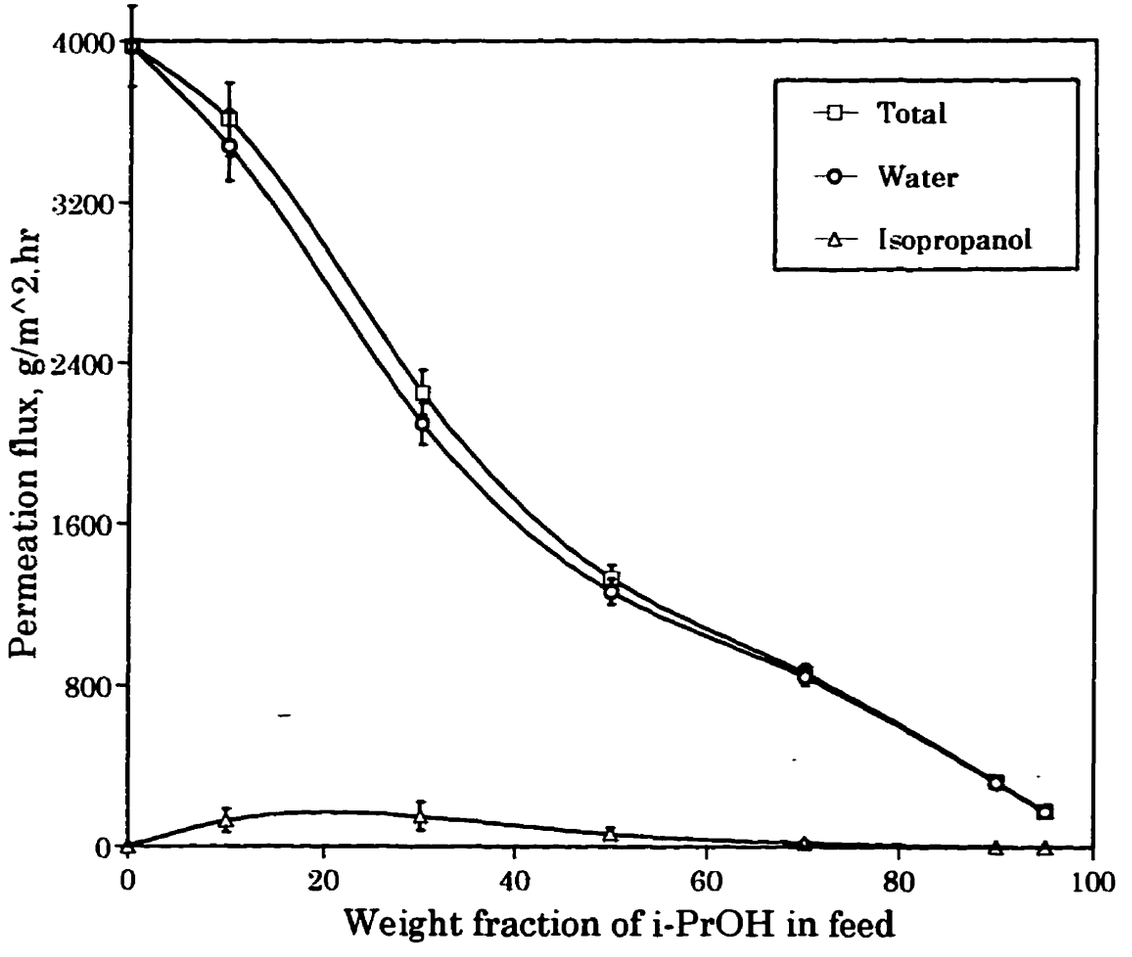


Figure 3.9 The total and partial permeation fluxes versus feed concentration. Temperature 30 °C.

water flux decreases more significantly, resulting in a decrease in the total flux of the binary mixture of isopropanol/water. It should be noted that for the whole range of feed composition the water flux is almost identical to the total flux and the isopropanol flux reaches a maximum at an isopropanol feed concentration about 0.20 corresponding to the maximum isopropanol sorption. Owing to high hydrophilicity of the chitosan material, the chitosan membranes swell more significantly in the solution with high water content. As the water concentration in the feed increases, the amorphous regions of the membrane are more swollen, and the polymer chains become more flexible and increase the space available for diffusion, thus decreasing the energy required for diffusive transport the membrane. As a result, the water flux increases with an increase in water concentration in the feed.

The permeation ratio as a function of feed isopropanol concentration is shown in Figure 3.10. At low isopropanol concentration, the isopropanol permeation ratio is well above unity, indicating positive deviation from ideal permeation, corresponding to the positive deviation from ideal sorption. At isopropanol feed concentration higher than 0.50, the isopropanol permeation ratio decreases below unity suggesting negative deviation from ideal permeation. On the other hand, the water permeation deviates from ideal behavior negatively for the whole feed isopropanol concentration, indicating the water permeation is impaired by the presence of isopropanol in the feed

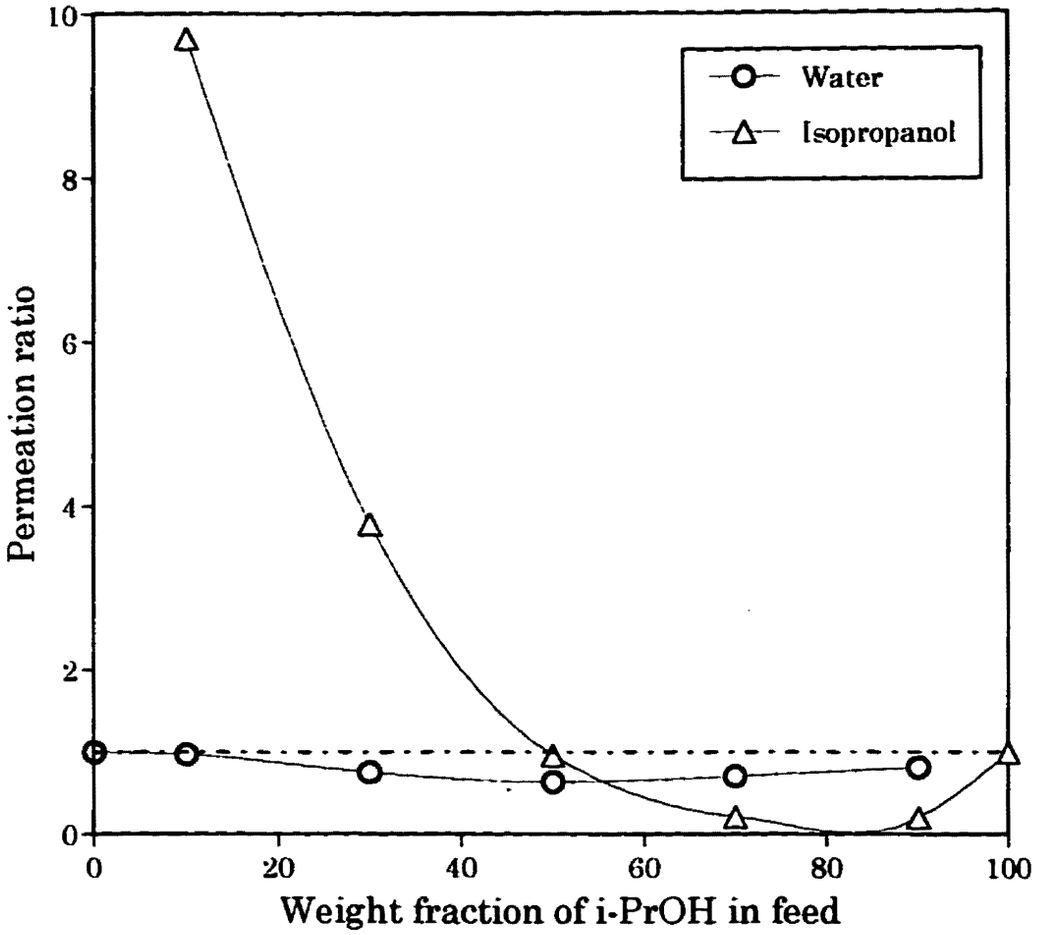


Figure 3.10 Permeation ratio versus feed concentration. Temperature 30 °C.

mixture.

Figure 3.11 shows the corresponding data for weight fraction of isopropanol in the permeate versus the weight fraction of isopropanol in the feed solution. Over the whole range of composition of isopropanol/water feed mixtures, the water component is enriched in the membrane permeated product, indicating that water was preferentially permeated. The stronger affinity of chitosan to water and the fact that molecular size of water is relatively smaller than that of isopropanol make the chitosan membrane more selective to water.

3.4.4 Sorption versus Diffusion

It is well known that, if the transport through a pervaporation membrane follows the solution-diffusion mechanism, preferential sorption usually leads to preferential permeation. This is also the case for pervaporation dehydration of isopropanol/water mixtures with chitosan membranes. As can be seen from Fig. 3.8 and 3.11, water is preferentially sorbed and permeated over the entire concentration range, i.e., the chitosan membrane is selective to water. Fig. 3.12 shows the individual permeation and sorption for the isopropanol component as a function of isopropanol weight fraction in feed solution. As can be seen, both the permeation and the

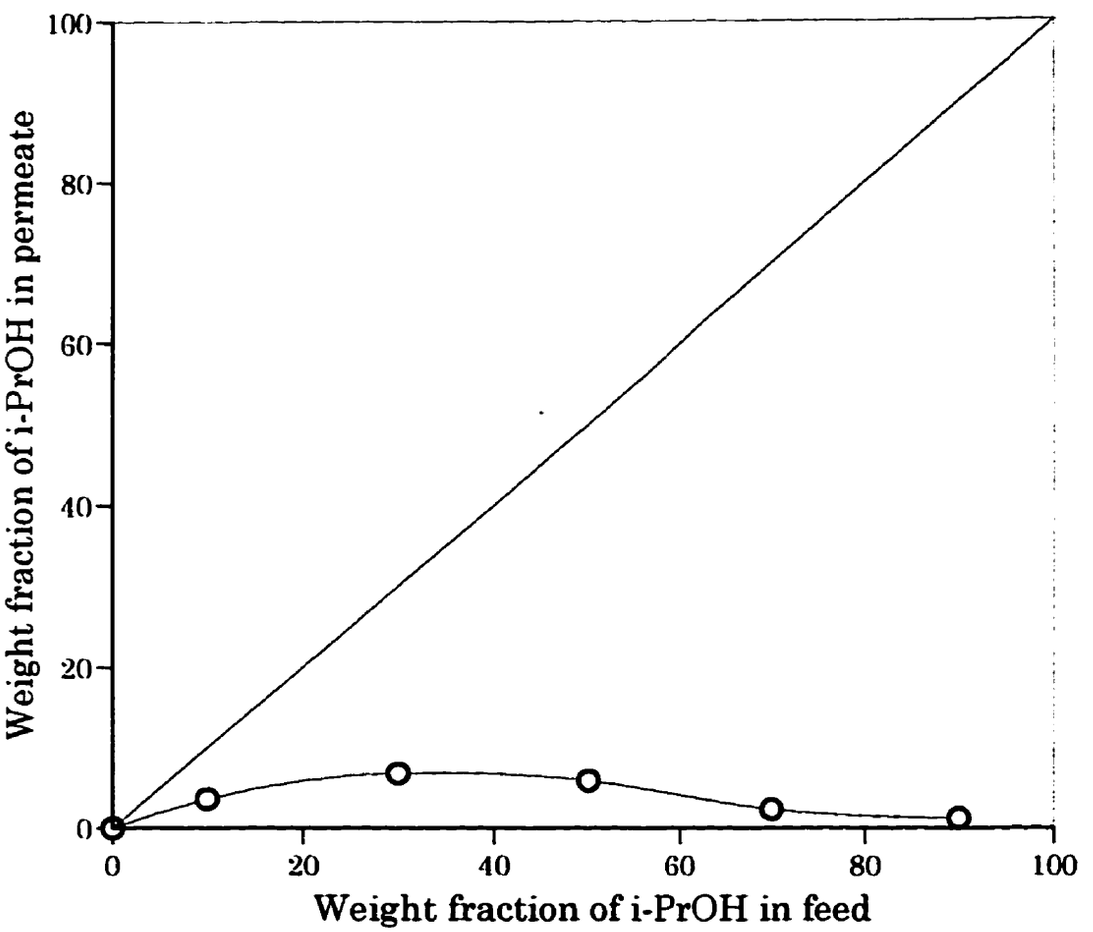


Figure 3.11 Weight fraction of isopropanol in the permeate versus weight fraction of isopropanol in liquid feed. Temperature 30 °C.

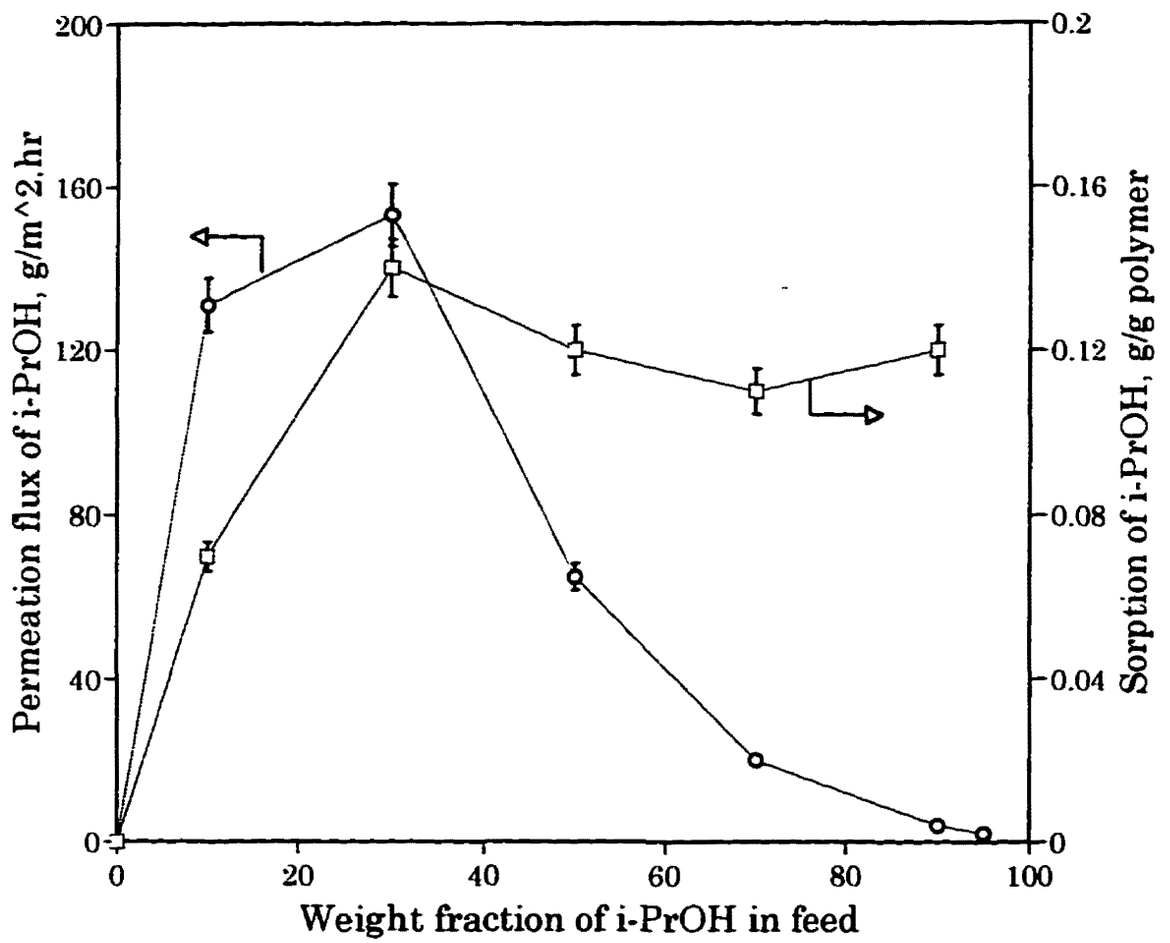


Figure 3.12 Partial permeation and sorption of isopropanol versus weight fraction of isopropanol in feed.

sorption of isopropanol reach a maximum at an isopropanol weight fraction in the feed about 0.30. The maxima in the isopropanol flux in this figure can be attributed to two effects: decrease of swelling at increased isopropanol feed concentration; decrease of water flux at increased isopropanol concentration. The latter effect reduces the friction between water molecules and isopropanol molecules in the membrane and so the "drift" transport of isopropanol or the transport of isopropanol caused by the transport of water, is reduced.

By comparing Figures 3.10 and 3.7, it can be seen that both the permeation ratio and the sorption ratio for isopropanol change with an increase in feed isopropanol concentration and the permeation and the sorption of isopropanol deviate from the ideal behaviors in a relatively similar pattern; positively at low isopropanol concentration and negatively at high isopropanol concentration. On the other hand, the deviation of the permeation ratio for the water component is relatively different from the deviation of its sorption ratio. These observations may be attributed to the fact that the feed concentration affects the mobilities of different permeating components to a different degree, as is generally observed [Sferazza *et al.*, 1988; Camera-Roda *et al.*, 1991]. Figures 3.10 and 3.7 also suggest that both the sorption and permeation for the isopropanol component are greatly

enhanced by the presence of the water component in the solution, especially at low concentration of isopropanol, and the reverse situation is observed for the water component. At high isopropanol weight fraction, the permeation and sorption for the water component are impaired by the presence of the isopropanol. Figure 3.8 and 3.11 show that the water component is enriched in both the membrane sorbed phase and in the membrane permeated product over the entire range of composition of isopropanol/water feed mixtures. This means that preferential sorption does give rise to preferential permeation for the chitosan membrane.

Figure 3.13 shows the separation factor as a function of feed isopropanol concentration. For comparison, the sorption selectivity is also presented in Figure 3.13. As can be seen, both the separation factor and sorption selectivity increase with an increase in the concentration of isopropanol in the feed. For a given feed concentration, the separation factor of pervaporation is significantly higher than the sorption selectivity, indicating that water molecules are more mobile in the membrane than isopropanol molecules. This is obvious because the water molecule is smaller than the isopropanol molecules. It should be noted that based on the definition of diffusion selectivity as described in eqn. (3.5), Figure 3.13 indicates that the diffusion selectivity α_D values are much greater than the

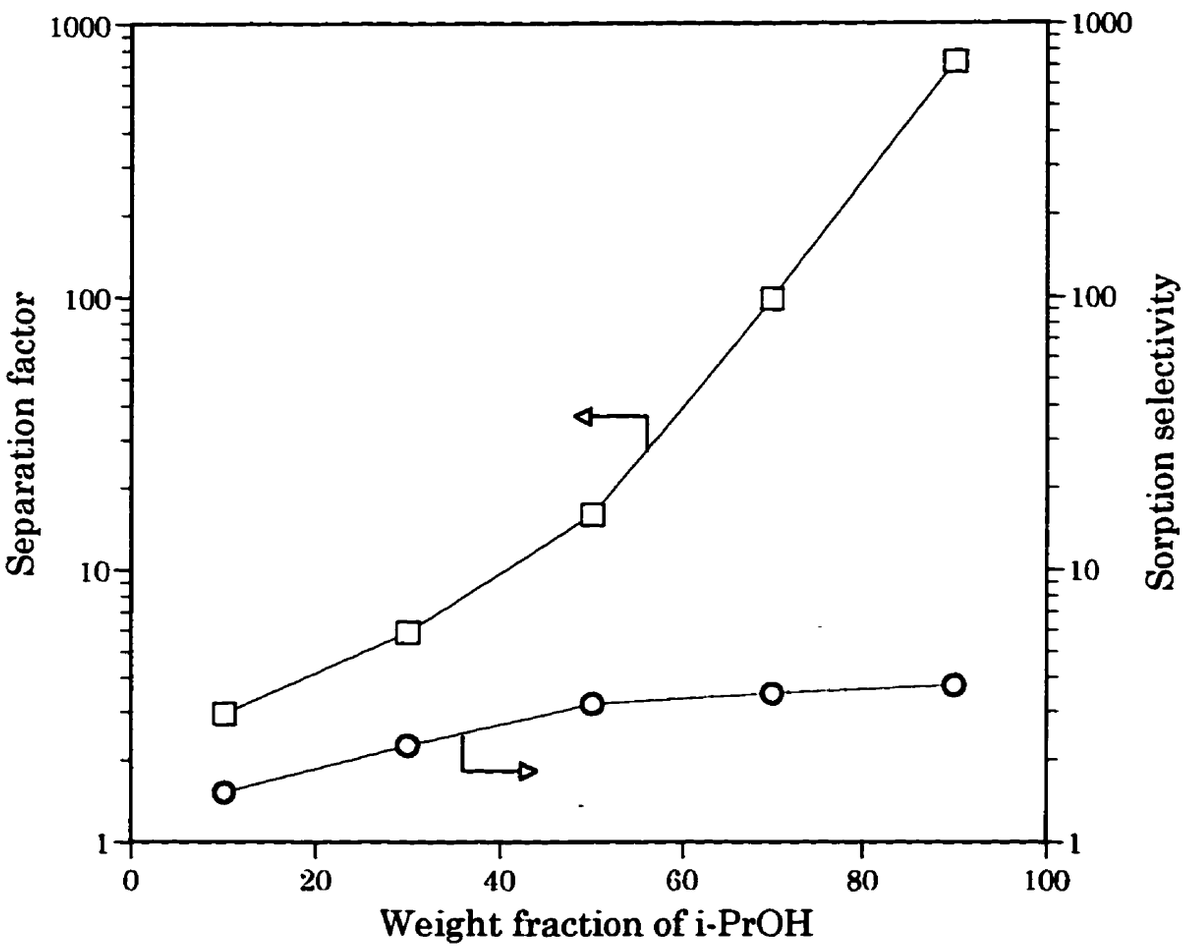


Figure 3.13 Separation factor and sorption selectivity versus weight fraction of isopropanol in feed.

corresponding α_S, especially at high isopropanol weight fraction in feed. This means that preferential diffusion contributes more to pervaporation than does preferential sorption of chitosan membrane, i.e., the increase in the separation factor of chitosan membrane is mainly caused by the increase in diffusion selectivity.

3.4.5 Temperature Effect

Figure 3.14 illustrates the effect of temperature on the individual permeation flux for the pervaporation dehydration of 90 wt. % isopropanol aqueous solution using chitosan membrane, while Figure 3.15 illustrates the typical separation factor with respect to temperature. It can be observed that the permeation flux increases progressively with the increase in temperature. In general, as the temperature increases, the thermal motion of the polymer chains is intensified, creating more free volume in the polymer matrix, through which the permeating molecules of water and isopropanol can diffuse. As a result, the transport of both the permeants is enhanced, leading to an increase in the total permeation flux and a decrease in the separation factor.

The dependence of the permeation flux on temperature can be related by an Arrhenius-type expression of the form

$$J = A\exp(-E/RT) \qquad (3.7)$$

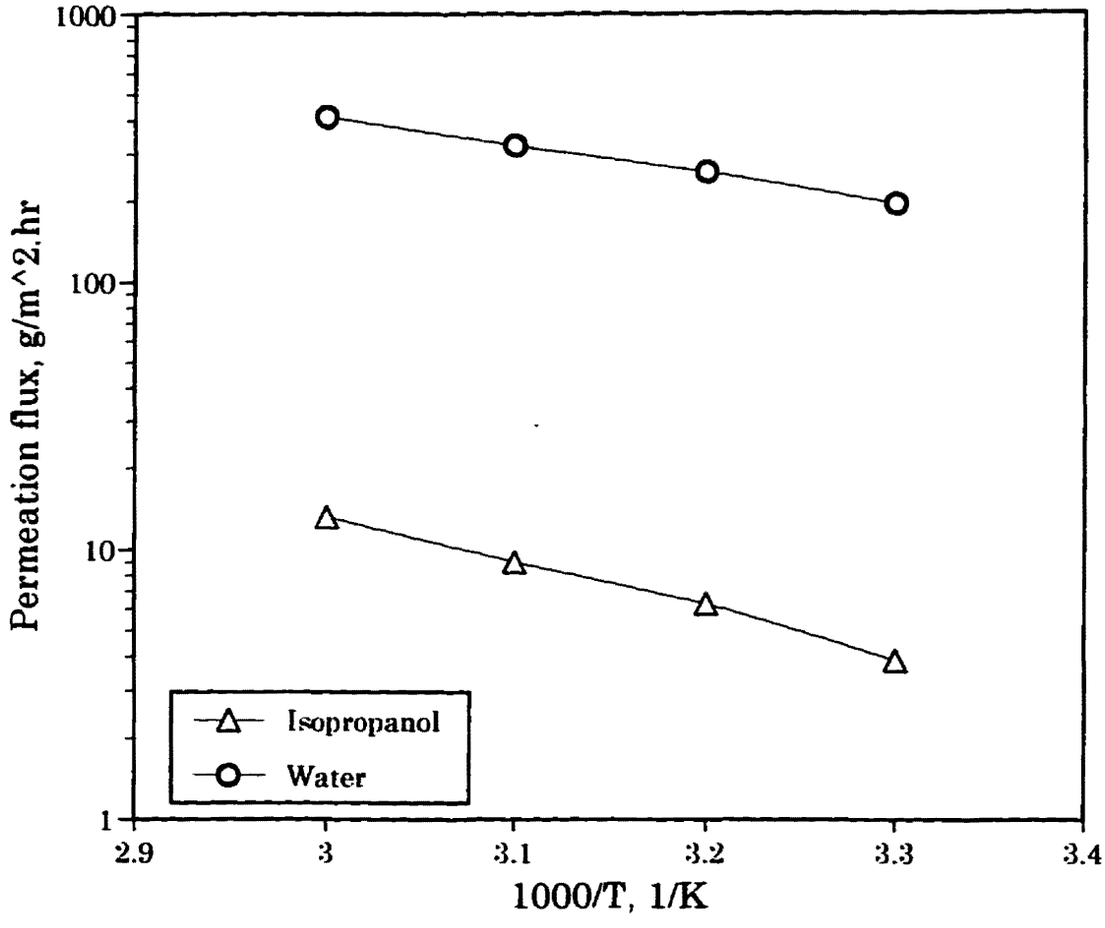


Figure 3.14 Effect of temperature on permeation flux. Isopropanol weight fraction in feed : 0.90.

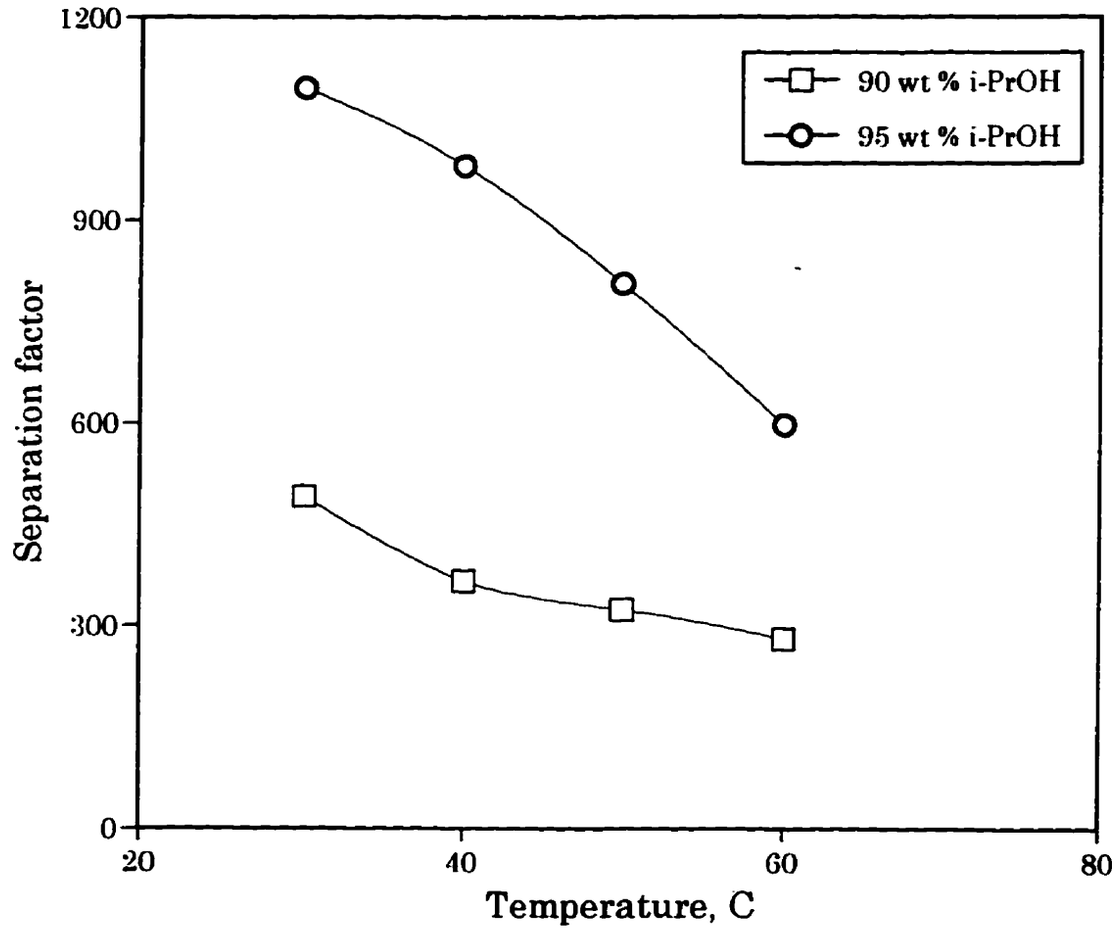


Figure 3.15 Effect of temperature on the separation factor.

where A is a constant, E the apparent activation energy for permeation, T the absolute temperature, and R the gas constant. The apparent activation energy for transport of each component, water and isopropanol, could be calculated from the slope of the Arrhenius plot of the flux as shown in Figure 3.14. The apparent activation energy thus calculated for water and isopropanol are 20.59 KJ/mol and 35.49 KJ/mol, respectively. The activation energy for transport of water is lower than that of isopropanol, indicating that water molecules requires less energy than isopropanol molecules do to facilitate permeation through the membrane. The significant difference in the activation energy for water and isopropanol suggests that isopropanol molecules and water molecules permeate by different mechanisms and through different pathways; isopropanol permeates by a random molecular diffusion within the amorphous matrix while water permeates by a selective transport through hydrophilic moiety in the polymer. The difference in the activation energy for each component may arise from several material factors such as the molecular size and the affinity between permeates and membrane. As a consequence, water molecules are preferentially absorbed and permeate more easily as compared with isopropanol due to the smaller molecular size as well as the higher affinity for the membrane.Note however that the activation energy for transport is only an empirical parameter that shows the relationship between the permeation flux and temperature. Since

flux in a membrane is determined by both the solubility and the diffusion of the permeants, the activation value should depend on both the activation energy for diffusion through the membrane and the heat of sorption [Bungay, 1986].

3.5 Conclusions

Liquid phase sorption with reference to pervaporation dehydration of isopropanol/water systems using chitosan membrane was investigated, and the effects of some operating conditions on the pervaporation performance were studied. The following conclusions can be drawn:

(1) The chitosan membrane exhibits preferential sorption and preferential permeation to the water component over the whole range of feed compositions; the chitosan membrane is water selective.

(2) The preferential permeation is affected and determined by the permeation sorption from the liquid phase; preferential sorption leads to preferential permeation.

(3) The pervaporation of isopropanol/water mixtures is a diffusion controlled process rather than a sorption controlled process.

(4) The pervaporation performance of the membrane is affected by such operating parameters such as temperature and feed concentration.

CHAPTER 4

Composite Chitosan Membranes for Dehydration of Isopropanol

4.1 Introduction

In membrane separation processes, pervaporation appears to be promising for separations involving liquid-organic or aqueous-organic mixtures, i.e, azeotropes or mixtures consisting of components with nearly equal boiling points [Sander, 1988; Rautenbach *et al.*, 1988; Hirotsu, 1988; Reineke, 1987]. However, the permeation fluxes of the early membranes were too low for practical uses. An approach to increase permeation flux is by minimizing the effective thickness of the membrane by the use of asymmetric or composite membranes. In fact, the rapid progress in membrane separation

technology has been very much a consequence of the development of the asymmetric membranes which were first reported by Loeb and Sourirajan [1960]. Integrally skinned asymmetric membranes have been widely used in reverse osmosis and gas separation [Sourirajan and Matsuura, 1985], but their applications in pervaporation are less developed.

Many studies on water-alcohol separations have been carried out from a practical point of view in commercial industries. Since the development and industrial applications of the PVA composite membrane by the GFT company in Germany in the 1980's, progress in the development of membrane materials and improvements in the membrane performance have been made in various fields. Almost all industrial pervaporation membranes are manufactured in composite fashions not only to achieve high membrane productivity but also to retain the necessary mechanical strength. Integrally skinned asymmetric membranes are made by phase inversion processes [Kesting, 1985]. Composite membranes are in general an improvement over phase inversion membranes. The composite technique allows one to produce support and active (skin) layers from different materials which are selected for optimum function in each case. Recently, Wang *et al.* [1996] developed a novel composite membrane for pervaporation dehydration of alcohol-water mixtures by coating a microporous polyacrylonitrile (PAN) support layer with a thin dense film of chitosan membrane.Feng [1996] performed pervaporation separation

of water from ethylene glycol by using a composite membrane consisting of a selective layer of chitosan film coated on a porous polysulfone substrate. Shieh [1996] studied pervaporation performance of composite and homogeneous membranes based on polyelectrolyte complexes of chitosan and polyacrylic acid for the separation of water/ethanol mixtures. A comparison between the performance of the homogeneous and the composite membranes led him to a development of a transport mechanism consisting of dense layer and porous substrate in series which can be used to explain the effects of porous substrate on the overall pervaporation performance of the composite membranes.

Composite solution-diffusion membranes can be made in two different ways:

(1) the dense separating layer can be coated on top of a microporous sublayer which acts as a mechanical support. Both layers can be prepared from different materials. They can therefore be selected and optimized separately to meet their specific functions.

(2) the microporous substructure itself can be cast as a dense integral asymmetric membrane with a few imperfections tolerated. Then the top layer has the function to clog these pinholes in order to prevent any convective flow through the membrane.

Both types of composite membrane have already been introduced into

gas separation processes. In most cases the selectivities of the top layer and the support material are preferring the same component. In pervaporation, however, because of permeant-polymer interactions, polymeric materials may exhibit inverse selectivities towards a given feed mixture, thus type (1) is generally used.

One of the objectives of this work is to develop composite chitosan membranes applicable to the dehydration of isopropanol by pervaporation. Homogeneous chitosan membrane has excellent thermal stability, mechanical strength, and chemical resistance. In order to improve the permeation rate, composite chitosan membrane supported by microporous layer of polysulfone was prepared and its pervaporation performance for pervaporation of isopropanol/water systems is investigated.

4.2 Theoretical

In general, dense composite membranes are used to improve permeation flux by reducing the active membrane thickness. A composite membrane which consists of two different materials, is normally prepared by coating a very selective dense separating layer on top of a microporous support. The membrane combines the high selectivity of the dense membrane with the high permeation rate of the very thin membrane. Ideally, the actual

permselectivity is determined by the thin top layer, whereas the porous sublayer merely serves as a mechanical support.

The basic equation for solution-diffusion transport of a permeating component in pervaporation membrane can be written phenomenologically as [Feng, 1994],

$$[PR] = KA\frac{\gamma p_s X - pY}{l} \tag{4.1}$$

where *[PR]* is the permeation rate, γ is the activity coefficient, K is the effective permeability coefficient that accounts for non-ideality of the permeation, p and p_s refer to the permeate pressure and the saturated vapor pressure, respectively, and A and l are the area and thickness of the membrane, respectively. The permeation flux is linearly proportional to the reciprocal of the membrane thickness.

Defining permeation rate for both homogeneous membrane and composite membrane, which consists of a thin layer of dense homogeneous membrane supported on a porous sublayer, according to equation (4.1) at the same operating conditions results in,

$$[PR]_h = KA\frac{\gamma p_s X - pY}{l_h} \tag{4.2}$$

and

$$[PR]_c = KA\frac{\gamma p_s X - pY}{l_c} \tag{4.3}$$

where subscripts h and c represent homogeneous membrane and composite membrane, respectively.

Defining an ideal composite membrane as that membrane in which the permselectivity is completely determined by the thin dense homogeneous top layer l_c, we introduced permeation rate ratio (to differentiate from the permeation ratio defined in Chapter 3) to measure the relative effect of the porous support.

$$\Phi = \frac{[PR]_h l_h}{[PR]_c l_c} \tag{4.4}$$

where Φ is the permeation rate ratio. Based on eqn. (4.4), only when Φ is equal to unity the composite membrane performs ideally; i.e., its permselectivity is determined by the thickness of the dense top layer. For the practical application of pervaporation, the membrane must have a high permeation rate J, and a large separation factor α. However, in general a so-called trade-off relationship exists between the permeability and selectivity. In view of this trade-off, Huang and Rhim [1993] proposed the pervaporation separation

index (PSI) to measure the membrane overall pervaporation performance

$$PSI = J(\alpha - 1) \qquad (4.5)$$

4.3 Experimental

4.3.1 Materials

Polysulfone in powder form (Udel P-3500) was supplied by Amoco Performance Products, Inc., USA. Dimethyl formamide (DMF) was purchased from BDH Chemicals Co. and methyl Cellosolve (ethylene glycol monomethyl ether) from Fisher Scientific Co.A non-woven polyester fabric was used as the backing material for the composite membrane. All the other chemicals were the same as specified in Chapter 3.

4.3.2 Membrane Preparation

The porous polysulfone substrate was prepared via phase inverse process from a casting solution containing 12 wt. % polysulfone, 11 wt. % methyl Cellosolve, and 77 wt. % N,N-dimethyl formamide (DMF). The casting solution was cast onto a non-woven fabric held on a glass plate with the aid of a Gardner knife. The cast film was immediately immersed into a gel bath consisting of 50 wt. % dimethyl formamide in deionized water at room temperature for 10 minutes. The resulted porous membrane was washed with

deionized water for 24 hours and dried in air at room temperature. The substrate membrane exhibited a pure water permeation rate of 235 kg/m2.hr at a cross-membrane pressure difference of 100 psi.

The composite membrane was prepared by coating 0.5 wt. % chitosan solution onto the porous polysulfone membrane with the aid of a dropper and a glass rod adjusting to the appropriate thickness. Then the coated membrane was dried at room temperature for 24 hours, immersed in 3 wt. % aqueous sodium hydroxide solution containing 50 wt. % isopropanol for another 24 hours, washed thoroughly in deionized water and redried in air at room temperature.

4.3.3 Scanning Electron Microscopy (SEM)

The membrane morphology was studied by using a Hitachi S-5700 scanning electron microscope at an accelerating voltage of 15 KV. The membrane specimens were first dried under vacuum at room temperature for 24 hours. Then the specimens were fractured in liquid nitrogen to avoid spoiling the polymer structures. The so prepared samples were mounted onto top of metal aluminium stub and sputter-coated with gold prior to the macroscopic observation. Both the surface layer and the cross-section of the membrane were photographed by the SEM.

4.3.4 Pervaporation

The apparatus for the pervaporation experiment and the chromatographic analysis were essentially the same as that used and specified in Chapter 3. The pervaporation dehydration of isopropanol was performed for the whole range of concentration of isopropanol/water mixtures.

4.4 Results and Discussion

4.4.1 Membranes Morphology

The SEM photograph of the surface layer and cross-section of the homogeneous chitosan membrane is shown in Figure 4.1. Note the absence of pores at a very high level of magnification in the solid chitosan surface layer and cross-section indicating the dense structure of the homogeneous chitosan membrane.

SEM photographs of the composite membrane are shown in Figure 4.2 and 4.3. Figure 4.2 shows the entire thickness of the composite chitosan/polysulfone membrane. The top dense layer consists of a solid homogeneous chitosan film. This thin layer is supported by the sponge-like porous polysulfone substrate which is attached onto a non-woven polyester fabric layer. Figure 4.3 (a) shows the SEM photograph of the dense chitosan layer on top of the composite membrane. Note the absence of pores in this

Figure 4.1 Scanning electron microscopy (SEM) photographs of homogeneous chitosan membranes:
(a) cross-section; (b) surface layer

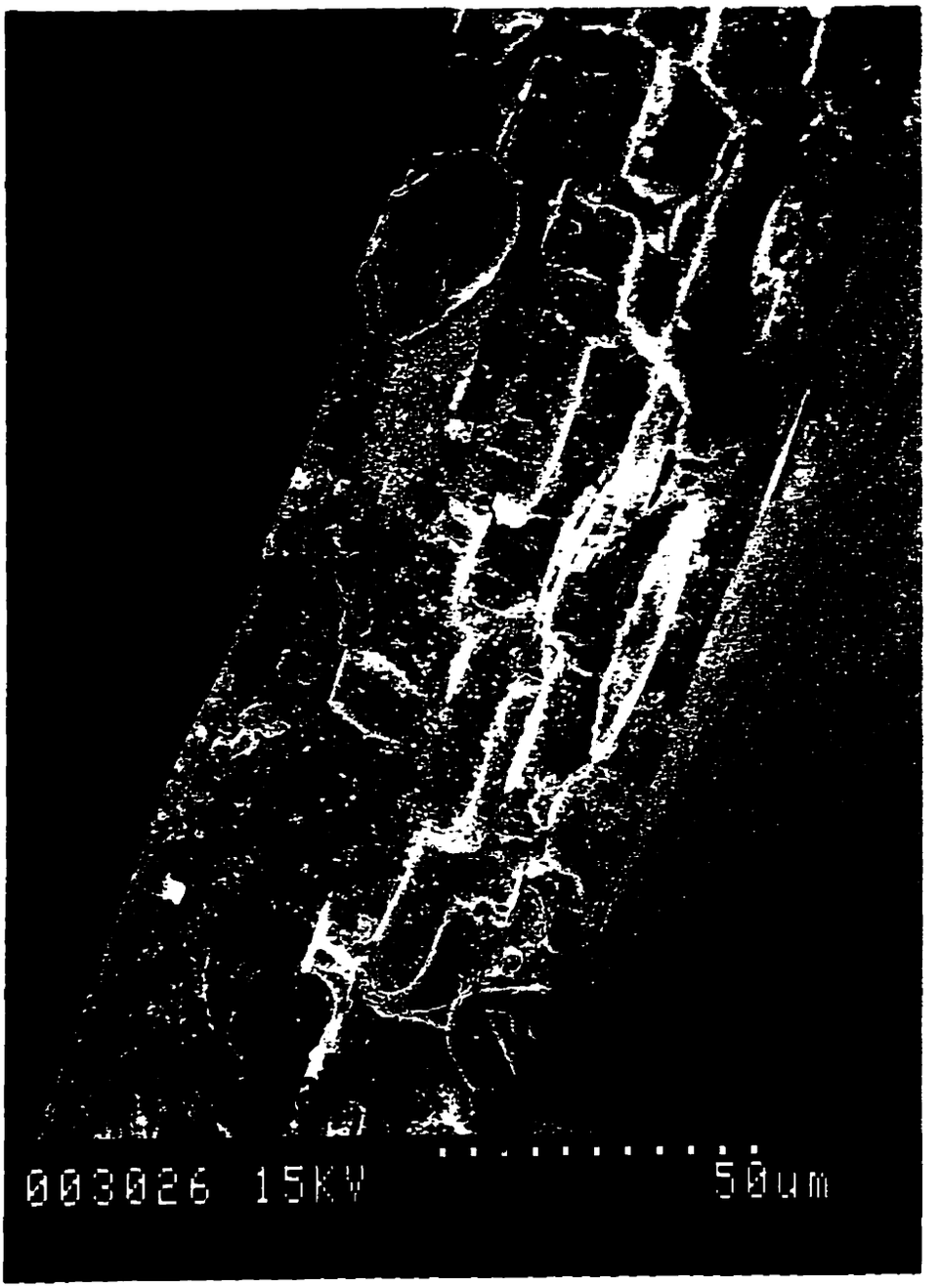
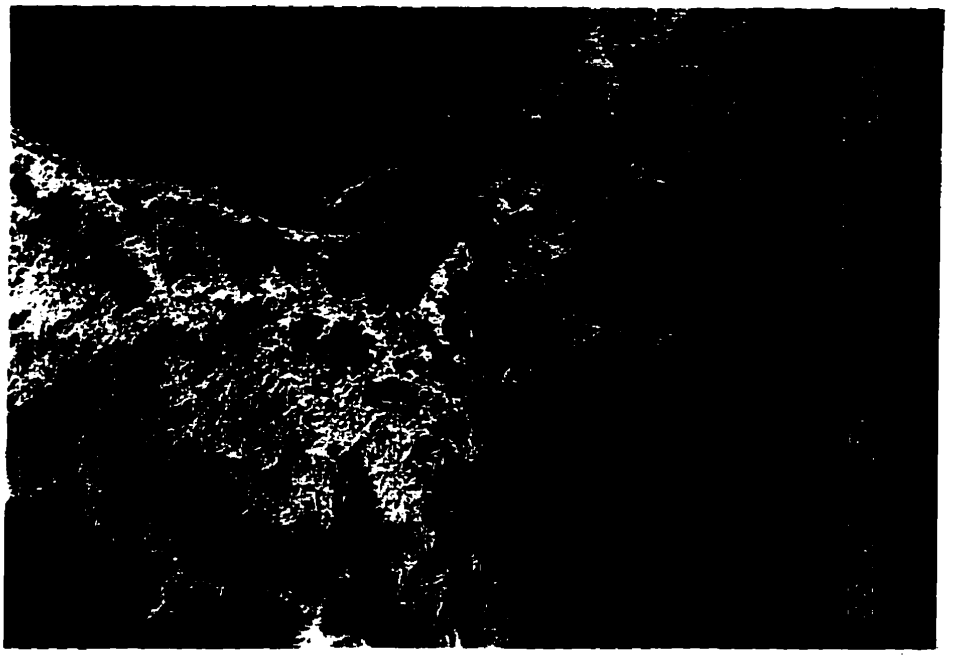

003026 15KV
50um

Figure 4.2 SEM photographs of cross section of composite chitosan membranes showing both (a) the chitosan top layer and (b) the polysulfone porous substrate.



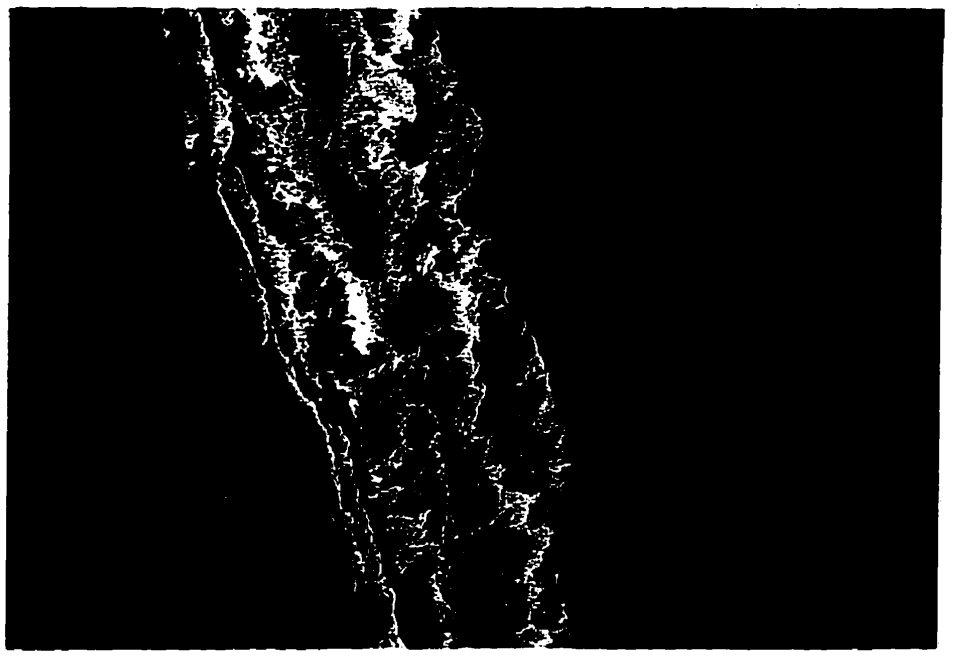
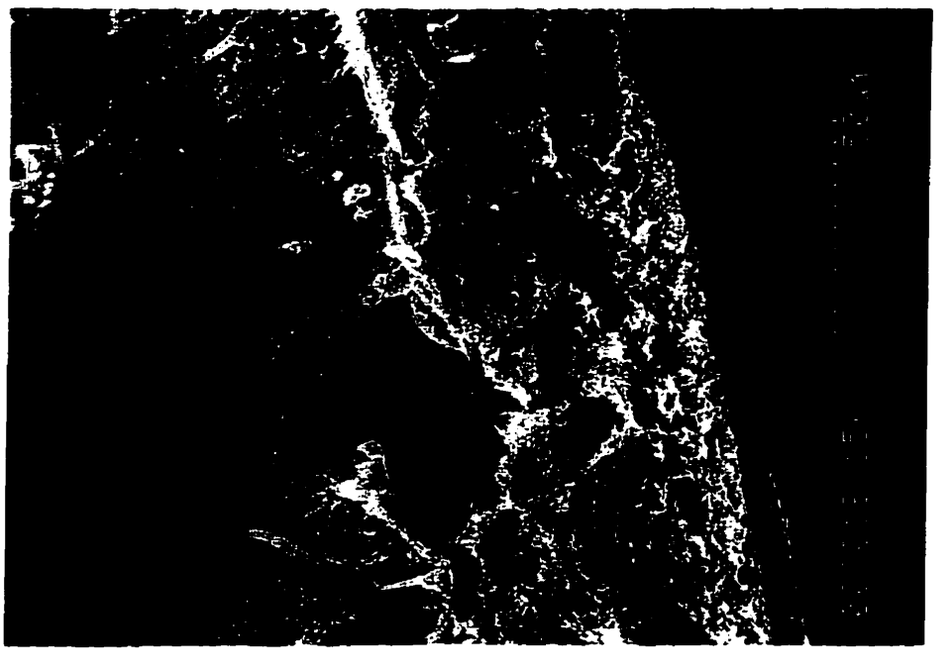


Figure 4.3 SEM photographs of composite chitosan membranes taken from the opposite angle and without the nonwoven fabric:
(a) polysulfone support ; (b) chitosan dense layer.





layer consistent with the structure of the homogeneous chitosan membrane shown in Figure 4.1. Figure 4.3 (b) shows the structure of the composite membrane after the non-woven polyester fabric was peeled off from the composite membrane. This figure clearly reveals the structure of the sponge-like porous polysulfone substrate, both the surface layer and cross-section. Note the distinctive structure between the dense chitosan layer with the porous sponge-like structure of the polysulfone substrate.

It is generally accepted that certain phase inversion membrane structures can be correlated with the rate of precipitation of the polymer solution. Very high precipitation rates (short gelation times) always lead to a finger-like structure, while slow precipitation rates (long gelation times) lead to asymmetric membrane with a sponge-like structure [Porter, 1990]. In this study, a quench medium consisting of 50 wt. % aqueous DMF was used as the precipitation bath. The presence of dimethyl formamide which is also a solvent for polysulfone would slow down the exchange rate between the nonsolvent (water) in the quench medium and solvent in the polymer solution. As a result the precipitation rate would be slow and the so formed membrane would feature a sponge-like structure. As can be seen from the SEM photographs of the composite membranes, the ratio of the thickness of this spongy structure to that of the chitosan thin dense layer can be estimated to be 6 to 1.

4.4.2 Pervaporation Performance of the Composite Membranes

The individual permeation fluxes of the permeating species were calculated from the total permeation rate and the permeate composition. Figures 4.4 shows the permeation fluxes as a function of isopropanol concentration for the composite chitosan membranes. In the entire composition range, water permeates predominantly and the total flux is almost the same as the water flux suggesting that water is preferentially permeable through the composite membrane. The total and water permeation fluxes decrease with isopropanol concentration in the feed solution. Owing to the high hydrophilicity of the chitosan material, the chitosan membranes swell more significantly in the solution with high water content. As the water concentration in feed increases, the amorphous regions of the membrane are more swollen, and the polymer chains become more flexible and increase the space available for diffusion, thus decreasing the energy required for diffusive transport through the membrane.

The data for the separation factor as a function of feed concentration are plotted in Figure 4.5. Interestingly, high separation factors for water removal are observed at high isopropanol concentrations. Hence, the membranes are effective especially for the dehydration of high concentrations

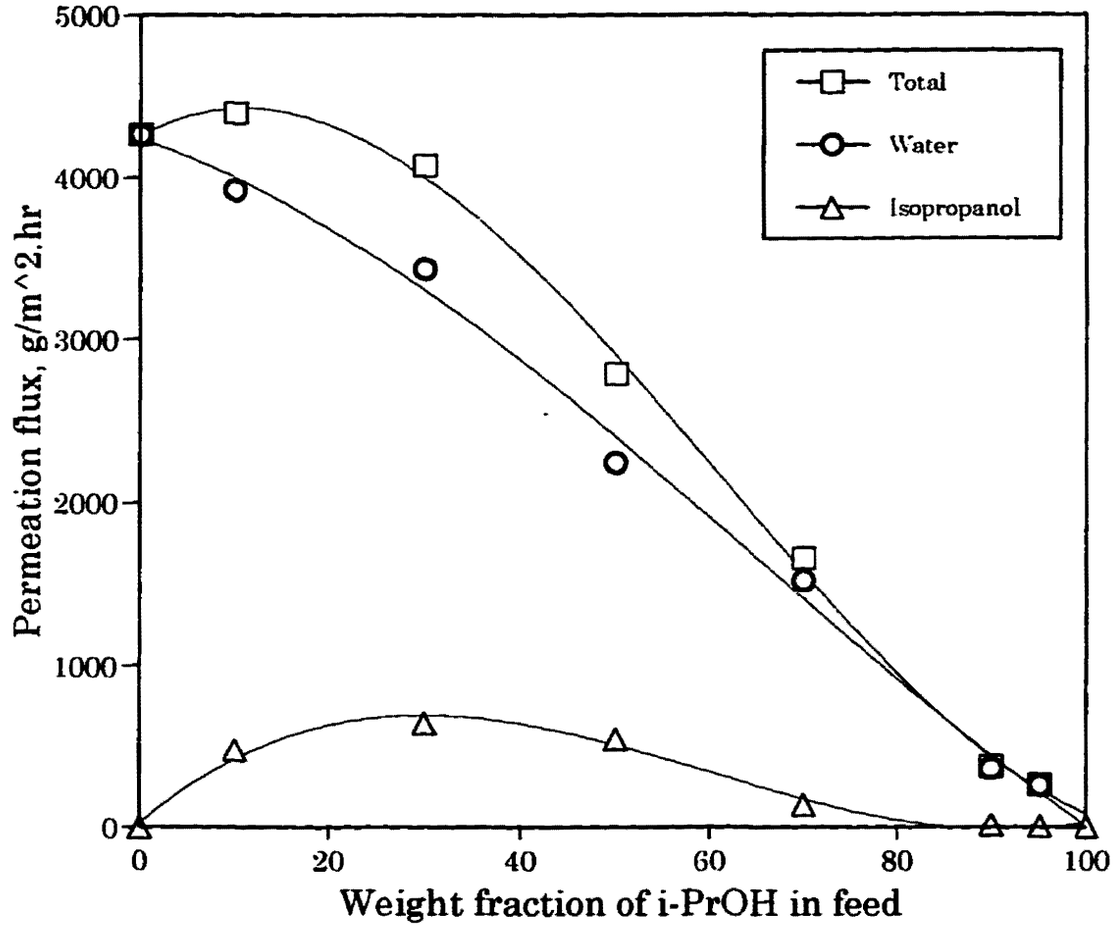


Figure 4.4 **The total and partial permeation fluxes versus feed concentrations for the composite chitosan membrane. Temperature 30 °C.**

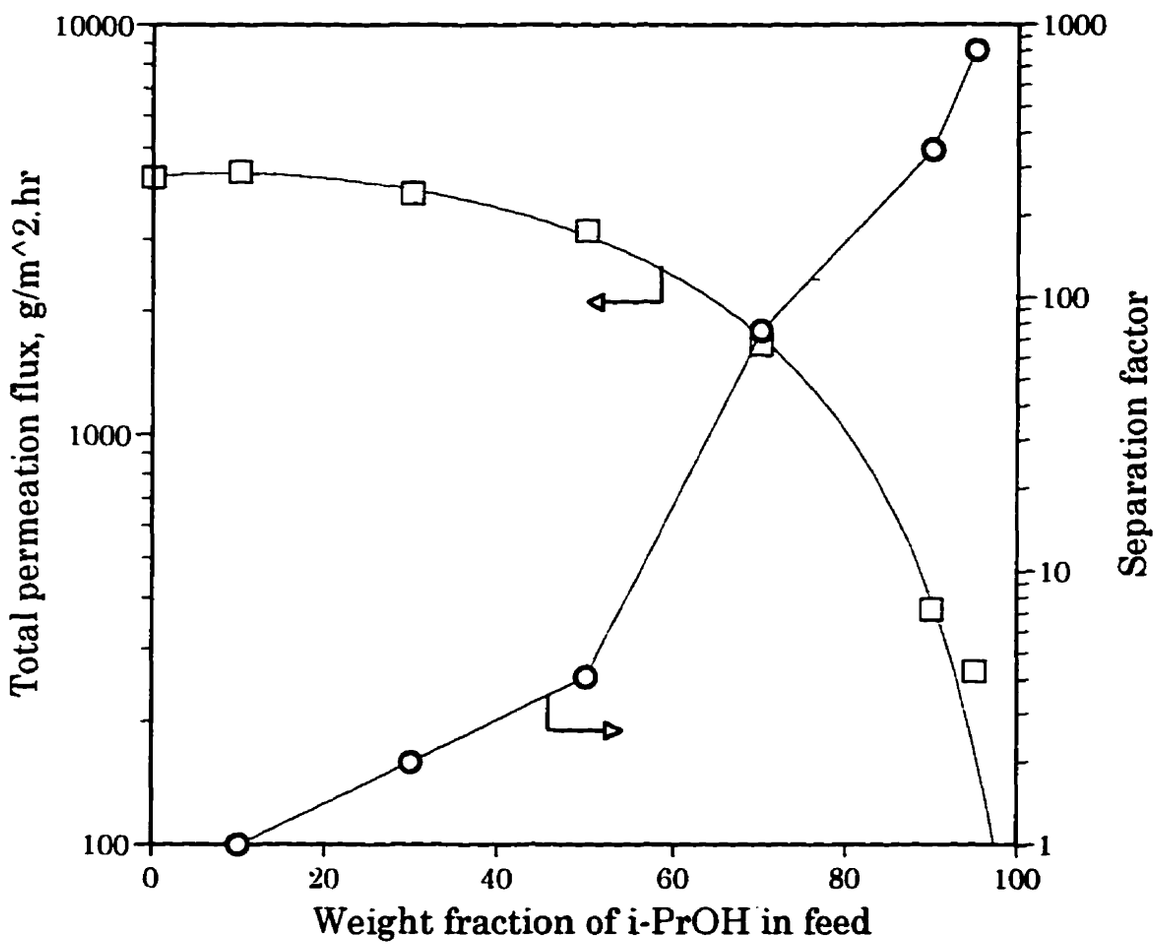


Figure 4.5 **Separation performance for the composite chitosan membrane as a function of feed concentration. Temperature 30 °C.**

of isopropanol including isopropanol/water azeotrope.This is what we desired for the proposed separation using chitosan based membranes.

The composite membrane was also tested for the dehydration of the isopropanol/water mixtures at high concentrations of isopropanol at elevated temperatures. The experimental results are shown in Figure 4.6, where the pervaporation data are plotted against the reciprocal of the operating temperature. In general, increasing temperature leads to a higher permeation flux and a lower separation factor. The temperature dependence of permeation flux seems to follow an Arrhenius type of relation in the temperature range tested. As the temperature increases, the thermal motion of the polymer chains in the membrane is amplified to create more free volume in the polymer matrix, which leads to an increase permeation for both water and isopropanol. The increase in the water flux causes further plasticization of the pervaporation system, which may cause a larger increase in the isopropanol flux, therefore decreases the separation factor with an increase in temperature.

4.4.3 Composite Membranes vs. Homogeneous Membranes

Interestingly, for both the homogeneous and composite membranes, the isopropanol permeation flux did not increase monotonically with the increase

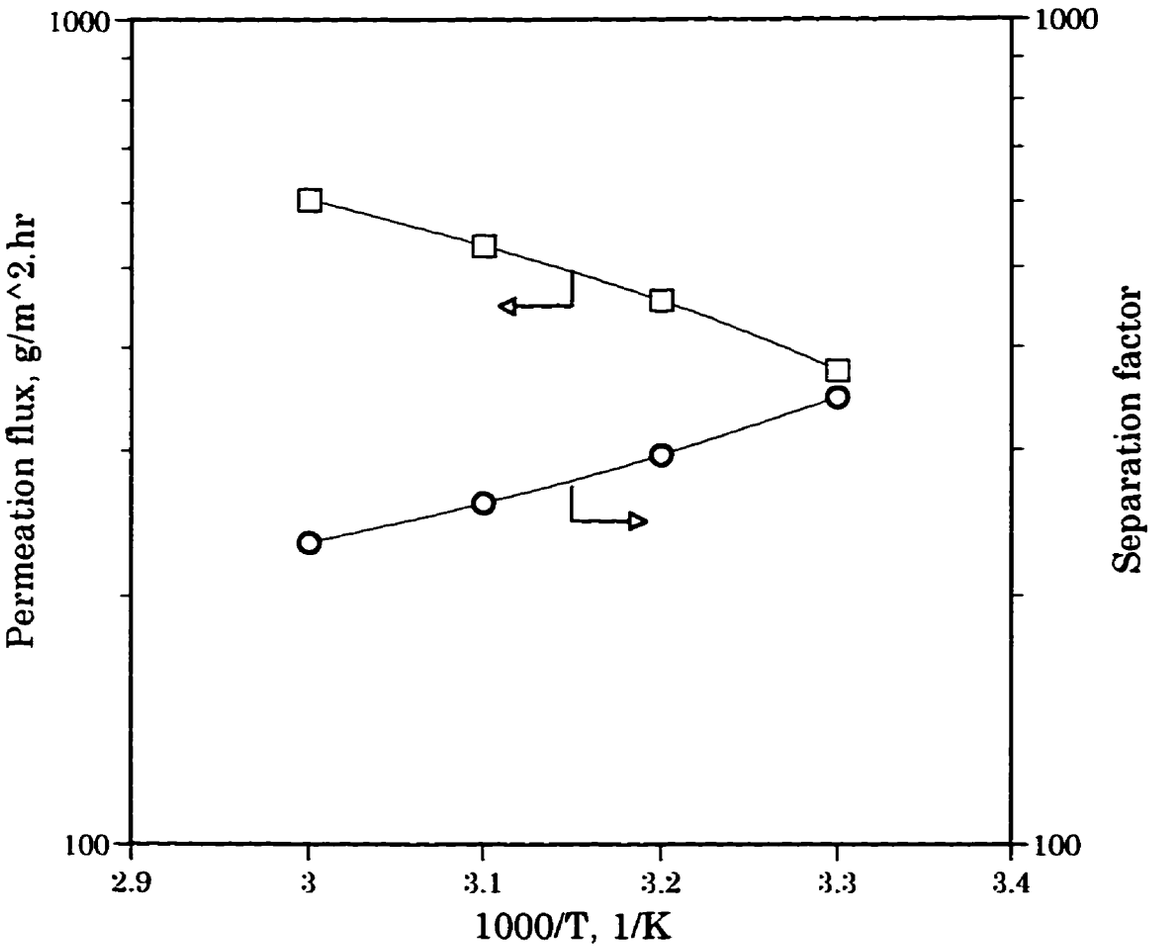


Figure 4.6 The effect of temperature on the permeation flux and the separation factor for the composite membrane. Feed composition : 90 wt. % isopropanol.

in isopropanol in feed as shown in Figure 4.7. As can be seen, an increase in feed isopropanol concentration increased both the isopropanol fluxes in the homogeneous and the composite chitosan membranes when the isopropanol concentration is less than about 30 wt. %, whereas after this point a reverse trend was observed. The existence of the maximum flux suggests that the permeation flux of isopropanol was greatly affected by the presence of water in the feed. Evidently the presence of water increase the diffusivity of isopropanol and this plasticizing effect of water on the membrane was especially significant in the feed with high water content.

As the feed isopropanol concentration increases from 70 to 95 wt. % the decrease of isopropanol flux is more significant than that of water, resulting in an exponential increase in the separation factor as illustrated in Figure 4.8. The increase in the isopropanol concentration restricts the degree of swelling of the membranes, thus reducing the diffusivity of the permeating species. Since the molecular size of isopropanol is greater than those of water, the permeation flux of the former is more affected than that of the latter. At 30 °C, the separation factor for the homogeneous and composite membranes for 90 wt. % isopropanol feed concentration were 491 and 348, respectively. When the isopropanol concentration was increased to 95 wt. %, the separation factor for the homogeneous and composite membranes increased to 1096 and 807,

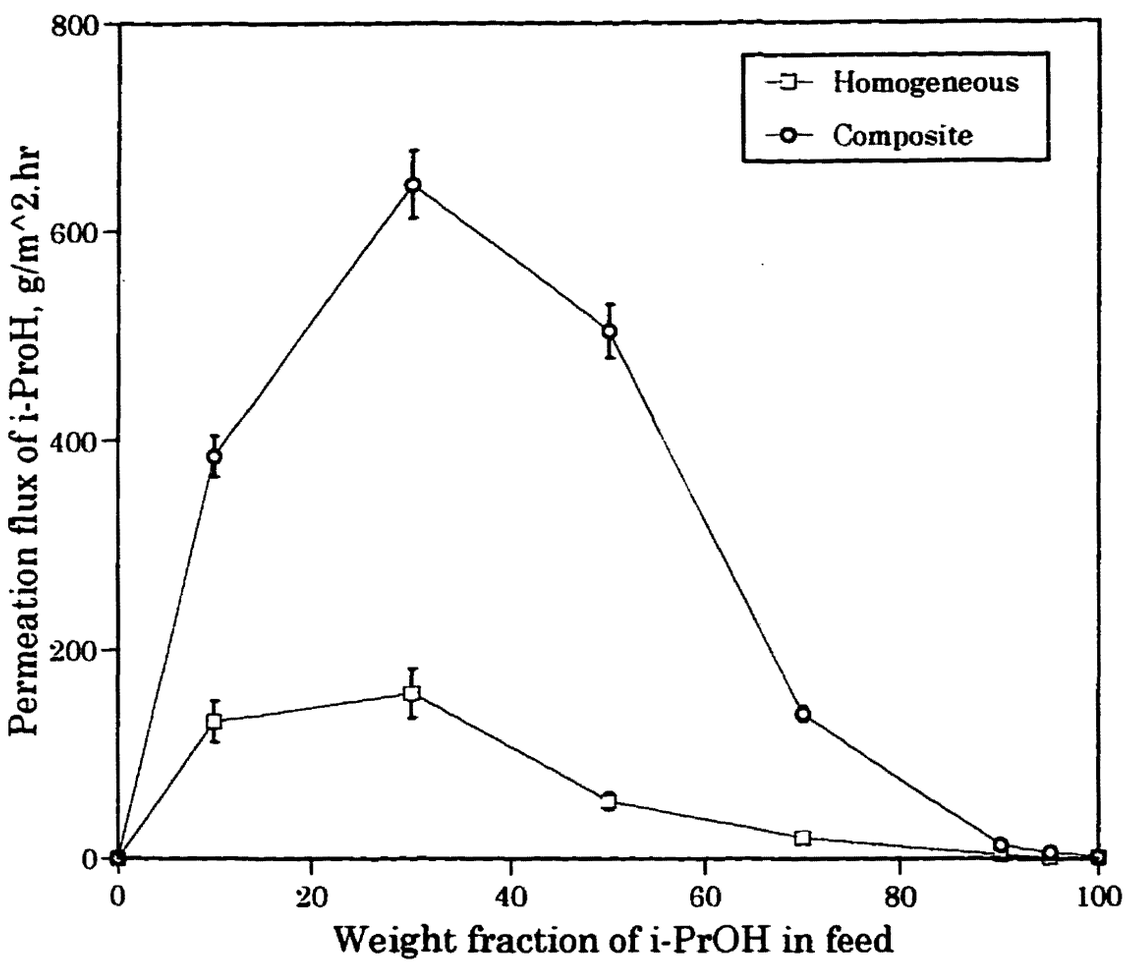


Figure 4.7 The isopropanol partial permeation for the homogeneous membrane and composite membrane as a function of feed concentration. Temperature 30 °C.

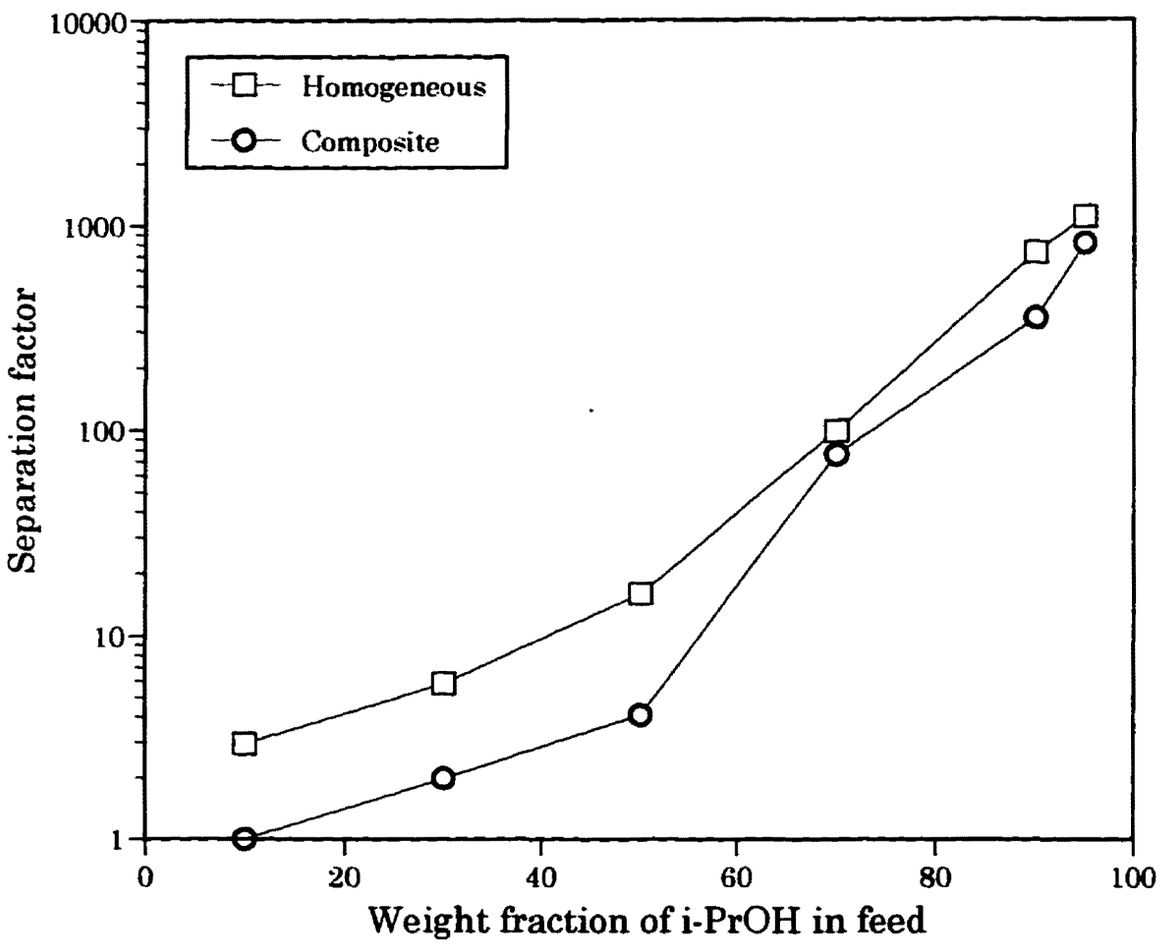


Figure 4.8 **The separation factor for the homogeneous membrane and composite membrane as a function of feed concentration.**

for the homogeneous and composite membranes increased to 1096 and 807, respectively. Note that for the whole range of feed composition, the separation factor for the homogeneous membrane is higher than that of composite membrane.

Figure 4.9 shows the permeation rate ratio and the separation factor ratio between the homogeneous chitosan membrane and the composite of chitosan/polysulfone membrane. These figures suggest that the composite membrane does not perform ideally, i.e., the porous support provides a mechanical strength as well as an additional *"thickness"* to the composite membrane, thus creating an additional resistance for the transport of the permeating components through the membrane. From eqns. (4.2) and. (4.3) we can see that a high permeation rate can be obtained if the permeate pressure can be kept as low as possible and the vapor can leave the phase boundaries without any restrictions. However, in the case of the composite membrane, the permeate vapor from the dense top layer may create a significant pressure build-up at the interface between the dense layer and the porous substrate. This may reduce the driving force across the selective dense membrane and in turn decreases the overall membrane performance. Feng [1994] developed a resistance model approach to asymmetric membranes to rationalize between membrane selectivity and resistance to mass transport offered by different component parts of the membrane. He reported that the permeation

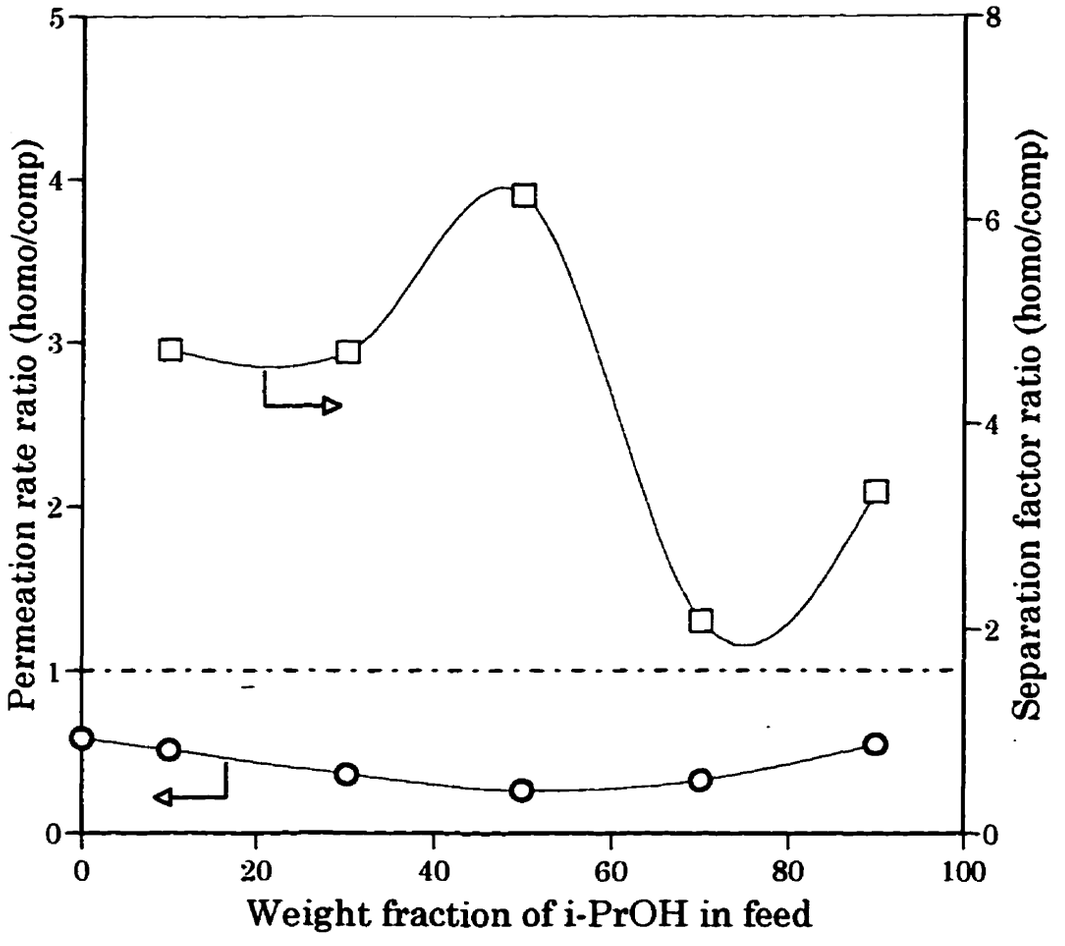


Figure 4.9 **The permeation rate ratio and the separation factor ratio of homogeneous membrane and composite membrane.**

selectivity in an asymmetric membrane was affected not only by the relative resistance of the dense layer and the porous substrate, but also by the relative resistance of the polymer matrix and the pores in the substrate.

The composite membrane comprising of a thin chitosan barrier and a porous polysulfone support was prepared to increase the permeation flux with a minimal sacrifice of separation factor. In order to measure the performance of the composite membrane as compared to the homogeneous one, both factors have to be taken into consideration. The pervaporation separation index (PSI) is used to evaluate the overall membrane pervaporation performance and the experimental results are illustrated in Figure 4.10. As can be observed, in terms of the PSI, the composite membrane is more productive for the feed with high isopropanol content especially when the isopropanol feed concentration exceeds 70 wt. %, whereas for the feed with low isopropanol content the reverse trend is observed. This implies that if the PSI were the determining factor, composite chitosan would be more effective for the pervaporation of aqueous isopropanol near its azeotropic concentration, while homogeneous chitosan membrane would be useful for the separation of dilute aqueous isopropanol solutions. Similar results were reported by Shieh [1996] for the pervaporation dehydration of ethanol/water systems using both homogeneous and composite membranes of polyelectrolyte complexes based on chitosan and polyacrylic acid; based on the PSI values he found that the

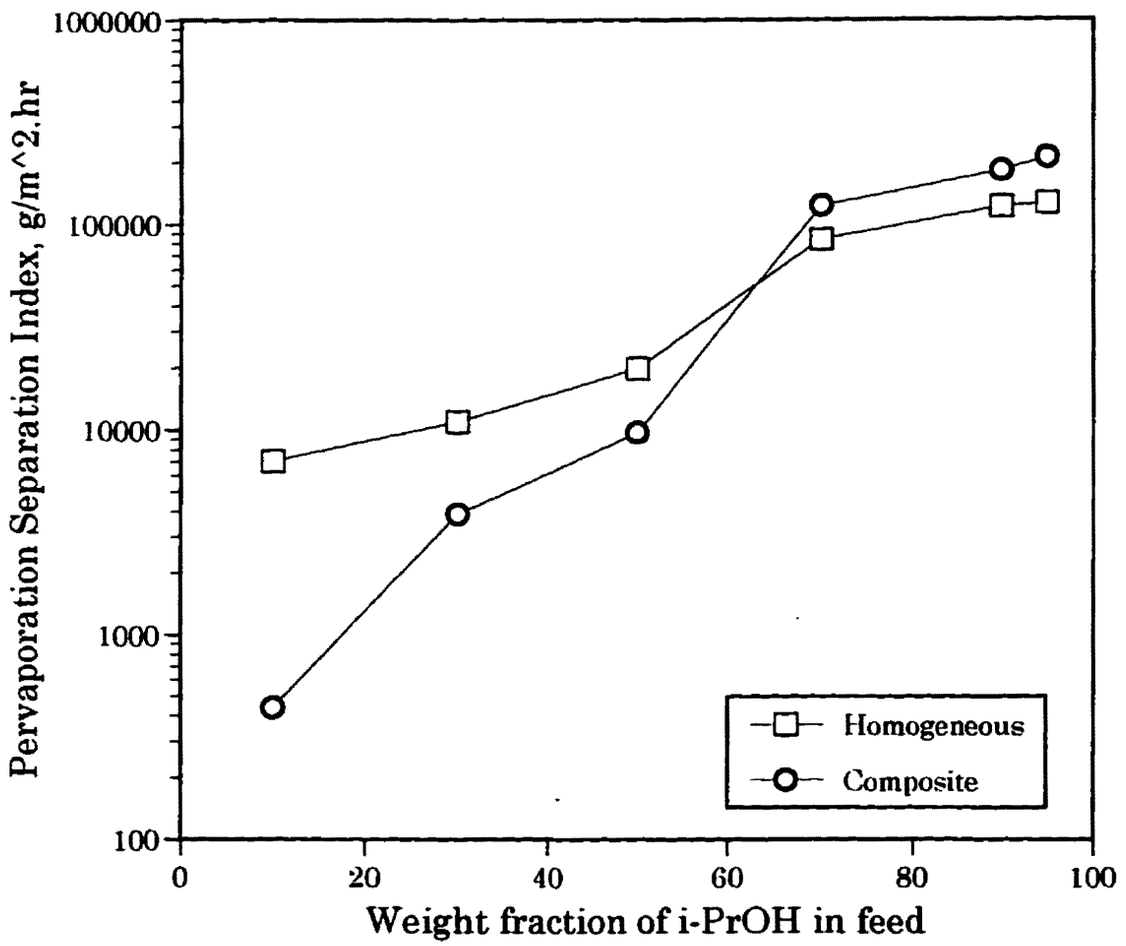


Figure 4.10 The pervaporation separation index for the homogeneous and composite membrane versus feed isopropanol concentration.

composite membrane was superior to homogeneous membrane at high concentration of ethanol in feed solution. These results demonstrate the potential of pervaporation using composite chitosan membranes as an alternative to conventional distillation for the separation of water/isopropanol mixtures as well as for water/ethanol mixtures [Shieh, 1996] and water/ethylene glycol mixtures [Feng, 1996]. Note that separation of azeotropic and close-boiling point mixtures by pervaporation through a number of different membranes including dehydration of ethanol and isopropanol is the best developed application of pervaporation due to commercial interest in combining pervaporation and conventional hybrid systems [Rautenbach *et al.*, 1992; Bungay, 1986].

4.5 Conclusions

Composite chitosan membranes with chitosan dense top layer supported by polysulfone microporous substrate were prepared and investigated for the pervaporation dehydration of isopropanol. The following conclusions can be drawn:

(1) The pervaporation properties of the composite membranes are similar to that of the corresponding homogeneous membranes; the membranes are water selective and their permselective performance is affected by

the feed composition, the permeation flux decreases while the corresponding separation factor increases more significantly with an increase in isopropanol concentration.

(2) The separation factor for the composite membranes, in general, decreases with an increase in temperature, whereas the corresponding permeation flux increases to follow an Arrhenius type of relationship.

(3) The permselective performance of the composite chitosan membrane relative to that of homogeneous chitosan membrane was affected by the presence of the polysulfone porous substrate.

(4) The PSI shows that the composite membrane was superior to the homogeneous membrane only at high feed isopropanol concentrations.

This study demonstrates the applicability of composite chitosan membranes for pervaporation dehydration of isopropanol, especially at high feed isopropanol concentrations. However, the membranes were not prepared under optimized conditions; the addition of porous support creates additional resistance for the transport of the permeating components. In order to further improve the performance of the composite membranes a continuous effort to minimize the effect of the porous substrate on the permselectivity of the membrane should be considered.

CHAPTER 5

Modified Chitosan Membranes for the Pervaporation of Isopropanol/Water Mixtures

5.1 Introduction

Chitosan has been studied as membranes [Yang and Zall, 1984; Mochizuki *et al*., 1989 a,b,c, 1990 a,b; Shieh, 1996; Feng, 1996] because of its good film forming properties, highly hydrophilic, and good chemical resistant properties. However, because of the amino group, chitosan has a poor stability in water and in aqueous mixtures. Its stability in aqueous solution has to be improved to fully utilize its potential as a membrane. In general, heat treatment can be adopted to enhance the water resistance of the chitosan by promoting crystallization. The membrane with the crystallization

pretreatment may be used in aqueous mixtures at low temperature; at high temperature the stability may change significantly. The stability of the chitosan against water and aqueous mixtures at high temperatures can be increased by crosslinking. Chitosan, being a high molecular weigh polymer, is a linear polyamine whose amino groups are readily available for chemical reactions and salt formation with acids.

The selectivity may also be improved by modification. Some researchers have reported modified chitosan membranes used for pervaporation separation of water/ethanol mixtures [Lee and Shin, 1991; Uragami and Takigawa, 1990; Watanabe and Kyo, 1992]. Wang *et al.* [1996] reported the pervaporation of alcohol/water mixtures using a novel three-layer composite membrane prepared from chitosan (CS) and microporous polyacrylonitrile (PAN) and found that the intermolecular crosslinks between CS and the hydrolyzed support PAN significantly increased both the selectivity and flux of the membrane. Uragami *et al.* [1994] reported the characteristics of permeation and separation for aqueous ethanol solutions through a glutaradehyde (GA) crosslinked chitosan membrane in vapor permeation. They found that both the permeation rate and the separation factor of water/ethanol increased with increasing crosslinked GA content in the membrane.

Polymer blending provides simpler, more feasible technology than do

other methods that combine different polymers to yield new polymeric material. Since the homogeneous polymer blends are compatible at the molecular level, the new distinctive polymeric material thus combines the properties of the polymeric components. Shieh [1996] developed a series of highly water-selective blend membranes of chitosan and polyacrylic acid for pervaporation of water/ethanol mixtures. He found that the blend membranes with higher molecular weight chitosan exhibited better pervaporation performance than the ones with lower molecular weight. In this study, chitosan - poly(vinyl alcohol) blends are investigated as pervaporation membranes for the dehydration of water-isopropanol mixtures.

Poly(vinyl alcohol) (PVA), a 1,3-diglycol polymer with a monomer weight of 44, has been studied intensively as a membrane in many various ways [Greenlaw *et al.*, 1977; Shantora and Huang, 1981; Zhang *et al.*, 1988] for its excellent film-forming properties and is used mainly when dissolved in water. Its many hydroxyl groups cause it to have high affinity to water, with strong hydrogen bonding between the intra- and intermolecular hydroxyl groups, greatly impeding its solubility in water. Because of the hydroxyl group, which reacts with difunctional agents such as diacid, PVA is readily crosslinked in aqueous solutions.

In this work, chemically crosslinked and chitosan-poly(vinyl alcohol) blend membranes are developed for the pervaporation dehydration of

isopropanol. The membranes pervaporation performances in terms of selectivity and permeability are investigated. The effects of crosslinking reaction times and blend compositions are also studied to further utilize the potential of chitosan membranes as pervaporation membranes.

5.2 Experimental

5.2.1 Materials

Poly(vinyl alcohol) polymer (mole % hydrolysed : 99; MW: 133,000) was supplied by Polyscience Inc., USA. Reagent grade 1,6-Hexamethylene diisocyanate (HMDI) (see Scheme 5.1) was purchased from Sigma Inc., USA and maleic acid was obtained from Fisher Scientific, USA. Methanol and ethanol were purchased from Commercial Alcohols Inc., Toronto. All other materials including chitosan are the same as those used in Chapter 3.

$$O=C=N-CH_2-(CH_2)_4-CH_2-N=C=O$$

Scheme 5.1 Molecular structure of 1,6-Hexamethylene diisocyanate

5.2.2 Membrane Preparation

Crosslinked Chitosan Membranes. The procedure and sequence of

preparing homogeneous chitosan membrane is as described in Chapter 3. 1,6 - Hexamethylene diisocyanate with a flexible spacer between reactive groups was used as the crosslinking agent in order not to rigidify the membrane. The solution technique was used to modify chitosan membrane by using HMDI in acetone/water solution. Acetone was used to control the swelling of the membrane. The prepared homogeneous chitosan was soaked in a reaction bath containing HMDI at room temperature for a certain period of times and then heated at 150 °C in an oven. The modified membranes were dried at room temperature under vacuum. The thickness of the modified chitosan membranes was 20 - 30 μm.

Chitosan-Poly(vinyl alcohol) Blend Membranes. Aqueous 10 wt. % PVA solutions were prepared by dissolving preweighed quantities of dry PVA in deionized water, followed by a continuous heating at 90 °C for 6 hours. 0.5 wt. % chitosan solutions were prepared by dissolving preweighed quantities of chitosan in 10 wt. % acetic acid solution and stirring them at room temperature for 24 hours. The casting solutions were prepared by mixing the PVA and chitosan solutions at a different blend ratios at room temperature for 24 hours. The blended casting solutions were cast onto PVC plates with the aid of a Gardner casting knife and dried at room temperature for 24 hours. The films were peeled off from the plates,treated in 3 wt. % NaOH solution

containing 50 wt. % isopropanol solution for 24 hours at room temperature, washed thoroughly with deionized water to completely remove NaOH. The solution technique was used to modify the blended membranes by using maleic acid in acetone/water system. The modified membranes were dried at temperature under vacuum. The thickness of the membranes was measured manually and was between 50 to 70 μm.

5.2.3 Fourier Transform Infrared Spectroscopy (FT-IR) Measurement

A BOMEM Michelson Series 100 FT-IR spectrometer was used to identify and characterize structural changes in the crosslinked chitosan membranes. The experiments were run with air as the background and the resolution and number of scans were 4.0 cm^{-1} and 20 respectively. Films were sandwiched between rectangular sheets, whose insides were circularly cut. The sample thickness was between 20 - 50 μm.

5.2.4 Scanning Electron Microscopy (SEM) Experiment

The SEM experiment was carried out by using the same apparatus and procedure as described in Chapter 4 . The membrane samples were completely dried under vacuum before the SEM experiment. The thickness of the dried

samples was 50-70 μm.

5.2.5 Differential Scanning Calorimeter (DSC)

The glass transition temperatures (T_g) of the chitosan-poly(vinyl alcohol) blend membranes were measured by using a Thermal Analysis 2100 equipped with a DSC 2920. Samples size was between 2 to 5 mg. The samples were heated from 10 to 300 °C and cooled down from 300 to 10 °C at constant heating and cooling rate of 10 °C/min. During the experiments, helium gas was purged at a constant rate of 40 ml/min. The T_g measurements were based on the second run of the experiments.

5.2.6 Swelling Measurement

The predried membranes were immersed in water/isopropanol mixtures in closed bottles at room temperature for 2 days. The membranes were removed, pressed between Kimwipes tissue paper, and weighed immediately. The membranes were dried under vacuum at room temperature and weighed again.

The swelling degree was expressed as a relative weight increase;

$$Swelling\ degree = \frac{weight\ of\ swollen\ membrane}{weight\ of\ dry\ membrane}$$

5.2.7 Pervaporation Experiment

The apparatus for the pervaporation experiment and the chromatographic analysis were essentially the same as that used and specified in Chapter 3. The membrane performances were investigated in terms of selectivity and permeability.

5.3 Results and Discussion

5.3.1 Crosslinking of Chitosan Membranes

The solution technique modification of chitosan using HMDI in water was carried out to improve chitosan stability in aqueous solution. Being hydrophilic, chitosan is easily swollen in water. The swelling of chitosan promotes the penetration of HMDI into the chitosan polymer, making the crosslinking reaction possible. The $-NH_2$ groups on the chitosan molecule form an activated complex with water through strong hydrogen bonding. The activated complex then gives rise to the complex form with cyanate group on the HMDI to produce the structure of crosslinked chitosan membrane. Isocyanates undergo facile reactions with compounds containing active hydrogen [Saunders, 1964]. Therefore, in the crosslinking process, the diisocyanate reacts with the amine group to form urea linkages as illustrated in Scheme 5.2 [Damusis, 1971].

$$-N=C=O + RNH_2 \rightarrow -NH-\overset{\overset{O}{\|}}{C}-NH-R$$

Scheme 5.2 Reaction between cyanate and amine group to form urea

When chitosan is reacted with HMDI a crosslinked chitosan membrane as shown in Figure 5.1 is formed. The chemical reaction between chitosan and 1,6-Hexamethylene diisocyanate (HMDI) is believed to be similar to the type of reaction when chitosan is reacted with glutaraldehyde as reported by Uragami *et. al* [1994]. Depending on the extent of the crosslinking reaction, for the D-glucosamine unit in the chitosan molecule, there are

(1) a crosslinked structure between two cyanate groups in the HMDI molecule and two amino groups in the chitosan molecule,

(2) a pendant structure due to the reaction of cyanate group in the HMDI molecule with one amino group in the chitosan molecule,

(3) unreacted structure in the chitosan molecule

In Figure 5.2, the IR and absorption spectra of the unmodified and crosslinked chitosan membranes are shown. Figure 5.2 (a) shows the stretching vibration amide II band appears near 3220 cm^{-1}. For crosslinked chitosan membranes, the amide II bands appear near 3250 cm^{-1}. If a free cyanate group in the membrane exists, a strong absorption should appear around 2275-

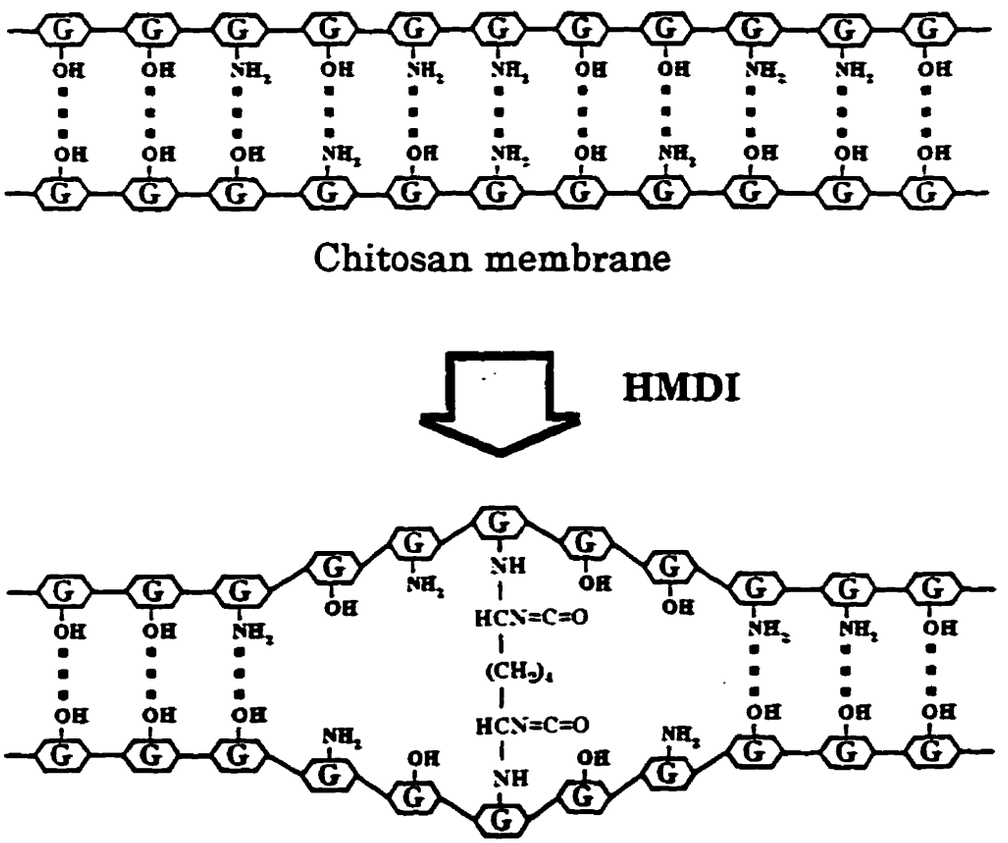
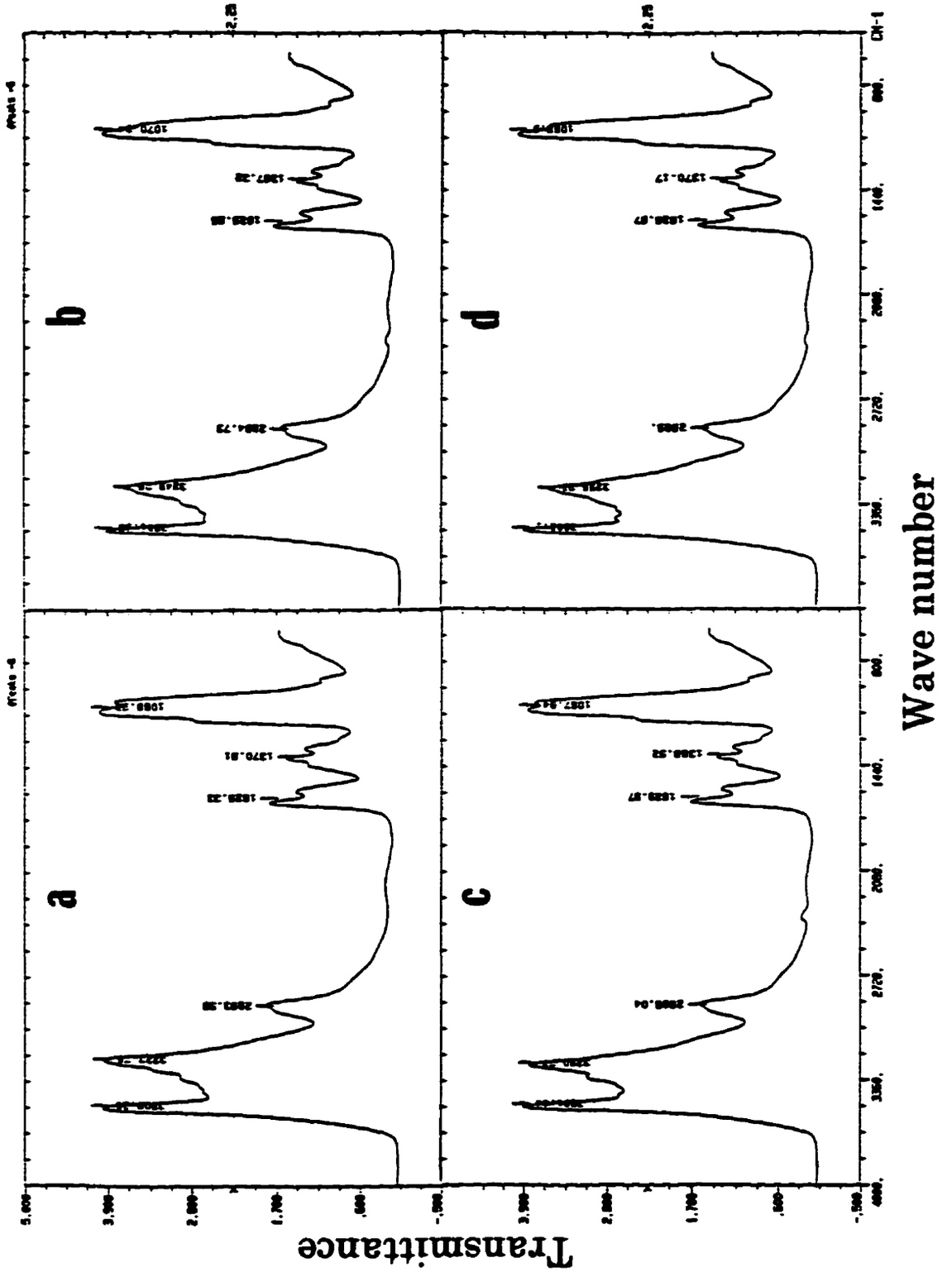


Figure 5.1 A model of the structural change between the chitosan membrane and the crosslinked chitosan membrane.

Figure 5.2 Fourier transform infrared spectroscopy (FT-IR) spectra of the chitosan and crosslinked chitosan membranes :
(a) unmodified, (b) 24-hr-crosslinked, (c) 30-hr-crosslinked, and (d) 48-hr-crosslinked chitosan membranes.

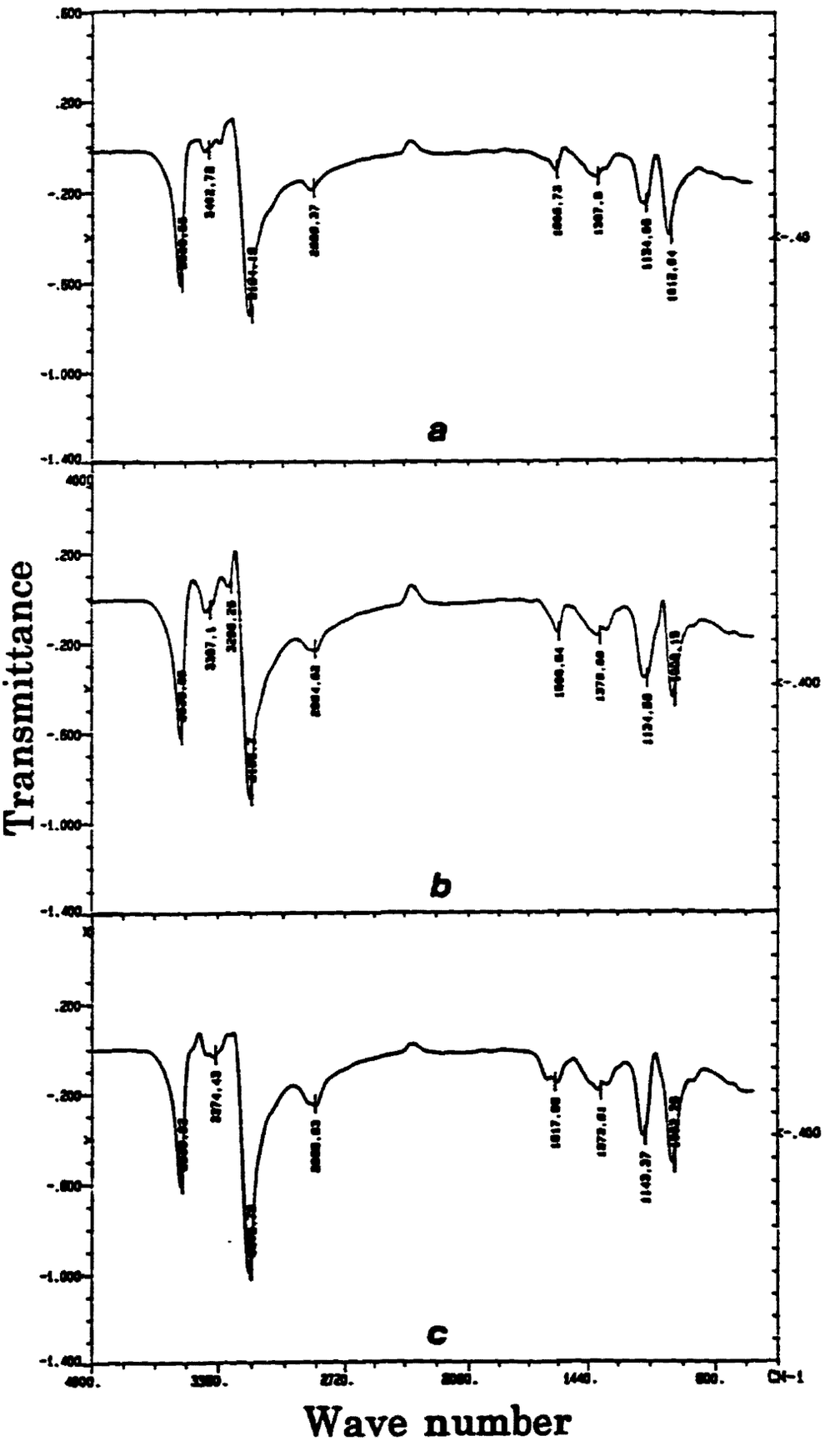

a
b
c
d
Transmittance
Wave number

2250 cm^{-1}. Such an absorption band, however, can not be even observed in any of the crosslinked chitosan membranes. These results suggest that there no free cyanate groups, i.e., there is no pendant structure in the crosslinked membranes.

One of the spectral processing operations most widely used in polymer analysis is the digital substraction of absorbance spectra in order to reveal or emphasize subtle differences between two samples or a sample and a reference material. When a polymer is examined before and after a chemical or physical treatment, and substraction of original spectrum from the final spectrum is done, positive absorbances (negative transmittances) reflect the structures that are formed during the treatment and negative absorbance (positive transmittances) reflect the loss of structure [Koenig, 1984]. The resulted IR and absorption for the crosslinked chitosan membranes are shown in Figure 5.3. The negative transmittances indicate formation of structures due to the reaction between the chitosan and HMDI. Among others, functional group C=N absorbs in 1700 to 1615 cm^{-1} [Pasto and Johnson, 1979] and Figure 5.3 (a), (b), and (c) show the appearances of the absorption bands at around 1600, which increase relatively with crosslinking time. These observations support the existence of the crosslinked structure between the chitosan-HMDI molecules.

Functional group RNH_2 absorbs 3500-3400 cm^{-1}, and such and

Figure 5.3 The resulting FT-IR subtraction spectra for the crosslinked chitosan membranes after : (a) 24 hr crosslinking, (b) 30 hr crosslinking, and (c) 48 hr crosslinking.


Transmittance
Wave number
a
b
c
4000.
3200.
2400.
1600.
800.
CM-1

absorption band can be clearly seen Figure 5.3. Interestingly, the absorption bands increase with an increase in the reaction time (from 24 to 30 hours) and then decrease with further increase in reaction time (from 30 to 48 hours). These results suggest that the crosslinking agent has reacted with the $-NH_2$ groups of chitosan and the reaction between the chitosan and the cyanate molecules is time dependent, i.e., the relative degree of crosslinking is dependent on the reaction time. Since the chemical crosslinks are obtained by treating the chitosan membrane in a HMDI solution, the formation of the crosslinked structures, thus the degree of crosslinking, is controlled by the membrane treatment time. This is understandable since the reaction first occurs at the surface of the chitosan membrane and then proceeds across the membrane, i.e., the penetration of the HMDI molecules increases with the crosslinking time.

Table 5.1 summarizes the relative intensity of the IR peaks for three different types of chitosan membranes. Not unexpectedly, the data indicate that the formation of the different structures increases relatively with an increase in the reaction time. The facts that the -N=C=O group in isocyanate prepolymers is highly reactive and polymerizable [Deanin, 1972] and that isocyanates react with amine groups at a sufficient rate at room temperature to cause crosslinking in a short time [Trafara, 1980] suggest that the

Table 5.1 Relative IR peaks intensity for crosslinked chitosan membranes

Wavenumber Range	Relative Intensity[a]		
	Type I[b]	Type II[c]	Type III[d]
1000-1013	-0.391	-0.452	-0.519
1134-1144	-0.251	-0.367	-0.399
1373-1388	-0.134	-0.176	-0.196
1598-1618	-0.105	-0.158	-0.159
2884-2890	-0.191	-0.233	-0.252
3194-3203	-0.743	-0.886	-0.991
3374-3403	-0.019	-0.058	-0.032
3538-3540	-0.606	-0.617	-0.605

[a]Relative Intensity : Treated - Unmodified
[b]Type I : Treated in HMDI solution for 24 hours
[c]Type II : Treated in HMDI solution for 30 hours
[d]Type III : Treated in HMDI soltuion for 48 hours

structures were formed by the crosslinking reaction between isocyanate groups on HMDI molecules and amine groups on chitosan molecules and the degree of crosslinking increases with the reaction time.

5.3.2 Polymer Blending of Chitosan-Poly(vinyl alcohol) (CS-PVA)

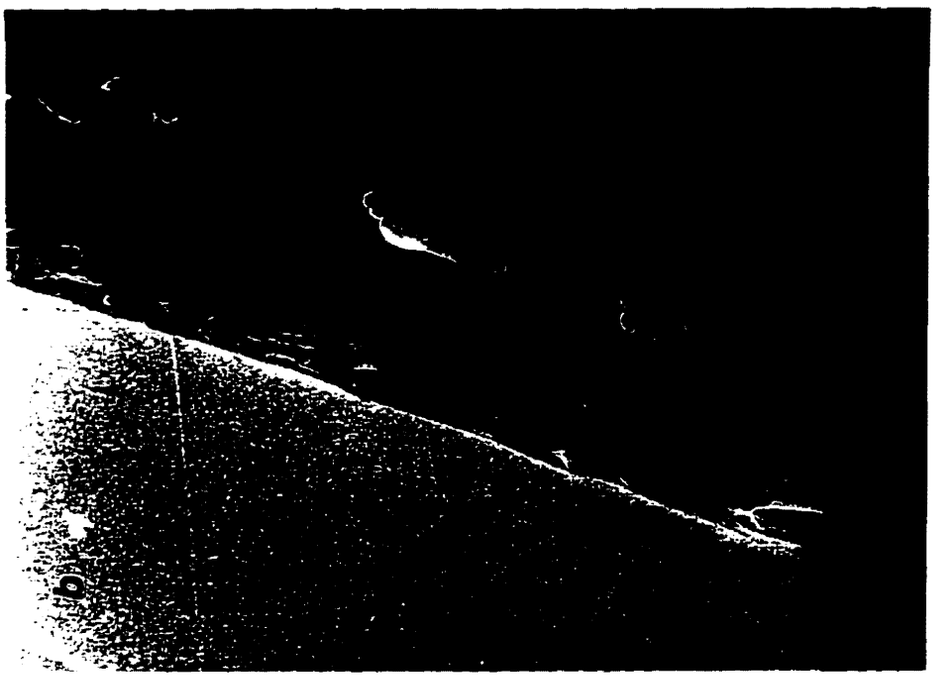
The blends of chitosan-poly(vinyl alcohol) are homogeneous for the whole range of chitosan and poly(vinyl alcohol) concentrations. The blend membranes investigated in this work are smooth, physically strong and transparent. Chitosan is insoluble in water, however, PVA is water soluble. The CS-PVA blended membrane shows better characteristics with respect to physical strength, stability and resistance to water, in comparison with both PVA and CS membranes.

As shown by SEM in Figure 5.4, no obvious phase segregation phenomenon is observed. Strong hydrogen bonding between hydroxyl groups on PVA structure and amino groups on chitosan structure apparently provides sufficient driving force for the miscibility of the blends. The compatibility of polymer blends is promising when the T_g of the polymer blends is single and constant, generally between the T_g's of the two individual components.

In this study, DSC was used to measure transitions in the polymer

Figure 5.4 SEM photograph of CS-PVA blended membranes :

(a) 5:5 CS to PVA weight ratio; (b) 8:2 CS to PVA weight ratio.





blends and hence to test the compatibility of the CS-PVA blends. Typical results are shown in Figure 5.5 and the data as summarized in Table 5.2 show that the different ratios of CS and PVA have different single T_g's, and are between the T_g of CS and the T_g of PVA.

Table 5.2 Glass Transition Temperature of CS-PVA Blends Membranes

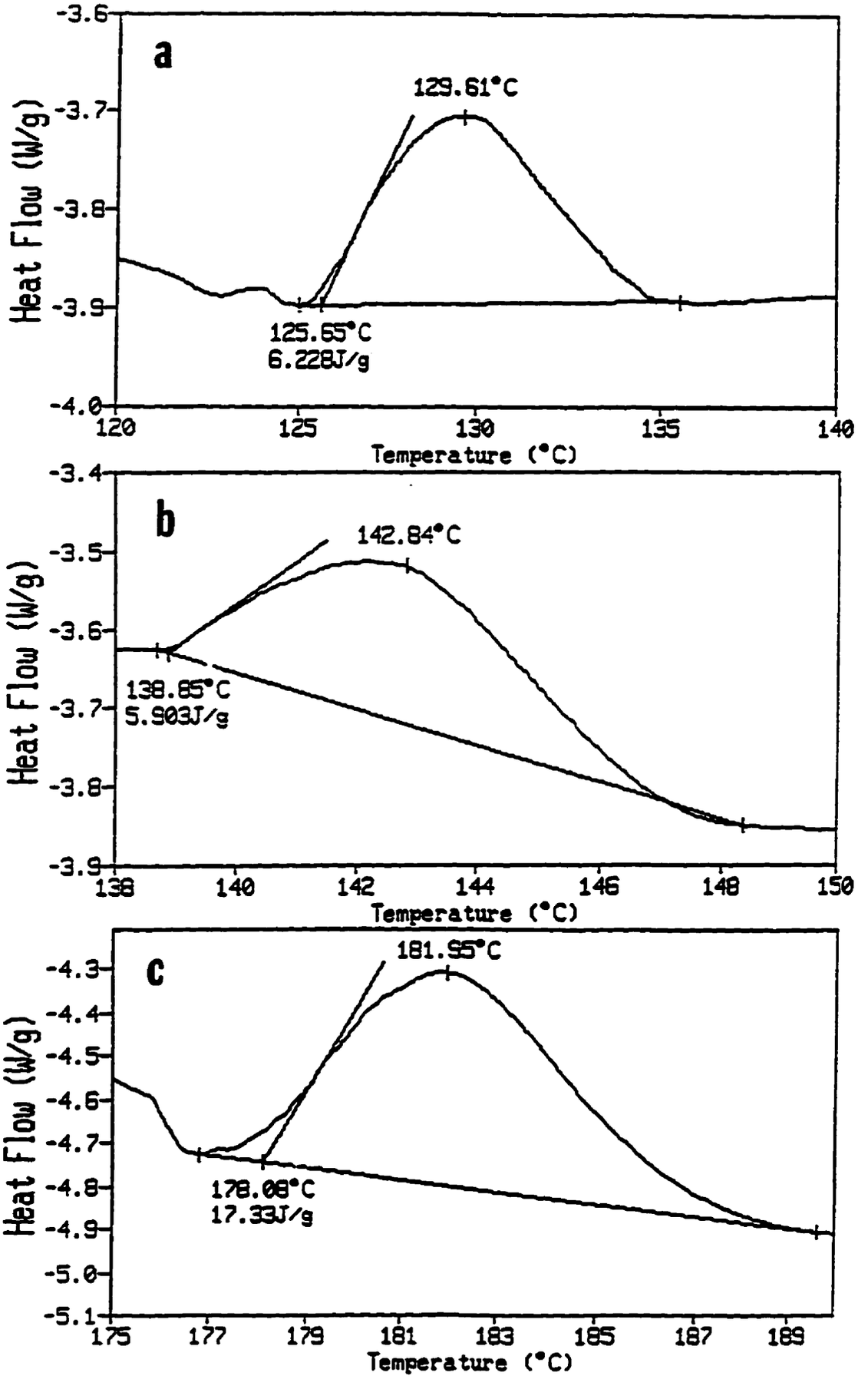
CS content in polymer blend (wt %)	0	10	30	70	100
T_g (°C)	205	178	139	126	101

The thickness of the membranes varies with the weight ratios of the chitosan and PVA in the polymer blends. This is understandable because as the chitosan weight percent in the polymer blends increases, the total polymer concentration in the casting solutions decreases, thus decreases the thickness of the dried membrane. Note that, no apparent structural differences could be observed under the SEM as the chitosan content in the polymer blends was varied from 10 to 90 wt. %.

5.3.3 Relative Degree of Swelling

Figure 5.6 shows the relative degree of swelling of the crosslinked

Figure 5.5 The Differential scanning calorimeter (DSC) thermogram of some of the blended CS-PVA films. Weight fraction of chitosan (a) 70 %, (b) 30 %, and (c) 10 %.


a
129.61°C
125.65°C
6.228J/g
Heat Flow (W/g)
-3.6
-3.7
-3.8
-3.9
-4.0
120
125
130
135
140
Temperature (°C)
b
142.84°C
138.85°C
5.903J/g
Heat Flow (W/g)
-3.4
-3.5
-3.6
-3.7
-3.8
-3.9
138
140
142
144
146
148
150
Temperature (°C)
c
181.95°C
178.08°C
17.33J/g
Heat Flow (W/g)
-4.3
-4.4
-4.5
-4.6
-4.7
-4.8
-4.9
-5.0
-5.1
175
177
179
181
183
185
187
189
Temperature (°C)

chitosan membranes as a function of the membrane treatment time. As expected, the swelling degree of the membranes decreases relatively with an increase in isopropanol concentration, which indicates that the crosslinked membrane has a better affinity with water than with isopropanol. However, more importantly, Figure 5.6 shows that the degree of swelling of the crosslinked membranes decreases relatively with an increase in the membrane treatment time. These results are consistent with the FT-IR experiments which indicate that the degree of crosslinking increases with the crosslinking reaction time. As the crosslinking density increases (with time), the membrane becomes more compact and thus less permeable to penetrant molecules. In terms of hydrophilic balance of the membranes, the crosslinking of the chitosan membrane, which is induced by the reaction of $-NH_2$ groups on the chitosan molecule, reduces the total hydrophilicity ability of the membrane surface. As a result, the membrane affinity with water decreases and the membrane becomes less permeable to water ; the swelling decreases.

Note that swelling measurement is widely used to determine the degree of crosslinking experimentally. However, in many cases experimental values do not agree with the degree of crosslinking calculated from knowledge of the chemistry of the crosslinking reaction. Reasons for this deviation include the simplifying assumptions made in deriving the relationships between

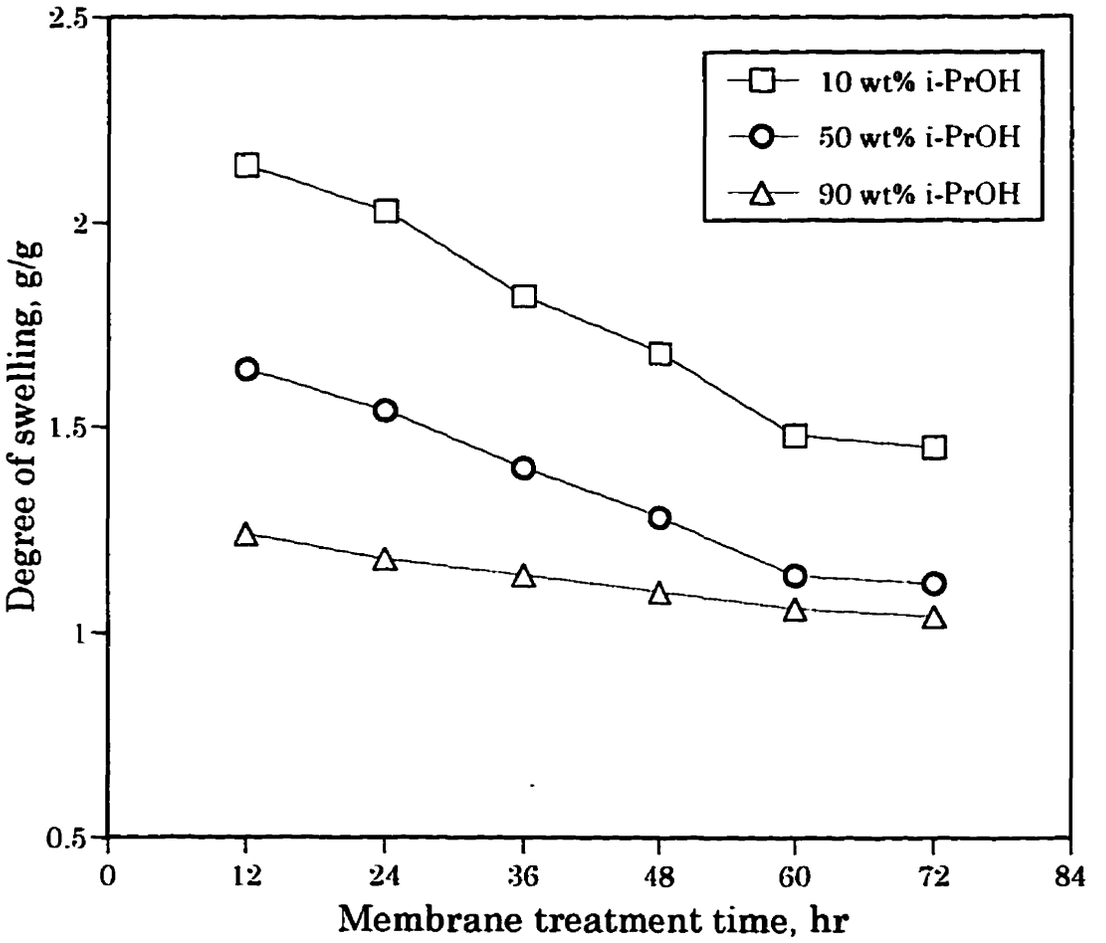


Figure 5.6 **The swelling degree of chitosan membranes as a function of membrane treatment time.**

swelling properties and crosslink density. For example, it is argued that not all chemical bonds connecting polymer chains together are mechanically effective. The presence of a finite length of dangling chain leads to a lower degree of measured crosslink density. On the other hand, trapped entanglements of infinite chain lead to higher values of crosslink density [Pearson, 1968]. Therefore, it is rather difficult and misleading to measure quantitatively the degree of crosslinking of the chitosan polymer membranes.

5.3.4 Pervaporation with Chemically Crosslinked Chitosan Membranes

The chemically crosslinked chitosan membranes were investigated for the pervaporation separation of isopropanol from water mixtures. The pervaporation performances of the chemically crosslinked chitosan membrane in comparison with the unmodified chitosan membrane are shown in Figures 5.7 - 9. Comparably, the permeability of the membranes decreases while the separation factor increase with an increase in feed isopropanol concentration. At high water concentration, the membranes would be comparatively more swollen and enable the nonpreferential components to enter the polymer matrix and diffuse through the membrane. As expected, for the entire range of feed isopropanol concentration, the permeation flux of the crosslinked

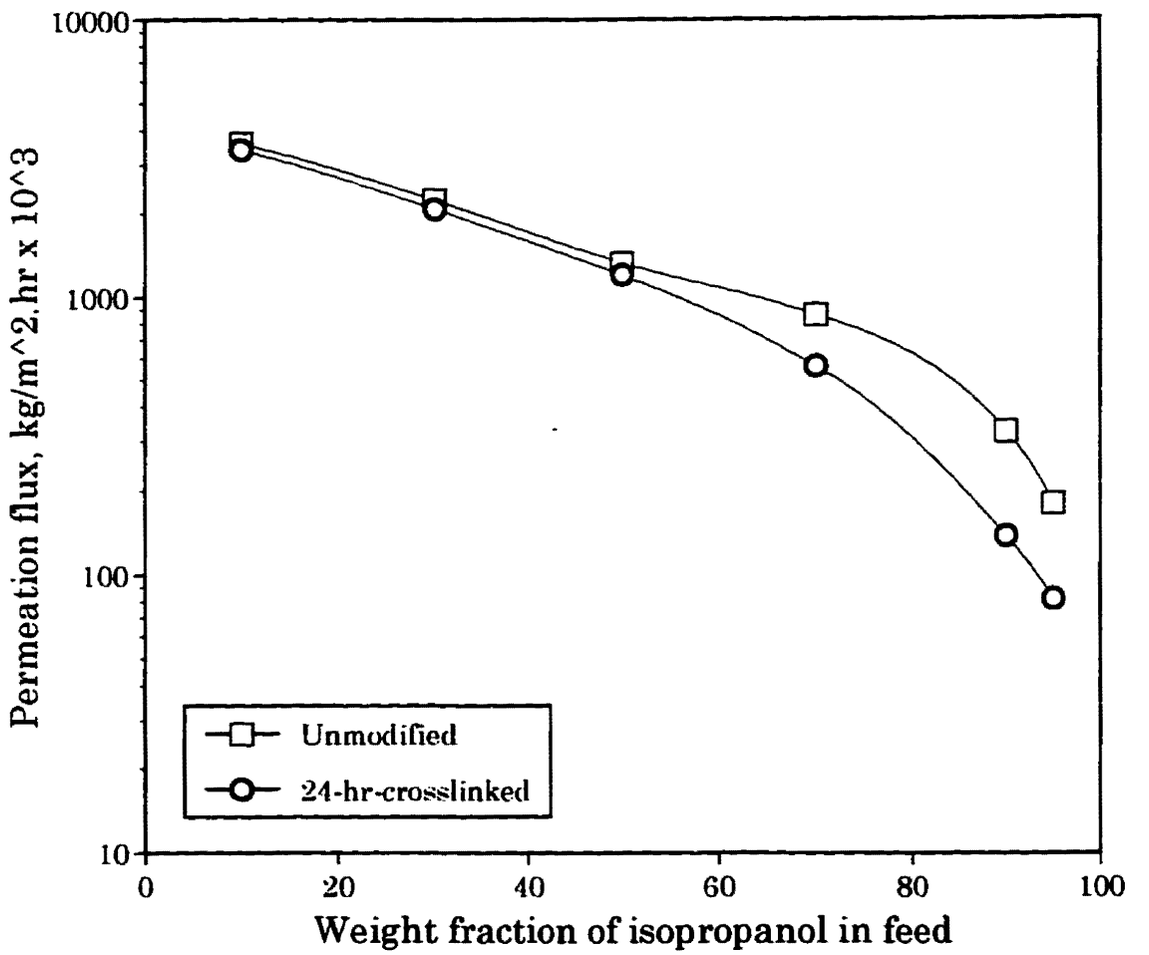


Figure 5.7 The total permeation fluxes for crosslinked and uncrosslinked chitosan membranes versus feed composition.

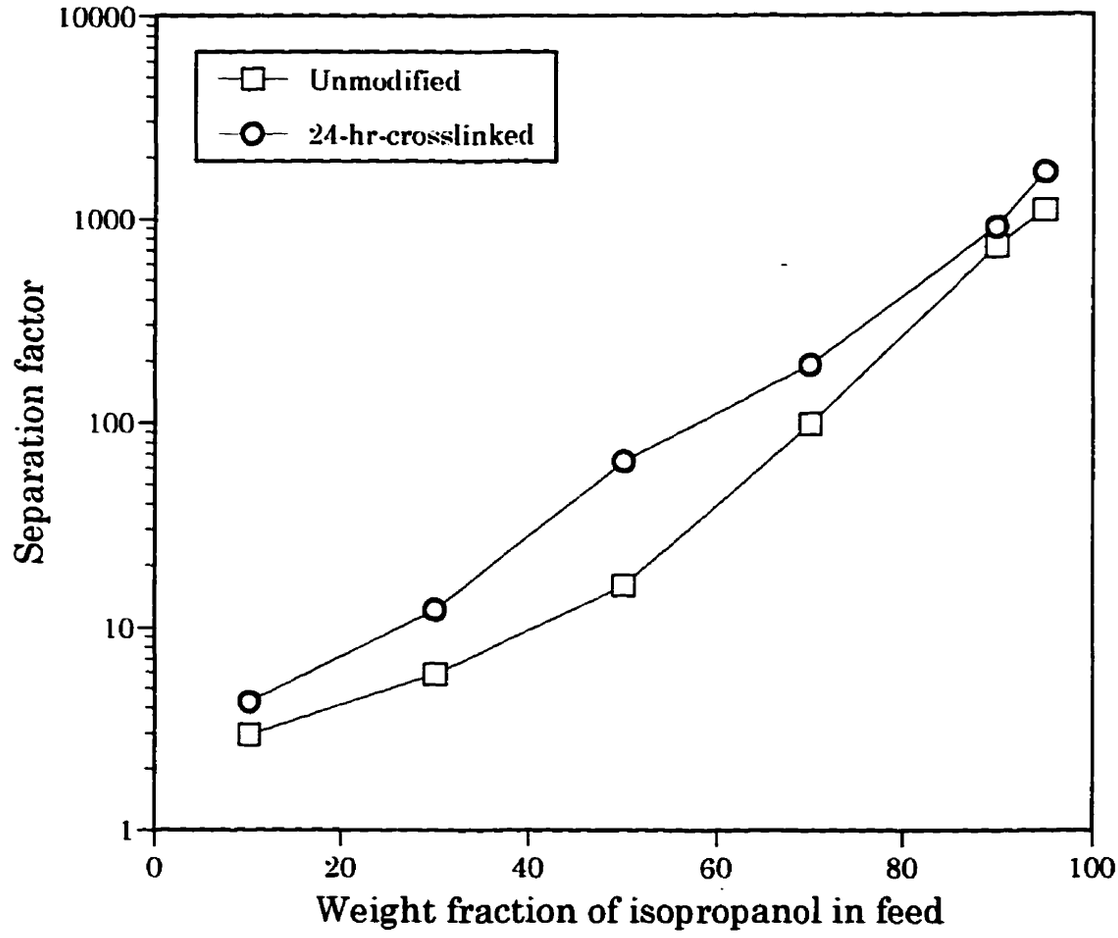


Figure 5.8 **The separation factor for the crosslinked and uncrosslinked chitosan membranes versus feed composition.**

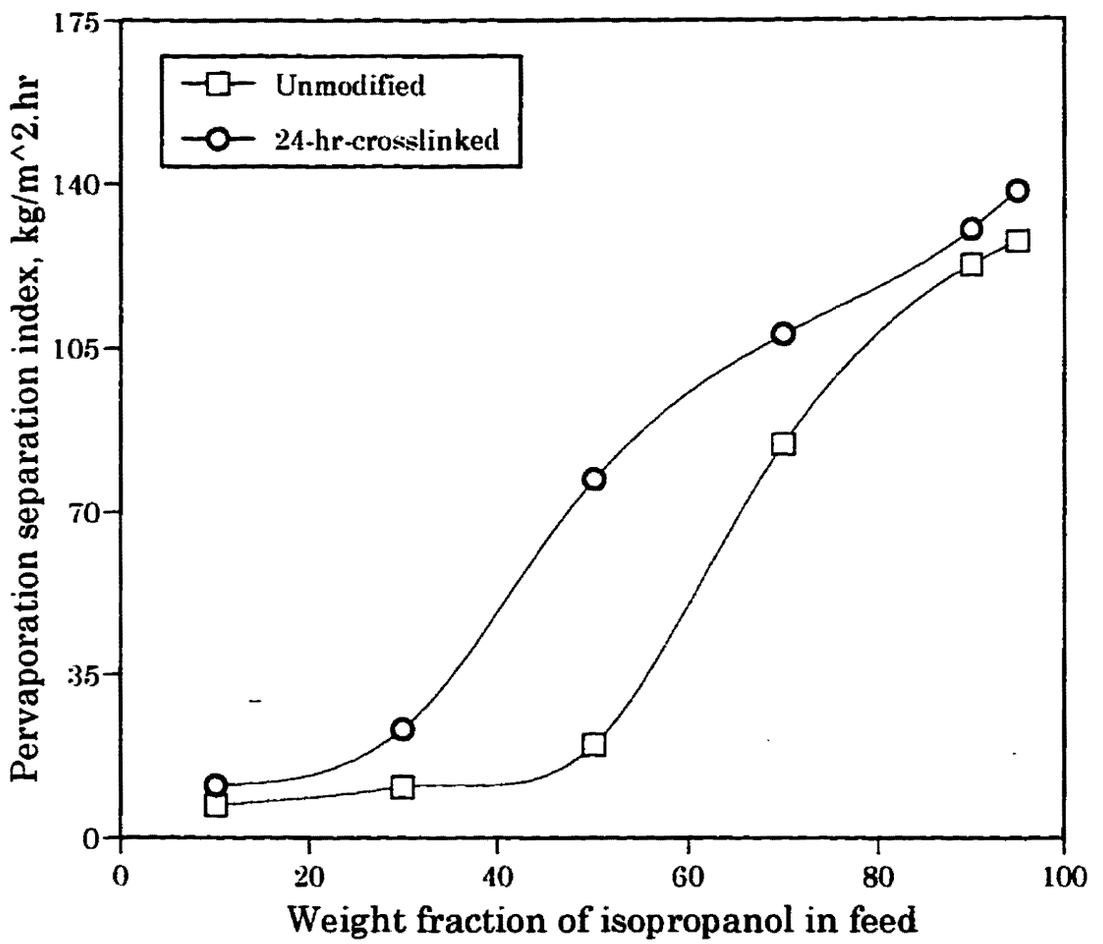


Figure 5.9 The pervaporation separation index for the crosslinked and uncrosslinked chitosan membranes versus feed composition.

membrane is lower than that of unmodified membrane, but the separation factor of the former is higher and that of the latter.

In general, crosslinking leads to the formation of strong primary homopolar covalent bonds between polymer molecules which converts them into large three-dimensional crosslinked networks, and pulls the molecular chain closer together, leaving less free volume [Deanin, 1972]. As shown in Figure 5.6, crosslinking reduces the swelling of the chitosan membranes. The crosslinking of chitosan reduces their segments mobility to the point that sorption and diffusion of the permeants in the polymeric matrix are both reduced, and thus the permeability is reduced and separation factor is increased for both reasons.

The overall performance of the crosslinked chitosan relative to the unmodified chitosan membranes measured qualitatively in terms of the pervaporation separation index is shown in Figure 5.9. The results indicate that crosslinking improves the overall pervaporation performance of the chitosan membrane for the entire composition of the isopropanol/water mixtures. Consequently, it may be manifested that the chemical modification technique is a useful and effective tool in improving the overall pervaporation characteristics.

Figures 5.10 and 5.11 show the effects of the membrane treatment time on the pervaporation performance of the crosslinked membranes for the

separation of 90 weight percent of isopropanol in water. In general, the permeability decreases and the separation factor increases with an increase in membrane treatment time; the permeation flux decreases linearly and more significantly when the membrane treatment time is less than 36 hours after which a saturation point is reached, while the separation factor increases almost linearly and more significantly when the treatment time is less than 48 hours after which a saturation point is reached and the membranes exhibit no significant change in their respective properties.

The crosslinking of the chitosan membranes was carried out via the solution technique so that the relative degree of crosslinking was qualitatively controlled by the membrane treatment time. The crosslinking reactions occur through the diffusion of the HMDI into the chitosan membrane network and interacts with the amine groups, from the membrane surface across the membrane. Upon increasing the membrane treatment time, the chain mobility of the chitosan molecules in the membrane may be reduced due to the high concentration of crosslinks, resulting in low flux. As the crosslinking reaches a saturation point, crosslinks forming on many, most or even all of the monomer units in the polymer chains, and these highly crosslinked polymers are more completely three-dimensional networks, leaving very little mobility for the polymer molecules. Consequently, the diffusion of penetrants decreases rapidly as the crosslinking approaches the saturation point.

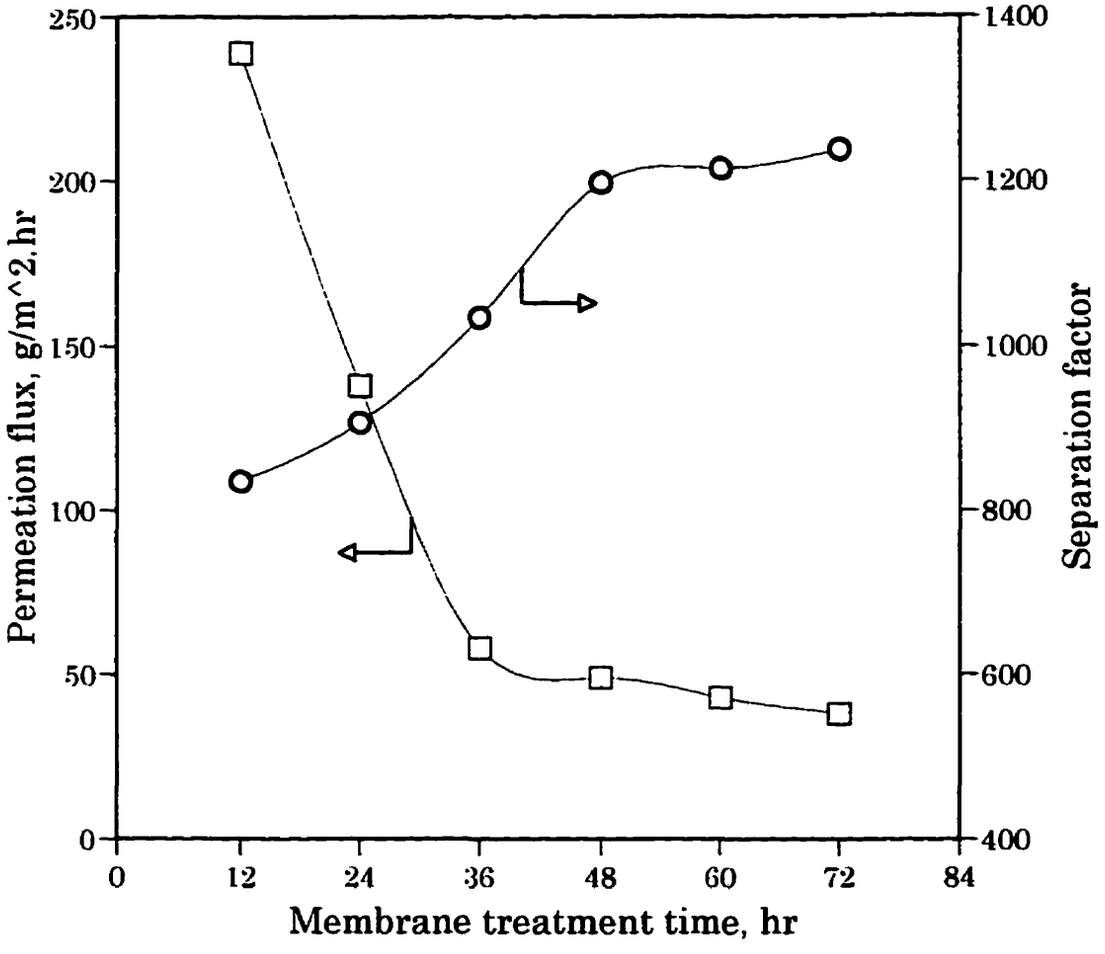


Figure 5.10 **The pervaporation data of the crosslinked membranes as a function of the membrane treatment time. Feed isopropanol concentration: 90 wt.. %.**

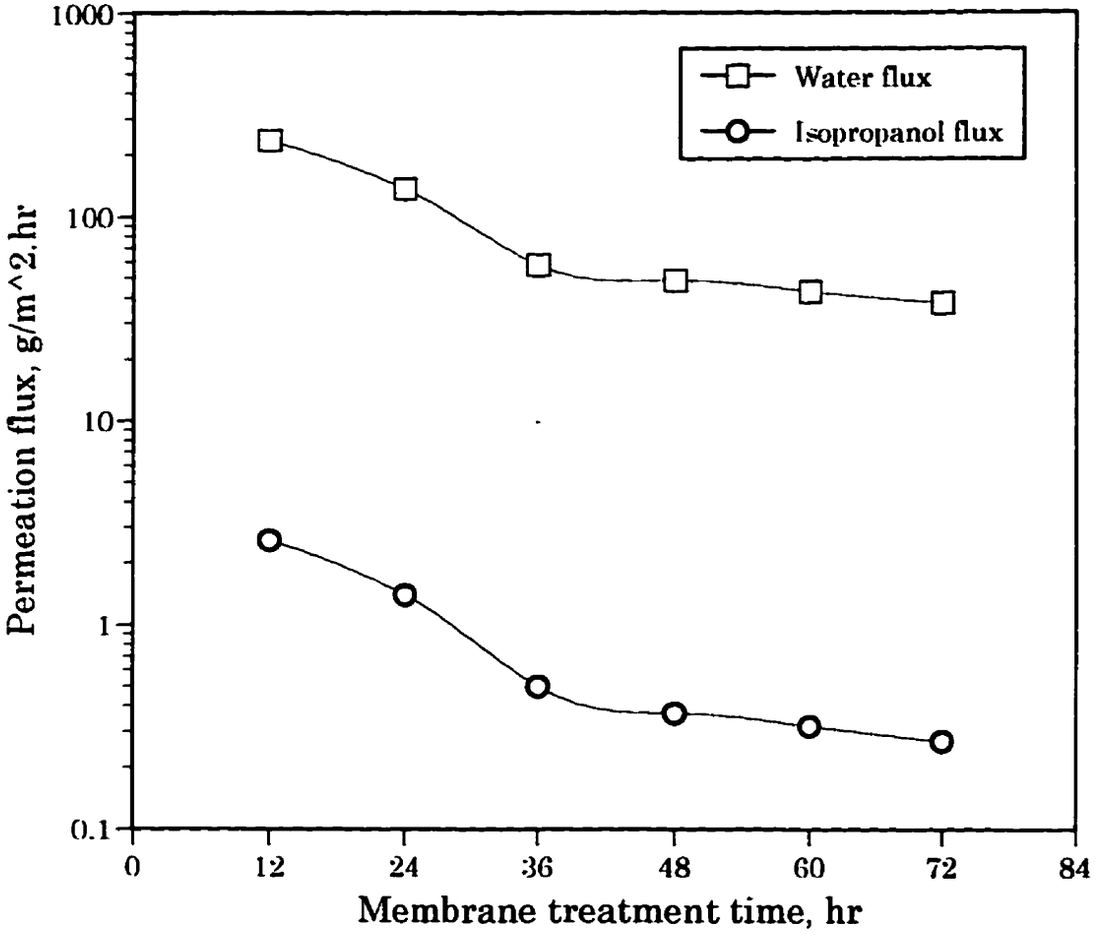


Figure 5.11 **The individual fluxes for the crosslinked chitosan membranes as a function of the membrane treatment time. Feed isopropanol concentration: 90 wt. %.**

The shrinkage of the free volume available to the polymer matrix and the fact that molecular size of isopropanol is larger than that of water may be responsible for the increase in the separation factor with an increase in membrane treatment time. This is not surprising since generally the permeation flux and the permselectivity are in conflict in membrane processes; an increase in permeability normally leads to decrease in selectivity, and *vice versa*.

5.3.5 Pervaporation with CS-PVA Blends Membranes

The performance of CS-PVA blends membranes was investigated in terms of their permeation flux and separation factor for the separation of isopropanol/water mixtures. Figures 5.12 shows the pervaporation characteristics in the CS-PVA blended membranes. The feed solution was fixed at 10 wt.. % water. The total permeation flux increases almost linearly with an increase in the chitosan content the polymer membrane. This may be attributed to a decrease in the density of blended membrane; the membranes were prepared by mixing 0.5 wt. % CS in aqueous acetic acid with 10 wt. % PVA in water, thus an increase in the CS to PVA ratio leads to a relative decrease in the total polymer concentration. As the membrane becomes relatively less dense and the polymer network becomes more loose, thus

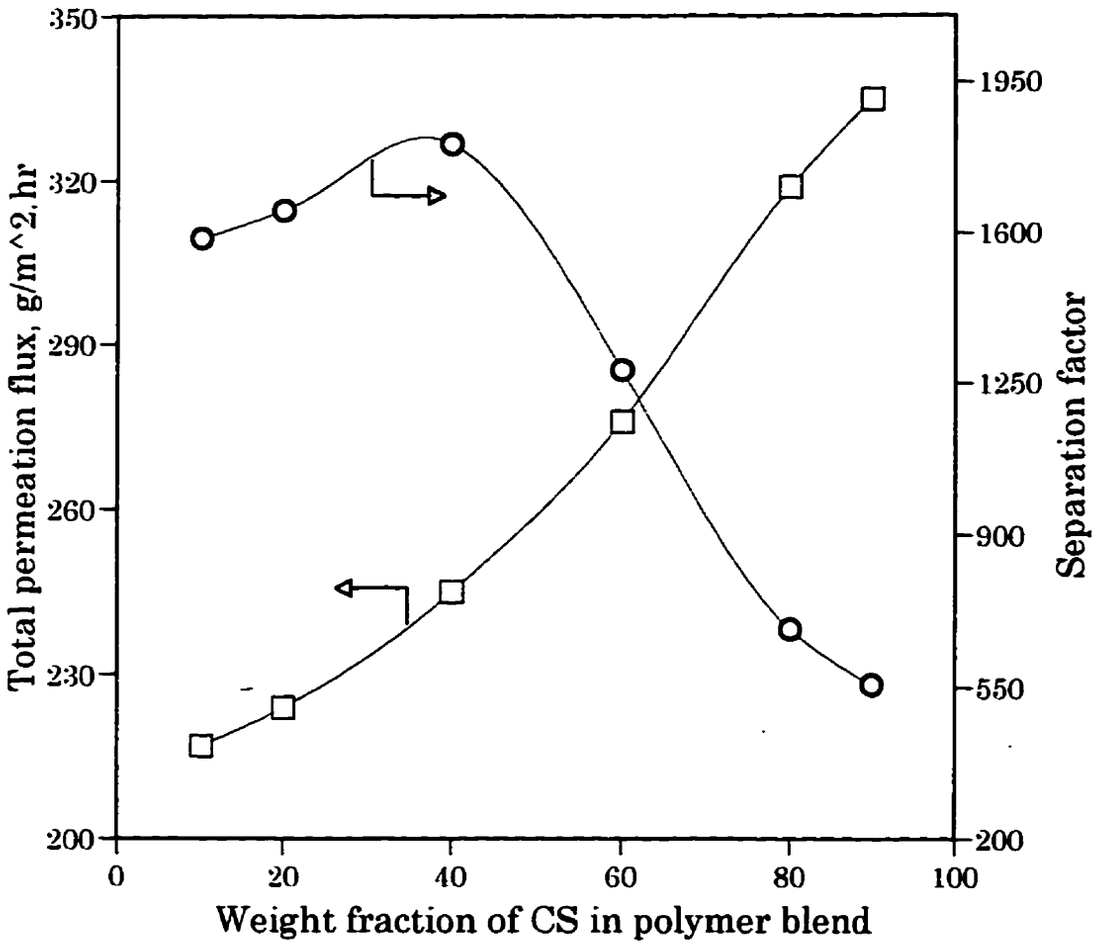


Figure 5.12 The pervaporation data for the CS-PVA blended membranes as a function of blend compositions. Feed isopropanol concentration: 90 wt. %.

imparting greater segmental mobility and larger free volume, consequently the permeation increases. However, the loosening of the polymer network makes the membranes less selective. In fact, the permselectivity increases initially with CS content, passes through a maximum at chitosan content around 40 wt. %, and then decreases. The increase of the permselectivity at lower CS content seems to be related to plasticization effect of chitosan for water to permeate.

Figure 5.12 also suggests that appropriate blend ratios are necessary to fully utilize the potential of CS-PVA blended membrane for the pervaporation separation of isopropanol/water mixtures, especially at feed isopropanol concentrations higher than the azeotrope mixture The CS content of 40 wt. % was chosen for subsequent studies since maximum overall pervaporation characteristics measured in terms of PSI as illustrated in Figure 5.13, is obtained at this blend composition.

Figures. 5.14 and 5.15 show the sorption and pervaporation data as a function of feed isopropanol concentration for the CS-PVA membrane with a 40:60 blend composition. Interestingly, both the sorption and permeation plots of isopropanol show maximum points at isopropanol concentration around 30 - 40 wt. %. These results indicate that the aqueous isopropanol solution extensively swells the blended membranes, and exerts a very strong plasticization effect on the membrane. However, the sorption and permeation

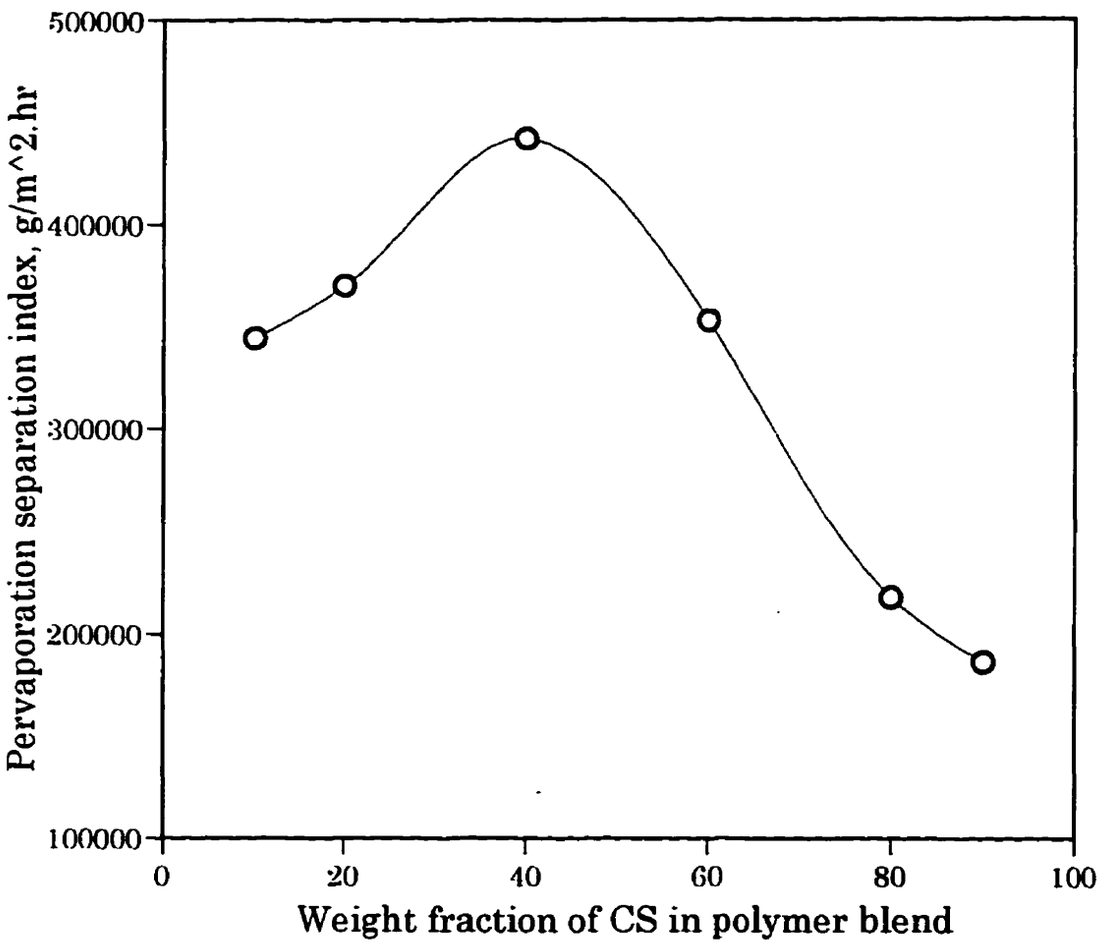


Figure 5.13 The pervaporation index for the CS-PVA membranes as a function of blend compositions. Feed isopropanol concentration: 90 wt. %.

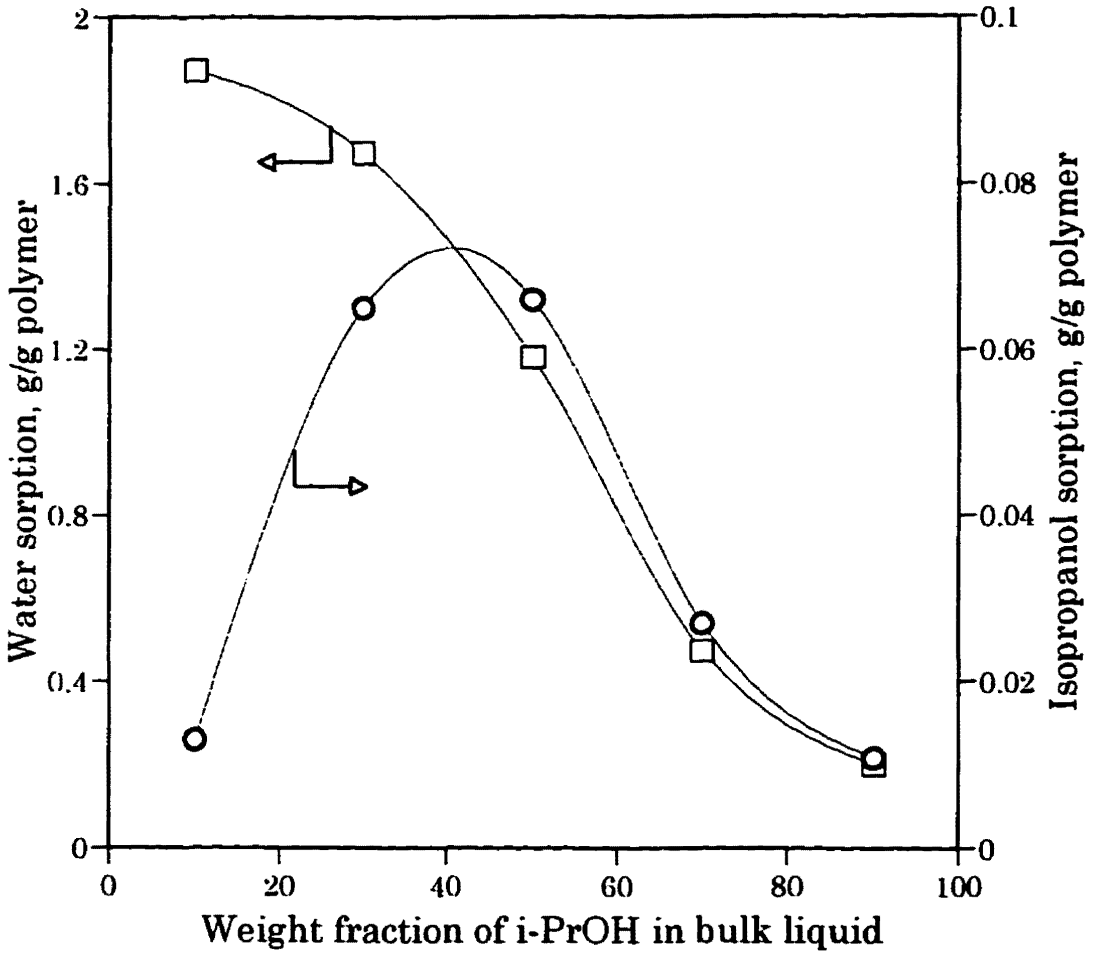


Figure 5.14 The individual sorptions for the CS-PVA blended membrane versus feed composition. Blend composition: 40/60.

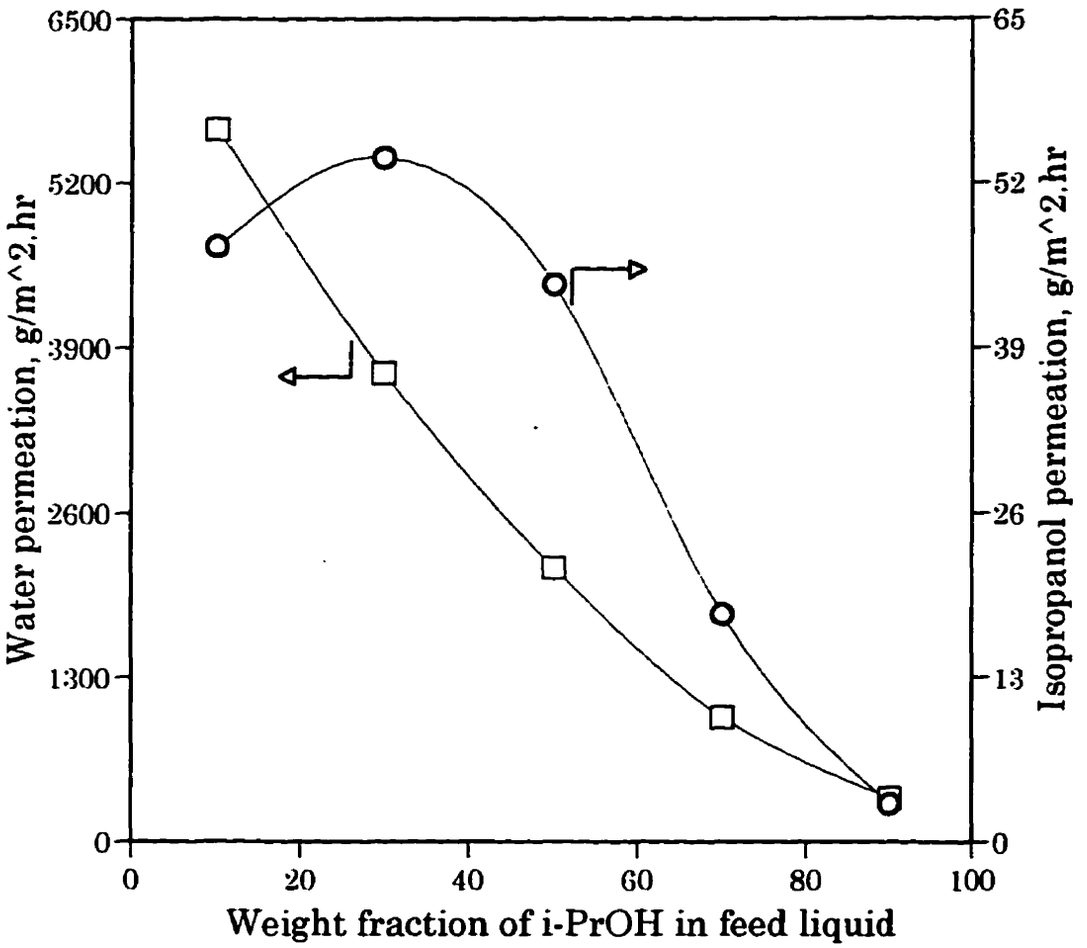


Figure 5.15 The individual permeation for the CS-PVA blended membrane versus feed composition. Blend composition: 40/60.

plots of water show no such phenomenon. As can be seen, for the entire isopropanol concentration, the water sorption is significantly higher than the isopropanol sorption, which suggest that water is preferentially sorbed. Figure 5.16 shows the separation factor and the sorption selectivity of the blended membrane as function of feed composition. Note that for the entire feed composition, both the separation factor and sorption selectivity are significantly higher than unity. Therefore, the selective sorption of isopropanol/water mixtures in the membrane contributes to preferential permeation of the water component positively for the whole range of isopropanol concentrations. Also, as in the case of homogeneous chitosan previously discussed in Chapter 3, the separation factor of pervaporation is higher than the sorption selectivity, indicating that water molecules are more mobile in the membrane than isopropanol molecules.

In light of the permeability-selectivity trade-off, the PSI is used to evaluate the pervaporation performance of the blended membrane in comparison with the homogeneous chitosan membrane. Figure 5.17 is a plot of the PSI versus the feed composition. It is shown that the PSI tends to increase with an increase in the feed isopropanol concentration. More importantly, the PSI for the CS-PVA membrane is higher than that for the homogeneous CS membrane, indicating the effectiveness of polymer blending technique to improve the overall pervaporation performance of chitosan membranes for the

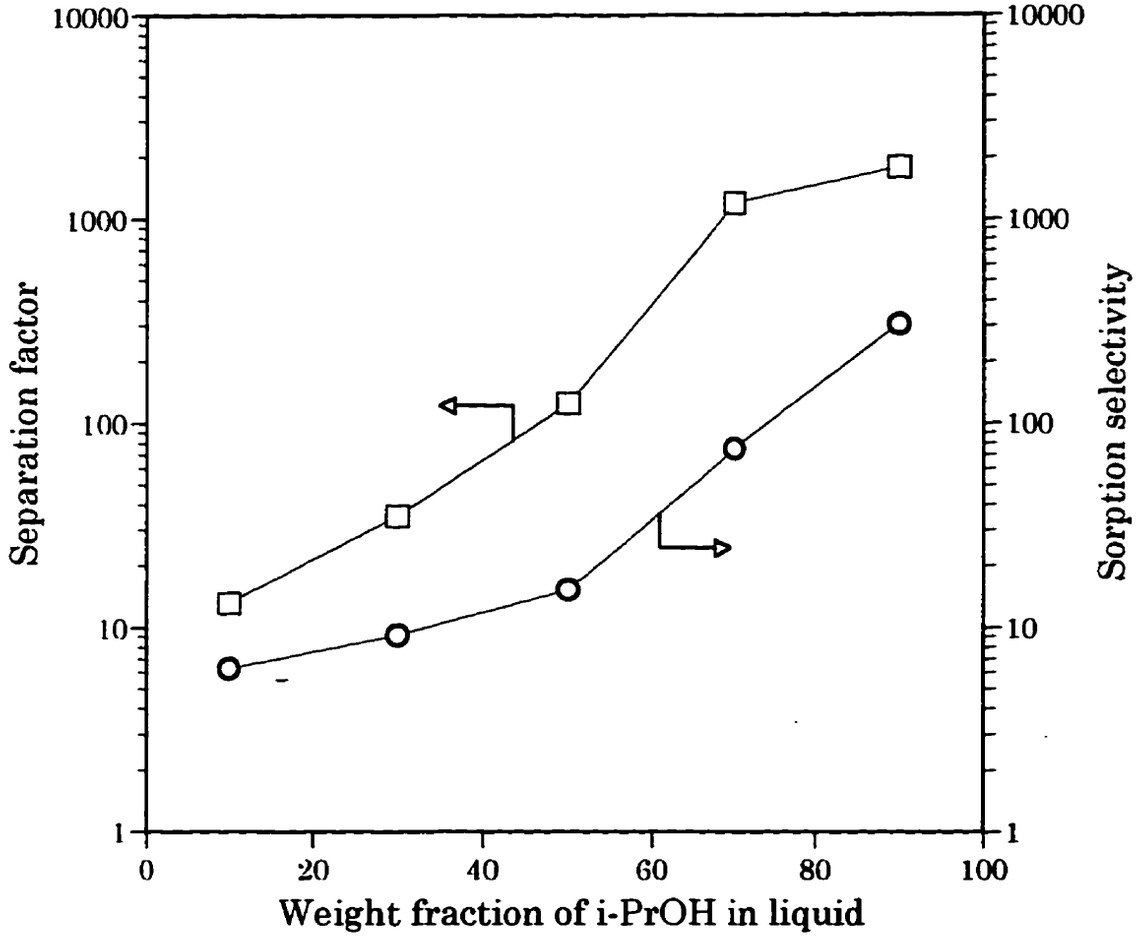


Figure 5.16 The separation factor and sorption selectivity of the CS-PVA blended membrane versus feed composition. Blend composition: 40/60.

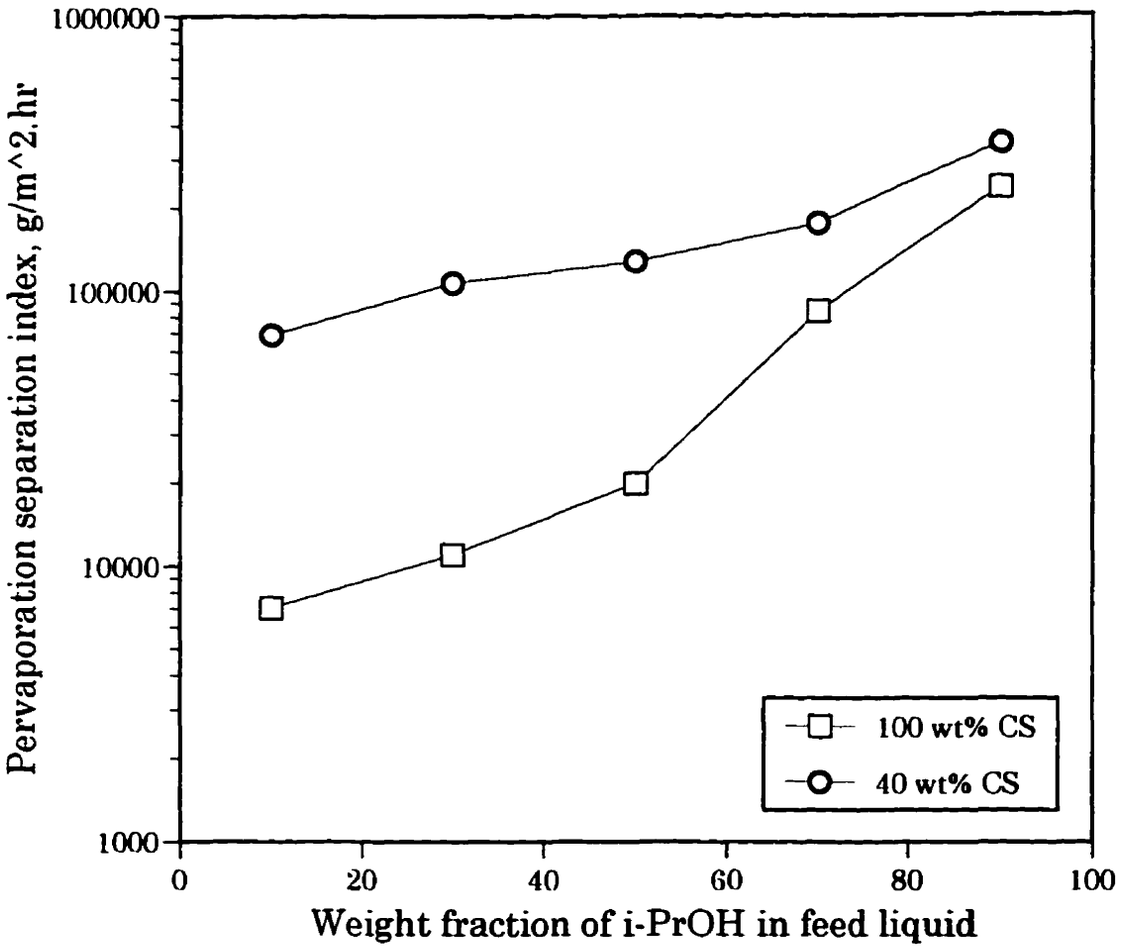


Figure 5.17 The pervaporation separation index of chitosan membranes as a function of feed composition.

separation of isopropanol/water mixtures. It has to be noted however that, at high feed isopropanol concentrations, the PSI values for the two types of membranes do not differ significantly since a high selectivity is compensated for by a low permeability, or *vice versa*. These results are of special importance for effective pervaporation separation of isopropanol/water mixtures since the azeotrope of isopropanol water is located at about 88 wt. % isopropanol and the fact that the blend compositions of the CS-PVA membranes can be adjusted according to the priority of separation objectives; to obtain optimal selectivity with a minimal sacrifice in permeability, or *vice versa*. A specific example of pervaporation of isopropanol/water mixtures using polymeric membranes mixtures is pervaporation dehydration of 6,000 l/d of isopropanol to allow in-plant recycle as a cleaning agent in compact disk manufacturing [Koros, 1995]. In this case, the ultimate objective of the separation is to produce high purity of isopropanol solvent, so selectivity is the determining criteria of the separation.

The membrane was further tested for the dehydration of 90 wt. % isopropanol aqueous solution at elevated temperatures. The experimental results are illustrated in Figure 5.18 where the pervaporation data are plotted against the reciprocal of the operating temperature. In general, temperature leads to a higher permeation flux and a lower separation factor. The temperature dependence of the permeation flux seems to follow an Arrhenius

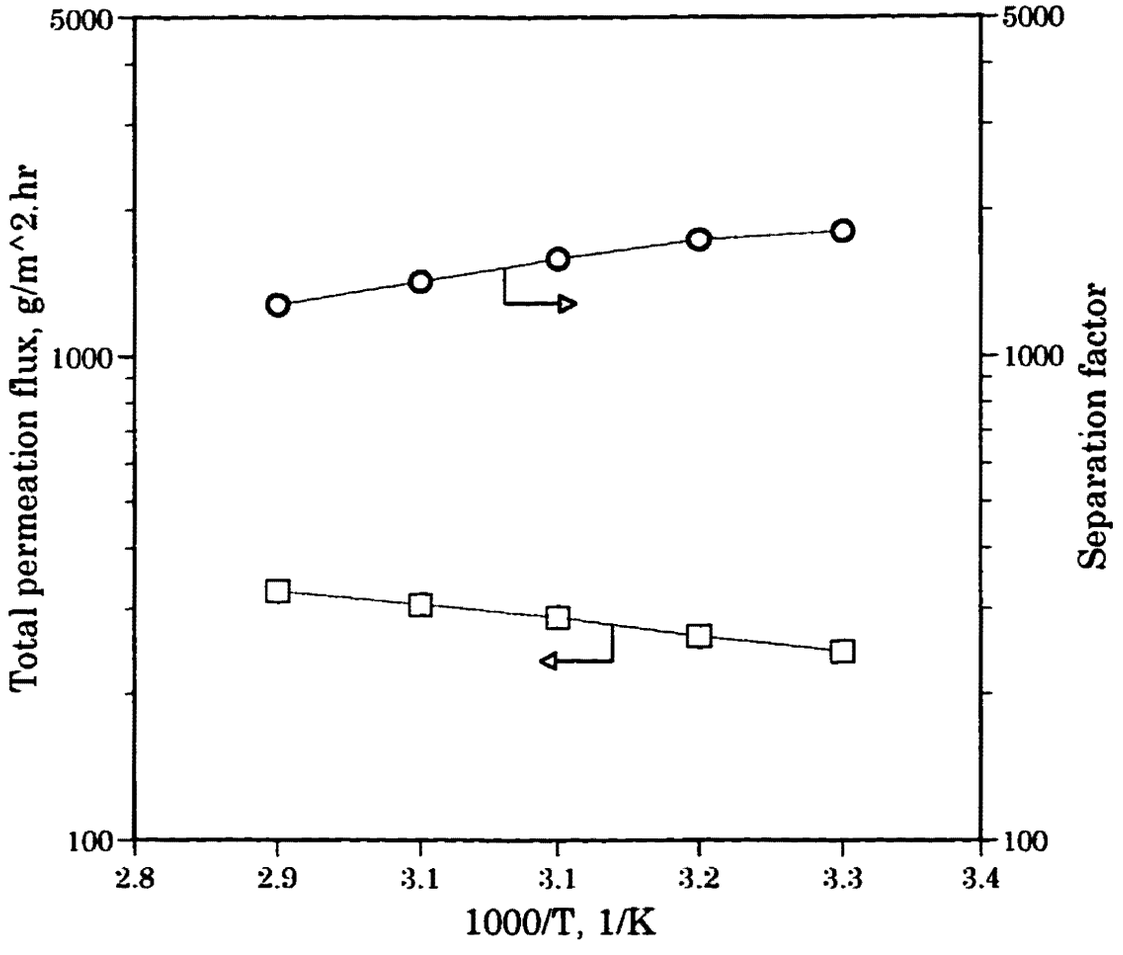


Figure 5.18 The pervaporation data of the CS-PVA blended membrane versus operating temperature. Feed isopropanol concentration: 0.90; blend composition: 40/60.

type of relation in the temperature range tested.

5.4 Conclusions

The chemically crosslinked chitosan membranes and CS-PVA blended membranes were prepared and tested for the pervaporation dehydration of isopropanol/water mixtures. The following conclusions can be drawn from the current study:

(1) The solution technique crosslinking of chitosan with HMDI is potentially effective to modify the structure of chitosan membranes for the pervaporation separation of isopropanol/water mixtures; the membranes performance is greatly affected by the extent of the crosslinking reaction which is controlled by the treatment time.

(2) The crosslinked structure of chitosan membranes show improved overall pervaporation performances; the membranes are preferentially permeable to water and the membranes permselectivity increases with an increase in feed isopropanol concentration.

(3) Chitosan is fully compatible with poly(vinyl alcohol) in the entire range of blend composition.

(4) The CS-PVA membranes are effective for the pervaporation of isopropanol/water mixtures; the blended membranes are preferentially

permeable to water over the entire feed composition and the membranes performance is greatly affected by the blend composition.

(5) The preferential permeation for the CS-PVA membranes is affected and determined by the preferential sorption in the liquid phase.

(6) The pervaporation performance of the CS-PVA is affected by the feed composition and the operating temperature.

CHAPTER 6

Vapor Phase Pervaporation Dehydration of Isopropanol with Chitosan Membranes

6.1 Introduction

Vapor phase pervaporation (VPVAP) is a relatively new membrane separation technique developed based on the concept of pervaporation (PVAP). VPVAP differs from PVAP in that the operating module is then fed not with a liquid mixture but with a saturated mixed vapor. Compared to PVAP, VPVAP process seems, at first sight, to be advantageous for several reasons [Neel, 1991].

i) The membrane technique often compliments a distillation step, providing fractions which are already in the vapor state,

ii) In vapor phase pervaporation, mass-transport through the membrane does not result in a phase-change. It is therefore not necessary to supply heat to the operating module to compensate the vaporization enthalpy and to make the system work under virtually isothermal conditions,

iii) The problem of concentration polarization, which is sometimes encountered in the case of PVAP, no longer exists if the feed is processed in the vapor state.

In the PVAP method, polymer membranes are swollen or shrunk because the feed solutions are directly in contact with the polymer membranes, and consequently the original functionalities of the polymer membranes, designed chemically and physically, are sometimes impaired by such swelling or shrinking of membrane. Since in the VPVAP technique the feed solutions are fed without direct contact with the polymer membrane, the swelling or shrinking of polymer membranes due to the feed solutions can be prevented.

The VPVAP method consists in [Uragami *et al.*, 1989]:

i) dissolution of vapor molecules evaporated from the feed mixtures into the polymer membrane,

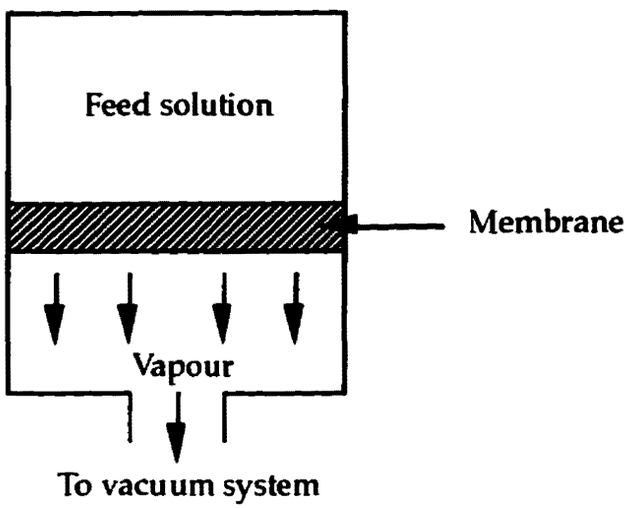
ii) diffusion of these molecules through the polymer membrane, and

iii) evaporation of these molecules from the polymer membrane.

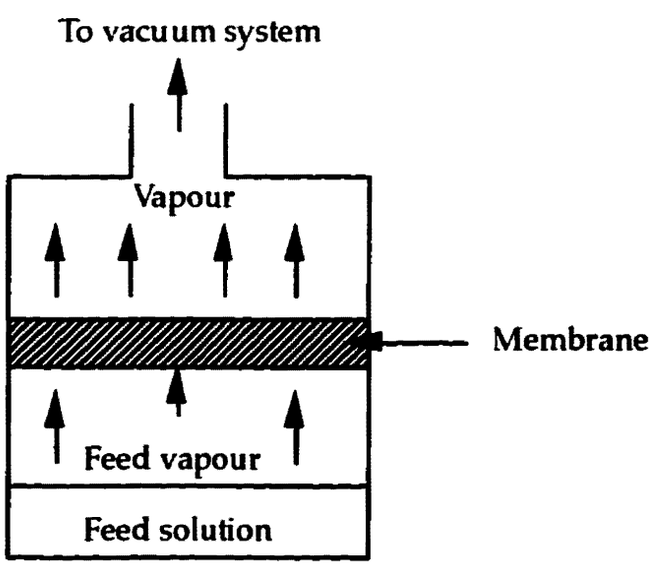
The separation factor is enhanced by these three processes so that in general permeation rates in the case of VPVAP are smaller than those of PVAP, but the separation factors in the former case are greater than those in the latter. The comparison between the principles of PVAP and VPVAP is shown in Figure 6.1.

Despite these favorable features, VPVAP has not yet been developed on an industrial scale. This fact is probably due to technical difficulties, such as the possibility of undesirable condensations in the feed-stream, induced by variations in its composition, pressure or temperature, as it proceeds along the module. Furthermore, it has not yet been experimentally demonstrated that a given membrane always displays equivalent performance (permeability and selectivity) when it is used to separate a given mixture investigated successively in the liquid state and as a saturated mixed vapor.

The question as to whether the liquid charge could be indiscriminately replaced by a saturated vapor of the same composition has often been raised. Experimenting at 30 °C, with a low-density polyethylene film, Michaels *et al*. [1962], claimed that the steady-state permeation rate observed with pure liquid xylene was more than ten times that obtained with a charge of saturated vapor. Long [1965] has stated that the equilibrium solubility of both liquid and saturated vapor are equal and that the lower permeation rate



(a)



(b)

Figure 6.1 Comparison between the (a) PVAP and (b) VPVAP

for saturated vapor mainly resulted from a lower rate of replenishment of surface permeant during vapor permeation experiments. More recently, Pineri *et al.* [1988], by means of the Small Angle Neutron Scattering technique (SANS), succeeded in revealing the concentration-profile of the penetrant within the entire thickness of a homogeneous membrane made from a perfluorinated ionomer (NAFION^{R}), during the steady-state PVAP of pure water. Two comparative experiments were run respectively with liquid water and saturated steam. The two water concentration-profiles determined by SANS technique were found to be significantly different, the profile generated from the saturated vapor showing a steep drop within the upstream layer of film. Stannett and Yasuda [1962, 1963], on the other hand, have reported good agreement between liquid and saturated vapor permeation rates for benzene, cyclohexane and water through low-density polyethylene sheets and rubber films. It thus appears that the literature contains some inconsistencies with regard to this question, which is important, since it partly determines the respective advantages of PVAP and VPVAP.

From the thermodynamic standpoint, it is hardly conceivable that the swelling of the membrane polymer could be noticeably different when this material is successively contacted, at the same temperature, with a pure liquid and its saturated vapor. In both cases, indeed, the activity of the

penetrant is the same and equilibrium sorption uptakes should therefore be equivalent. Nevertheless, one may conceive that the sorption taking place at the upstream surface of the membrane could be slower in the case of a saturated vapor than in that of a liquid/polymer interface.

In this present study, we design a VPVAP column to investigate the performance of chitosan based membranes for the separation of isopropanol/water mixtures. Fundamental VPVAP experiments of isopropanol/water mixtures using chitosan membranes are performed and the permeation data in VPVAP are compared with those in PVAP.

6.2 Experimental

6.2.1 Materials

All the chemicals including chitosan flakes, acetic acid, isopropanol, PVA, and polysulfone used in this present study are the same as those used in the previous chapters.

6.2.2 VPVAP Permeation Cell Design

The VPVAP permeation cell is designed based on the design concept of the VPVAP cell structure adapted from Uragami [1994]. The schematic diagram of the VPVAP tube-and-shell permeation cell is shown in Figure 6.2.

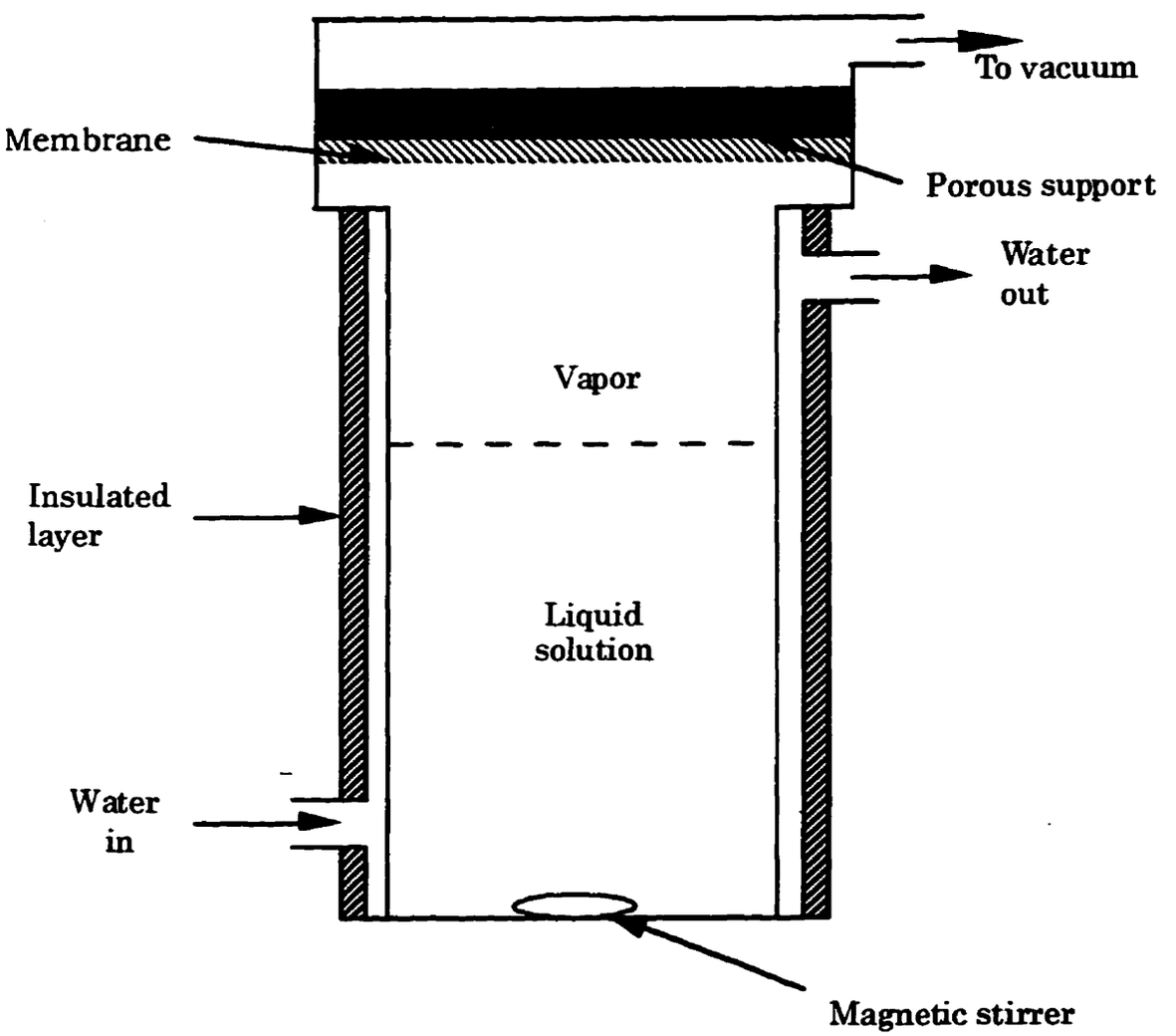


Figure 6.2 A schematic diagram of the VPVAP permeation cell.

The liquid mixture is kept in the tube surrounded by a shell filled with a circulated water bath to maintain a constant uniform temperature throughout the whole length of the cell. The entire length of the permeation cell is tightly *wrapped* with an insulation cloth to minimize heat lost. The cell capacity is about 500 ml and the effective area of the membrane is 47.8 cm^2. The cell permeate outlet is connected to a VPVAP separation apparatus shown in Figure 6.3.

6.2.3 Membrane Preparation

All the homogeneous CS and the composite CS/PS membranes used in the present study were prepared by using the same techniques and procedures as those previously used in Chapters 3, 4 and 5.

6.2.4 Vapor Phase Pervaporation

The separation experiments were conducted using the VPVAP permeation cell. The feed liquid is supplied to a half volume of the tube, then the upstream air in tube is degassed by a vacuum pump. The feed liquid is stirred by a magnetic stirrer. The temperature of the liquid feed and the vapor in the tube can be controlled by adjusting the temperature of the circulated water bath which is controlled by an electric heater. The downstream

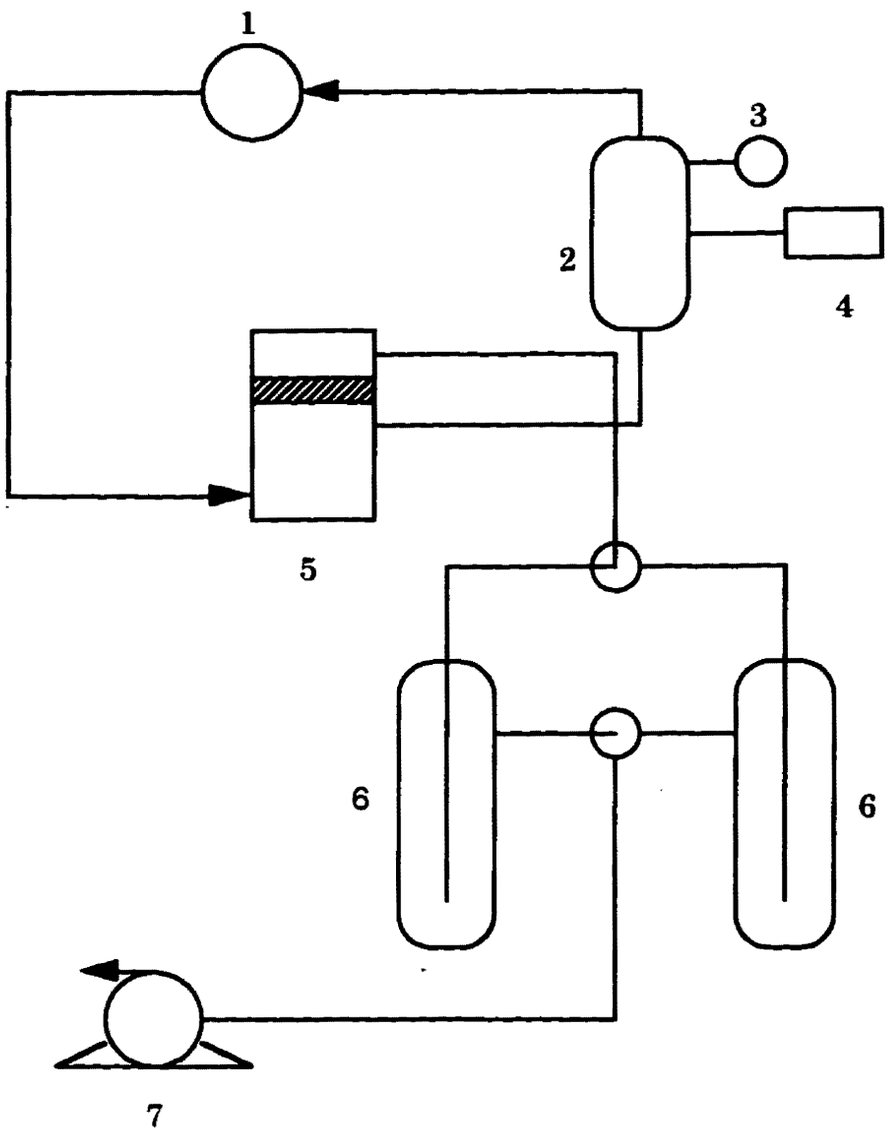


Figure 6.3 A schematic diagram of the VPVAP separation apparatus. (1) Circulation pump; (2) Water bath; (3) Temperature indicator; (4) Electric heater; (5) VPVAP permeation cell; (6) Glass traps; (7) Vacuum pump.

pressure is normally maintained to 3 mm Hg. Each VPVAP process was run for at least two hours to reach the steady state before the collection of permeant. The permeant was collected in one of the glass traps which were immersed in liquid nitrogen. The isopropanol concentration in the permeate is analyzed by a Hewlett Packard 5890 Series II gas chromatography previously described in Chapter 3.

6.3 Results and Discussion

The total and partial permeation fluxes for the binary isopropanol/water mixtures at 30 °C and at a permeate pressure of 3 mm Hg are plotted against feed composition in Figure 6.4. As shown for the entire range of feed composition, the total permeation flux is mainly constituted by the water permeation flux, and the water permeation flux is almost proportional to the water concentration of the feed. Thus it can be understood that water is preferentially permeated in the highly hydrophilic membrane. These results suggest that higher volatility does not necessarily lead to a higher permeation flux, *vice versa*. Figure 6.5 shows the effects of feed composition on the total permeation flux in PVAP and in VPVAP. The total permeation flux decreases with an increase in the feed isopropanol concentration. Furthermore, the total permeation rate in PVAP is

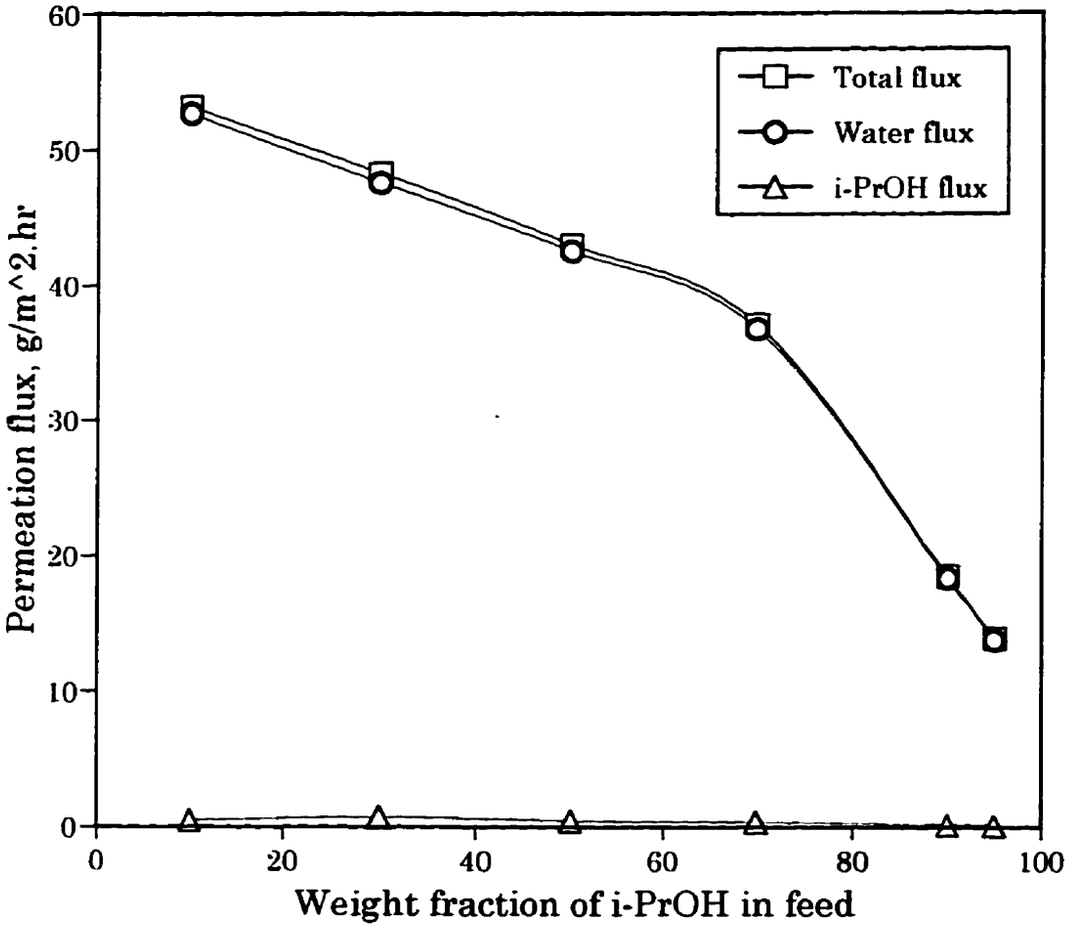


Figure 6.4 **The total and partial permeation fluxes as a function of feed composition. Temperature 30 °C.**

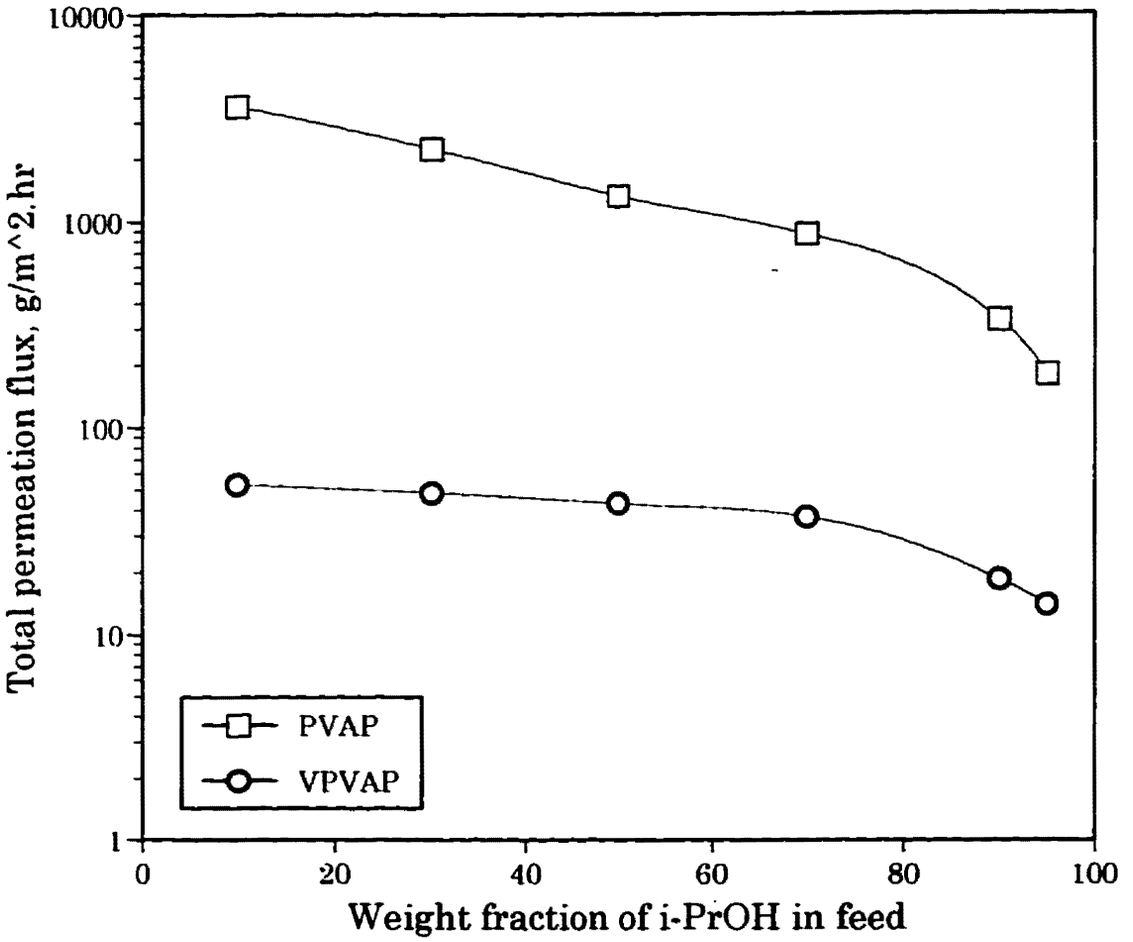


Figure 6.5 The total permeation flux in PVAP and in VPVAP as a function of feed composition. Temperature 30 °C.

significantly higher than that in VPVAP over the full range of feed composition measured. These results depend on the fact that swelling of the chitosan membrane in VPVAP is remarkably prevented as compared to that in PVAP. Theoretically, the two rates should be equal. But from early stage of researches, difference of behavior has been noticed and reported. Kataoka *et al.* [1991] performed PVAP and VPVAP experiments for the separation of ethanol/water systems using polyacrylonitrile (PAN) and cellulose acetate (CA) to investigate reasons for discrepancy in permeabilities in PVAP and VPVAP. They found that results with PAN membranes showed good agreement between PVAP and VPVAP, but the results with CA membranes showed larger permeation flux and a lower separation factor in PVAP than in VPVAP. They attributed the discrepancy to higher sorption characteristic of CA than that of PAN.

The relations of isopropanol flux to the feed composition at 30 °C are shown in Figure 6.6. As a comparison, the isopropanol flux in PVAP is also plotted. In both cases, isopropanol flux increases slightly , passes a maximum and then decreases with an increase in feed isopropanol concentration. The appearance of the maximum point of isopropanol flux in VPVAP at feed isopropanol around 30 weight percent confirms the existence of the plasticization effects of water on the chitosan membrane discussed in

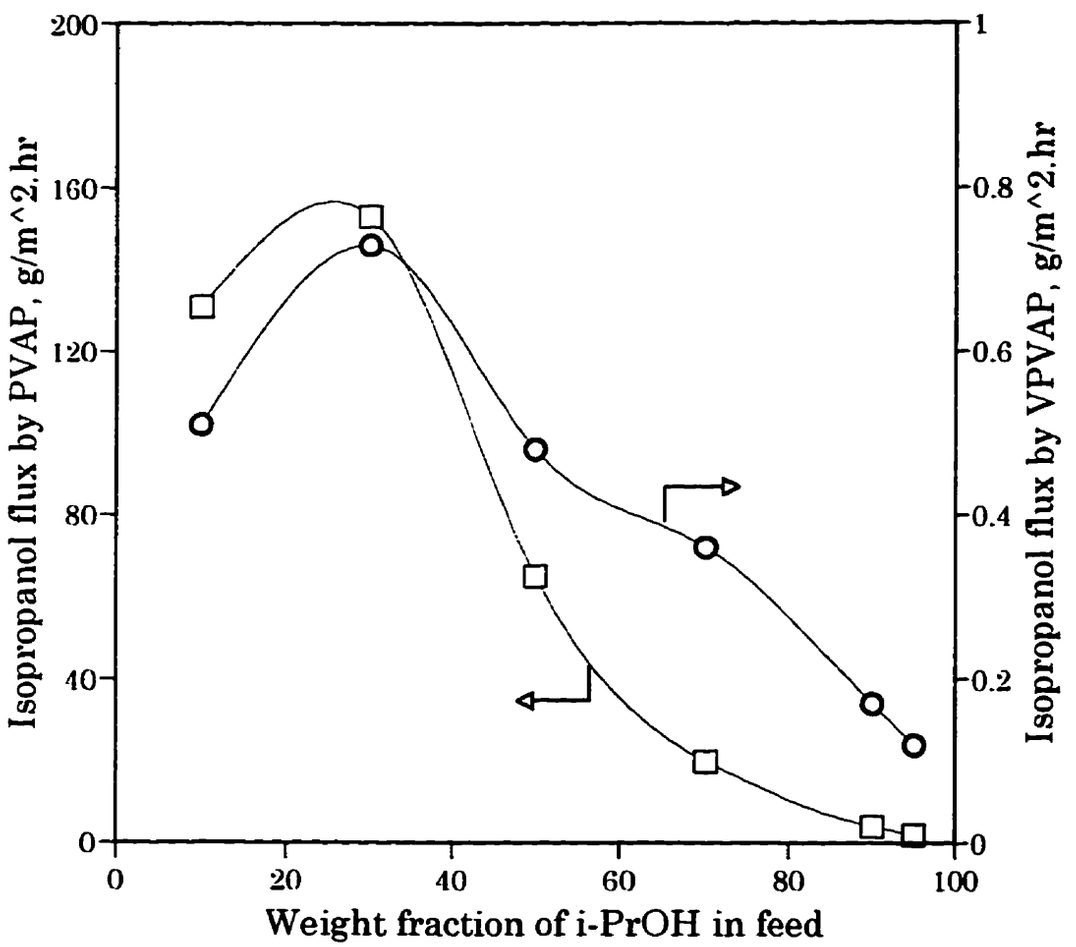


Figure 6.6 **The isopropanol fluxes in VPVAP and in PVAP versus feed composition. Temperature 30 °C.**

Chapter 3. Note that for full range of feed composition the isopropanol flux in PVAP is higher than that in VPVAP. This fact supports the assumption that the chitosan membrane in VPVAP can almost keep the dense structure existing prior to the VPVAP experiment and that consequently the diffusivity of the permeating species during the diffusion process is lowered. In fact, degree of swelling before measurement was also identified as one of the important factors in the permeability measurements that caused discrepancy in permeabilities for benzene and xylenes through polyethylene membranes measured in PVAP and those measured in VPVAP by Blackadder and Keniry [1972]..

The separation factors for the VPVAP and PVAP are shown in Figure 6.7. Here, both the separation factors in PVAP and in VPVAP are plotted for the compositions of aqueous isopropanol solutions. The separation factors in VPVAP are greater than those in PVAP for the entire range of liquid feed isopropanol concentration. These results are attributed to the fact that denser membrane structures in the VPVAP remain unchanged. From physical observation, wrinkles on membrane surfaces were clearly seen in PVAP experiments, but were not observed in VPVAP experiments. It has to be noted that, the separation factors in VPVAP would have been much higher if they were plotted for the compositions of liquid-vapor equilibria for isopropanol solutions instead of the aqueous isopropanol solutions.

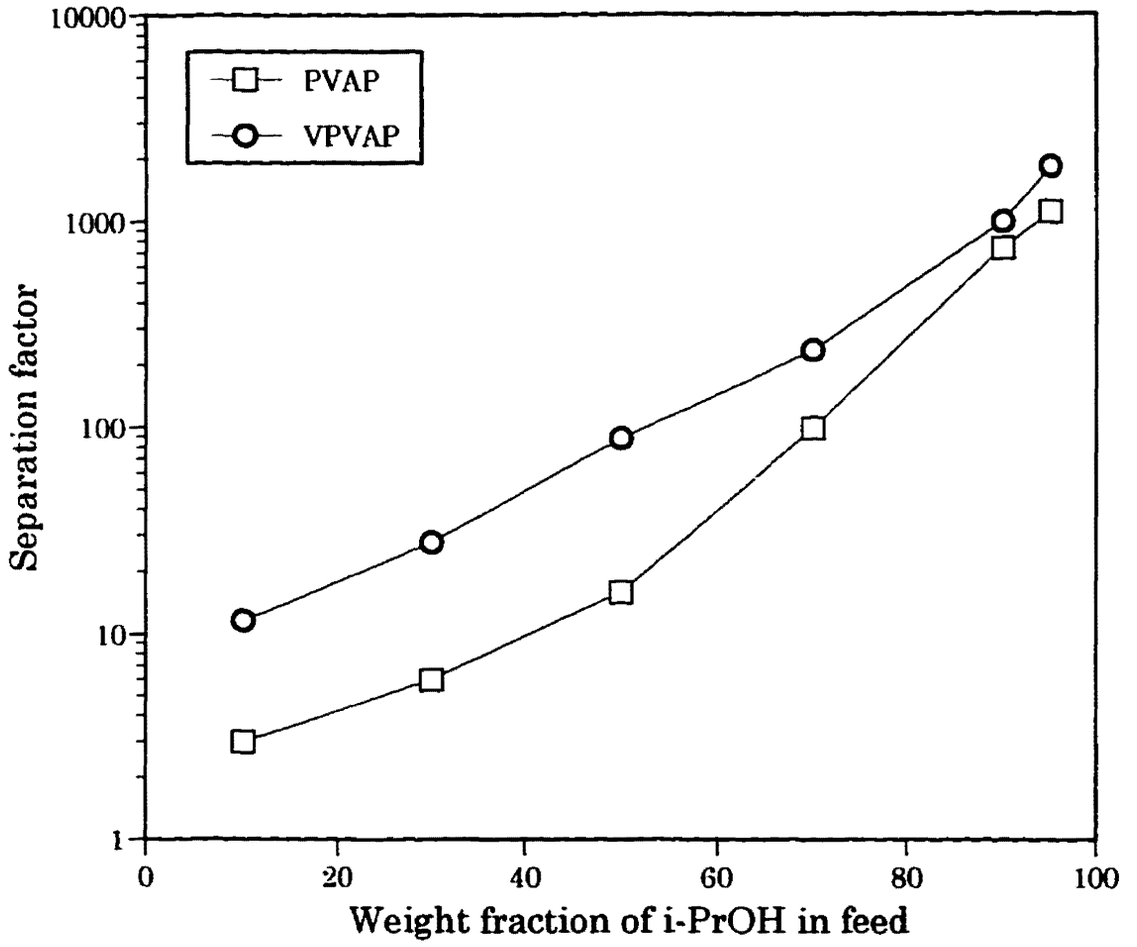


Figure 6.7 The separation factors for PVAP and VPVAP versus feed composition.

In order to more accurately evaluate the effectiveness of the VPVAP process as compared to the PVAP, both the permselectivity and permeability have to be considered, and the results are illustrated in Figure 6.8. As can be seen, in terms of the PSI, the PVAP is more productive than the VPVAP for the separation of isopropanol/water mixtures. These results depend greatly on the permselectivity-permeability trade-off; high selectivity is compensated with low permeation flux, *vice versa*.

The use of composite chitosan membranes for the separation of isopropanol/water mixtures by VPVAP at 30 °C was also investigated. The results are plotted in Figures 6.9 and 6.10. The effects of feed composition on the permeability of the composite membranes are shown in Figure 6.9. The results indicate that the permeation rate of the composite chitosan membranes is greater than that of homogeneous membranes for the entire range of feed composition measured. This is understandable because the permeation rate of a membrane is dependent on the membrane thickness and the effective thickness of the composite chitosan membranes is less than that of the homogeneous ones. Note however that the values of the permeation flux for the two types of the chitosan dense membranes do not differ significantly, indicating that the permeation flux for the composite membrane is not linearly dependent on the effective thickness of thin top layer of chitosan, i.e.,

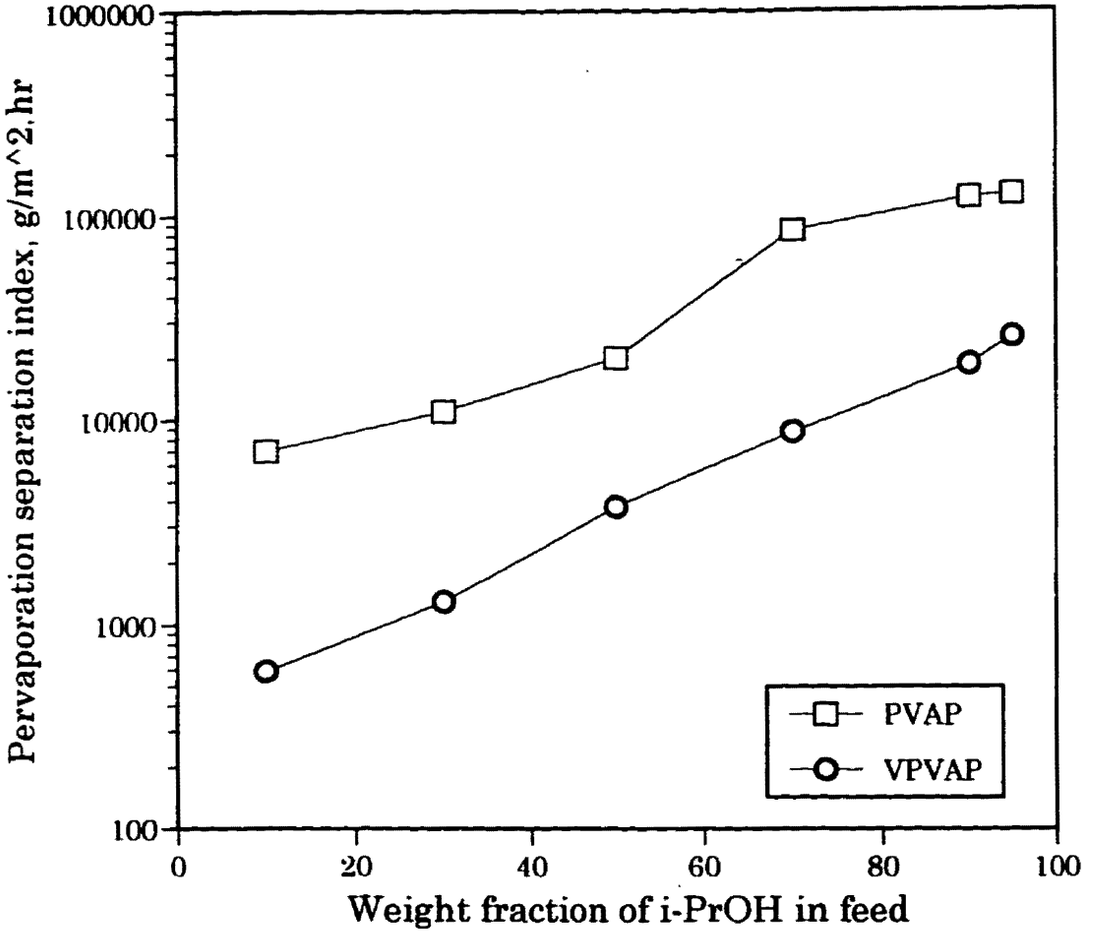


Figure 6.8 **The pervaporation separation index in PVAP and in VPVAP as a function of feed composition.**

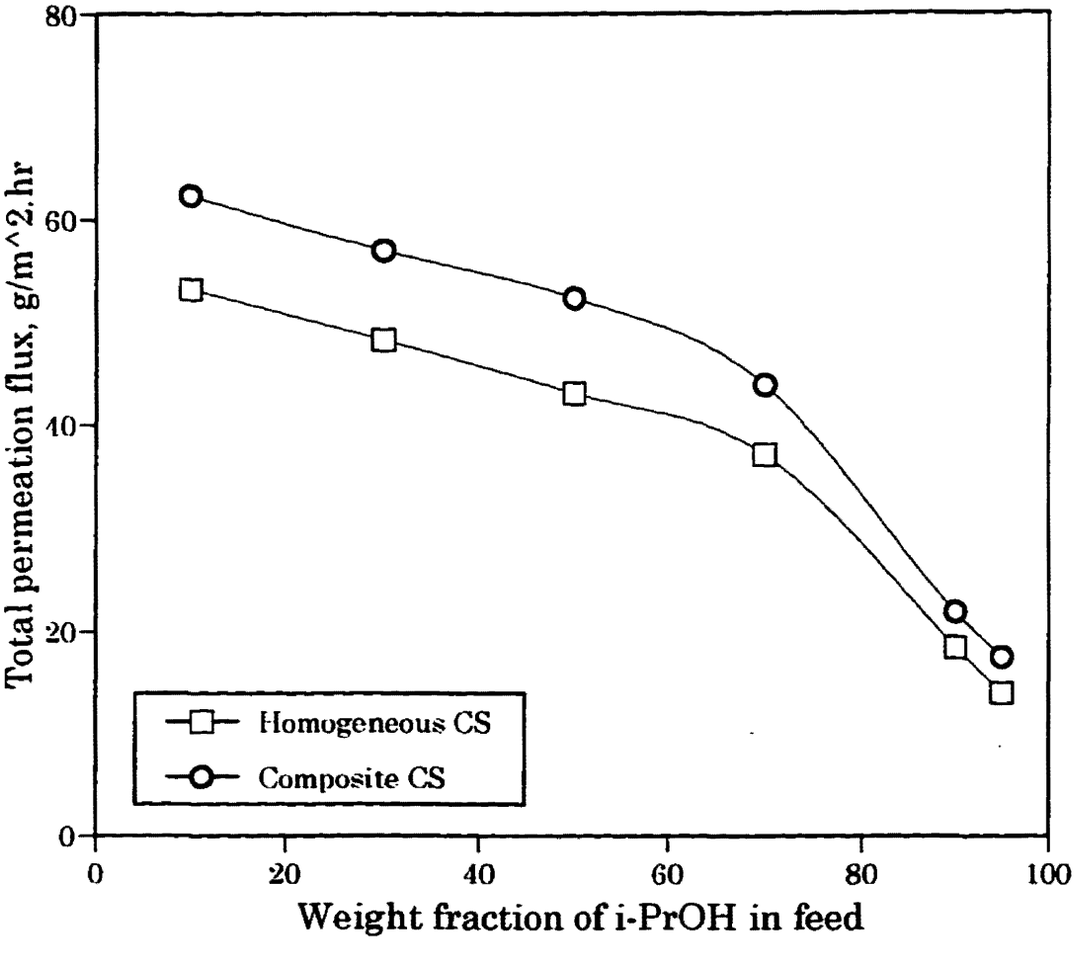


Figure 6.9 **The permeability of composite chitosan membranes in VPVAP as a function of feed composition.**

to some extent the polysulfone porous support does play a role in the permeability of the composite membrane as suggested in Chapter 4 for the PVAP process.

The separation factors for the composite and the homogeneous chitosan membranes are plotted against the feed compositions in Figure 6.10. Note that the compositions of the feed aqueous isopropanol solutions were used as the basis for calculations. Interestingly, the separation factors for the homogeneous chitosan membrane is only slightly higher than that of composite ones. This may also related to the fact that in VPVAP, membranes do not swell as much as in PVAP. In other words, since membrane swelling is limited in the VPVAP and thus dense structures of the membranes are generally remain unaltered, then in terms of permselectivity, composite membranes do not behave significantly different than the corresponding homogeneous ones. These results are of special importance because of the facts that most commercially available dehydration membranes are of the composite type and normally composite membranes have good mechanical strength and are used to increase permeation of permeating species and in general the permeation and separation factor are always in conflict in membrane processes. These results demonstrate the potential of VPVAP using composite chitosan membranes in combination with distillation or other separation technologies for the dehydration of isopropanol as a solvent of very

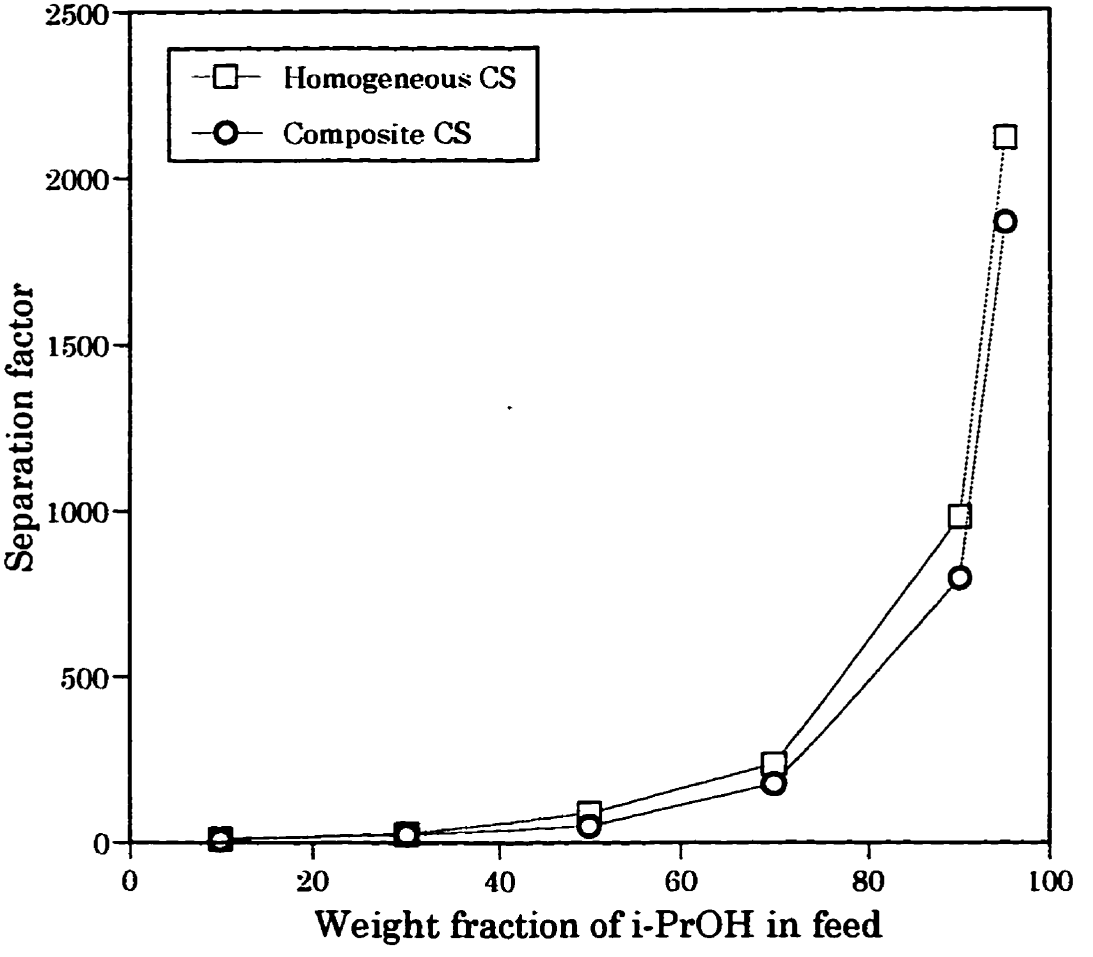


Figure 6.10 The separation factors of homogeneous and composite chitosan membranes versus feed composition.

high purity and very low residual of water content as required in compact disk and semiconductor manufacturing. Further, the advantage of composite membranes is that each layer can be optimised independently to obtain optimal membrane performance with respect to selectivity, permeability, chemical and thermal stability.

6.4 Conclusions

Preliminary experimental studies on vapor phase pervaporation separation of isopropanol/water mixtures using chitosan membranes were performed. The following conclusions can be drawn:

(1) VPVAP provides an alternative technique to the more common PVAP for the dehydration of isopropanol using chitosan membranes.

(2) The separation factor in VPVAP is higher than that in PVAP while the total permeation rate in the VPVAP is lower than that in PVAP; in terms of PSI, PVAP is more productive than the VPVAP.

(3) The composite chitosan membranes do not perform significantly different than the homogeneous chitosan membranes in VPVAP for the dehydration of isopropanol at a constant temperature of 30 °C.

The present study was performed preliminarily to investigate the effectiveness of VPVAP process for the separation of isopropanol/water mixtures. The study

was carried out on the assumption that membrane swelling is restricted in VPVAP and thus membrane structures do not change significantly. From physical observation, wrinkles on membrane surfaces were seen in PVAP experiments, but were not observed in VPVAP experiments. The compositions of the feed solutions were used as the basis for the calculations of the separation factors. The more appropriate way is to use the composition of the vapor or to use the liquid-vapor equilibria data. Obviously further study is required to fully comprehend the significance of this VPVAP process.

CHAPTER 7

Diffusion Coefficient Estimations by Thin-Channel Column Inverse Gas Chromatography (IGC)

7.1 Background

Gas chromatography (GC) has become well established as an alternative for studying the interaction of polymers with volatile solutes years ago [Laub, 1978; Conder, 1979; Braun, 1975]. In a typical application, the polymer is used as the stationary phase in a chromatography column. The solute or probe is vaporized and injected into a carrier gas flowing through the column. As the probe is swept through the column, it can interact with the polymer via adsorption or absorption. The retention time of the probe and the

shape of the elution profile (i.e. chromatographic peak) will reflect the strength and nature of the interactions that occur between the polymer and the solute and can be used to study those interactions. Such an experiments is sometimes referred to as inverse gas chromatography (IGC), to differentiate it from the more common analytical application of gas chromatography.

In general, IGC has been used primarily for the measurement of solution thermodynamic parameters. When an IGC experiment is carried out at temperatures significantly higher than the glass transition temperature of the polymeric stationary phase, the retention time will be determined by the solubility of that component in the polymer. Consequently, measurements of retention time can be used to calculate such useful parameters as Henry's law constant, the activity coefficient, and various solution model interaction parameters. In comparison with bulk equilibrium methods (gravimetric sorption/desorption) for thermodynamic measurements, IGC offers several advantages. The foremost among these is speed: a single IGC experiment can be completed in minutes; a vapor sorption experiment may require hours or days to complete.

The IGC method is ideal for obtaining infinite dilution properties because very low solute concentrations can be measured with standard detector systems. In addition, changes in the solute and temperature can be readily made in a chromatographic experiment. These features enable

determination of the interactions of a large number of solutes with a given polymer in a relatively short period of time. Several studies have established the consistency of thermodynamic data obtained by IGC with data obtained by more conventional techniques [Summers *et al.*, 1972; Tewari, 1972; Tait, 1979; Vrentas *et al.*, 1983].

In principle, IGC experiments can also be used to obtain information about the diffusion of the solute in the polymer phase. It has long been recognized that mass-transport limitations in the stationary phase result in significant spreading and distortion of a chromatography peak. A number of researchers have attempted to exploit this phenomenon as a means of measuring the diffusion coefficient of the solvent in the stationary phase [Tait, 1979; Braun., 1975; Kong, 1975; Galin, 1978]. In all of these studies, packed-column chromatography was used and diffusion coefficient estimates were extracted from the elution curve data using the van Deemter equation. None of these efforts has provided a convincing demonstration that the method can be used to obtain meaningful information; difficulties inherent in the use of a packed column make it nearly impossible to relate the measured elution curve to the diffusion coefficient. The major limitation is the irregular distribution of polymer with the column, which prohibits the application of realistic models for stationary phase transport processes. The van Deemter analysis assumes a uniform distribution of polymer. In any real packed

column, the distribution will not be uniform and will be difficult to characterize.

In a pervaporation process, diffusion coefficients of permeating components in polymers in general depend strongly on the state of swelling of the polymer because of the plasticizing action of the liquid on the segmental motions of the polymer. In general, two methods have been widely used to obtain diffusion coefficients: the absorption experiment method [Crank, 1968, 1979] and the desorption experiment [McCall, 1957; Fels and Huang, 1970; Rhim and Huang, 1989]. The two methods are based on the unsteady state process and complicated. The experimental results are very sensitive to the accuracy of measurements. Fels and Huang [1970] and Rhim and Huang [1989] tried to determined the diffusion coefficients of organic components in polyethylene from desorption experiments and applied the resulting diffusion coefficients to their equations for predicting the behavior of the pervaporation process. However, the results of the comparison of the calculated data with the experimental data were not fully satisfactory. Despite the advantages and despite the widespread use of IGC, to date no attempts to utilize the use of gas chromatography to determine diffusion coefficients applicable to pervaporation process have been reported in the literature.

In this study we present a significant improvement in the IGC method for the measurement of diffusivities applicable to the pervaporation process.

The technique depends on the use of a specifically designed column based on the concept of a thin-channel system with highly uniform layer of polymer membrane film used as the stationary phase. The thin-channel column offers great improvements over the conventional packed columns.

7.2 Theoretical

Diffusion processes on gas chromatographic columns lead to broadening of the chromatographic peak. In traditional gas chromatography, the peak broadening is directly related to the resolving power of the columns and as such has received extensive theoretical interest [Schupp, 1968; Conder, 1979]. There are two major factors that contribute to peak broadening: diffusion of the injected compound (probe) in the carrier gas and diffusion of the probe in the stationary phase. The former is characterized by the gas-phase mutual diffusion coefficient, D_g, and the latter factor is related to the liquid-phase mutual diffusion coefficient, D_L.In the case of IGC experiments, where a polymer is the stationary phase, D_L is a polymer-probe diffusion coefficient.

We will follow the standard chromatographic approach in expressing the distribution of a probe on the column by means of the height equivalent to a theoretical plate (HETP), H. We may define HETP as a unit of column length sufficient to bring the gas issuing from it into equlibrium with the

solute in the immobile phase throughout the unit [Conder, 1979]. HETP is related to the number of theoretical plates N and to the physical length of the column L as

$$H = \frac{L}{N} \tag{7.1}$$

The measurements of effective diffusion coefficients is based on the well known equation developed by van Deemter *et al.* [1956] for a gas chromatographic column

$$H = A + \frac{B}{u} + Cu \tag{7.2}$$

where u is the linear velocity of carrier gas and A, B and C are constants of the column, gases and operating conditions.

On packed columns, A is called the eddy diffusion term and is related to the size of the support particles and the irregularity of packing. The constant B describes the time-dependent factors; only the longitudinal diffusion of the probe, along the stream of the carrier gas, contributes significantly to B. The third term in eqn. (7.2) is related to peak broadening, which is due to solute/stationary phase resistance to mass transfer within the column. The constant C is given by

$$C = \frac{8}{\Pi^2} \frac{K}{(1+K)^2} \frac{d^2}{D_L} \tag{7.3}$$

where d is the thickness of the stationary phase, D_L is the solute diffusion coefficient in the liquid phase, and K is the partition ratio given by

$$K = \frac{t_r - t_m}{t_m} \tag{7.4}$$

where t_r and t_m are the retention time to peak maximum of the probe molecule and a non interacting material such as methane, respectively. The retention time t_r is the time the average molecule of solute takes to travel the length of the column and is measured to the midpoint of the symmetrical breakthrough curve. A part, t_m, of this time is required by the solute simply to pass through the mobile phase space from inlet to outlet [Conder, 1979], hence the partition ratio, K, measures the relative amounts of time the solute spent in the mobile and the stationary phase [Laub, 1978].

The simple version of the van Deemter equation, eqn. (7.3), does not consider broadening effects due to the noninstantaneous equilibration of vapor phase across the column by molecular or hydrodynamic mass transfer [Littlewood, 1970]. Trans-column diffusion in the gas phase is assumed to be fast compared with diffusion through the stationary phase. Furthermore, the

assumptions used to derive the C term are unrealistic for most practical gas chromatography columns where the geometry of the column packing is very complex.

Giddings [1965] has developed a nonequilibrium treatment which enables calculation of peak dispersion in more complex cases by redefining the C term to take account of various dispersion factors. In the case of uniform film thickness, Giddings' result is the same as that for the van Deemster C term but with the constant $8/\pi$ replaced by $2/3$. So eqn. (7.3) becomes,

$$C = \frac{2}{3}\frac{K}{(1+K)^2}\frac{d^2}{D_L} \tag{7.5}$$

Equation (7.2) is only valid for describing the elution of symmetric peaks, which requires that mass-transfer resistances be small but not negligible. The determination of D_L involves the measurement of H at several relatively high flow rate, where the term B/u is negligible and A remains suitably small. The slope obtained in a plot of H versus u enables one to calculate D_L, since K can be directly obtained from these experiments.

$$H = \frac{2}{3}\frac{K}{(1+K)^2}\frac{d^2}{D_L}u \tag{7.6}$$

From plate theory, it can be shown that for a column producing

Gaussian-shaped peaks H , is related to the peak width or variance by [Conder, 1979]

$$H = L\left(\frac{\sigma_t}{t_r}\right)^2 = \frac{L}{5.54}\left(\frac{W_{1/2}}{t_r}\right)^2 \qquad (7.7)$$

where σ_t^2 is the variance of the peak and $W_{1/2}$ is the peak width at half the peak height.

7.3 Experimental

7.3.1 Materials and Equipment

Chitosan polymer used for the stationary phase was the same as those used for the preparation of chitosan membranes in Chapter 3 and 4. Gases used for the operation of the chromatograph were supplied by the Praxair, Kitchener, Ontario. A high-purity helium was used as the carrier gas, dry-grade compressed air and hydrogen were used for the flame ionization detector (FID), and methane was used as the non-interacting material. The equipment required for the inverse gas chromatography was similar to that used in analytical applications as discussed in Chapter 3 and 4, with a few modifications. Figure 7.1 gives a schematic of the apparatus. A hydration system was used to saturate the carrier gas with water vapor in

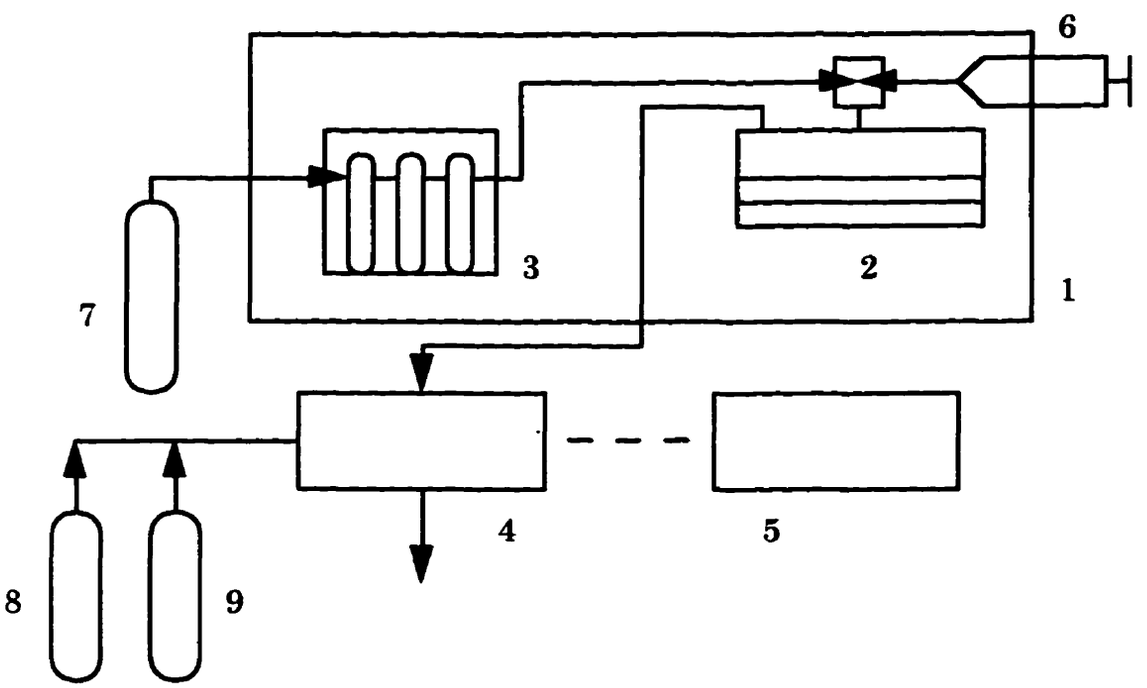


Figure 7.1 Schematic diagram of apparatus used for the IGC. (1) GC oven; (2) Thin-channel column; (3) Hydration system; (4) FID/TCD Detector; (5) Integrator; (6) Injector; (7) Hydrogen; (8) Helium; (9) Air.

order to swell the stationary phase to a certain extent.The flow rate of the carrier gas was controlled by a thermostated precision needle valve and was measured by soap bubble flowmeter. A 10-μl Hamilton syringe was used to inject the probes. A specially designed column was used and will be further discussed in the next section.

7.3.2 Column Design

The column was designed based on the concept of a spiral thin-channel system normally used for a cross-flow ultrafiltration unit. Figure 7.2 gives a schematic of the column. The column consisted of two parts: the top part or the thin-channel plate and the bottom part where the stationary phase was placed. The parts were sealed together with bolts and nuts. The finished column had a thin-channel with the dimensions of 3 mm in depth, 3 mm in width and 126 cm in length. The solute concentration-time profile was observed by the detector from the introduction of the solute at the injection point to its emergence at the outlet. The stationary phase which was actually a thin layer of homogeneous dense chitosan membrane was prepared according to the preparations of the pervaporation membranes, as discussed in Chapter 3.

Theoretically this thin-channel gas chromatography column features a

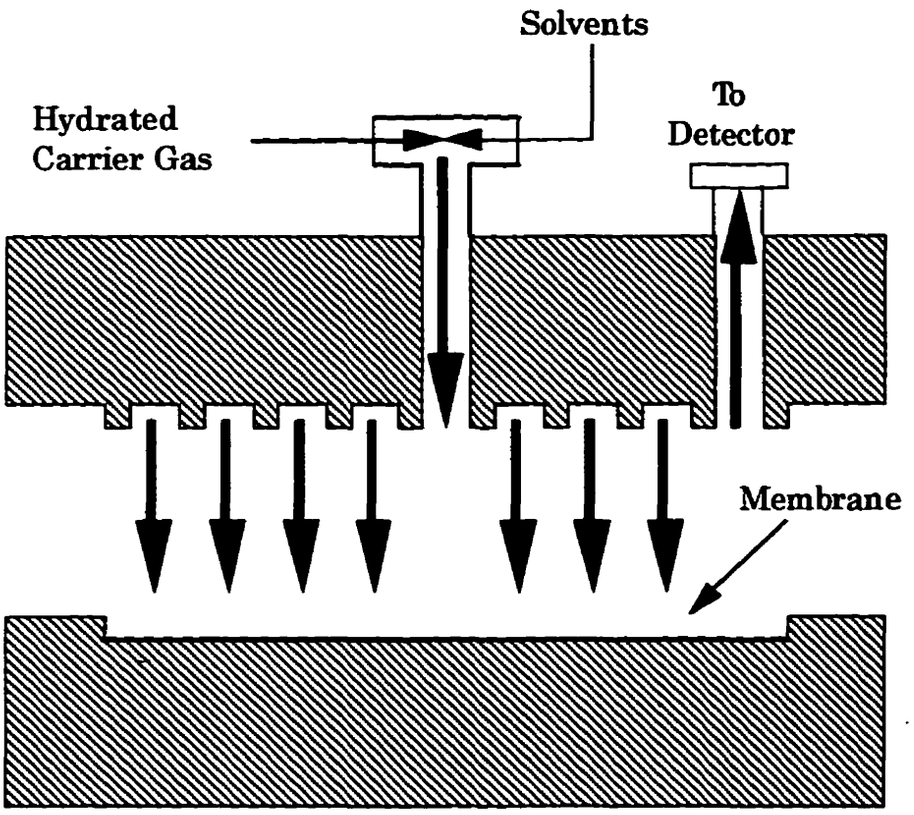


Figure 7.2 Schematic diagram of the thin-channel GC column.

significant improvements over the more conventional packed columns, because

(1) a thin layer of dense membrane can be used as the stationary phase ; i n general, casting a dense membrane layer is less difficult and less time-consuming than preparing a packed column or coating the inner wall of a small tube,

(2) the thickness of the stationary phase can be easily adjusted (as in the preparation of a membrane),

(3) a dry or swollen membrane film can be used as the stationary phase,

(4) the membrane can be directly cast onto the column, and most importantly,

(5) a more regular polymer distribution can be obtained.

7.3.3 Stationary Phase Preparation

The stationary phase used to "coat" the column consisted of a thin layer of chitosan dense membrane. The membrane was prepared from a homogeneous 0.5 wt% chitosan in acetic acid aqueous casting solution. The procedure and the sequence of the membrane preparation were the same as those described in Chapter 3.

7.3.4 Experimental Procedure

The procedure for obtaining an elution curve was simple. After the GC reached stable, steady-state operations, a small amount of solvent, in liquid or vapor state, was injected into the carrier gas depending on the type of detector used, flame ionization (FID) or thermal conductivity detector (TCD). FID is only sensitive to organic substances, whereas TCD is sensitive to both organic substances and water. Vapor samples were injected into the carrier gas at the injection point (Figure 7.3) to obtain elution curves and retention times of the probes in the swollen stationary phase and FID was used to measure the amount of solvent in the carrier gas leaving out of the column. The injection unit was designed using a Swagelok T fitting with an outside diameter of 3.18 mm (and inside diameter of approximately 3 mm) which was directly connected to the column to minimize dead spaces or mixing; sudden diameter changes of the fitting at the injection point that may create dead spaces or mixing was minimized. The injection unit was used in which the needle of the syringe can be extended to the head of the column to further reduce dead spaces or mixing at the injection point. Similar design was used at the outlet point; a Swagelok fitting with an inside diameter of 3 mm allowed the column to be fastened directly to the detector.

In contrast, liquid samples were injected into the carrier gas to obtain

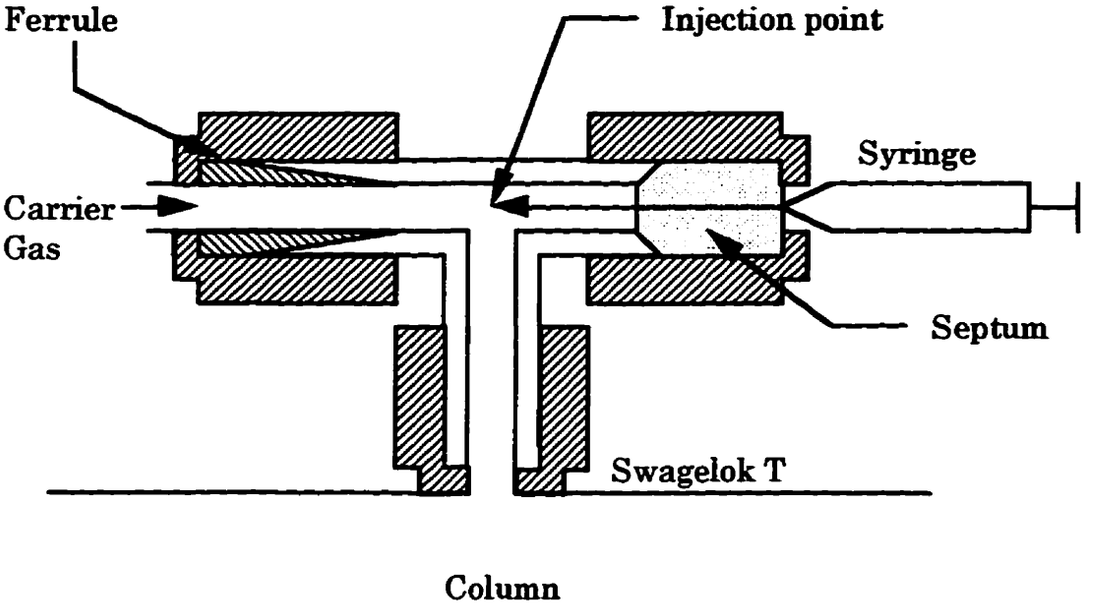


Figure 7.3 A schematic of the injection unit of the TC column.

elution curves and to determine retention times of the probes in dry stationary phase and TCD was used to measure the amount of solvent in the carrier gas leaving out the column. The liquid samples were injected through a heated injection point at 200 °C to ensure complete vaporization of the liquids. The carrier gas flow outlet flow rate was measured using a soap bubble flow meter.

The output from the gas chromatographic detector was fed to a Hewlett Packard HP 3396 Series II integrator. The experimental determination of $W_{1/2}$ and t_r was performed in triplicate for each flow rate and temperature, and an average plate height, H, was calculated. The linear portion of a graph of H vs. u was used to calculate C in the van Deemter equation (eqn. 7.2). The value of the diffusion coefficient in the polymer membrane was calculated from C using eqn. (7.3). The thickness of the membrane was measured manually by using a Mitutoyo MDC Series 293 digimatic micrometer.

7.3.5 Measurement of Retention time , Peak Variance, Partition Coefficient, and Diffusion Coefficient.

Measurement of Retention Time of Methane, t_m. The so-called column dead-time [Heftmann,1992] is an important chromatographic parameter and it corresponds to the retention time for non-retained sample component such as methane. The methods used to measure t_m depends on the detector; with

FID, t_m could be measured directly from the retention time to peak maximum of methane, while with TCD, t_m could be calculated from the following relation [Heftmann, 1992],

$$t_m = \frac{L}{u} \tag{7.7}$$

where L is the length of the column and u is the velocity of the carrier gas. In this study, since both the TCD and FID were used, the t_m values at different velocities of the carrier gas were calculated from equation (7.7) for consistency.

Measurement of Partition Ratio, K. The normal elution mode of GC was used to measure K values. The time required for the center of gravity of the solute band to pass completely through the column (the solute retention time) is a function of the relative amounts of time spent in the mobile and stationary phase, hence K. From equation (7.4)

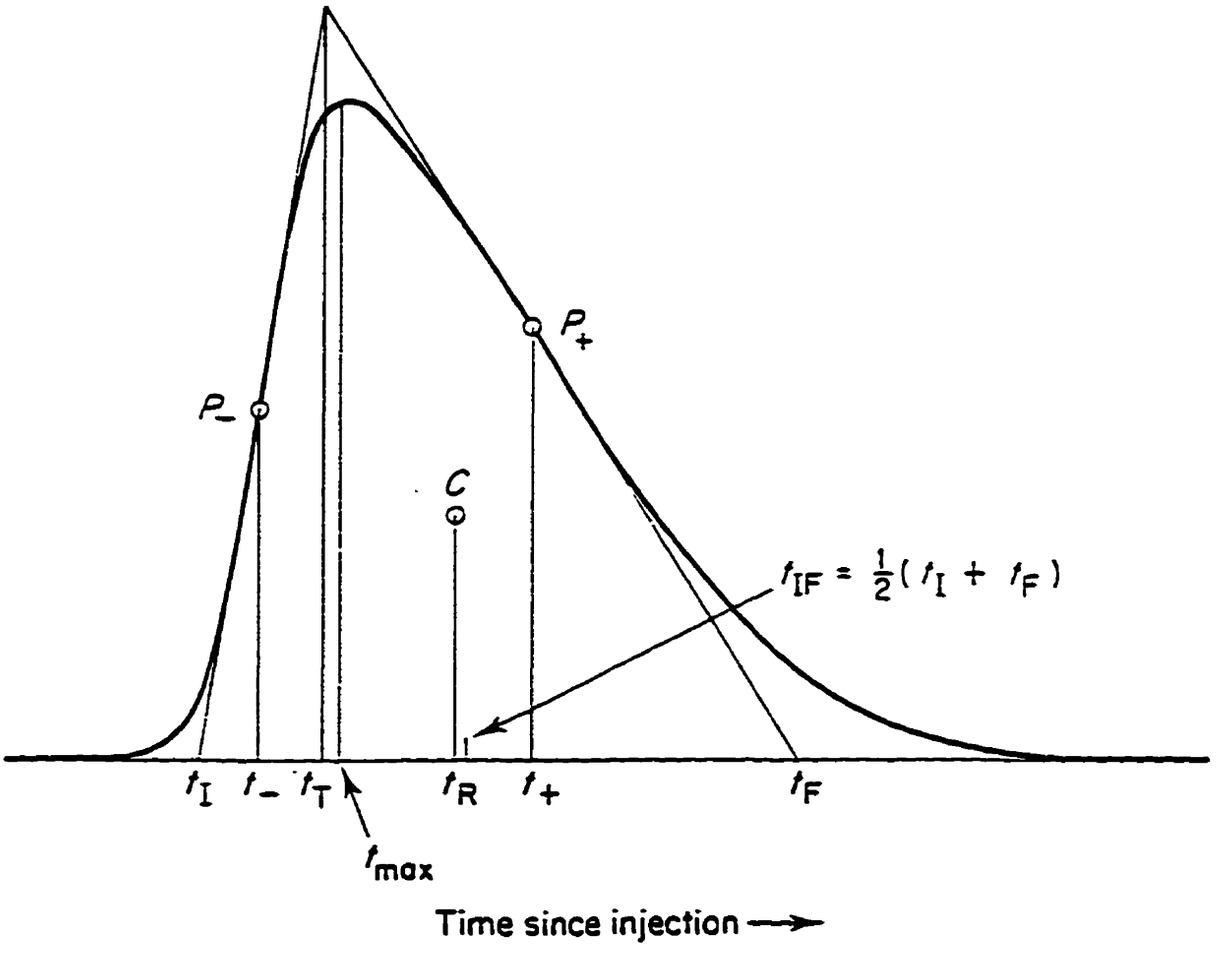
$$K = \frac{t_r - t_m}{t_m} \tag{7.4}$$

Measurement of Variance of Peak σ_t, on Slightly Asymmetrical Peaks. When the eluted peak has a symmetrical, Gaussian profile, both the plate

height, H, and the peak variance, σ_t are easily measured. However, peaks are rarely perfectly symmetrical and the methods used to determine the necessary parameters depends very much on the degree of the asymmetry of the peaks.. In this study, a simple method was used to estimate peak variance from tailed peaks obtained from the chromatogram of the solutes. This method of finding the variance involved drawing tangents on the strip-chart chromatogram through the points of inflection, i.e., steepest-slope tangents on the sides of the peak. In Figure 7.4, the tangents are shown as intersecting the baseline at "initial" and "final" peak times, t_I and t_F. The peak variance was determined by using the equation [Conder, 1979]

$$\sigma_t = \frac{1}{2}(t_+ + t_-) \tag{7.8}$$

Determination of Diffusion Coefficient, D_L. The determination of D_L involved the measurement of C, the slope in a linear plot of H versus u, and the use of equation (7.5). The application of the van Deemter equation to determine the diffusion coefficient depended greatly on the assumption that thermodynamic equilibrium was achieved in the column, the partition ratio, K, was assumed accordingly to be invariant with the amount of solute and phases extant in the system [Laub, 1978]; i.e., K was assumed to be



.Figure 7.4 Times on peak concentration profile, measured from mass center of injection profile. P_- and P_+ are the points of inflection.

independent of the velocity of the carrier gas, u.

7.4 Results and Discussion

Table 7.1 shows a comparison between the t_m values obtained directly from methane peaks with FID at various carrier gas velocities and those calculated from equation (7.4). As can be seen, the experimental t_m values are in a very good agreement with the theoretical values. The agreement suggests that the t_m values were appropriately calculated by using equation (7.4) for whole range of carrier gas velocities investigated.

The thin-channel column with the chitosan membrane stationary phase was used to investigate the partition coefficients of water and isopropanol. Figure 7.5 shows the effects of carrier gas velocity, u, on the partition coefficient K for both water and isopropanol at 30 °C. The small variations (near-zero slope) of K with u indicate that the partition coefficients of water and isopropanol are not dependent on the carrier gas velocity. Hence, we are justified to use the van Deemter equation to estimate diffusion coefficients of water and isopropanol in chitosan stationary phase using the thin-channel column.

The thin-channel column GC technique was then used to determine

Table 7.1 A comparison between the experimental and theoretical retention time of methane, t_m[a].

Carrier Gas Velocity (cm/sec)	Experimental[b] t_m (min)	Theoretical[c] t_m (min)	Ratio[d]
5	0.40	0.42	0.95
10	0.22	0.21	1.05
15	0.14	0.14	1.00
20	0.12	0.105	1.14
25	0.08	0.084	0.95
30	0.07	0.070	1.00

[a] at 30 °C.

[b] obtained directly from peak maximum of methane.

[c] calculated from eq. (7.4)

[d] Ratio = Experimental t_m/Theoretical t_m.

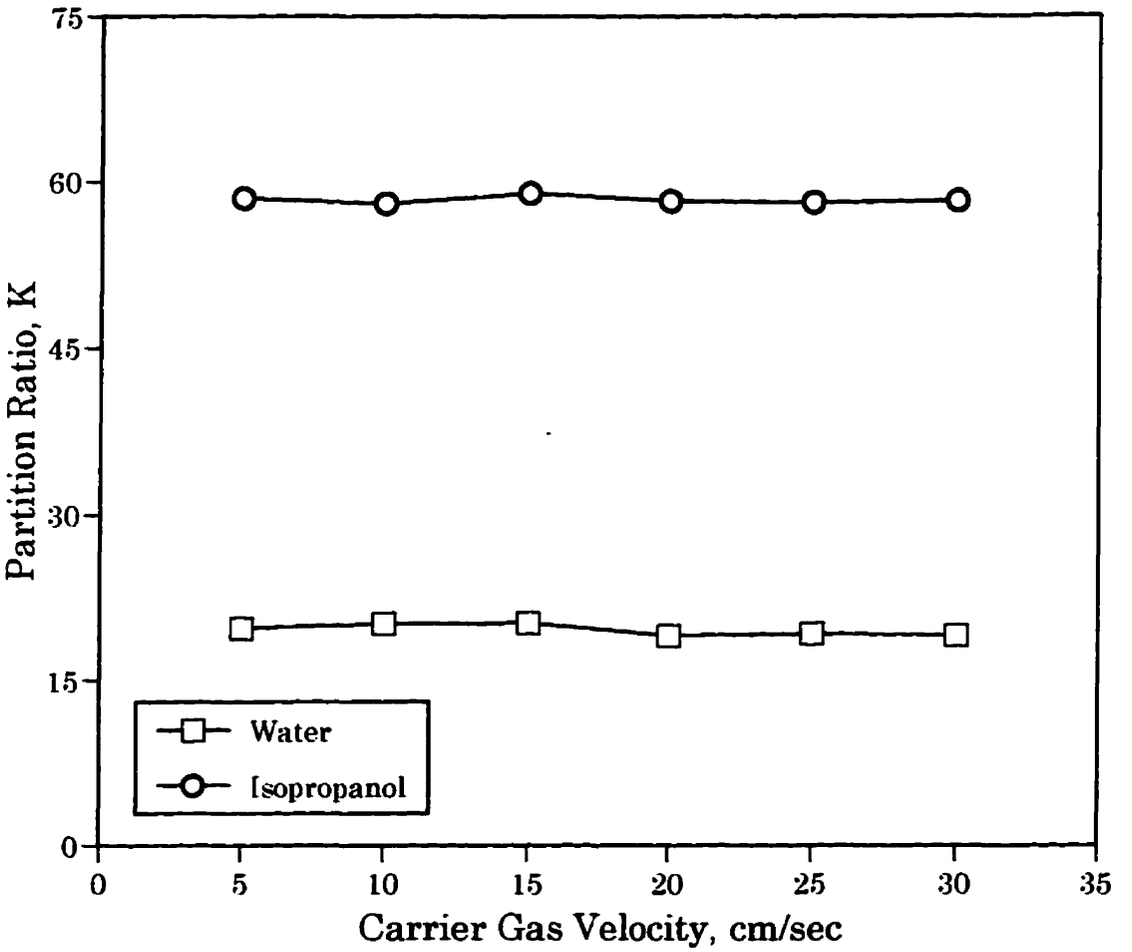


Figure 7.5 Partition coefficient of water and isopropanol as a function of carrier gas velocity. Operating temperature 30 °C.

diffusion coefficients of isopropanol and water in the chitosan membrane. The results of a series of experiments to measure the amount of peak spreading as a function of flow rate at 30 °C are shown in Figure 7.6. At sufficiently high flow rates, H increases linearly with u, with gradient C given by the simple van Deemter expression. In general, the plate heights for these experiments on polymer stationary phases are much higher than the 0.5-2 mm values for H aimed for in analytical gas chromatography [Littlèwood, 1970]. High plate heights may be rationalized by considering the nature of the chitosan polymer with a glass transition temperature, T_g about 101 °C. At room temperature chitosan contains crystalline regions which were not penetrated by the probe molecule and amorphous or rubbery regions. The rate of diffusion through this material was much slower than through the usual liquid stationary phases used in gas chromatography. At temperatures below T_g, the molecular movements of the chitosan chains are limited to segmental vibrations about a relatively fixed position. The amptitude of segmental vibration increases with increasing temperature up to T_g and at T_g, the chain segments have sufficient energy to perform rotational and translational motions or short-range diffusion motion. The plate heights of isopropanol are higher than that of water indicating that the rate of diffusion of isopropanol through the chitosan

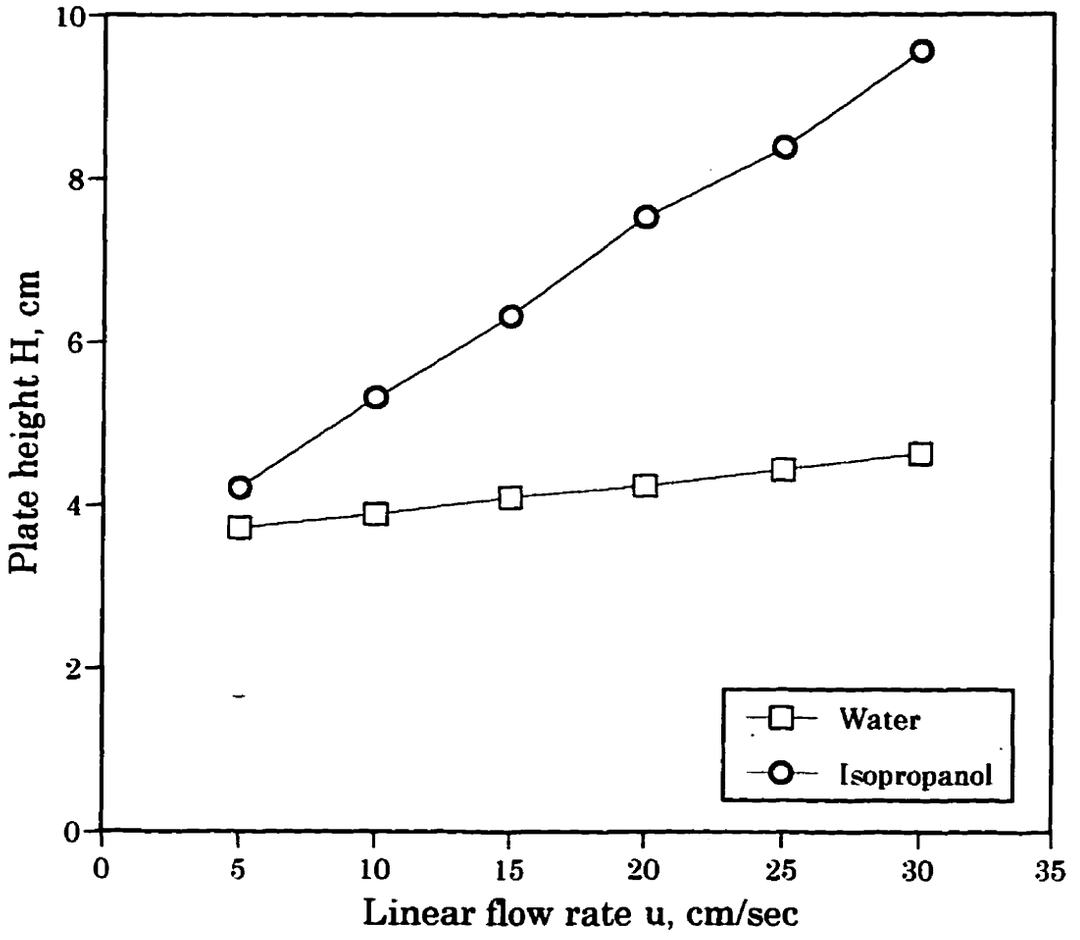


Figure 7.6 Van Deemter curves for thin-channel column with chitosan stationary phase. Operating temperature 30 °C.

stationary phase is slower than that of water. This is not unexpected because water molecule is smaller than isopropanol molecule and generally, highly hydrophilic chitosan stationary phase exhibits stronger affinity to water relative to isopropanol. Note that this is consistent with the results obtained in the pervaporation experiments with isopropanol/water mixtures where the permeation flux of water was significantly higher than that of isopropanol for the entire range of feed composition.

The chromatographic parameters were measured based on the assumption that the mass transfer between the mobile/stationary phase in the column was the only primary source of normal band-peak spreading. Note however that, the plate height, H, is equal to the increment in the variance of the peak profile per unit length of column, i.e., in a uniform column

$$H = \frac{\sigma_l^2}{L} \tag{7.9}$$

where σ_l is the standard deviation of the peak in units of column length, observed when the peak reaches the outlet, and L is the total length of column. When several, independent sources of peak spreading are present together, the law of additivity applies [Conder, 1979]:

$$\sigma_{Total} = \sum_i \sigma_i^2 \tag{7.10}$$

$$H_{Total} = \sum_i H_i \qquad (7.11)$$

In other words, the standard deviation of peak, σ, and hence the plate height, H, measured from the thin-channel column characterized the overall band-spreading processes. From a practical point of view, the peak spreading in the thin-channel column may also be due to several apparatus effects including finite width of peak at point of injection and "mixing" or dead spaces in column. These effects can be major causes of tailed chromatographs and should be kept to the minimum when accurate measurements are intended.

In order to qualitatively estimate the contributions of the undesirable apparatus effects in the total band-spreading processes, the peak-spreading of methane, an inert gas, was compared to that of water and isopropanol at the same operating conditions. We assumed that for methane, the peak-broadening which due to solute/stationary phase resistance to mass transfer within the column was sufficiently small and negligible, i.e., the peak-broadening of methane was due to phenomenon other than mass transfer of gas/stationary phase . The results are shown in Table 7.2. As can be seen, the numerical value of σ_{Total} of methane is significantly smaller than that of water and isopropanol. This indicates that the apparatus effects including

Table 7.2 Experimental data of the peak-spreading processes of methane, water and isopropanol[a].

	Methane	Water	Isopropanol
t_r (min)	0.4	8.7	23.8
σ_{Total} (min)	0.05	1.5	2.8
$W_{1/2}$ (min)	0.1	3.6	6.6
H_{Total} (cm)	0.8	3.8	5.6

[a]Measured at 30 °C with a gas carrier velocity of 5 cm/s.

dead spaces or mixing in column was reasonably small, thus indicates a high level of certainty in the true retention time in the column.

Dead spaces or mixing which may lead to band spreading and asymmetry are primarily created by sudden changes in tube diameter which occur at fitting and where the injector, column, and detector are joined to each other by connecting tubing [Conder, 1979]. The injector, thin-channel column and detector used in this study were also joined to each other by connecting tubing. However, all the tubing including the Swagelok T fitting that was used to connect the injector to the column had relatively the same size of inside diameters of about 3 mm . Note that the dimension of the rectangular thin-channel was 3 mm x 3 mm x 126 cm. The rectangular cross-section of the channel was expected to contribute more dispersion in the column than a circular cross-section, but the effect on the total peak-spreading processes was considered small [Hoff, 1997]. Therefore, we believe that dead spaces created by sudden changes in tubes diameter were minimal.

In general, the possible causes of asymmetry or tailing in the eluted peaks observed in this study are as follow [Conder, 1979]:

(a) presence of a second, unresolved component in the sample,

(b) extra-column band spreading (apparatus effects), and

(c) non-ideality - normal band-spreading process.

Since pure samples were injected and considering that the thin-channel

column was properly designed, the first two factors may not be responsible for the asymmetry and tailing in the peaks. Non-ideal peak-spreading processes may be classified in two groups. The first, there are processes which are present in every column which includes axial diffusion and non-equilibrium due to resistance to mass transfer between phases. These "normal" processes are responsible for the term in the van Deemter equation. The second group of peak-spreading processes are not inherent in the chromatographic process. Examples are slow desorption from sites of high adsorption energy, slow reactions involving the solute and occurring in the column, and very slow diffusion-controlled mass transfer between phases. Such processes usually lead to more asymmetrical, tailed peaks than normal processes. As shown in Figure 7.2 there is a part of the membrane which is not in direct contact with the gas stream, which may contribute to the adsorption of vapor. In fact, we believe the part of the membrane which is not in direct contact with the gas phase may be responsible for the peak asymmetry and tailing.

The accuracy of the chromatographic parameters measured in this study depends greatly on the design of the thin-channel column. Based on the aforementioned discussions we can say that the thin-channel column was sufficiently well designed to prevent any significant apparatus contributions to asymmetry; apparatus effects including dead spaces did not significantly

effect the peak broadening of the solutes in the column. These lead us to suggest that, the chromatographic parameters were measured to a high degree of accuracy, and hence, we were justified to proceed with our investigations.

The diffusion coefficients of water and isopropanol in the dry chitosan membrane at 30 °C were determined from the slope of the corresponding H versus u plots shown in Figure 7.5. Since the slope of such a plot is equivalent to the C term in equation (7.5), the numerical values of the diffusion coefficients of water and isopropanol in the chitosan stationary phase could be calculated for the corresponding K values. The results are tabulated in Table 7.3. As expected, the diffusion coefficient of water in the chitosan membrane is larger than that of isopropanol.

7.4.1 Effect of Temperature

Diffusion coefficients of water and isopropanol for the chitosan stationary phase were calculated from the slopes of H vs. u. In Table 7.4, the diffusion coefficients of water and isopropanol are summarized along with the operating temperatures. The diffusion coefficients of water are consistently higher than that of isopropanol and the diffusion coefficients increase with temperature from 30 to 70 °C. An increase in temperature provides energy for

Table 7.3 Diffusion coefficients in chitosan membrane determined by the thin-channel column GC technique[a]

Component	C[b] (sec)	K_{ave}[c]	D_L ($cm^2/sec \times 10^7$)
Water	0.18	19.7	10.6
Isopropanol	0.96	58.5	0.72

[a]measured using a 25 μm chitosan stationary phase at 30 °C.

[b]obtained from the slopes of plots in Figure 7.5

[c]calculated from Figure 7.4

Table 7.4 Diffusion coefficients from gas chromatographic measurements on dry chitosan membrane.

Probe	Temp (°C)	Retention Time (min)	Partition Coef. K	D_L ($cm^2/sec \times 10^7$)
Water	30	8.7	19.7	10.60
	40	7.7	18.3	10.70
	50	7.1	16.6	10.78
	60	6.3	14.6	10.82
	70	5.3	12.3	10.90
Isopropanol	30	23.8	58.5	0.72
	40	19.3	47.3	0.87
	50	15.3	37.2	1.07
	60	12.2	29.3	1.28
	70	8.2	19.2	1.65

a general increase in segmental motion. If the energy density is sufficient, the polymer may pass through structural transitions such as the *Tg*, which further affect the diffusion process. Above *Tg*, in the rubbery state, the segmental motion is rapid and but molecular motion is still restricted by chain entanglements. As temperature increases, the degree of entanglement decreases and molecular slip increases. The effects of an increase in temperature may also be expressed in terms of the increase in free volume directly related to the bulk expansion of the polymer due to the increased segmental motions.

As shown in Fig. 7.7, the temperature dependence of the diffusion coefficient, D_L over small temperature range can be represented by an Arrhenius type relation,

$$D_L = D_o exp\left(-\frac{E_a}{RT}\right) \tag{7.12}$$

where D_o is a constant, E_a the activation energy for diffusion, R is the gas constant, and T is the operating temperature. The activation energy for diffusion for water and isopropanol was calculated from the slopes of Fig. 7.7 and are summarized in Table 7.5. The activation energy for diffusion of isopropanol is higher than that for water, which suggests that the water molecules require less energy than isopropanol do to facilitate diffusion

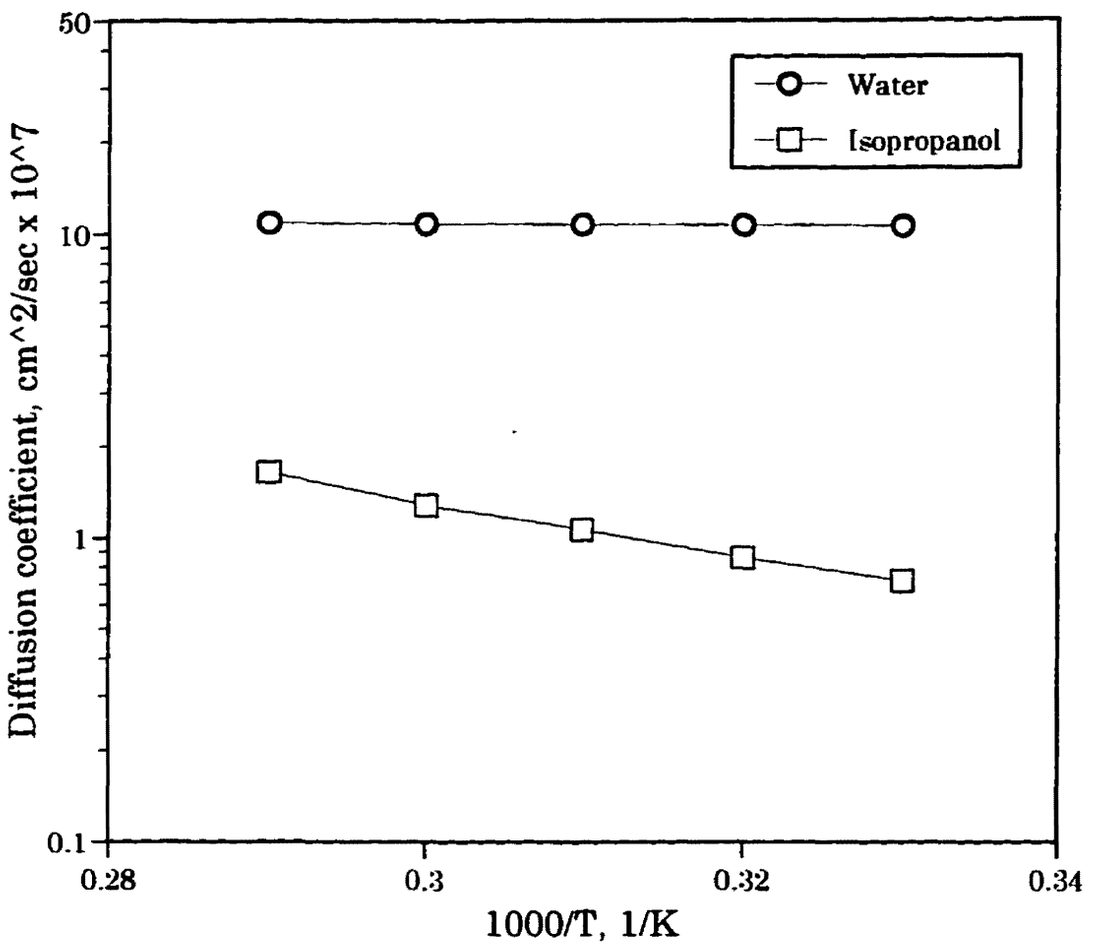


Figure 7.7 Arrhenius plots of diffusion coefficients for water and isopropanol in chitosan.

Table 7.5 Diffusion activation energy for water and isopropanol determined by inverse gas chromatography technique.

Stationary Phase	Activation Energy, KJ/mol[a]	
	Water	Isopropanol
Dry Chitosan	0.59	1.91
Swollen Chitosan	No data[b]	1.08

[a]Gas constant, R = 8.314 KJ/mol.K

[b]No experiment was done.

through the stationary phase.

Note that from practical point of view, the difference in the activation energy for each probe may arise from several factors including molecular size and probe/stationary phase interaction. Interestingly, activation energy for diffusion of isopropanol through the swollen stationary phase is lower than that through the dry stationary phase. This indicates that the diffusion of isopropanol is also affected by the nature of the stationary phase; the presence of sorbed water in the water swollen stationary phase apparently decreases the energy required for the diffusion of isopropanol. Water apparently depresses the T_g of the chitosan membrane and changes the properties of the stationary phase induced by plasticisation and swelling processes.

Note also that plasticisation and swelling of the stationary phase caused by prolonged exposure to water saturated carrier gas are both reversible processes. The amorphous chitosan polymer exhibits a significant change from glass-like behavior when dry to soft, rubbery-like behavior when swollen and *vice-versa*.

7.4.2 Effect of Penetrant Size

An increase in the size of a penetrant in a series of chemically similar penetrants generally leads to an increase in solubility and a decrease in

diffusion coefficients. The effect of penetrant size on the diffusion coefficients is illustrated in Fig. 7.8 at various temperatures for a series of alcohols: methanol, ethanol and isopropanol. As can be seen, as the size of the alcohols increases from methanol to isopropanol, the corresponding diffusion coefficients decrease. The decrease in diffusion coefficients is a reflection of the need to create or utilize a critical activation volume in the polymer stationary phase proportional to that of the penetrant molecule; the size of the hole required to accommodate the molecule, the length and the size of the path the molecule must follow during its diffusion, and the free volume available to the polymer segment to exchange positions with the probe molecules.

Therefore, the diffusion coefficient shows inverse proportionality to the size of the molecule. This result agrees well with Einstein's equation for the diffusion coefficient relating to the chain length of the solvent which has the form

$$D = RT/f \tag{7.13}$$

where f is called the friction factor and is directly proportional to the chain length. The validity of such a relationship has also been confirmed by other workers [Prager and Long, 1951; Prager *et al.*, 1953]. According to Fujita's free volume theory [Fujita, 1961], the thermodynamic diffusion coefficient, D, is

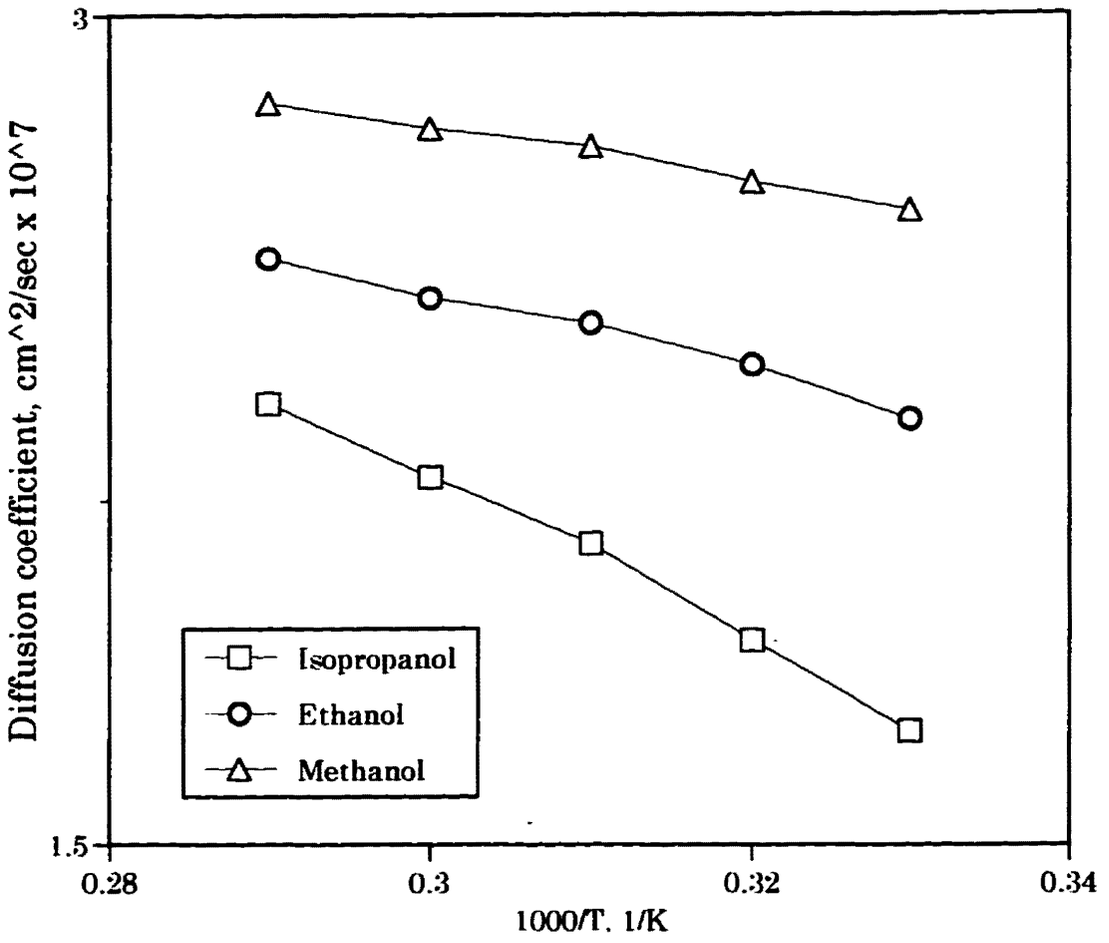


Figure 7.8 **Arrhenius plots of diffusion coefficients of methanol, ethanol and isopropanol in swollen chitosan membrane.**

related to the free volume by the following expression:

$$D = ARTexp\left(-\frac{B}{f}\right) \tag{7.14}$$

where A and B are parameters that are assumed to be independent of diffusant concentration and temperature. However, A is pre-exponential factor which depends on the properties of the diffusant and the polymer, whereas B is a constant characterizing the size of the hole needed for a diffusion jump. The fractional free volume of the pure polymer is denoted by f.

On the basis of eqn. (7.10), the following equation can be written for the diffusion coefficient at zero penetrant concentration, D_L:

$$D_L = ARTexp\left(-\frac{B}{f_L}\right) \tag{7.15}$$

where f_L is the fractional free volume of the pure polymer. Hence, increasing the diffusant size will, in general, cause an increase in B and possibly a decrease in A, which in turn decrease the diffusion coefficient.

Table 7.6 gives the summary of the activation energy for diffusion of methanol, ethanol and isopropanol calculated from the corresponding Arrhenius plot of diffusion coefficients. The apparent activation energy for diffusion increases proportional to the relative size of the penetrants and have the following order;

Table 7.6 Diffusion activation energy of alcohols determined by gas chromatography technique.

Chitosan Stationary Phase	Activation Energy, KJ/kgmol					
	MeOH	R_M^{2a}	EtOH	R_E^{2a}	i-PrOH	R_I^{2a}
Dry	0.85	0.97	0.90	0.96	1.91	0.97
Swollen	0.51	0.93	0.62	0.94	1.08	0.98

[a] Regression coefficient.

isopropanol > ethanol > methanol

Evidently, the presence of sorbed water in the stationary phase causes a significant decrease in the activation energy. As previously discussed, swelling and plastization of the chitosan stationary phase increase the free volume available to the system to enhance the diffusion of the solvents.

7.5 Accuracy of Measurements

It is difficult to determine the accuracy of the diffusion coefficients measurements by the thin-channel column inverse gas chromatography technique. Comparison of the present results with literature data was somewhat difficult, due to unavailability of reported data on similar probe/stationary phase systems and different temperature range involved. Generally, the diffusion coefficients for polymer/probe systems lie in the range of 10^{-6} to 10^{-9} cm^2/sec [Price, *et al.* 1978]. Table 7.7 gives some of the literature data of diffusion coefficients determined by IGC technique as reported by various workers. The overall accuracy of the diffusion coefficients measured by the thin-channel column IGC method, as evidenced by the linearity of the Arrhenius plot of the diffusion coefficients indicated by the numerical value of the regression coefficient of determination, R^2, (see Table 7.6) was reasonably good.

Table 7.7 Literature data of experimental diffusion coefficients measured by gas chromatography technique.

Column Type	Stationary Phase	Probe	Diffusion Coefficient ($cm^2/sec \times 10^7$)	Temp .(°C)	Reference
Packed Column	P(VdC/VC)[a]	Water	0.200 0.255	30 50	Demertzis, 1989
Packed Column	P(VdC/AcN)[b]	Water	0.120 0.175	30 50	Demertzis, 1989
Packed Column	PAN	Water Ethanol -	0.034 0.047 0.008 0.147	30 50 30 50	Kim, 1994
Capillary Column	PMMA[c]	Methanol	0.007 0.044	70 100	Arnould, 1989
Thin-channel Column	Chitosan	Water Isopropanol	10.6 0.72	30 30	This study

[a]Poly(vinylidene chloride-vinyl chloride)
[b]Poly(vinylidene chloride-acrylonitrile)
[c]Polymethyl methacrylate

In this work, no apparent sample-size dependent effects on the retention times was observed, tailing and asymmetric peaks were minimal. This supports our belief that the thin-channel column *"coated"* with the chitosan membrane layer was sufficiently well prepared, apparatus effects were small and negligible, and that adsorption was minimized. Therefore, it was assumed that thermodynamic equilibrium was achieved in the column, and hence that we were justified in using the van Deemter equation to calculate the diffusion coefficients with a high degree of accuracy. The design of the column parameters can be adjusted, within limits, to suit certain purposes and the thickness of the polymer film can be readily varied to allow for the study of a range of diffusion coefficients of components in polymeric membranes.

7.6 Conclusions

A spiral thin-channel column was designed and used for the study of diffusion in chitosan stationary phase based on inverse gas chromatography technique. The followings conclusions can be drawn from this work:

(1) The uniquely designed column presents a reliable alternative to the conventional packed and capillary columns, with special applications to pervaporation membranes, for the measurements of diffusion

coefficients by inverse gas chromatography technique.

(2) Inverse gas chromatography technique provides a simple, fast and objective alternative to estimate the diffusion in polymer membrane.

(3) The measured diffusion coefficients are dependent on both temperature and molecular size; the diffusion coefficients increase with an increase in temperature and decrease with a relative increase in molecular size of the probes.

(4) The diffusion coefficients in water swollen stationary phase are higher than that obtained in dry stationary phase; the sorbed water affects the diffusion of alcohols through the polymer film.

(5) It may be possible to apply this technique for determining diffusion coefficients of other solutes in other hydrophilic polymers.

CHAPTER 8

Pervaporation Transport Mechanism in Hydrophilic Chitosan Membranes

8.1 Introduction

Transport phenomena in polymer films have been extensively studied because of their significance from both practical and fundamental viewpoints [Hopfenberg, 1974; Kumins, 1973; Vergnaud, 1991]. These investigations have shown that, for most part, gas and liquid transport through a polymeric film can be described in terms of sorption and diffusion. For most pervaporation systems, permeate transport behaves non-ideally, especially when particular interactions exist. Several theories on sorption and diffusion have been proposed which seek to relate experimental data to polymer morphology,

chemical structure and other physical properties [Hopfenberg, 1974; Zaikov *et al.*, 1988; Crank, 1968].

Transport through membranes usually can lead to the separation of different molecules. For many membrane systems, the process complexity often makes it difficult to come up with an accurate explanation of the transport mechanisms. The transport of permeants through a polymer membrane in a pervaporation separation, which is the only membrane process where a phase transition occurs from the upstream side to the downstream permeate side, is still unclear.

The solution-diffusion model has been the most widely accepted transport mechanism for pervaporation because of its satisfactory description of mass transport in terms of physicochemical nature of pervaporation process. The pervaporation through moderately swollen membrane has also been analyzed as a solution-diffusion process. However, several authors indicated that the mechanism of water transport through a membrane containing polar moiety is not easily explained by random solution and diffusion through the polymer matrix. Rather, transport through highly water selective continuous paths (channels) within the membrane may probably be responsible for the low activation energy and high fluxes obtained in such system.

The model of continuous micelles proposed by Gierke [1983] indicates

that the transport of hydrophilic permeates indeed takes place through a continuous (extended) micelle with relatively high charge density. Preferential transport of water by hydrogen bonding between water and carboxylic acid through poly(acrylonitrile-co-acrylic acid) was investigated by Yoshikawa *et al.* [1984]. They suggested that water permeates through a hydrogen bond channel according to a so-called *push-pull* mechanism. Recently, Kim [1994] modified the free volume model by considering the polar path in order to interpret the pervaporation transport mechanism for a containing hydrophilic groups. By using this modified model, they were able to calculate the concentration profile and the local selectivity profile in the membrane.

As shown and discussed in Chapter 3 and 4, the highly hydrophilic chitosan membranes are dense, homogeneous in which water is preferentially absorbed and permeated during pervaporation with water-isopropanol mixtures. Experimentally, it has been shown that the diffusion coefficient of water is significantly higher than that of isopropanol as measured by the inverse gas chromatography technique in Chapter 5. These observations lead us to an interpretation that the water molecules may permeate through an additional channel, so-called polar pathway which is only available to water molecules, whereas the isopropanol molecules travel through the regular polymer matrix available for both the water and isopropanol molecules. In other words, the significantly high water fluxes is due the co-existence of the

polar pathway and the polymer matrix.

8.2 Theoretical

8.2.1 Single Component Permeation

According to the solution-diffusion theory, each component of the permeating molecules dissolves in the membrane in accordance with an equilibrium distribution law and diffuses through the membrane in response to the concentration gradient. Thus, the flux J for component i is given by a relationship of the type

$$J_i = -\frac{D_i C_i}{RT}\frac{d\mu_i}{dX} \tag{8.1}$$

and

$$\mu_i = \mu_{i0} + RT\ln a_i + \int_{P_r}^{P} \overline{V_i}\, dP - \int_{T_r}^{T} S_i dT \tag{8.2}$$

where J_i is the flux rate of component i through the membrane at the position X in the membrane, D_i is the mobility for component i at the position X in the membrane, C_i is the concentration of component i at the position X in the membrane, μ_i is the chemical potential of component i at the position X in

the membrane, μ_{i0} is the chemical potential of component i at the reference state, a_i is the activity of component i at the position X in the membrane, $\overline{V_i}$ is the partial molar volume of component i at the position X in the membrane, P is the pressure at the position X in the membrane, and P_r, T_r are the reference pressure and temperature, respectively.

In the case of a flat membrane and one dimensional isothermal permeation, the flux J_i at steady state will become

$$J_i = -\frac{D_i C_i}{RT}\left[RT\frac{d}{dX}\ln a_i + \overline{V_i}\frac{d}{dX}P\right] \tag{8.3}$$

Thus, the permeation rate will depend on the diffusion constant, the concentration, the activity gradient, and the pressure gradient in the membrane.

A single component permeation through a polymer membrane can be considered as a binary system, a membrane system consists of the component i and the polymer itself. The mass balance of this membrane system for a stationary coordinate is described by [Bird, 1960]

$$J_i = \omega_i\left(J_i + J_p\right) + J_{iD} \tag{8.4}$$

where J_i and J_p are the mass flux of component i and polymer, respectively;

J_{iD} is the mass flux of component i due to diffusion; ω_i is the mass fraction of component i in the membrane system.

The equation shows that the mass flux of component i through the membrane system is the resultant of the mass flux resulting from the bulk motion of the membrane system (the first term on the right-hand side) and the diffusion superimposed on the bulk flow (the second term on the right-hand side). Since the polymer is stationary, there is no mass flux of polymer. Thus, eqn. (8.4) can be reduced to

$$J_i = \frac{J_{i_D}}{1 - \omega_i} \tag{8.5}$$

8.2.2 Binary Components Permeation

The permeation of a component of a binary mixture is not only affected by its own presence but also by the movement of the other component. This phenomenon is known as the coupling effect. Coupling can be divided into two parts : a thermodynamic and a kinetic part.

From a thermodynamic view, the change in concentration of one component in the membrane due to the presence of another component is caused by mutual interactions between the permeants in the membrane as

well as by that between the permeants and membrane material. For a thermodynamic coupling to occur, the affinity between permeants and that between permeants and membrane play a very important role in determining preferential sorption.

On the other hand, kinetic coupling is due to the concentration dependence of the diffusion coefficients of low molecular weight components in polymers, particularly in glassy polymers. Below the glass transition temperatures, the thermal motions of polymer chain segments are very restricted. When low molecular weight components are dissolved in such polymers, the mobility of the chain increases. In the case of a binary mixture, both components will exert a plasticizing effect on the segmental motions, and the mobilities of both permeants will be enhanced by the combined plasticizing action. Therefore, in a model description for the permeation of liquid mixtures by pervaporation, coupling phenomena have to be taken into account. A mathematical model based on the extension of the Fujita's free volume theory [Fujita, 1961] and the Flory-Huggins thermodynamics [Flory, 1953] was developed by Yeom [1991, 1992] for the pervaporation separation of ethanol-water mixtures through crosslinked poly(vinyl alcohol). The model includes the diffusion coefficient of the individual penetrants and terms that explain the plasticization actions of a penetrant and the coupling effect of the permeation through the membrane of one penetrant on permeation of the

other penetrant.

A binary mixture permeation through a polymer membrane can be considered as a ternary membrane system consisting of permeants i, j and the polymer.

The mass balance for this system can be expressed as

for permeant i

$$J_i = \omega_i(J_i + J_j + J_p) + J_{iD} \tag{8.6}$$

for permeant j

$$J_j = \omega_j(J_i + J_j + J_p) + J_{jD} \tag{8.7}$$

for polymer p (stationary)

$$J_p = 0 \tag{8.8}$$

where J_i, J_j, and J_p are the mass fluxes of permeant i, j and polymer through the membrane system, respectively; ω_i and ω_j are the mass fractions of permeant i and j in the membrane system, respectively; J_{iD} and J_{jD} are the mass fluxes of permeants i and j through the membrane system due to diffusion, respectively. Expressing J_i and J_j in terms of J_{iD} and J_{jD}, we obtain

for permeant i

$$J_i = \frac{1 - \omega_j}{1 - \omega_i - \omega_j} J_{iD} + \frac{\omega_i}{1 - \omega_i - \omega_j} J_{jD} \tag{8.9}$$

for permeant j

$$J_j = \frac{1 - \omega_i}{1 - \omega_i - \omega_j} J_{jD} + \frac{\omega_j}{1 - \omega_i - \omega_j} J_{iD} \tag{8.10}$$

The first term of the Eqns. (8.9) and (8.10) on the right-hand side represents the mass flux of permeant i and j due to their own chemical potential. The second term represents the coupling flow resulting from the other chemical potential gradient.

8.3 Transport Through Chitosan Membranes

As previously cited, the transport of water through membranes containing hydrophilic groups such as carboxylic acid or vinyl pyridine was widely investigated by Yoskikawa *et al.* [1984]. They suggested that for the membrane containing carboxylic acid group, water might be able to permeate by a so-called "*push-pull*" mechanism as shown in Figure 8.1. In this way, water molecules might be pushed and pulled by direct hydrogen bonding interaction by carboxylic acid resulting in high value of permeation rate. Hence, the transport of water through the membrane containing hydrophilic functional group cannot be explained by a simple mechanism of diffusion described in the solution-diffusion model.

The chitosan membranes show a higher affinity for water than for

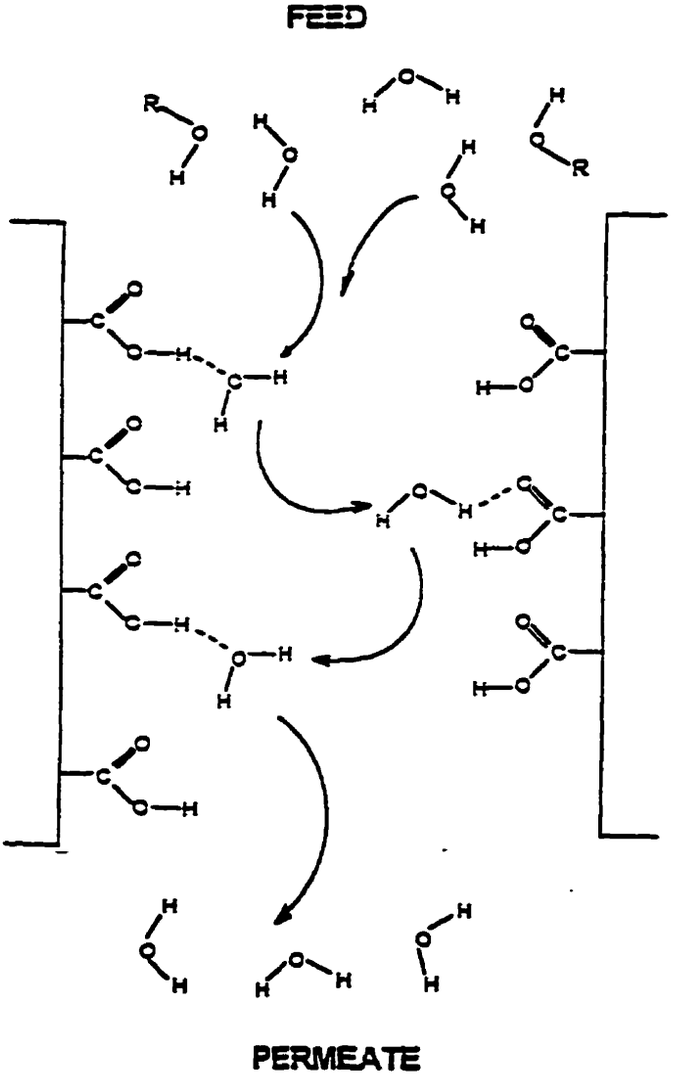


Figure 8.1 Transport mechanism of water by direct hydrogen bonding between water molecules and carboxylic acid [Yoshikawa *et al.*, 1984]

isopropanol; the water might be preferentially bound to the ionized amino group in the chitosan matrix by hydrogen-bonding force or hydrogen shell. Water should permeate through the hydrophilic region by virtue of a high exchange rate between the free water and ionized water in the hydration shells. For isopropanol, apart from a small part which may dragged along by flow coupling with water, transport through the membrane may take place mainly by random molecular solution and diffusion within the amorphous network of non-ionized species in the chitosan matrix.

Water transport through a highly water selective pathway seems to play a very important role in pervaporation separation of water-isopropanol mixtures through the chitosan membranes. Thus the solution-diffusion model is modified for the membrane containing polar moieties by taking polar pathway within the membrane into consideration. In this approach, as illustrated in Figure 8.2, the total permeation flux, J, through the membrane is broken into two parts: the permeation flux through the polar pathway, J_p, and the permeation rate through the membrane matrix, J_f.

It is worth noting here that the polar pathway is hydrophilic and has strong interaction with water but has negligible effect on isopropanol. Further more J_p may be greater than J_f. J_f is determined by the nature of the polymer and is relatively constant once the polymer structure is formed, while J_p can

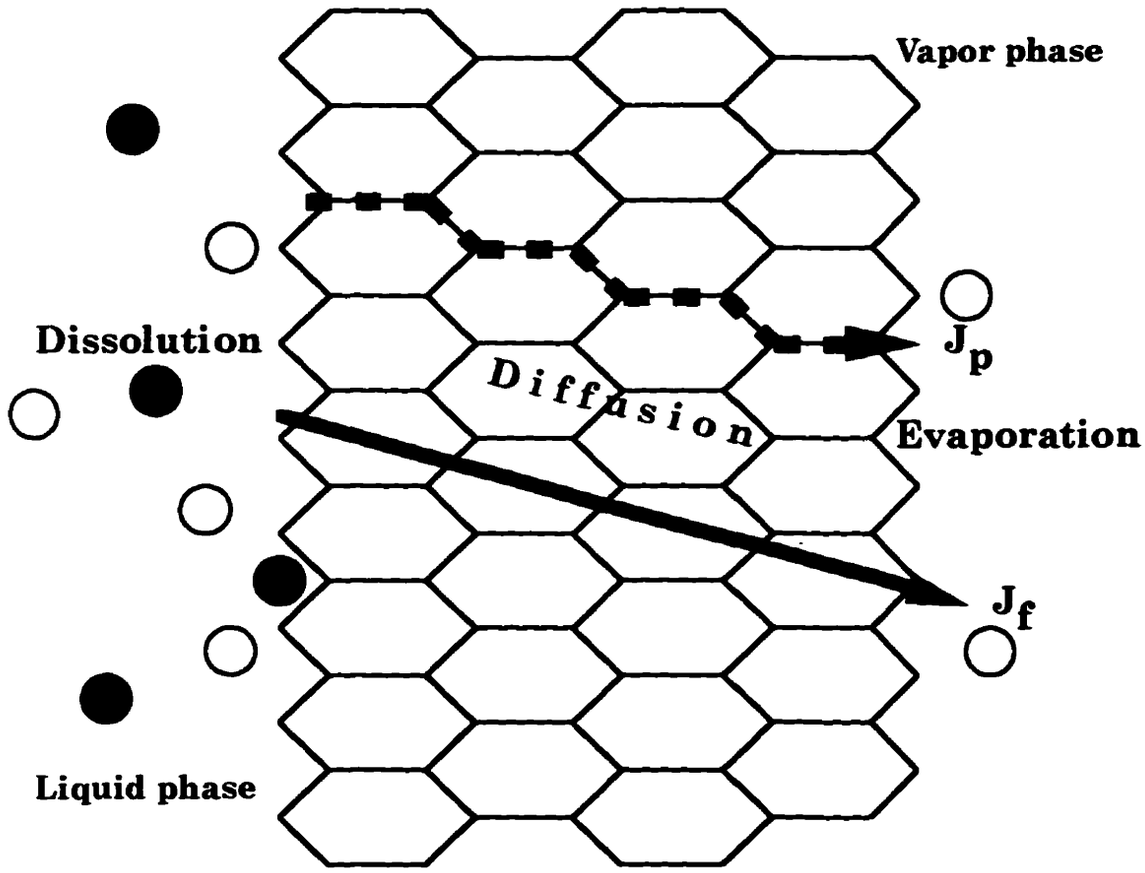


Figure 8.2 Schematic of transport mechanism through chitosan membrane.

vary according to different membrane treatment applied. As discussed in Chapter 5, crosslinking of chitosan leads to a change in hydrophilicity of the membrane, and should therefore change the diffusivity in the polar pathway and J_p.

The following assumptions are made to simplify the modelling procedure.

(1) Permeation through the membrane system obeys the solution-diffusion mechanism.

(2) The permeant(s) undergoes no phase change within the membrane system during the pervaporation.

(3) Isopropanol does not interact or permeate through the highly water selective paths.

(4) The diffusion coefficient of water in this path is constant,i.e., it is independent of water concentration.

(5) The membrane undergoes no structural changes during the steady-state separation process.

(6) The pressure within the membrane system is uniform.

(7) Thermodynamic equilibrium exists at the interfaces of the membrane system.

8.3.1 Single Component Permeation

The water flux through a hydrophilic membrane such as chitosan, J_{iD}, can be expressed as

$$J_{iD} = kJ_{ip} + (1 - k)J_{if} \tag{8.11}$$

where k is the surface area fraction of polar path in the membrane, and J_{ip} and J_{if} are the water fluxes through the polar pathway and the membrane matrix, respectively. The fraction of polar paths, k, can be recognized as the surface area fraction of polar group and can be assumed to be the same as $n^{2/3}$ [Kim, 1994] where n is the swelling ratio. J_{ip} and J_{if} can be expressed as

$$J_{ip} = -\frac{D_{ip}C_{ip}}{RT}\frac{d\mu_i}{dX} \tag{8.12}$$

$$J_{if} = -\frac{D_{if}C_{if}}{RT}\frac{d\mu_i}{dX} \tag{8.13}$$

where D_{ip} and D_{if} are the diffusion coefficient of component i through the polar pathway and in the membrane matrix, respectively. Substitution of Eqns. (8.12) and (8.13) into Eqn. (8.11) gives

$$J_{iD} = -\frac{1}{RT}\left[kD_{ip}C_{ip} + (1-k)D_{if}C_{if}\right]\frac{d\mu_i}{dX} \tag{8.14}$$

The mass flux of water through the membrane system can be rewritten by substituting Eqn. (8.14) into Eqn. (8.5)

$$J_i = -\frac{1}{1-\omega_i}\frac{1}{RT}\left[kD_{ip}C_{ip} + (1-k)D_{if}C_{if}\right]\frac{d\mu_i}{dX} \tag{8.15}$$

In the case of a flat membrane and one dimensional isothermal permeation and constant pressure, the water flux J_i and the isopropanol flux J_j at steady state will become

$$J_i = -\frac{1}{1-\omega_i}\left[kD_{ip}C_{ip} + (1-k)D_{if}C_{if}\right]\left[\frac{d}{dX}\ln a_i\right] \tag{8.16}$$

$$J_j = -\frac{1}{1-\omega_j}\left[(1-k)D_{jf}C_{jf}\right]\left[\frac{d}{dX}\ln a_j\right] \tag{8.17}$$

The concentration of penetrant at the boundary of the membrane may be calculated from thermodynamic principles.We assume that when the membrane is in contact with a system, either liquid or gas, the chemical potential at the boundary of the membrane as illustrated in Figure 8.3, $\mu_{i1}^m(\mu_{i2}^m)$, and that in the adjacent phase solution, μ_{i1}^s (μ_{i2}^s), must be equal. Therefore

$$\mu_{i1}^s = \mu_{i1}^m \quad \mu_{i2}^s = \mu_{i2}^m \tag{8.18}$$

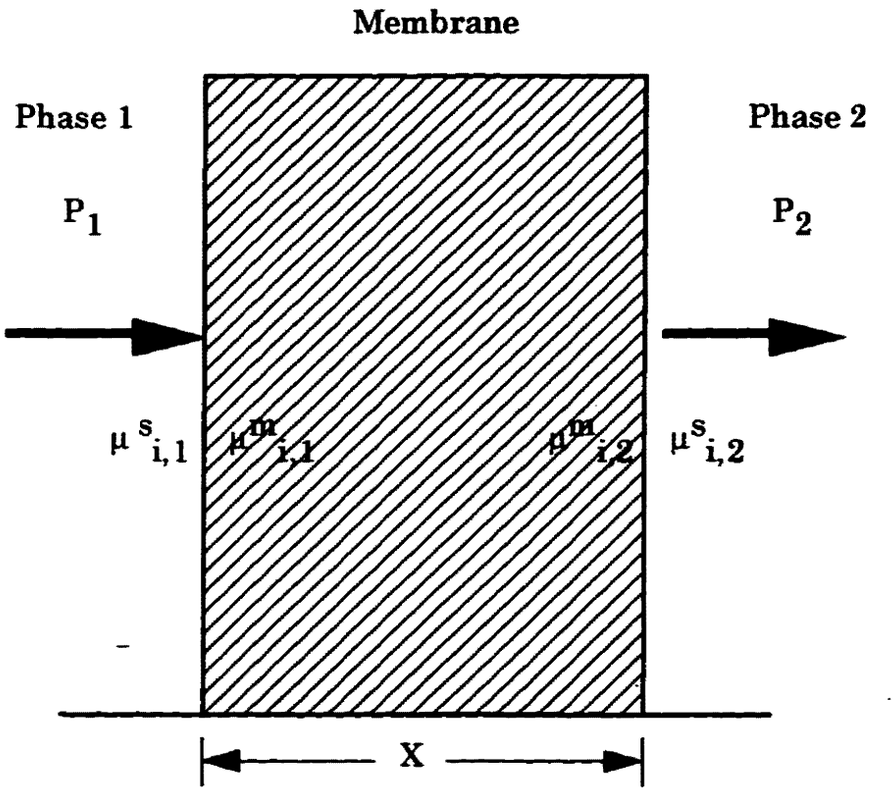


Figure 8.3 The schematic of the permeation through a membrane

where 1 and 2 refer to the upstream and downstream side, respectively.

In order to relate the activities of permeant at the membrane faces to the pressure upstream and downstream, we make use of the equality of chemical potential between dissolved permeant and contacting fluid which follows from the assumption of thermodynamic equilibrium [Greenlaw, 1977].

For the pure liquid upstream at pressure, P_1, assuming constant molar volume, $\overline{V}$,

$$\mu_1 = \mu^0 + \overline{V}\left(P_1 - P_0\right) \tag{8.19}$$

where μ^0 is the chemical potential of the pure liquid at its saturation pressure P_0.

For the dissolved liquid at the upstream face, assuming the effect of pressure on activity coefficient (but not chemical potential) is negligible, and assuming the partial molar volume of the permeant equal to the molar volume,

$$\mu_1 = \mu^0 + \overline{V}\left(P_1 - P_0\right) + RT \ln a_1 \tag{8.20}$$

For the dissolved liquid at the downstream face (and assuming the pressure in the membrane is constant at P_1),

$$\mu_2 = \mu^0 + \overline{V}\left(P_1 - P_0\right) + RT \ln a_2 \tag{8.21}$$

For pure vapor in contact with the downstream face, assuming perfect gas behavior,

$$\mu_2 = \mu^0 + RT\,In\left(\frac{P_2}{P_0}\right) \tag{8.22}$$

Equating equations (8.19) and (8.20), we find that the upstream activity must be unity. Thus the activity of component i at the upstream face is,

$$a_{il}^{m} = 1 \tag{8.23}$$

Equating equations (8.21) and (8.22) we obtain the following relation for a_2, applicable when we have vapor at the downstream face,

$$a_2 = \frac{P_2}{P_0} exp\left[-\frac{\overline{V_i}}{RT}\left(P_1 - P_0\right)\right] \tag{8.24}$$

where P_0 is the saturation pressure of water and if water vapor is assumed to be a perfect gas, the ratio P_2/P_0 is equal to the activity, a_{i2}^{s}.

The concentration and diffusion of component i is a function of permeant concentration in the membrane system. Using the simplest relationship [Greenlaw *et al.*, 1977]

$$D_i = k_{Di} c_i \tag{8.25}$$

and

$$c_i = k_{ci} a_i \tag{8.26}$$

where k_{Di} and k_{ci} are constants. c_i is the solubility of permeant i in the polymer with the unit of mass of permeant i per mass of polymer. The mass concentration, C_i, and the mass fraction, ω_i, can also be expressed in term c_i

$$C_i = \frac{c_i}{1+c_i} d_m \tag{8.27}$$

and

$$\omega_i = \frac{c_i}{1+c_i} \tag{8.28}$$

where d_m is the density of the membrane system which is assumed to be constant. Expressing D_{ip}, D_{if}, C_{ip}, and C_{if} in terms of c_i using similar relationships as in equations (8.25 - 27) we obtain

$$D_{ip} = k_{D_p} c_{ip} \tag{8.29}$$

$$D_{if} = k_{D_f} c_{if} \tag{8.30}$$

$$C_{ip} = \frac{c_{ip}}{1 + c_{ip}} d_m \tag{8.31}$$

$$C_{if} = \frac{c_{if}}{1 + c_{if}} d_m \tag{8.32}$$

$$c_{ip} = k_{c_{ip}} a_i \tag{8.33}$$

$$c_{if} = k_{c_{if}} a_i \tag{8.34}$$

where $k_{D_{ip}}$, $k_{D_{if}}$, $k_{c_{ip}}$, $k_{c_{if}}$ are constants. c_{ip} and c_{if} are the solubilities of permeant i in the polar pathway and polymer matrix, respectively.

Combining equations (8.28-34) and (8.16), we obtain

$$J_i = -\left(1 + c_i\right)\left[k k_{D_{ip}} k_{c_{ip}} \frac{c_{ip}}{1 + c_{ip}} d_m a_i + (1 - k) k_{D_{if}} k_{c_{if}} \frac{c_{if}}{1 + c_{if}} d_m a_i \right] \frac{d}{dX} \ln a_i \tag{8.35}$$

Combining c_{ip} and c_{if} in terms of c_i

$$c_{ip} + c_{if} = c_i \tag{8.36}$$

and for simplicity, assuming

$$c_{if} * c_{ip} < 1 \tag{8.37}$$

we obtain

$$J_i = -d_m \left[k k_{D_{ip}} k_{c_{ip}} c_{ip} + (1-k) k_{D_{if}} k_{c_{if}} c_{if} \right] \frac{d}{dX} a_i \ln a_i \tag{8.38}$$

Substituting c_{ip} and c_{if} in terms of a_i using equations (8.33) and (8.34) we obtain

$$J_i = -d_m \left[k k_{D_{ip}} k_{c_{ip}}{}^2 + (1-k) k_{D_{if}} k_{c_{if}}{}^2 \right] \frac{d}{dX} a_i{}^2 \ln a_i \tag{8.39}$$

Integrating with the boundary conditions at the downstream and the upstream sides,

$$J_i \int_0^x dx = -d_m \left[k k_{D_{ip}} k_{c_{ip}}{}^2 + (1-k) k_{D_{if}} k_{c_{if}}{}^2 \right] \int_{a_1}^{a_2} a_i da_i \tag{8.40}$$

$$J_i = -\frac{d_m}{2X} \left[k k_{D_{ip}} k_{c_{ip}}{}^2 + (1-k) k_{D_{if}} k_{c_{if}}{}^2 \right] a_i{}^2 \Big|_{a_1}^{a_2} \tag{8.41}$$

where X is the thickness of the membrane.

With boundary conditions,

$$a_1 = 1 \tag{8.42}$$

and

$$a_2 = \frac{P_2}{P_0} exp\left[-\frac{\overline{V}}{RT}(P_1 - P_0)\right] \tag{8.43}$$

we obtain

$$J_i = \frac{d_m}{2X}\left[kk_{D_{ip}}k_{c_{ip}}{}^2 + (1-k)k_{D_{if}}k_{c_{if}}{}^2\right]\left\{1-\left(\frac{P_2}{P_0}\right)^2 exp\left[-\frac{\overline{2V}}{RT}(P_1 - P_0)\right]\right\} \tag{8.44}$$

or

$$J_i = \frac{d_m}{2X}\left[kk_{D_{ip}}k_{c_{ip}}{}^2 + (1-k)k_{D_{if}}k_{c_{if}}{}^2\right]\left(1-a_{i2}{}^2\right) \tag{8.45}$$

Introducing K_i to equation (8.45) where,

$$K_i = \frac{d_m}{2X}\left[kk_{D_{ip}}k_{c_{ip}}{}^2 + (1-k)k_{D_{if}}k_{c_{if}}{}^2\right] \tag{8.46}$$

the mass flux of water ,J_i, through the membrane system in a single component pervaporation process can be rewritten as

$$J_i = K_i\left[1-a_{i2}{}^2\right] \tag{8.47}$$

similarly for isopropanol flux, J_j,

$$J_j = K_j\left[1 - a_{j2}^{\ 2}\right] \tag{8.48}$$

where

$$K_j = \frac{d_m}{2X}\left[(1-k)k_{D_{jf}}k_{c_{jf}}^{\ 2}\right] \tag{8.49}$$

The resulting equation for water flux and isopropanol flux is characterized by a single empirical constant. Its corresponding value can be obtained experimentally.

8.3.2 Estimation of Parameters

Surface area fraction of polar path, k. The numerical values of k were determined from the swelling measurement as previously described in Chapter 5. The swelling measurement was carried using unmodified chitosan membrane and crosslinked chitosan membranes. We assumed that the numerical value k is equivalent to $n^{2/3}$ [Kim, 1994], where n is the ratio of swelling degree of highly crosslinked chitosan and that of unmodified chitosan membrane.

Constants $k_{D_{wp}}$, $k_{D_{wf}}$, $k_{c_{wp}}$, $k_{c_{wf}}$, $k_{D_{jf}}$, and $k_{c_{jf}}$. The constants were estimated from the relationships shown in equations (8.29 - 34). D_{if} was measured from

the thin-channel IGC experiment, while c_{if} was measured from the sorption experiment using highly crosslinked chitosan membranes. The corresponding D_{ip} and c_{ip} were calculated from the relationships

$$D_i = D_{ip} + D_{if} \tag{8.50}$$

and

$$c_i = c_{ip} + c_{if} \tag{8.51}$$

with the assumptions that the diffusion coefficient and solubility of component i in unmodified chitosan membranes were equivalent to D_i and c_i, respectively. We also assumed that for isopropanol

$$D_j = D_{jf} \tag{8.52}$$

The constants $k_{c_{ip}}$, $k_{c_{if}}$, and $k_{c_{jf}}$ were determined using equations (8.33 and 34) using the solubility data of water and isopropanol at unit activity.

Membrane thickness X, and density d_m. The average thickness of the dry chitosan membrane was 25 μm and the density of the membrane was 0.9 g/cm^3.

8.4 Binary Component Permeation

Although a binary component transport mechanism has also been proposed by incorporating the polar pathway concept and the basic equations were derived (see Appendix F), however, it was found the predictions of pervaporation properties based on these equations is too complicated and is not practical. As an alternative, the free volume approach which was developed by Yeom and Huang [1992] was employed to model the pervaporation of isopropanol/water mixture in chitosan membrane system. Individual permeabilities of isopropanol and water through the membrane can be estimated by the utilization of the equilibrium sorption data.

8.4.1 Free Volume Model Approach

The steady state permeation of a single component can be related by the Fick's first law with a concentration dependent diffusion coefficient.

$$J_i = -D_i \frac{\partial c_i}{\partial x} \tag{8.53}$$

where J_i is the flux of single component i, D_i is the concentration dependent diffusion coefficient of component i, and $\partial c_i / \partial x$ is the concentration gradient across the membrane.

According to Fujita's free volume theory [Fujita, 1961], the diffusion coefficient D_i is related to the thermodynamics diffusion coefficient of component i $(D_T)_i$

$$D_i=(D_T)_i\frac{\partial \ln a_i}{\partial \ln v_i} \tag{8.54}$$

where a_i and v_i are the chemical and volume fraction of component i in the membrane, respectively. $(D_T)_i$ is expressed by

$$(D_T)_i=RTA_{di}\exp\left[\frac{-B_{di}}{f(v_i,T)(1-\phi_c)}\right] \tag{8.55}$$

where A_{di} and B_{di} are the free volume parameters which are characteristic for a given polymer-penetrant pair, $f(v_i,T)$ is the free volume fraction of the membrane system at temperature T, ϕ_c is the degree of crystallinity of the membrane, and R is the gas constant.

The free volume parameter B_{di} is a characteristic parameter of an amorphous polymer. In order to get B_{di} applicable to semi-crystalline polymers as well as amorphous polymers, the new defined free volume parameter was introduced by Yeom and Huang [1992] as

$$B_i = \frac{B_{di}}{1-\phi_c} \tag{8.56}$$

Thus, the measurement of crystallinity is not necessary because the generalized parameter B_i, already includes the effect of crystallinity. The free volume fraction of a binary system (pure liquid-membrane) is given by

$$f(v_i,T) = f(0,T) + \beta_i(T)\, v_i \tag{8.57}$$

where $f(0,T)$ is the free volume fraction of the polymer itself and β_i is a proportional constant relating the amount of free volume created by the diffusing species i. When $v_i = 0$ in equation (8.57), the diffusion coefficient at zero concentration D_{i0} is given by

$$D_{i0} = RT A_{di} exp\left(\frac{-B_{di}}{f(0,T)}\right) \tag{8.58}$$

The free volume fraction of a ternary system (binary mixture) is expressed by

$$f(v_i,T) = f(0,T) + \beta_1(T)\, v_1 + \beta_2(T)\, v_2 \tag{8.59}$$

Therefore in a ternary system the thermodynamic diffusion coefficient of component 1, $(D_T)_1$ can be expressed as

$$(D_T)_1 = RT A_{d1} exp\left[\frac{-B_{d1}}{f(0,T) + \beta_1(T)\, v_1 + \beta_2(T)\, v_2}\right] \tag{8.60}$$

where A_{dl} and B_{dl} are the free volume parameters of component 1 in a ternary system. In pure liquid permeation, $\beta_l(T)$ can be calculated with the definition (when $v_l = 1$) in equation (8.57)

$$f(1,T)=f(0,T)+\beta_i(T) \tag{8.61}$$

The free volume fraction f(1,T) is related to [Doolittle, 1951]

$$f(1,T)=\frac{v_f - v_0}{v_f} \tag{8.62}$$

where v_f is the specific volume of the liquid at any temperature T, and v_0 is the specific volume of the liquid extrapolated to the temperature 0 °K without phase change.

The free volume fraction of polymer at a temperature below its glass transition temperature (T_g) was related by Robert and White [1973] to the pre-requisite for the motion of chain segments. In the Yeom and Huang model [1992], $f(0,T)$ is assumed to be proportional to temperature in the temperature range shortly below T_g with a slope of $0.025/2T_g$, which is an average value of the extreme cases (increasing free volume above 0 °K and constant free volume at T_g)

$$f(0,T)=0.025-\frac{0.025\left(T_g-T\right)}{2T_g} \tag{8.63}$$

The partial differential term in equation (8.54) of a binary system is given by the Flory-Huggins thermodynamics [Flory, 1953]

$$\frac{\partial \ln a_i}{\partial \ln v_i}=1-\left(1-\frac{V_i}{V_p}\right)v_i-2\chi_{ip}v_i v_p \tag{8.64}$$

$$\approx 1-v_i-2\chi_{ip}v_i\left(1-v_i\right)$$

where V is the molar volume, subscript p represent polymer, χ_{ip} is the interaction parameter characterizing the interactions between penetrant and the polymer membrane, which is related by

$$\frac{\Delta G_{mix}}{RT}=n_1\ln\phi_1+n_p\ln\phi_p+\chi_{1p}n_1\phi_p \tag{8.65}$$

where ΔG_{mix} is the Gibbs free energy of mixing, n is the mole fraction and ϕ is the volume fraction in equilibrium sorption. It has been shown that [Rhim, 1989]

$$\chi_{ip}=-\frac{\ln\left(1-v_p\right)+v_p}{v_p^2} \tag{8.66}$$

In order to calculate the individual permeability in a ternary system, it is assumed both penetrants diffuse independently, i.e, they are treated as two independent binary systems. For each binary system, the permeation rate of component i is expressed by

$$J_i = -\rho_i \int_0^{v_{i0}} (D_T)_i \frac{\partial \ln a_i}{\partial \ln v_i} \frac{dv_i}{dX} \tag{8.67}$$

For a ternary system, the sorption data of the same system can be used as the boundary conditions in conducting the integration. Integrating across the membrane thickness using these boundary conditions, the permeability of component i, P_i, in the ternary system is given by

$$P_i = J_i X = \int_0^X J_i dX$$

$$= \rho_i \int_0^{v_{i0}} (1 - v_i)(1 - 2\chi_{ip}) v_i (D_T)_i dv_i \tag{8.68}$$

where v_0 is the v_i value corresponding to ϕ_i at equilibrium sorption, ρ is the density of component.

In order to obtain the concentration profile of the individual

component in the chitosan membrane, Wei [1993] defined a relative distance in the membrane ($X_R = X/l$). Incorporating this definition with equation (8.67) we obtain

$$X_R = \frac{X}{l} = \frac{\int_{v_{i,0}}^{v_i} (1-v_i)(1-2\chi_{ip}) exp\left[\frac{-B_{di}}{f(0,T)+\beta_i(T)v_i}\right] dv_i}{\int_{0}^{v_{i,0}} (1-v_i)(1-2\chi_{ip}) exp\left[\frac{-B_{di}}{f(0,T)+\beta_i(T)v_i}\right] dv_i} \qquad (8.69)$$

Since X_R ranges between 0 - 1, the volume fraction of individual component v_i can be computed from equation (8.69).

In order to characterize the plasticization effect caused by the permeant, Yeom and Huang [1992] defined a plasticizing coefficient, O, which is related to the free volume parameters, β_i and B_{di}

$$O_{ii} = \frac{\beta_i(T)}{B_{di}} \qquad (8.70)$$

$$O_{ij} = \frac{\beta_j(T)B_j}{B_{di}} \qquad (8.71)$$

8.5 Results and Discussion

8.5.1 Single Component Permeation

The numerical values of the diffusion coefficients and all other parameters used for predicting permeation fluxes of water and isopropanol using the modified polar pathway model are summarized in Table 8.1. and 8.2. The parameters were measured experimentally from either the thin-channel IGC method, sorption or swelling experiments using homogeneous chitosan membranes. In the determinations of the model parameters we assumed that the crosslinking of chitosan membranes with HMDI decreased the hydrophilicity of the membranes and at a sufficiently high degree of crosslinking, water permeation occurred mainly through the polymer matrix. Furthermore, we assumed that isopropanol only permeated through the polymer matrix. As indicated by the numerical values of the diffusion coefficients, the diffusion of water in the polar pathway play a significant role in the overall water permeation through the highly hydrophilic homogeneous chitosan membrane.

The experimental data were applied to the modified polar pathway model for the single component pervaporation of water and isopropanol through homogeneous chitosan membranes at 30 °C. The numerical values of the calculated permeation fluxes are compared with the experimental

Table 8.1 Surface area fraction of polar pathway, diffusion coefficients, and solubility in chitosan membrane for the polar pathway model[a].

Component	k	D_p (m^2/hr) x 10^7	D_f (m^2/hr) x 10^7	c_p (g/g)	c_f (g/g)
Water	0.83	2.2	1.6	0.79	0.18
Isopropanol	0.83	-	0.24	-	0.14

[a]Membrane thickness : 25 μm; temperature 30 °C.

Table 8.2 Estimated polar pathway model parameters for water and isopropanol in chitosan membrane[a].

Component	k_{D_p} (m^2/hr) x 10^7	k_{D_f} (m^2/hr) x 10^7	k_{c_p} [b] (g/g)	k_{c_f} [b] (g/g)
Water	3.3	5.2	0.79	0.18
Isopropanol	-	1.7		0.14

[a]Membrane thickness : 25 μm; temperature 30 °C.

[b]Estimated at unit activity.

permeation fluxes of each component and the results are tabulated in Table 8.3. Note that here we assumed that the permeate pressure was small and negligible so that the activity of component in the permeate side is zero. In general, the prediction of the polar pathway model for the single component permeation of water is in good agreement with the experimentally observed behavior, but the prediction for the isopropanol permeation is not as good.

The deviations between the calculated permeation and the experimental fluxes of water and isopropanol may be attributed to the complexity of solution-diffusion mechanism in pervaporation processes, especially in the pervaporation using highly hydrophilic polymer membranes. Because of the complicated penetrants-membrane interactions it is often difficult to formulate a single explanation to the complex pervaporation process. For a swollen membrane [Nakagawa,1993] suggested that the diffusion of the permeate in the swollen layer and in the active layer in the membrane is very different. . The presence of sorbed water increases the free volume of the chitosan membrane and the polymer chain segmental motion is thereby enhanced to the same extent it would be a corresponding temperature increase leading to the same free volume increase. Because chitosan is a highly swollen membrane, it is difficult to use an ideal model to describe the actual diffusion mechanism. This may explain the deviation between the theoretical and the experimental water permeation fluxes.

Table 8.3 **Comparison between the experimental permeation and theoretical permeation based on the polar pathway model of pure components in chitosan membrane[a].**

Component	Experimental Permeation ($g/m^2.hr$)	Theoretical Permeation[b] ($g/m^2.hr$)	Ratio[c]
Water	3976	3140	0.79
Isopropanol	2.1	10	4.8

[a] Measured at 30 °C.

[b] d_m = 0.9 g/cm^3, $\bar{X}$ = 25 μm, and zero activity at downstream side.

[c]Ratio : Theoretical Permeation/Experimental Permeation

For isopropanol, the comparison shows more significant deviation between the calculated value and the experimental data. Note that the permeation of isopropanol is significantly small compared with that of water or total permeability for the chitosan membranes. Even though the measuring error in the large scale of the total system is trivial, this can be magnified when the results is applied to a small scale of the system.

Considering the numerous assumptions and approximations of the proposed model and the fact that the empirical constants were fitted to the data obtained from different nonpervaporation methods using different samples of chitosan membranes , the deviations were not unexpected. Besides the experimental errors, deviation caused by the assumptions made in carrying out the calculations may be significant.

8.5.2 Equilibrium Sorption of Individual Component

The sorption of individual component in the chitosan membrane was determined in terms of its volume fraction. The sorption results are given in Table 8.4. Form this table, it can be seen that pure water causes a greater degree of membrane swelling than that of isopropanol. It is also observed that for the chitosan membrane, the degree of membrane swelling increases to a maximum at 10 wt. % of isopropanol in the liquid, due to the coupled sorption.

Table 8.4 Equilibrium sorption of chitosan membrane with isopropanol-water mixtures at 30 °C[a].

Liquid Comp. (wt. %)[b]	Volume Fraction, ϕ		
	Water	Isopropanol	Polymer
0	0.467	0.000	0.533
10	0.448	0.036	0.516
30	0.369	0.078	0.553
50	0.239	0.082	0.679
70	0.121	0.087	0.792
90	0.038	0.111	0.851
100	0.00	0.139	0.861

[a]Density : Water = 1.0 g/cm^3; isopropanol = 0.78 g/cm^3; chitosan = 0.90 g/cm^3.

[b]Liquid Comp : Wt. % of isopropanol in liquid

8.5.3 Free Volume Parameters

To obtain the predicted permeability, the free volume parameters should be obtained first. For water, its free volume, v_f-v_0, in the temperature range of 0 - 150 °C can be found from the literature [Miller, 1963]. The calculation of vf and extrapolating of the specific volume to 0 °K is done by using a density function in the form of Taylor expansion [Yeom and Huang, 1992]. The parameters , f(0,T), f(i,T) and β(T) can be obtained from equations (8.61) to (8.63), and are listed in Table 8.5.

The free volume parameters, A_{di} and B_{di}, are obtained from equation (8.58) by solving for the equation with the thermodynamic diffusion coefficient of pure component at different temperatures which were determined by the IGC method. As shown by the free volume theory [Fujita, 1961], B_{di} is an arbitrary parameter corresponding to the minimum size of the *jumping cell*, or *hole* required for a given permeant molecule *i* to complete diffusional displacement, thus is related to the size of the permeant molecules. The B_{di} value for water is smaller than that of isopropanol because water has a smaller molecular size, and require a smaller cell to permit the jump.

The binary interaction parameter characterizing the interaction

Table 8.5 Free volume parameters of water and isopropanol at 30 °C.

Parameters	Water	Isopropanol
f(0,T)	0.023	0.023
f(1,T)	0.299	0.245
β(T)	0.276	0.222
$R(A)_{di}$	2.5E-10	4.3E-7
B_{di}	0.016	0.297
χ_{ip}	0.804	1.488

between the individual component and the membrane, χ_{ip}, was calculated from equation (8.66) using the equilibrium sorption data, and are given in Table 8.5. The interaction parameter is assumed to be concentration independent.

8.5.4 Concentration Profile of Individual Component

The concentration profile within the membrane system is also an important issue for pervaporation modelling. The concentration profiles of individual component in the chitosan membranes can be calculated from equation (8.69) by using the parameters in Table 8.5. The concentration profiles at feed composition of 50 weight percent isopropanol is given as typical example and is shown in Figure 8.4.

8.5.5 Estimation of the Individual Permeability

Knowing the diffusion coefficients, the concentration profile and the equilibrium sorption data, which are used as the boundary conditions, the individual permeabilities of the components in a ternary system can be calculated using equation (8.68). The calculated permeabilities are listed in Table 8.6, together with the experimental results at the same feed temperature and concentration. The ratio of the experimental to the

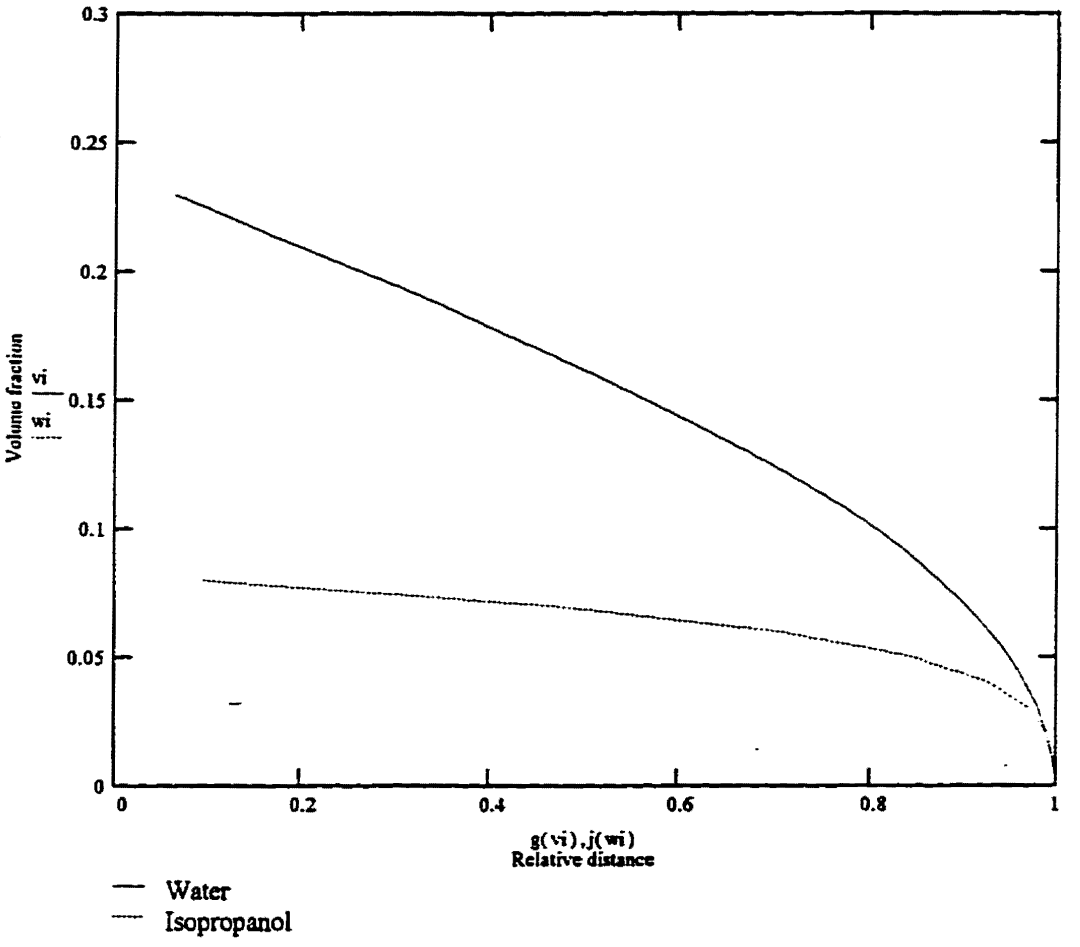


Figure 8.4 Calculated concentration profile inside the chitosan membrane. Feed isopropanol concentration: 50 weight. %; feed temperature 30 °C.

Table 8.6 **Experimental and calculated permeability based on the free volume model of individual component through the chitosan membrane at 30 °C.**

Liquid Comp. (wt. %)[a]	Water Flux (g/m.hr)		i-PrOH Flux (g/m.hr)x10		Ratio[d]	
	Exp.[b]	Calc.[c]	Exp.	Calc.	Water	i-PrOH
10	0.871	0.292	0.33	0.18	2.9	1.8
30	0.525	0.211	0.38	0.70	2.5	0.5
50	0.317	0.100	0.16	0.38	3.2	1.3
70	0.211	0.030	0.05	0.14	7.0	0.4
90	0.081	0.010	0.01	0.07	8.1	0.1

[a]Liquid Comp : Wt. % of isopropanol in feed.

[b]Experimental value.

[c]Calculated value.

[d]Ratio =Experimental Value/Calculated Value

calculated permeabilities are also given as an indication of the discrepancy. From the data in this table, it is seen that the estimation gives reasonable agreement with the experimental results for the individual permeabilities of isopropanol and water in chitosan membranes.

For water permeability, the model gives better estimations at low isopropanol concentration in feed liquid.The deviations from the experimental values at higher isopropanol concentration in the mixtures is not clear. This can possibly arise from some inaccuracy in the assumption that equilibrium sorptions exist at the upstream side of the membrane during pervaporation. In the real system, the interfacial resistance may contribute to large extent to the total resistance during permeation. Mulder *et l.* [1985] observed that there was a difference between equilibrium sorption values and real concentration just inside membrane in investigating the concentration profiles of the water-ethanol-cellulose system. This is because the chemical potential of a component in the feed is not equal to the chemical potential of the component just inside the membrane. However, in this study, the interfacial resistance was assumed to be negligible.

For isopropanol, the free volume model gives reasonably good estimations for the whole range of the feed composition studied. Furthermore, it is observed that the free volume model gives better isopropanol permeation estimations in the middle of the feed composition range. The deviation can be

considered as being caused by sensitivity to the error that may occur in the total system.

8.5.6 Plasticization by Permeant during Pervaporation

In general, the permeation of a binary mixture is characterized by the coupling and plasticizing actions of permeants. From this point of view, the plasticizing coefficient can be said to provide a measure of the coupling and plasticizing actions for analyzing the transport properties of a membrane.

The plasticizing coefficients were computed from equations (8.70) and (8.71) using the free volume parameters and are shown in Table 8.7 From this table, it can be seen that the self-plasticizing coefficient of water, O_{11}, is significantly higher than that of isopropanol, O_{22}. This is why the permeability of pure water is significantly higher than that of pure isopropanol. These self-plasticizing coefficients seem to be strongly related to the interactions between liquid and membrane material. The chitosan membrane is highly hydrophilic and shows higher affinity for water than for isopropanol. The cross-plasticizing coefficient of water, O_{12}, is also higher than that of isopropanol,O_{21}. This suggests that the enhancement of isopropanol permeation by the presence of water is more pronounced than that of water

Table 8.7 Plasticizing coefficients of individual component at 30 °C.

	Water		Isopropanol	
Membrane	O_{11}	O_{12}	O_{22}	O_{21}
Chitosan	17.3	4.12	0.75	0.02

due to the presence of isopropanol in the diffusion step.

The amount of individual plasticization action can be expressed as the product of the volume fraction of individual permeant and its plasticizing coefficient, which reflects the coupling actions of permeants in the diffusion step as well as the sorption step. Table 8.8 shows the resulting data for isopropanol and water for the entire range of feed composition at 30 °C. It is observed that the self-plasticizing of water and isopropanol in the chitosan membrane increase with the increase in its own concentration in feed, leading to the increase in its permeability, which agrees with the experimental results in Chapter 3. The cross-plasticizing data give the same conclusion as from the cross-plasticization coefficient, O_{12} and O_{21}.

Table 8.8 The amount of plasticization action of individual component on the upstream side of chitosan membrane at 30 °C.

	Water		Isopropanol	
Feed Comp. (wt. %)[a]	$\phi_1 \times O_{11}$	$\phi_1 \times O_{12}$	$\phi_2 \times O_{22}$	$\phi \times O_{21}$
0	8.08	1.92	0	0
10	7.75	1.85	0.15	5.4E-4
30	6.38	1.52	0.32	1.2E-3
50	4.13	0.98	0.34	1.2E-3
70	2.09	0.50	0.36	1.3E-3
90	0.66	0.16	0.46	1.7E-3
100	0	0	0.57	2.1E-3

[a]Feed comp. : isopropanol concentration in feed mixture.

8.6 Conclusions

Two alternatives approaches were employed to describe the transport mechanism of water and isopropanol through the chitosan membranes; the polar pathway solution-diffusion approach and the free volume approach. The solution-diffusion model was modified by incorporating diffusion in polar pathway to describe the pervaporation transport mechanism of single component permeation of pure isopropanol and pure water in the chitosan membranes. The estimated permeations of isopropanol and water were in the same of magnitude as the experimental values. However, the predicted permeation of isopropanol based on the polar pathway model was not as good as that of water.

The binary component permeations of isopropanol-water mixtures through the chitosan membranes were predicted by employing the free volume model developed by Yeom and Huang [1992] for the water-ethanol-crosslinked poly(vinyl alcohol) system taking into account the coupling of fluxes. Reasonable agreements between the predicted permeations of water and isopropanol and the experimental values were obtained, especially at low concentration of isopropanol in the feed mixtures.

The following conclusions can be drawn from the present study:

(1) The proposed polar pathway model assumes that they are two different

"channels" for permeation of components through hydrophilic membrane systems. The diffusion in polar pathway which is only accessible to water molecules, and in polymer matrix accessible to all , coexist.

(2) The diffusion of water through the polar pathway plays a role in the permeation of water through chitosan membranes; the co-existence of the diffusion in the polar pathway and that in the polymer matrix should be considered for interpreting transport of isopropanol-water mixtures through chitosan membranes.

(3) The free volume approach based on the free volume theory and the thermodynamic was employed to conduct the modelling and estimation of the pervaporation property of the chitosan membrane for the binary component permeation of isopropanol/water mixtures. By using the free volume parameters of the pure component and the equilibrium data , the permeability of individual component was predicted. The calculated permeabilities were shown to be reasonable estimates of the experimental results.

CHAPTER 9

Conclusions and Contributions to Original Research

The various specific conclusions of the research have been summarized in the respective chapters. The following general conclusions can be drawn as they relate to the contributions to the original research:

(1) Chitosan membranes are water selective and are potentially applicable for the separation of water/isopropanol systems by pervaporation. The chitosan membranes preferentially sorb and permeate water relative to isopropanol; preferential sorption leads to preferential permeation. High selectivity especially at high isopropanol concentrations makes the chitosan membranes potentially effective for the pervaporation dehydration of water/isopropanol

azeotrope.

(2) Composite chitosan/polysulfone membranes developed for the pervaporation of aqueous isopropanol solutions are shown to be promising; high permeability with good selectivity proved to be the characteristics of the composite membranes. It is shown qualitatively that the microporous sublayer create an additional resistance to the mass transport through the membranes.

(3) Modifications via chemical crosslinking and polymer blending are shown to be effective to improve the overall pervaporation performance of the chitosan based membranes. The performance of the crosslinked chitosan membranes and CS-PVA blended membranes could be optimized by controlling the solution technique membrane treatment time and the blend composition, respectively.

(6) Vapor phase pervaporation using chitosan based membranes could be potentially useful for dehydrating isopropanol.The selectivity is higher than that of the common pervaporation, but the permeability of the former is significantly lower than that of the former. In terms of PSI, pervaporation is more effective than vapor phase pervaporation for the dehydration of isopropanol.

(7) A novel technique for measuring diffusion coefficients by inverse gas chromatography has been developed and shown to be applicable to

pervaporation membranes. The technique presents a simple but efficient method to measure the diffusion coefficients of alcohols and water in a polymer stationary phase. The specifically designed thin-channel column features a significant improvements over the conventional packed column.

(8) A modified model based on the solution-diffusion model was developed to describe single component permeation through chitosan membrane; the mathematical model was specifically designed to describe permeations of component through hydrophilic polymer films with the incorporation of the highly selective polar pathways which were assumed to only available to water.

(9) The free volume model [Yeom and Huang, 1992] based on the Fujita's free volume theory and the Flory-Huggins thermodynamics were employed for the modelling of binary component permeation of isopropanol-water mixtures through the chitosan membranes taking into account the coupling fluxes. The coupling parameters were used to explain the coupling behavior and the plasticization action of isopropanol and water.

CHAPTER 10

Recommendations for Future Work

There are possibilities of extending this study which would prove interesting, instructive and beneficial.

(1) Composite chitosan membranes potentially effective for pervaporation dehydration of water/isopropanol mixtures were developed. However, the membranes were not prepared under optimized conditions. One possibility would be to optimize the variables involved in the membrane preparation procedure in order to fully utilize the separation potential of the membrane. In light of the additional resistance created by the porous sublayer of the composite membrane, future work should also be attempted to minimize this effect to ensure high permeability and good selectivity.

(2) Crosslinking of chitosan membranes proved to be effective to improve selectivity of the membranes, however the chemical structures of the modified membranes were not clearly identified. Identification of the structurally modified membranes may lead to a better understanding of the pervaporation performance of these membranes. A further effort to properly analyze and thus identify the structures of the crosslinked membranes should be considered.

(3) Vapor phase pervaporation using chitosan based membranes for the separation of isopropanol/water mixtures could be useful if high permselectivity were the primary objective. The operating conditions mainly temperature and pressure, should be optimized for the separation potential of the membrane in this separation process to be fully worked out. Further, in light of the good permselectivity ,it would be of interest to combine vapor phase pervaporation using chitosan membranes with other appropriate separation techniques such as distillation as a hybrid process for dehydrating isopropanol.

(4) The technique of the thin-channel column for measuring diffusion coefficients applicable to pervaporation is promising. Another possibility of extending this study is to compare diffusion coefficients of the same components obtained by the conventional methods, i.e., the desorption and absorption methods. By comparing the data of the

diffusion coefficients obtained by these different methods, a critical evaluation on the thin-channel IGC technique could be done.

(5) The diffusion coefficients of water were measured using a dry chitosan film due to the difficulty of detecting water signal with TCD when the stationary phase was saturated with water. A better approach would be to incorporate an Electron Capture Detector (ECD) (sensitive to both water and alcohols) to the available GC unit, so that a swollen chitosan film could be used as the stationary phase.The use of swollen stationary phase would prove to be more representative of the pervaporation conditions.

(6) The polar pathway mathematical model was developed to interpret transport of permeants in chitosan membrane. A further study should also be focused on the application of this model to other membrane systems where such polar pathway may exist.

(7) Shieh [1996] developed a Phase-change solution-diffusion (PCSD) model to consider the phase-change phenomenon in describing pervaporation transport mechanism. It may be interesting to further expand this model by incorporating the co- existence of the polar pathway and membrane matrix proposed in this study to interpret the transport of permeating species through pervaporation membranes using the PCSD model.

Nomenclature

a	Activity of component
A	Membrane area, m^2
A	A constant in Eqn. (7.2)
A	A constant in Eqn. (7.10)
A_{di}	Free volume parameters
B	A constant in Eqn. (7.2)
B	A constant in Eqn. (7.10)
B_{di}	Free volume parameters
c_i	solubility of permeant i, g/g polymer
c_{ip}	solubility of permeant i in polar pathway, g/g polymer
c_{if}	solubility of permeant i in polymer matrix, g/g polymer
C	A constant in Eqn. (7.2)

C Mass concentration of feed, g/m^3

d Thickness of stationary phase, m (Chapter 7)

d_m Density of membrane system, g/cm^3

D Diffusion coefficient in membrane, cm^2/s

D_L Diffusion coefficient in liquid phase, cm^2/s

D_o A constant in Eqn. (7.8)

$(D_T)_i$ Thermodynamic diffusion coefficient, cm2/s

E_a Activation energy for diffusion. Kcal/mol

E_p Activation energy of pervaporation, Kcal/mol

f Friction factor (Chapter 7)

f_L Fractional free volume of pure polymer (Chapter 7)

ΔF Interfacial free energy parameter

$f(0,T)$ Free volume fraction of the polymer

$f(v_i,T)$ Free volume fraction of the membrane system at temperature T

ΔG_M Free energy of mixing

H Height equivalent to theoretical plate, m (Chapter 7)

ΔH_M Enthalpy of mixing

J Permeation flux, g/m^2.hr

J_i Permeation flux of component i, g/m^2.hr

J_{iD} Permeation flux of component i due to diffusion, g/m^2.hr

J_{if} Permeation flux of component i in polymer matrix, g/m.hr

J_{ip} Permeation flux of component i in polar pathway, g/m.hr

J^o Permeation flux of pure component, g/m^2.hr

k Surface area fraction of polar path in membrane (Chapter 8)

k_{c_i} Constant in equation (8.26), g/g

$k_{c_{ip}}$ Constant in equation (8.33), g/g

$k_{c_{if}}$ Constant in equation (8.34), g/g

k_{D_i} Constant in equation (8.25), cm^2/s

$k_{D_{ip}}$ Constant in equation (8.29), cm^2/s

$k_{D_{if}}$ Constant in equation (8.30), cm^2/s

K Permeability coefficient, g.m/m^2.Pa.s

K Partition ratio (Chapter 7)

K_i Constant in equation (8.46), g/m^2.hr

K_j Constant in equation (8.47), g/m^2.hr

l Membrane thickness (Chapter 4)

L Column length, m (Chapter 7)

l_h Thickness of homogeneous membrane, m

l_c Thickness of skin layer in a composite membrane, m

N Number of theoretical plates (Chapter 7)

O Plasticization coefficient

P_1 Feed pressure, atm or mm Hg

P_2 Permeate pressure, atm or mm Hg

P_s Saturated vapor pressure

$[PR]$ Permeation rate, g/s

$[PR]_h$ Permeation rate in homogeneous membrane, g/s

$[PR]_c$ Permeation rate in composite membrane, g/s

PSI Pervaporation separation factor, g/m^2.hr

Q Amount of a liquid sorbed in polymer, g/g-polymer

Q^o Pure liquid sorption amount in polymer, g/g-polymer

R Gas constant, J/mol.K

ΔS_M Entropy of mixing

t Time, sec or hour

T Absolute temperature, K

T_g Glass transition temperature, K

t_m Retention time of methane, s

t_r Retention time of solute, s

u Linear velocity of carrier gas, cm/s

v Volume fraction

v_f specific volume of the liquid at any temperature T

v_0 specific volume of the liquid extrapolated to the temperature 0 oK without phase change

$\overline{V}$ Partial molar volume

$W_{1/2}$ Peak width at half the peak height, m (Chapter 7)

X Mass fraction of the more permeable component in feed

X Thickness of membrane, m (Chapter 8).

X_p Mass fraction of the more permeable component in polymer sorbed phase

Y Mass fraction of the more permeable component in permeate

Greek Letters

α Separation factor

α_D Diffusion selectivity

α_S Sorption selectivity

β Enrichment factor

$\beta_i(T)$ A proportional constant relating the amount of free volume created by the diffusing species i

γ Activity coefficient (Chapter 4)

μ Chemical potential, joule/gmol

Δ Solubility parameter difference, $(MPa)^{0.5}$

δ Membrane thickness, m

θ Permeation ratio

Φ Permeation rate ratio

ϕ Sorption ratio or volume fraction in equilibrium sorption

ϕ_c Degree of crystallinity of the polymer

σ Variance of peak, s

ρ Mass concentration, kg/m^3

χ_{ip} Interaction parameter characterizing the interactions between the

penetrant and the polymer membrane

ω Mass fraction of component in membrane system

Bibliography

Aptel, P., N. Challard, J. Cuny,and J. Neel, "Application of the pervaporation process to the separation of azeotropic mixtures", *J. Membrane Sci.*, **1**, 271 (1976).

Aptel, P., J. Cuny, J. Jozefowics, G. Morel and J. Neel, "Liquid transport through membranes prepared by grafting of polar monomer onto poly(tetrafluoroethylene) films. I. Some fractions of liquid mixtures by pervaporation", *J. Appl. Polym. Sci.*, **16**, 1061 (1972).

Aptel, P., J. Cuny, J. Jozefowics, G. Morel and J. Neel, "Liquid transport through membranes prepared by grafting of polar monomer onto poly(tetrafluoroethylene) films. II. Some factors determining pervaporation rate and selectivity", *J. Appl. Polym. Sci.*, **18**, 351 (1974).

Aptel, P., J. Cuny, J. Jozefowics, G. Morel and J. Neel, "Liquid transport through membranes prepared by grafting of polar monomer onto poly(tetrafluoroethylene) films. II. Steady-state distribution in membrane during pervaporation", *J. Appl. Polym. Sci.*, **18**, 365 (1974a).

Arnould, D. and R.L. Laurence, "Solute diffusion in polymers by capillary column inverse gas chromatography", in *Inverse Gas Chromatography*, D.R Lloyd, T.C. Ward, H.P. Schreiber, and C.C. Pizana (Eds.), American Chemical Society, Washington, DC (1989).

Asada, T., "Dehydration of organic solvents. Some of the actual results of the pervaporation plants in Japan", in *Proc. 3rd. Int. Conf. Pervaporation process in Chem. Ind.*, R. Bakish (Ed.), Bakish Materials Corp., Englewood, NJ (1988).

Baker, R.W.,E.L Cussler, W. Eykamp, W.J. Koros, R.L. Riley, and H. Strathmann, "Membrane separation system, recent development and future

directions", Noyes, Park Ridge, New Jersey (1991).

Baranowski, B., "Non-equilibrium thermodynamics as applied to membrane transport", *J. Membrane Sci.*, **57**, 119 (1991).

Bell, C.M., F.J. Gerner and H. Strathmann, "Selection of polymers for pervaporation membranes", *J. Membrane Sci.*, **36**, 315 (1988).

Binning, R.C. and F.E. James, "New separations by membrane separation", *Petroleum Refining*, **27**, 214 (1958a).

Binning, R.C. and F.E. James, "Permeation : A new way to separate mixtures", *Oil Gas J.*, **56**, 104 (1958b).

Binning, R.C., R.J. Lee, J.F. Jennings, and E.C. Martin, "Separation of liquid mixtures by permeation", *Ind. Eng. Chem.*, **53**,45 (1961).

Bird, R.B., W.E. Stewart, and E.N. Lightfoot, *Transport Phenomena*, Wiley, New York (1960).

Blackadder, D.A. and J.S. Keniry, "The measurement of the permeability of polymer membranes to solvating molecules", *J. Appl. Polym. Sci.*, **16**, 2141 (1972).

Blume, I., J.G. Wijmans, and R.W. Baker, "The separation of dissolved organics from water by pervaporation", *J. Membrane Sci.*, **49**, 253 (1990).

Boddeker, K.W., G. Bengston and E. Bode, "Pervaporation of low volatility aromatics from water", *J. Membrane Sci.*, **53**, 143 (1990).

Boddeker, K.W., G. Bengston and H. Pingel, "Pervaporation of isomeric butanols", *J. Memb. Sci.*, **54**, 1 (1990a).

Boddeker, K.W., G. Bengston, H. Pingel, and S. Dozel, "Pervaporation of high boilers using heated membranes", *Desalination*, **90**, 249 (1993).

Braun, J.M. and J.E. Guillet, "Studies of polystyrene in the region of the glass transition temperature by inverse gas chromatography", *Macromolecules*, **8**, 883 (1975).

Brueschke, H.E.A., "Thermodynamics of pervaporation", in *Proc. 2nd. Int.*

Conf. on Pervaporation Processes in the Chem. Ind., R. Bakish (Ed.), Bakish Materials Corp., Englewood, NJ (1987).

Brueschke, H.E.A, "State of the art of pervaporation", in *Proc. 3rd. Intl. Conf. on Pervaporation Processes in Chem. Ind.*, R. Bakish (Ed.), Bakish Materials Corp., Englewood, NJ (1988).

Brun, J.P., C. Larchet, R. Melet, and G. Bulvester, "Modelling of the pervaporation of binary mixtures through moderately swelling, non-reacting membranes", *J. Membrane Sci.*, **23**, 257 (1985).

Bungay, P.M., " *Synthetic Membrane : Science, engineering and application*", D. Reidel Publishing Company, New York, 1986.

Cabasso, I., J. Jagur-Grodzinski and D. Vofsi, " A study of organic solvents through polymeric membranes based on polymeric alloys of polyphosphonate and acetyl cellulose. II. Separation of benzene, cyclohexane and cyclohexene ", *J. Appl. Polym. Sci.*, **18**, 2137 (1974).

Cabasso, I., E. Korngold, and Zhong-Zhou Liu, "Thermal decomposition of poly(ethylene oxide),poly(methyl methacrylate),and their mixture by thermogravimetric method", *J. Polym. Sci., Polym. Lett. Ed.*, **23**, 577 (1985).

Cabasso, I. and C.N. Tran, " Polymer alloy membrane. I. Cellulose acetate poly(bromophenylene oxide phosphonate) dense and asymmetric membrane", *J. Appl. Polym. Sci.*, **23**, 2967 (1979).

Camera-Roda, G., A. Bottino, G. Capannelli, G. Costa, and G.C. Starti, "Pervaporation of organic compounds through poly[1-(trimetylsilyl)-1-propyne]", in *Proc. 5th Intl. Conf. Pervaporation Process in Chem. Ind.*, R. Bakish (Ed.), Bakish Materials Corp., Englewood, NJ (1991).

Charles, J.B., *Introduction to Chitin: Accomplishments and Perspectives, in Chitin, Chitosan and Related Enzymes*, J.P. Zikakis (Ed.), Academic Press Inc., New York (1984).

Chen, M.S.K., G.S., Markiewiez, and K.G. Venugopal, "Development of membrane pervaporation TRIM^{TM} process for methanol recovery from CH_3OH/MTBE/C_4 mixtures", *AIChE Symp. Ser.* **85**, 272 (1989).

Conder, J.R. and C.L. Young, *Physicochemical Measurement by Gas Chromatography*, Wiley, New York, 1979.

Crank, J., *The Mathematics of Diffusion, 2nd. Edn.*, Oxford University Press, Oxford (1979).

Crank, J. and G.S. Park, *Diffusion in Polymers*, Academic Press, New York, NY (1968).

Damusis, A and K.C. Frisch in *Treatise and Coatings: Film-Forming Compositions*, Vol. 1, Part 1, R.Myers and J.S. LOng (Eds.), Marcel Dekker, New York (1971).

Daubert, T.E. and R.P. Danner, *Physical and Thermodynamic Properties of Pure Chemicals. Data Compilation*, Hemisphere Publishing Corporation (1989).

Deanin, R.D., *Polymer Structure, Properties and Applications*, The Maple Press Co., Pennsylvania (1972).

Demertzis, P.G. and M.G. Kontominas," Thermodynamic study of water sorption and water vapor diffusion in poly(vinylidene chloride) copolymers", in *Inverse Gas Chromatography*, D.R Lloyd, T.C. Ward, H.P. Schreiber, and C.C. Pizana (Eds.), American Chemical Society, Washington, DC (1989).

Deng, S., S. Shiyao, S. Sourirajan, and T. Matsuura, "A study of the pervaporation of isopropyl alcohol/water by cellulose acetate membranes", *J. Colloid Interface Sci.*, **136**, 283 (1990).

Doolittle, A.K., "Studies in newtonian flow. II. The dependence of the viscosity of liquids on free-space", *J. Appl. Phys.*, **22(12)**, 1471 (1951).

Doong, S.J., W.S. Ho, and R.P. Mastondrea, "Prediction of flux and selectivity in pervaporation through a membrane", *J. Membrane Sci.*, **107**, 129 (1995).

Duggal, A. and E.V..Thompson, "Dependence of diffusive permeation rates on upstream and downstream pressures. IV. Experimental results for the water-ethanol system", *J. Membrane Sci.*, **27**, 13 (1986).

Elyassini, J., Q.T. Nguyen and J. Neel, "Preparation and study of poly(vinyl alcohol)-poly(ethylene glycol) blends films in dehydration of ethanol by

pervaporation", in *Synthetic Polymeric Membranes*, Walter de Gruyter, Germany (1987).

Farnand, B.A. and S.H. Noh, "Pervaporation as an attractive process for the separation of methanol from C_4 hydrocarbons in the production of MTBE and TAME", in *Membrane Separations in Chemical Engineering*, A.E. Faouda, J.D. Hazlett, T. Matsuura and J. Johnson (Eds.), AIChE, New York (1989).

Fels, M. and R.Y.M. Huang,"Diffusion coefficient of liquids in polymer membranes by a desorption method", *J. Appl. Polym. Sci.*, **14**, 523 (1970).

Fels, M. and R.Y.M. Huang, "The effect of styrene grafting on the diffusion and solubility of organic liquids in polyethylene", *J. Appl. Polym. Sci.*, **14**, 537 (1970a).

Fels, M. and R.Y.M. Huang, "Theoretical interpretation of the effect of mixture composition on separation of liquids in polymers", *J. Macromol. Sci. Phys.*, **B5 (1)**, 89 (1971).

Feng, X., *Studies on Pervaporation Membranes and Pervaporation Processes*, Ph.D Thesis, University of Waterloo, Canada (1994).

Feng, X. and R.Y.M. Huang, "Pervaporation with chitosan membranes. I. Separation of water from ethylene glycol by a chitosan/polysulfone composite membrane", *J. Membrane Sci.*, **116**, 67 (1996).

Fleming, H.L., "Consider membrane pervaporation", *Chem. Engr. Progress*, **88**, 46 , (1992).

Flory, P.J., *Principles of Polymer Chemistry*, Conell Univ. Press, Ithaca (1953).

Fujita, H., "Diffusion in polymer-diluent systems", *Fortschr. Hocpolym. Forsch.*, **3**, 1 (1961).

Galin, M. and M.C. Rupprecht, "Study by gas-liquid chromatography of the interactions between linear or branched polystyrenes and solvents in the temperature range 60-200 °C", *Polymer*, **19**, 506 (1978).

Giddings, J.C., *Dynamics of Chromatography*, Part 1, Marcel Dekker Inc., New York, NY (1965).

Gierke, T.D., "The cluster network model of ion clustering in perfluorosulfonated membrane", *J. Membrane Sci.*, **13**, 307 (1983).

Greenlaw, F.W., R.A. Shelden and E.V. Thompson, "Dependence of diffusive permeation rates on upstream and downstream pressures. I. Single component permeant", *J. Membrane Sci.*, **2**, 141 (1977a).

Greenlaw, F.W., R.A. Shelden and E.V. Thompson, "Dependence of diffusive permeation rates on upstream and downstream pressures. I.Two component permeant", *J. Membrane Sci.*, **2**, 333 (1977b).

Hauser, J., A. Heintz, G.A. Reinhardt, R. Schmittecker, M. Weisslein, and R.N. Lichtenthaler, "Sorption, diffusion and pervaporation of water/ethanol mixtures in PV-membrane : Experimental results and theoretical treatment", in *Proc. 2nd. Int. Conf. on Pervaporation Process in the Chem. Ind.*, R. Bakish (Ed.), Bakish Materials Corp., Englewood, NJ (1987).

Hauser, J., R. Schmittecker, and R.N. Lichtenthaler, "Experimental investigations of sorption and diffusion in polymeric materials", *in Proc. 3rd. Int. Conf. on Pervaporation Process in the Chem.Ind.*, R. Bakish (Ed.), Bakish Materials Corp., Englewood, NJ (1988).

Heftmann, E., (Ed.), *Chromatography, 5th. Ed.. Fundamental and Applications for Chromatography and Related Differential Migration Methods*, Elsevier Science Publishing Co. Inc., New York, USA (1992).

Heintz, A. and W. Stephan, "A generalized solution-diffusion model of the pervaporation process through composite membranes. Part II. Concentration polarization, coupled diffusion and influence of the porous support layer", *J. Membrane Sci.*, **89**, 153 (1994).

Hickey, P.J. and C.S. Slater, "The selective recovery of alcohols from fermentation broths by pervaporation", *Sep. Puri. Methods*, **19**, 93 (1990).

Hirotsu, T., "Water-ethanol separation by pervaporation through plasma graft polymerized membranes", *J.Appl. Polym. Sci.*, **34**, 1159 (1987).

Hirotsu, T., "Plasma grafted pervaporation membranes", in *Pervaporation Membrane Separation Processes*, R.Y. M. Huang (Ed.), Elsevier, Amsterdam (1991).

Hirotsu, T. and S. Nakajima, "Water-ethanol permseparation by pervaporation through the plasma graft copolymeric membranes of acrylic acid and acrylamide", *J. Appl. Polym. Sci.*, **36**, 177 (1988).

Ho, W.S., G. Sartori, Thaler, W.A., Dalrymple, R.P. Mastondrea, and D.W. Savage, "Hard/soft segment copolymer membranes for aromatic/saturates separation", in *Proc. of Inter. Congress on Membranes and Membrane Processes (ICOM)*, Yokohama, Japan (1996).

Hoff, J., Department of Earth Science, University of Waterloo, Canada (1997).

Hopfenberg, H.B., *Permeability of Plastic Films and Coatings to Gases, Vapors and Liquids*, Plenum, New York (1974).

Huang, R.Y.M., *Pervaporation Membrane Separation Processes*, Elsevier, Amsterdam (1991).

Huang, R.Y.M. and X. Feng, "Pervaporation with chitosan membranes. I. Separation of water from ethylene glycol by a chitosan/polysulfone composite membrane", *J. Membrane Sci.*, (1996).

Huang, R.Y.M. and N.R. Jarvis, "Separation of liquid mixtures by using polymer membranes. II. Permeation of aqueous alcohols solution through cellophane and poly(vinyl alcohol)", *J. Appl. Polym. Sci.*, **14**, 2341 (1970).

Huang, R.Y.M. and V.J.C. Lin, "Separation of liquid mixtures by using polymer membranes. I. Permeation of binary organic liquid mixtures through polyethylene", *J. Appl. Polym. Sci.*, **12**, 2165 (1968).

Huang, R.Y.M., A. Moreira, R. Notarfonzo, and Y.F. Xu, "Pervaporation separation of acetic acid-water mixtures using modified membranes. I. Blended polyacrylic acid (PAA)-nylon 6 membrane", *J. Appl. Polym. Sci.*, **35**, 191 (1988).

Huang, R.Y.M. and J.W. Rhim, "Separation characteristics of pervaporation membrane separation processes", in *Pervaporation Membrane Separation Processes*, R.Y.M. Huang (Ed.), Elsevier, Amsterdam (1991).

Huang, R.Y.M. and J.W. Rhim, "Theoretical estimations of diffusion coefficients", *J. Appl. Polym. Sci.*, **42**, 535 (1990).

Huang, R.Y.M. and J.W. Rhim,"Separation characteristics of pervaporation membrane separation processes using modified poly(vinyl alcohol) membranes", *Polym. Int.*, **30**, 123 (1993).

Huang, R.Y.M. and J.W. Rhim, "Modification of poly(vinyl alcohol) using maleic acid and its application to the separation of acetic acid-water mixtures by pervaporation technique", *Polym. Int.*, **30**, 129 (1993a).

Huang, R.Y.M. and Y.F. Xu, "Pervaporation separation of acetic acid-water mixtures using modified membranes. II. Gamma-ray-induced grafted polyacrylic acid (PAA)-nylon 6 membrane", *J. Membrane Sci.*, **43**, 143 (1989).

Huang, R.Y.M., Y.F. Xu, Y. Jin and C. Lipski, "Novel blended nylon membranes for the pervaporation of acetic acid-water and ethanol-water liquid mixture system", in *Proc. of the 2nd. Int. Conf. on Pervaporation Process in the Chem. Ind.*, R.Bakish (Ed.), Bakish Materials Corp., Englewood, NJ (1987).

Huang, R.Y.M. and C.K. Yeom, " Pervaporation separation of aqueous mixtures using crosslinked poly(vinyl alcohol) membranes. II.Permeation of ethanol-water mixture", *J. Membrane Sci.*, **51**, 273 (1990).

Huang, R.Y.M. and C.K. Yeom, "Pervaporation separation of aqueous mixtures using crosslinked poly(vinyl alcohol)membranes. III. Permeation of acetic acid-water mixtures", *J. Membrane Sci.*, **58**, 33 (1991a).

Huang, R.Y.M. and C.K. Yeom, "Development of crosslinked poly(vinyl alcohol) (Type II) and permeation of acetic acid-water mixtures", *J. Membrane Sci.*, **62**, 59 (1991b).

Jia, M.D., K.V. Peimemann, and R.D. Behling, "Preparation and characterization of thin film zeolite PDMS composite membranes", *J. Membrane Sci.*, **73**, 119 (1992).

Jian, K. and P.N. Pintauro, "Integral asymmetric poly(vinylidene fluoride) (PVDF) pervaporation membranes", *J. Membrane Sci.*, **85**, 301 (1993).

Jopski, J., H. Strathmann, and P. Eyerer, "Separation of ethanol-water mixtures by pervaporation with silicon-containing polymer membranes", in *Proc. of the 4th. Int. Conf. on Pervaporation in the Chem. Ind.*, R. Bakish (Ed.), Bakish Materials Corp., Englewood, NJ (1989).

Karakane, H., T. Tsuyumoto, Y. Maeda, and Z. Honda, "Separation of water-ethanol by pervaporation through polyion complex composite membrane, *J. Appl. Polym. Sci.*, 42, 3229 (1991).

Kataoka, T., Tsuru, T., Nakao, S.I., and Kimura, S., "Membrane transport properties of pervaporation and vapor permeation in ethanol/water system using polyacrylonitrile and cellulose acetate membranes", *J. Chem. Eng. Japan*, 24, 234 (1991).

Katz, M.G. and T. Wydeven Jr., "Selective permeability of poly(vinyl alcohol) membranes. II. Heat-treated membranes", *J. Appl. Polym. Sci.*, 27, 79 (1982).

Kim, H.J., *A Study on the Mechanism of the Separation of Water/Ethanol Mixture through PAN based Copolymer Membranes by Pervaporation*, Ph.D Thesis, Korea (1994).

King, C.J., *Separation Processes, 2nd. Ed.*, McGraw Hill, New York (1980).
Kober,P.A.,"Pervaporation,perstillation,and percrystallization", *J. Amer. Chem. Soc.*, 39, 944 (1917).

Kong, J.M. and Hawkes, S.J., "Diffusion in uncrosslinked silicones", *Macromolecules*, 8, 148 (1975).

Koros, W.J., "Membranes: learning a lesson from nature", *Chem. Eng. Prog.*, 91, 68 (1995).

Koros, W.J. and H.W. Hullems, "Transport properties", in *Encyclopedia of Polymer Science*, 2nd. ed., Supplement Volume, Wiley, New York (1989).

Kumins, C.A., "Transport phenomena through polymer films", *J. Polym. Sci., Polym. Symp.*, 41 (1973).

Larchet, C., G. Bulvester and M. Guillou, "Separation of benzene-n-heptane mixtures by pervaporation with elastomeric membranes. I. Performance of membranes", *J. Membrane Sci., 15*, 81 (1983).

Laub, R.J. and R.L. Pecsok, *Physicochemical Applications of Gas Chromatography*, Wiley, New York (1978).

Lee, C.H., "Theory of reverse osmosis and some other membrane permeation operation", *J. Appl. Polym. Sci.*, 19, 83 (1975).

Lee, Y.M., D. Bourgeois, and G. Belfort, "Selection of polymer materials for pervaporation", *in Proc. of 2nd. Int. Conf. on Pervaporation in the Chem. Ind.*, R. Bakish (Ed.), Bakish Materials Corp., Englewood, NJ (1987).

Lee, Y.M., D. Bourgeois, and G. Belfort, "Sorption, diffusion and pervaporation of organics in polymer membranes", *J. Membrane Sci.*, **44**, 161 (1989).

Lee, K.R., R.Y. Chen, and J.Y. Lai, "Plasma deposition of vinyl acetate onto nylon-4 membrane for pervaporation and evaporation separation of aqueous alcohol mixtures", *J. Membrane Sci.*, **75**, 171 (1992).

Lee, Y.M. and E.M. Shin, "Pervaporation separation of water-ethanol through modified chitosan membrane. IV. Phosphorylated chitosan membranes", *J. Membrane Sci.*, **64**, 145 (1991).

Lipski, C. and P. Cote, "The use of pervaporation for the removal of organic contaminates from water", *Environ. Prog.*, **9**, 254 (1990).

Littlewood, A.B., *Gas Chromatography*, 2nd. ed., Academic Press, New York, NY (1970).

Lloyd, D.R. and T.B. Meluch, "Selection and evaluation of membrane materials for liquid separations", in *Membrane Science of Synthetic Membranes*, D.R. Lloyd (Ed.), ACS, Washington (1985).

Masuda, T., M. Takatsuka, B.Z. Tang, and T. Higashimura, "Pervaporation of organic liquid-water mixtures through substituted polyacrylene membranes", *J. Membrane Sci.*, **49**, 69 (1990).

Masuoka, T., T. Iwatsubo, and K. Mizoguchi, "Pervaporation membranes for ethanol-water prepared by plasma polymerization of fluorocarbons. II. per-fluoropropane membrane", *J. Membrane Sci.*, **69**, 109 (1992).

Matsumoto, Y., M. Kondo, and Fujita, "Transport mechanism in PEBA membrane", in *Proc. of the 6th. Int. Conf. on Pervaporation Process in the Chem. Ind.*, R. Bakish (Ed.), Bakish Materials Corp., Englewood, NJ (1992).

Matsuura, T., *Synthetic Membranes and Membrane Separation Processes*, CRC Press, Boca Raton, Fl (1994).

McCall, D.W., "Diffusion in ethylene polymers. I. Desorption kinetics for a thin

slab", *J. Polym. Sci.*, **26**, 151 (1957).

Merten, U., "Transport properties of osmotic membranes", in *Desalination by Reverse Osmosis*, U. Merten (Ed.), MIT Press., Cambridge, Mass. (1966).

Miller, A.A., "Free volume and the viscosity of liquid water", *J. Chem. Phys.*, **38(7)**, 1568 (1963).

Mochizuki, A., Y. Sato, H. Ogawara, and S. Yamashita, "Pervaporation separation of water-ethanol mixtures through polysaccharide membranes. I. The effects of salts on the permselectivity of cellulose membrane in pervaporation", *J. Appl. Polym. Sci.*, **37**, 3357 (1989).

Mochizuki, A., Y. Sato, H. Ogawara, and S. Yamashita, "Pervaporation separation of water-ethanol mixtures through polysaccharide membranes. II. The permselectivity of chitosan membranes", *J. Appl. Polym. Sci.*, **37**, 3375 (1989).

Mochizuki, A., Y. Sato, H. Ogawara, and S. Yamashita, "Pervaporation separation of water-ethanol mixtures through polysaccharide membranes.III. The permselectivity of neutralized chitosan membrane and the relationships between it s permselectivity and solid state structure", *J. Appl. Polym. Sci.*, **37**, 3385 (1989).

Mochizuki, A., Y. Sato, H. Ogawara, and S. Yamashita, "Pervaporation separation of water-ethanol mixtures through polysaccharide membranes. IV. The relationships between the permselectivity of alginic acid structure and its solid state structure", *J. Appl. Polym. Sci.*, **40**, 385 (1990).

Mulder, M.H.V., T. Franken and C.A. Smolders, "Preferential sorption versus preferential permeability in pervaporation", *J. Membrane Sci.*, **22**, 155 (1985).

Mulder, M.H.V. and C.A. Smolders, "Pervaporation, solubility aspects of the solution-diffusion model", *Sep. Puri. Method*, **15**, 1 (1986).

Mulder, M., *Basic Principles of Membrane Technology*, Kluwer Academic Publisher, Netherland (1991).

Neel, J., "Introduction to pervaporation", in *Pervaporation Membrane Separation Processes*", R.Y.M. Huang (Ed.), Elsevier, Amsterdam (1991).

Neel,J.,P.Aptel and R. Clement,"Basic aspects of pervaporation",*Desalination*, **53**, 297 (1985).

Neel, J., Q.T. Nguyen, R. Clement and D.J. Lin, "Influence of downstream pressure on the pervaporation of water-tetrahydrofuran mixtures through a regenerated cellulose membrane (CUPROPHAN)", *J. Membrane Sci.*, **27**, 217 (1980).

Neumann, A.W., R.J. Good, C.J. Hope, and M. Sejpal, "A equation-of-state approach to determine surface tensions of low energy solids from contact angles", *J. Colloid Interface Sci.*, **49**, 291 (1974).

Nguyen, T.Q., L.Le Blanc, and J. Neel,"Preparation of membranes from polyacrylonitrile-polyvinylpyrrolidone blends and the study of their behavior in the pervaporation of water-organic liquid mixtures", *J. Membrane Sci.*, **22**, 245 (1985).

Nguyen, T.Q. and K. Nobe, "Extraction of organic contaminants in aqueous solution by pervaporation", *J. Membrane Sci.*, **30**, 11 (1987).

Nijhuis, H.H., M.H.V. Mulder and C.A. Smolders, "Selection of elastomeric membranes for the removal of volatile organic components from water", in *Proc. of the 3rd. Int. Conf. on Pervaporation in the Chem. Ind.*, R.Bakish (Ed.), Bakish Materials Corp., Englewood, NJ (1988).

Okada, T. and T. Matsuura, " A new transport model for pervaporation", *J. Membrane Sci.*, **59**, 133 (1991).

Okada, T. and T. Matsuura, "Predictability of transport equations for pervaporation on the basis of pore flow mechanism", *J. Membrane Sci.*, **70**, 163 (1992).

Okada, T., M. Yoshikawa, and T. Matsuura, "A study on pervaporation of ethanol/water mixtures on the basis pore flow model", *J. Membrane Sci.*, **59**, 151 (1991a).

Okamoto, K., A. Butsuen, S. Tsuru, S. Nishioka, K. Tanaka, H. Kita, and S. Asaka, "Pervaporation of water-ethanol mixtures through PDMS block-copolymer membranes", *Polym. J.*, **19**, 747 (1987).

Osada, K. and T. Nakagawa, Membrane Science and Technology, Dekker, New

York (1993).

Park, H.C., R.M. Mertens, H.M.V. Mulder, and C.A. Smolders, "Pervaporation of alcohol-toluene mixture through polymer blend membranes of poly(acrylic acid)and poly(vinyl alcohol)", *J. Membrane Sci.*, **90**, 265 (1990).

Pearson, J.R., "On the gradient column method for measuring densities", *Polymer*, **9**, 283 (1968).

Porter, M.C., *Handbook of industrial membrane technology*, Noyes Publications, New Jersey (1990).
Prager, S. and F. Long, "Diffusion of hydrocarbon vapor into polyisobutylene", *J. Am. Chem. Soc.*, **73**, 4072 (1951).

Prager, S., E. Bagley, and F. Long, "Equilibrium sorption data for polyisobutylene hydrocarbon systems", *J. Am. Chem. Soc*, **75**, 1255 (1953).

Price, F.P., P.T. Gilmore, E.L. Thomas, and R.L. Laurence, "Polymer/polymer diffusion. I. Experimental technique", *J. Polym. Sci., Polym. Sypm.*, **63**, 33 (1978).

Psaume, R., P. Aptel, R. Aurelle, J.C. Mora, and J.L. Bersillon, "Pervaporation : Importance of concentration polarization in the extraction of trace organics from water", *J. Membrane Sci.*, **36**, 373 (1988).

Rapin, J.L., "The Betheniville pervaporation unit - the first large-scale production plat for dehydration of ethanol", in *Proc. 3rd. Int. Conf. on Pervaporation Process in Chem. Ind.*, R. Bakish (Ed.), Bakish Materials Corp., Englewood, NJ (1988).

Rautenbach, R. and R. Albrecht, "Separation of organic binary mixtures by pervaporation", *J. Membrane Sci.*, **7**, 203 (1980).

Rautenbach, R. and R. Albrecht, "The separation potential of pervaporation. Part I. Discussion of transport equations and comparison with reverse osmosis", *J. Membrane Sci.*, **25**, 1 (1985).

Rautenbach, R., C. Herion and M. Franke, "Dehydration of multicomponent organic systems by a reverse osmosis/pervaporation-hybrid process-module, process design and economics", in *Proc. 3rd. Intl. Conf. on Pervaporation Processes in Chem. Ind.*, R. Bakish (Ed.), Bakish Materials Corp., Englewood,

NJ (1988).

Rautebach, R.C., S. Klatt and J. Vier, "State of the art of pervaporation - 10 years of industrial pervaporation", in *Proc. 6th. Intl. Conf. on Pervaporation Processes in Chem. Ind.,* R. Bakish (Ed.), Bakish Materials Corp., Englewood, NJ (1992).

Reineke, C.E., J.A. Jagodzinski and K.R. Denslow, "Highly water selective cellulosic polyelectrolyte membranes for the pervaporation of alcohol-water mixtures", *J. Membrane Sci.*, **32**, 207 (1987).

Rhim, J.W. and R.Y.M. Huang, "On the prediction of separation factor and permeability in the separation of binary mixtures by pervaporation", *J. Membrane Sci.*, **46**, 335 (1989).

Robert, G.E. and E.F.T. White, The thermodynamics of the glass state, in : The Physics of Glass Polymers, R.N. Howard (Ed.), Applied Science Publications, London (1973).

Sander, U. and P. Soukup, "Design and operation of a pervaporation plant for ethanol dehydration", *J. Membrane Sci.*, **36**, 463 (1988).

Schupp, O.E., "Gas chromatography", in *Technique of Organic Chemistry*, E.S. Perry and A. Weissberger (Eds.), Interscience, New York (1968).

Saunders, J.H. and K.C. Frisch, *Polyurethane: Chemistry and Technology*, Vol. 1, Wiley Interscience, New York (1964).

Sferrazza, R.A., R. Escobosa and C.H. Goding, "Estimation of parameters in a sorption-diffusion model in pervaporation", *J. Membrane Sci.*, **35**, 125 (1988).

Shantora, V. and R.Y.M. Huang, "Separation of liquid mixtures by using polymer membranes. III. Grafted poly(vinyl alcohol) membranes in vacuum permeation and dialysis", *J. Appl. Polym. Sci.*, **26**, 3223 (1981).

Shieh, J.J., *Novel Pervaporation Membranes for the Separation of Ethanol-Water Systems and Development of a Phase-Change Solution-Diffusion Pervaporation Model,* Ph.D Thesis, University of Waterloo, Canada (1996).

Shelden, R.A. and E.V. Thompson, "Dependence of diffusive permeation rates on upstream and downstream pressures. III. Membrane selectivity and

implications for separation processes", *J. Membrane Sci.*, **4**, 115 (1978).

Shelden, R.A. and E.V. Thompson, "Dependence of diffusive permeation rates on upstream and downstream pressures. IV. Computer simulation of nonideal systems", *J. Membrane Sci.*, **19**, 39 (1984).

Sheng, J., "Separation of dichloroethane/trichloroethylene mixtures by means of a membrane pervaporation process", *Desalination*, **80**, 85 (1991).

Shimidzu, T. and H. Okushita, "Selective separation of cyclohexane-cyclohanone-cyclohexanol mixture through poly(N-vinylpyrroolidone-co-acrylonitrile) membrane", *J. Membrane Sci.*, **39**, 113 (1988).

Shimidzu, T. and M. Yoshikawa, "Synthesis of novel copolymer membranes for pervaporation", in *Pervaporation Membrane Separation Processes*, R.Y.M. Huang (Ed.), Elsevier, Amsterdam (1991).

Slater, C.S. and P.J. Hickey, "Pervaporation R & D: A chronological and geographic perspective", in *Proc. 4th Int. Conf. Pervaporation Processes in Chem. Ind.*, R. Bakish (Ed.), Bakish Materials Corp., Englewood, NJ (1989).

Slater, C.S., P.J. Hickey and F.P. Juricic,"Pervaporation of aqueous ethanol mixtures through poly(dimethyl siloxane) membrane", *Sep. Sci. Techn.*, **25**, 1063 (1990).

Sourirajan, S., S. Bao and T. Matsuura, "An approach to membrane separation by pervaporation", in *Proc. of the 2nd. Int. Conf. on Pervaporation in the Chem. Ind.*, R. Bakish (Ed.), Bakish Materials Corp., Englewood, NJ (1987).

Sourirajan, S. and T. Matsuura, *Reverse Osmosis/Ultrafiltration Process Principles*, National Research Council Canada , Ottawa (1985).

Speigler, K.S. and O. Kedem, "Thermodynamics of hyperfiltration (reverse osmosis). Criteria for efficient membranes", *Desalination*, 1, 311 (1966).

Spitzen, J.W.F., "Pervaporation Membranes and Models for the Dehydration of Ethanol", Ph.D. Thesis, University of Twente (1988).

Strathmann, H. and W. Gudernatsch, "Pervaporation in biotechnology", in *Pervaporation Membrane Separation Processes*, R.Y.M. Huang (Ed.),Elsevier,

Amsterdam (1991).

Summers, W.R., Y.B. Tewari and H.P. Schreiber, "Thermodynamic interaction in polymethylsiloxane-hydrocarbon systems from gas-liquid chromatograph", *Macromolecules*, **5**, 12 (1972).

Tait, P.J.T. and A.M. Abushihada, " The use of a gas chromatographic technique for the study of diffusion in polymer", *J. Chromatogr. Sci.*, **17**, 219 (1979).

Takegami, S., H. Yamada and S. Tsujii, "Pervaporation of water-ethanol mixtures using novel hydrophobic membranes containing poly (dimethyl siloxane)", *J. Membrane Sci.*, **75**, 93 (1992).

Takegami, S., H. Yamada and S. Tsuji, "Dehydration of water-ethanol mixtures by pervaporation using modified poly(vinyl alcohol) membranes", *Polym. J.*, **11**, 1239 (1992a).

Tanimura, S.,S. Nakao, and S. Kimura, "Ethanol-selective membrane for reverse osmosis of ethanol/water mixture", *AIChE J.*, **36**, 1118 (1990).

te Hennepe, H.J.C., D. Bargeman, H,M.V. Mulder, and C.A. Smolders, "Zeolite-filled silicone rubber membranes. Part I. Membrane preparation and pervaporation results", *J. Membrane Sci.*, **35**, 38 (1987).

Terada, I., M. Nakamura, and M. Nakao, "Water-ethanol permeation properties through poly(hydroxymethylene) and poly(hydroxymethylene-co-fluorolefin) membrane by pervaporation method", *Desalination*, **70**, 455 (1988).

Tewari, Y.B. and H.P. Schreiber, "Thermodynamic interactions in polymer systems by gas-liquid chromatography. II. Rubber-hydrocarbons, *Macromolecules*, **5**, 329 (1972).

Timmermans, J., *Physico-Chemical Constants of Pure Organic Compounds*, Elsevier Publishing Co. Inc., London (1950).

Trafara, G., "State of order in isotactic polyhexylethylene", *J. Polym. Sci. Polym. Chem. Ed.*, **18**, 321 (1980).

Tusel, G., "Market potential of pervaporation systems", in *Proc. 2nd. Int. Conf.*

on Pervaporation Process in the Chem. Ind., R. Bakish (Ed.), Bakish Materials Corp., Englewood, NJ (1987).

Uragami, T., T. Matsuda, H. Okuno, and T. Miyata, "Structure of chemically modified chitosan membranes and characteristics of permeation and separation for aqueous ethanol solutions", *J. Membrane Sci.*, **88**, 243 (1994).

Uragami, T. and K. Takigawa, "Permeation and separation characteristics of ethanol-water mixtures through chitosan derivative membranes by pervaporation and evapomeation", *Polymer*, **31**, 668 (1990).

van Deemter, J.J., F.J. Zuiderweg, and A.Klinkenberg, "Longitudinal diffusion and resistance to mass transfer as causes of nonideality in chromatography", *Chem. Eng. Sci.*, **5**, 271 (1956).

van Krevelen, D.W. and Hoftyzer, *Properties of Polymers: Their Estimation and Correlation with Chemical Structure*, 2nd. ed., Elsevier, Amsterdam (1976).

van Oss, C.J., J. Visser, D.R. Absolom, S.N. Omenyi, and A.W.Neumann, "The concept of negative Hamaker coefficient. II. Thermodynamics, experimental evidence and applications", *Adv. Colloid Interface Sci.*, **18**, 133 (1983).

Vergnaud, J.M., *Liquid Transport Processes in Polymeric Materials, Modelling and Industrial Applications*, Prentice Hall, Englewood Cliffs, NJ (1991).

Volkov, V.V., V.S. Khotimski, and N. Plate, "Organophilic polymers for pervaporation", in *Proc. of the 4th. Int. Conf. on Pervaporation Process in the Chem. Ind.*, R. Bakish (Ed.), Bakish Materials Corp., Englewood, NJ (1989).

Vrentas, J.S., J.L. Duda and S.T. Hsieh, "Thermodynamic properties of some amorphous polymer-solvent systems", *Ind. Eng. Chem. Res. Dev.*, **22**, 326 (1983).

Wang, X.P., Shen, Z.Q., Zhang, F.Y., and Zhang, Y.F., "A novel composite chitosan membrane for the separation of alcohol-water mixtures", *J. Membrane Sci.*, **119**, 191 (1996).

Weast, R. C. (Ed.), *CRC Handbook of Chemistry and Physics*, 58th. Edition, Chemical Rubber Publishing Co., USA (1977).

Wei, Y., *Pervaporation with Latex Membranes*, Ph.D Thesis, University of

Waterloo, Canada (1993).

Wessling, M., U. Werner, and S.T. Hwang, "Pervaporation of aromatic C_8-isomers", *J. Membrane Sci.*, **57**, 257 (1991).

Wijmans, J.G. and R.W. Baker, "A simply predictive treatment of the permeation process in pervaporation", *J. Membrane Sci.*, **79**, 101 (1993).

Wytcherley, R.W. and F.P. McCandles, "The separation of meta- and para-xylene by pervaporation in the presence of CBr_4, a selective feed complexing agent", *J. Membrane Sci.*, **67**, 67 (1992).

Yang, T. and Zall, R.R., "Chitosan membranes for reverse osmosis applications", *J. Food Sci.*, **49**, 91 (1984).

Yeom, C.K., *Pervaporation of Binary Liquid Mixtures using Modified Poly(vinyl alcohol) Membranes and Mathematical Modelling*, Ph.D Thesis, University of Waterloo, Canada (1991).

Yeom, C.K. and R.Y.M. Huang, "Modelling of pervaporation separation of ethanol/water mixtures through crosslinked poly(vinyl alcohol) membrane", *J. Membrane Sci.*, **67**, 39 (1992).

Yoshikawa, M., Y. Adachi, H. Yokoi, K. Sanui, and N. Ogata, "Synthesis of poly 1-[(2-methyl propenoyl)oxy]succinimide-co-acrylonitrile and the selective separation of a water-ethanol mixture through its membranes", *Macromolecules*, **19**, 47 (1986a).

Yoshikawa, M., N. Ogata, and T. Shimizu, "Polymer membrane as a reaction field. III. Effect of membrane polarity on selective separation of a water-ethanol binary mixture through synthetic polymer membrane", *J. Membrane Sci.*, **26**, 107 (1986).

Yoshikawa, M., H. Yokoi, K. Sanui, and N. Ogata, "Selective separation of water-ethanol mixture through synthetic polymer membranes having carboxylic acid as a functional group", *J. Polym. Sci. Chem.*, **24**, 1585 (1984).

Yoshikawa, M., H. Yokoi, K. Sanui, and N. Ogata, "Selective separation of water-alcohol binary mixture through poly(maleimide-co-acrylonitrile) membrane", *J. Polym. Sci., Polym. Chem. Ed.*, **22**, 2159 (1984).

Yoshikawa, M., H. Yokoi, K. Sanui, and N. Ogata, "Selective separation of ethanol-water mixture through synthetic membrane having carboxylic acid as a functional group", *J. Polym. Sci., Polym. Chem. Ed.*, **24**, 1585 (1986).

Yoshikawa, T., Wano and T. Kitao, "Specialty polymeric membranes. I. Modified polybutadiene membranes for alcohol separation",*J. Membrane Sci.*, **76**, 255 (1993).

Zaikov, G.E., A.P. Iordanskii and V.S. Markin, *Diffusion in Electrolytes in Polymers*, VSP, Utrecht, The Netherland (1988).

Zhang, W.Z., A. Nodera, M. Satoh, and J. Komiyama, "Effects of nonvolatile additives on permeabilities of O_2 and N_2 through water-swollen poly(vinyl alcohol) membranes", *J. Membrane Sci.*, **35**, 311 (1988).

Zhao, X.P. and R.Y.M. Huang, "Pervaporation separation of ethanol-water mixtures using crosslinked blended poly(acrylic acid)-nylon 66 membranes", *J. Appl. Polym. Sci.*, **42**, 2133 (1990).

APPENDIX A

Sorption Data of Isopropanol-Water Mixtures in Homogeneous Chitosan Membranes

Results of sorption experiments of isopropanol/water mixtures in homogeneous chitosan membranes at 30 °C.

Table A.1. Liquid sorption in homogeneous chitosan membranes at 30 °C.

Liquid Comp.[a] (wt. %)	Sorbed Amount (g/g polymer) Water	Isopropanol	Total
0	0.97	-	0.97
10	0.96	0.07	1.03
30	0.74	0.14	0.88
50	0.39	0.12	0.51
70	0.17	0.11	0.28
90	0.05	0.13	0.18
100	-	0.14	0.14

[a]Liquid Comp. : Isopropanol in bulk liquid

Table A.2. Preferential sorption in homogeneous chitosan membranes.

Isopropanol in Feed (wt. %)	Isopropanol in Membrane (wt. %)	Sorption Selectivity[a]
0	-	-
10	6.8	1.5
30	15.9	2.3
50	23.8	3.2
70	40.1	3.5
90	72.7	3.8
100	100	-

[a]Water was preferentially sorbed.

APPENDIX B

Degree of Swelling Data of Chitosan Membranes in Water/Isopropanol Mixtures

Typical results of the swelling degree of chitosan membranes in the water/isopropanol mixtures at 30 °C.

Table B.1. Degree of swelling of chitosan membranes in water/isopropanol mixtures[a].

	Isopropanol Concentrations in Liquid (wt. %)					
Membrane[b]	0	10	30	50	70	90
1	2.46	2.21	1.98	1.76	1.59	1.32
2	2.31	2.14	1.85	1.64	1.47	1.24
3	2.18	2.03	1.76	1.54	1.34	1.18
4	2.08	1.82	1.63	1.40	1.22	1.14
5	1.96	1.68	1.50	1.28	1.15	1.10
6	1.86	1.48	1.34	1.14	1.10	1.06
7	1.71	1.45	1.30	1.12	1.08	1.04

[a]Degree of swelling in (g/g).

[b]Membranes :(1) Unmodified, (2) 12-hr-crosslinked, (3) 24-hr-crosslinked, (4) 36-hr-crosslinked, (5) 48-hr-crosslinked, (6) 60-hr-crosslinked, and (7) 72-hr-crosslinked chitosan membranes.

APPENDIX C

Pervaporation Data of Water-Isopropanol Mixtures with Chitosan Membranes

Typical results of pervaporation of water/isopropanol mixtures using chitosan based membranes at 30 °C.

Table C.1 Permeation data of water/isopropanol mixtures in homogeneous chitosan membranes.

Feed Comp. (wt. %)[a]	Permeation Rate Water ($g/m^2.hr$)	Isopropanol ($g/m^2.hr$)	Separation Factor
0	3976	-	-
10	3484	131	2.7
30	2101	153	5.9
50	1267	65	19.5
70	845	20	98.7
90	324	4	891.1
100	-	2.1	-

[a]Feed Comp. : Isopropanol weight fraction in feed .

Table C.2. Permeation data of water/isopropanol mixtures using composite chitosan/polysulfone at 30 °C.

Feed Comp. (wt. %)[a]	Permeation Rate Water ($g/m^2.hr$)	Isopropanol (g/m2.hr)	Separation Factor
0	4265	-	-
10	3922	479	0.9
30	3432	645	2.3
50	2243	545	4.1
70	1520	138	25.8
90	362	9	362.0
95	259	6	820.2
100	-	2	-

[a]Feed Comp. : Isopropanol weight fraction in feed.

Table C.3. Permeation data of water/isopropanol mixture using crosslinked chitosan membranes at 30 °C.[a]

Treatment Time (hr.)	Permeation Rate		Separation Factor
	Water ($g/m^2.hr$)	Isopropanol ($g/m^2.hr$)	
12	237	2.6	820
24	137	1.4	881
36	58	0.5	1044
48	49	0.37	1191
60	43	0.32	1209
72	38	0.27	1267

[a]Isopropanol weight fraction in feed : 0.9

Table C.4. Permeation data of water/isopropanol mixtures in blend membranes of chitosan/poly(vinyl alcohol)[a].

Chitosan (wt.)	Permeation Rate ($g/m^2.hr$) Water	Isopropanol	Total	Separation Factor
10	215.8	1.2	217	1619
20	222.8	1.2	224	1671
40	243.8	1.2	245	1828
60	274.1	1.9	276	1298
80	314.9	4.1	319	700
90	329.7	5.3	335	559

[a]Feed isopropanol concentration : 90 wt %.

Table C.5. Vapor phase permeation data of isopropanol/water mixtures using chitosan membranes.

Feed Comp. (wt. %)[a]	Permeation Rate ($g/m^2.hr$) Water	Isopropanol	Total	Separation Factor
10	52.69	0.51	53.2	11.6
30	47.57	0.73	48.3	27.8
50	42.52	0.48	43.0	88.3
70	36.74	0.36	37.1	235.8
90	18.33	0.17	18.5	980.0
95	13.78	0.12	13.9	1816.4

[a]Feed Comp. :Feed isopropanol concentration (wt. %)

Table C.6 Variations of chitosan membrane pervaporation performance with run times.

Run Time (hr)	Separation Factor[a]	Total Permeation Flux ($g/m^2.hr$)[a]
2	878.3	324
4	891.1	328
6	880.4	331
8	885.3	323
10	875.8	325

[a]Feed concentration 90 wt. % isopropanol.

Table C.7 Variations of composite chitosan membrane pervaporation performance with run times.

Run Time (hr)	Separation Factor[a]	Total Permeation Flux ($g/m^2.hr$)[a]
2	786.6	274
4	795.7	269
6	820.2	265
8	808.7	259
10	815.3	261

[a]Feed concentration : 95 wt. % isopropanol.

APPENDIX D

Results of the Inverse Gas Chromatography (IGC) Experiment

Typical inverse gas chromatographic data of water and isopropanol through chitosan stationary phase: retention time, variance of peak, and peak width at half of peak height.

Table D.1. Retention time of water and isopropanol in chitosan membrane.

Temperature (°C)	Water (min)	Isopropanol (min)
	8.6	23.7
30	8.9	23.8
	8.5	23.8
	7.8	19.5
40	7.8	19.1
	7.5	19.3
	7.3	15.5
50	7.0	15.4
	6.9	15.0
	6.3	12.1
60	6.3	12.3
	6.2	12.1
	5.5	8.1
70	5.1	8.4
	5.3	8.2

Table D.2. Variance of peak of water and isopropanol in chitosan stationary phase.

Temperature (°C)	Water (min)	Isopropanol (min)
	1.6	4.2
30	1.5	4.4
	1.4	4.2
	1.6	3.4
40	1.4	3.5
	1.2	3.4
	1.1	2.6
50	1.3	2.6
	1.4	2.5
	1.0	2.3
60	1.1	2.1
	1.2	2.2
	0.9	1.8
70	1.0	1.8
	1.1	1.6

Table D.3. Peak width at half the peak height of water and isopropanol.

Temperature (°C)	Water (min)	Isopropanol (min)
	3.8	9.8
30	3.7	10.3
	3.3	9.9
	3.8	8.0
40	3.3	8.2
	2.9	8.0
	2.6	6.2
50	3.1	6.2
	3.3	6.0
	2.4	5.4
60	2.4	5.0
	2.8	5.2
	2.1	4.2
70	2.6	4.2
	2.3	3.8

APPENDIX E

Diffusion Coefficients Data of Components in Chitosan Membrane

Diffusion coefficients of isopropanol, ethanol and methanol in the chitosan membranes.

Table E.1. Diffusion coefficients of methanol, ethanol and isopropanol in dry chitosan membranes determined by the thin-channel IGC method.

Temp. (°C)	Average Retention Time (min)			Diffusion Coefficient ($cm^2/sec \times 10^7$)		
	MeOH	EtOH	i-PrOH	MeOH	EtOH	i-PrOH
30	15.4	16.8	23.8	1.64	1.41	0.72
40	13.5	14.9	19.3	1.74	1.52	0.87
50	11.7	12.7	15.3	1.85	1.65	1.07
60	9.8	10.9	12.2	1.96	1.76	1.28
70	7.6	7.9	8.2	2.07	1.85	1.55

Table E.2. Diffusion coefficients of methanol, ethanol and isopropanol in swollen chitosan membranes determined by the thin-channel IGC method.

Temp. (°C)	Average Retention Time (min)			Diffusion Coefficient ($cm^2/sec \times 10^7$)		
	MeOH	EtOH	i-PrOH	MeOH	EtOH	i-PrOH
30	13.1	15.1	20.4	2.55	2.14	1.65
40	11.8	13.2	17.1	2.61	2.24	1.78
50	10.1	11.8	13.9	2.69	2.32	1.93
60	8.7	9.5	11.5	2.73	2.37	2.04
70	7.1	7.4	7.9	2.79	2.45	2.17

APPENDIX F

Binary Component Permeation in Chitosan Membranes : Derivation of Model Equations

The permeation of a component of a binary mixture is not only affected by its own presence but also by the movement of the other component. This phenomenon is known as the coupling effect. The second terms in equations (F.1) and (F.2) on the right-hand side represent the coupling flow resulting from the other chemical potential gradient.

$$J_i = \frac{1-\omega_j}{1-\omega_i-\omega_j} J_{i_D} + \frac{\omega_i}{1-\omega_i-\omega_j} J_{j_D} \qquad \text{(F.1)}$$

$$J_j = \frac{1-\omega_i}{1-\omega_i-\omega_j} J_{j_D} + \frac{\omega_j}{1-\omega_i-\omega_j} J_{i_D} \qquad \text{(F.2)}$$

Using a highly crosslinked chitosan membrane system as an example where diffusion in polymer matrix is assumed to be predominant, i.e., $D_{i_p} \approx 0$, and thus $D_i = D_{i_f}$

$$J_{i_D} = -\frac{1}{RT}\left[(1-k) D_{i_f} C_{i_f}\right] \frac{d\mu_i}{dX} \qquad \text{(F.3)}$$

and

$$J_{j_D} = -\frac{1}{RT}\left[(1-k) D_{j_f} C_{j_f}\right] \frac{d\mu_j}{dX} \qquad \text{(F.4)}$$

Substituting equations (F.3) and (F.4) into equations (F.1) and (F.2) for a flat membrane, one dimensional isothermal permeation and constant pressure we obtain,

$$J_i = -\frac{1-\omega_j}{1-\omega_i-\omega_j}\left[(1-k) D_{i_f} C_{i_f}\right] \frac{d}{dX} \ln a_i$$

$$-\frac{\omega_i}{1-\omega_i-\omega_j}\left[(1-k) D_{j_f} C_{j_f}\right] \frac{d}{dX} \ln a_j \qquad \text{(F.5)}$$

and

$$J_j = -\frac{1-\omega_i}{1-\omega_i-\omega_j}\left[(1-k)D_{j_f}C_{j_f}\right]\frac{d}{dX}\ln a_j$$

$$-\frac{\omega_j}{1-\omega_i-\omega_j}\left[(1-k)D_{i_f}C_{i_f}\right]\frac{d}{dX}\ln a_i \qquad \text{(F.6)}$$

Integrating equation (F.5) and (F.6) with boundary conditions,

$$J_i X = -(1-k)\int_{a_{i1},a_{j1}}^{a_{i2},a_{j2}}\left(\frac{1-\omega_j}{1-\omega_i-\omega_j}D_{i_f}C_{i_f}\right)\frac{1}{a_i}da_i + \left(\frac{\omega_i}{1-\omega_i-\omega_j}D_{j_f}C_{j_f}\right)\frac{1}{a_j}da_j \qquad \text{(F.7)}$$

and

$$J_j X = -(1-k)\int_{a_{i1},a_{j1}}^{a_{i2},a_{j2}}\left(\frac{1-\omega_i}{1-\omega_i-\omega_j}D_{j_f}C_{j_f}\right)\frac{1}{a_j}da_j + \left(\frac{\omega_j}{1-\omega_i-\omega_j}D_{i_f}C_{i_f}\right)\frac{1}{a_i}da_i \qquad \text{(F.8)}$$

where

$$\omega_i = \frac{c_i}{1+c_i+c_j} \qquad \text{(F.9)}$$

$$\omega_j = \frac{c_j}{1+c_i+c_j} \qquad \text{(F.10)}$$

$$C_{i_f} = \frac{c_{i_f}}{1 + c_{i_f} + c_{j_f}} d_m \qquad \text{(F.11)}$$

and

$$C_{j_f} = \frac{c_{j_f}}{1 + c_{i_f} + c_{j_f}} d_m \qquad \text{(F.12)}$$

Equations (F.11 and (F.12) are both path-dependent line integrals. Only if the relationship between a_i and a_j is known,a direct evaluation of the integrals is possible.

APPENDIX G

Free Volume Approach : Calculation of the Individual Concentration Profile

The concentration profile of the individual component in the chitosan membrane is calculated using equation (8.69) and the free volume parameters of the respective component (Table 8.5). The equation is first integrated using the Mathcad then solved with its numerical solver. The concentration profile of isopropanol and water is calculated separately.

A sample calculation for isopropanol concentration profile in the chitosan membrane at 30 °C and 0.5 weight fraction of isopropanol in feed is given here as a typical example. Since the relative distance X_R varies between 0 -1, the corresponding volume fraction of isopropanol in the chitosan

membrane is calculated by solving for $g(v_i)$ using the Mathcad Numerical Solver with a step of 0.01.

$$v_i = 0, 0.01 .. 0.082$$

$$f(v_i) = (1 - v_i)(1 - 2.976 v_i) \exp\left(\frac{-0.326}{0.023 + 0.222 v_i}\right)$$

$$g(v_i) = \frac{\int_{v_i}^{0.082} f(v_i)\, dv_i}{\int_{0}^{0.082} f(v_i)\, dv_i}$$